2015

Adiponectin and Selenium Rich Diet can act as a Complimentary Medicine in the Treatment of Intestinal and Chronic Inflammation Induced Colon Cancer

Arpit Saxena
University of South Carolina

ADIPONECTIN AND SELENIUM RICH DIET CAN ACT AS A COMPLIMENTARY MEDICINE IN THE TREATMENT OF INTESTINAL AND CHRONIC INFLAMMATION INDUCED COLON CANCER.

by

Arpit Saxena

Bachelor of Technology, Biotechnology
Guru Gobind Singh Indraprastha University, 2009

Submitted in Partial Fulfillment of the Requirements

For the Degree of Doctor of Philosophy in

Exercise Science

Norman J. Arnold School of Public Health

University of South Carolina

2015

Accepted by:

Raja Fayad, Major Professor

James Carson, Committee Member

Ho-Jin Koh, Committee Member

Xuewen Wang, Committee Member

Anindya Chanda, Committee Member

Lacy Ford, Senior Vice Provost and Dean of Graduate Studies

DEDICATION

This dissertation is dedicated in the loving memory of Dr. Raja Fayad who inspired and motivated me throughout length of my study at the Department of Exercise Science, University of South Carolina. His ideology and his passion for research will be a guiding light in my future endeavors.

ACKNOWLEDGEMENTS

I would like to thank God, Dr. Fayad and my parents Pankaj and Poonam Saxena, whose blessings have made this journey possible and helped me to successfully finish this dissertation. They have acted as a guiding light throughout the length of my study. Dr. Fayad has not only been my PhD mentor but has been my life mentor and guided me towards my next goal of pursuing a DO degree. He is my inspiration for pursuing the medical profession and to continue my research in the field of colon cancer. I would extend my special thanks to my colleague and wife Kamaljeet Kaur, who has helped me at every step of my dissertation by running blots, ELISA and covering my TA responsibilities and providing me with the mental support that is needed to overcome difficulty during this eventful journey. I would also like to thank my sister, Paridhi Saxena whose kindness, determination and sacrifice had made me finish this dissertation. I cannot thank enough to our chair, former graduate coordinator and my committee member Dr. James Carson who acted as a shield to protect us during the time of great distress which we all faced during early part of this year and his continued guidance and motivation which pulled me through and made me focused on my dissertation. I would thank Alexander Sougiannis and Sarah Depaepe for helping me with different experiment and shared supports during painful times. I would thank Dr. Anindya Chanda for mental support, motivation and monetary help for the successful completion of my experiment. I would thank Samantha Truman and Mathew Rorro for their help with data collection. I would also thank not only the present and the future members of Dr. Fayad's lab but other labs in the Department of

Exercise Science and Dr. Murphy's lab at the medical school who had helped me to successfully conduct experiments required for this dissertation: Alexander Sougiannis, Sarah Depaepe, Shweta Hegde, Kirby Lattwein, Bianca Larsen, Emma Fletcher, Alexander Chumanevich, Reilly Enos, Kandy Velazquez, Jamie Mcclellan, Aditi Narsale, Justin Hardee, Dennis Fix, Kim Hetzler, Song Gao and anyone who is not specifically mentioned here.

Funding for this dissertation was provide by Dr. Fayad's Lab and Center for Colon Cancer Research at University of South Carolina.

ABSTRACT

Colon cancer is the second largest cause of cancer death in United States. Chronic inflammation and obesity predispose patients to colon cancer. Adipose tissue is a source of bioactive substances called adipokines. Adiponectin (APN), an adipokine has anti-inflammatory property and found at lower levels in obese patients. Selenium (Se), a trace mineral and a dietary supplement, is inversely associated with cancer risk and possess anti-inflammatory and anti-carcinogenic properties. The **overall purpose** of this dissertation is to determine if chronic inflammation leading to colon and intestinal cancer are regulated by APN or Se rich diet or both. The **working hypothesis** is that APN deficiency will decrease goblet cell mucous production in colon leading to greater chronic inflammation and exacerbate the clinical symptoms and tumor load related to colon cancer. Se rich diet alone or in combination with APN administration will increase goblet cell production and apoptosis of cancer cells leading to reduced clinical symptoms, tumor load and inflammation. The specific aim 1 studied the role of APN deficiency in chronic inflammation induced colon cancer (CICC) and its effect of goblet cell production. Absence of APN increased the severity of CICC and its administration on goblet cell lines decrease their apoptosis with increase Math-1 production and upregulated mucin (Muc-2) secretion through the activation of its receptors APN R1 and R2. Specific aim 2 was designed to study the effect of Se rich diet and APN deficiency in positive modulation of CICC. Our result indicated a sharp decline in the physical manifestations of colon cancer with Se rich diet and higher severity of CICC with APN deficiency providing another proof

for the protective role of APN in CICC. Specific aim 3 studied the effect of APN administration or Se rich diet or both on intestinal cancer. We found a protective effect of Se, APN and both in reducing the clinical score and tumor load of intestinal cancer. Several mechanism of action of both Se and APN were studied in all the 3 aims. In conclusion, APN and Se could be used as a complimentary medicine in the treatment of colon and intestinal cancer.

TABLE OF CONTENTS

LIST OF FIGURES

LIST OF ABBREVIATIONS

AKT or PKB ..... Protein Kinase B

AMP ..... Adenosine Mono Phosphate

AMPK ..... 5' adenosine monophosphate-activated protein kinase

ANOVA ..... Analysis Of Variance

AOM ..... Azoxymethane

APC ..... Adenomatous polyposis coli

APN ..... Adiponectin

ATP ..... Adenosine Tri Phosphate

Bax ..... Bcl_2 associated X protein

bFGF ..... Fibroblast Growth Factor

BMI ..... Body Mass Index

CD ..... Crohn's Disease

CDC ..... Center for Disease Control and prevention

CICC ..... Chronic Inflammation induced Colon Cancer

COX-2 ..... Cyclooxygenase-2

CRC ..... Colorectal Cancer

DMEM ..... Dulbecco's Modified Eagle's Medium

DMH ..... 1,2 Dimethylhydrazine

DSS ..... Dextran Sodium Sulfate

Dvl ..... Disheveled

EMT ..... Epithelial to Mesenchymal Transition

FAP ..... Familial Adenomatous Polyposis

FoxO3a..... Foxhead box O3a

Fzd..... Frizzled

Gpx..... Glutathione peroxidase

GSK3-β ..... Glycogen Synthase Kinase-3-β

HB-EGF ..... Heparin Binding- Epidermal Growth Factor

Hes ..... Hairy and Enhancer of Split

HNPCC ..... Hereditary Non-Polyposis Colorectal Cancer

IBD..... Inflammatory Bowel Disease

IL..... Interleukin

iNOS ..... inducible Nitric Oxide Synthase

JAK ..... Janus Kinase

JNK ..... c-Jun N-terminal Kinases

LKB..... Liver Kinase

MAP ..... Mitogen Activated Proteins

MAPK ..... Mitogen Activated Protein Kinase

Math ..... Mouse ATonal Homolog

MDA ..... Malondialdehyde

Min..... Multiple Intestinal Neoplasia

MMP ..... Matrix Metalloproteinases

mTOR ..... mammalian Target Of Rapamycin

MUC ..... Mucin

NFκB..... Nuclear Factor Kappa-light-chain-enhancer of active B cell

NO..... Nitric Oxide

PDGF .....Platelet-Derived Growth Factor

PI3K Phosphatidylinositol-4,5-bisphosphate 3-kinase

pNFκB..... phosphorylated-Nuclear Factor Kappa-light-chain-enhancer of active B cell

PTEN.....Phosphatase and Tensin Homolog

ROS.....Reactive Oxygen Species

Se..... Selenium

STAT..... Signal transducer and activator of transcription

TdT.....Terminal deoxynucleotidyl transferase -mediated dUTP-biotin nick-end labeling

TGF-β..... Transforming Growth Factor β

T_H ..... T Helper

TNF-α.....Tumor Necrosis Factor alpha

WHO .....World Health Organization

WT ..... Wild Type

CHAPTER 1

INTRODUCTION

Colorectal cancer is the second largest cause of cancer death in United States and ranks fourth in the estimated new cases every year (R. Siegel, Naishadham, & Jemal, 2013). Some of the physical symptoms associated with colon cancer include rectal bleeding, change in bowel habits including constipation and diarrhea, abdominal pain, anemia, weight loss and constant fatigue (Korsgaard, Pedersen, Sorensen, & Laurberg, 2006). Etiology of colon cancer is very complex and heterogeneous and ranges from dietary and lifestyle factors to genetic mutations (Fearon, 2011). Certain risk factors associated with colon cancer includes age greater than 50, history of polyps or colorectal cancer or inflammatory bowel disease (IBD), family history of familial adenomatous polyposis (FAP) and hereditary non-polyposis colorectal cancer (HNPCC), race and ethnic background, food choices, lack of exercise, obesity, smoking and alcohol use. People who are obese are at greater risk of developing colorectal or intestinal cancer (Bardou, Barkun, & Martel, 2013). Obesity or increased fat consumption leads to an increase in the size of adipocytes, which puts an undue pressure on the adipose tissue leading to the necrosis of adipocytes. This event then results in an increase in the pro-inflammatory markers like M1 macrophages, Interleukin (IL)-6, Tumor Necrosis Factor (TNF)-α and a concomitant decrease in the anti-inflammatory markers like M2 macrophages and IL-10 (Makki, Froguel, & Wolowczuk, 2013). This switch of phenotype form anti-inflammatory to pro-inflammatory leads to the chronic cycle of inflammation leading to the activation of Nuclear factor kappa-light-chain-enhancer of active B cell (NFκB) mediated pro-inflammatory cytokines and other inflammatory mediators. Repeated cycles of inflammation in addition to carcinogenic exposure or mutation or increase gut permeability could result in pre-cancerous lesions which if could get transformed in to tumors. Studies

have shown that obesity leads to a decrease level of serum APN and exercised or trained individual have higher serum APN (Sakurai et al., 2013). APN is a protein secreted predominantly by adipocytes. Levels of serum APN has been inversely related with body weight and visceral fat accumulation. Our preliminary data indicated that APNKO mice given DMH to induce colon cancer showed significantly higher clinical score when compared to WT mice given the same treatment. Tumor number was also found to be significantly higher in APNKO mice given DMH when compared to its WT counterpart. Otani et al., 2010 has shown that intraperitoneal injection of APN (1.5mg/kg/week) 10 times from age 6 weeks to age 15 weeks significantly reduced adenomatous polyps in small intestines. Another recent study by Moon and Mantzoros 2013, have shown that co-administration of APN and Metformin, an anti-diabetic drug reduced malignant potential in Signal transducer and activator of transcription **(**STAT) 3 and Liver Kinase B1 / 5' adenosine monophosphate-activated protein kinase (LKB1/AMPK) dependent manner (Moon & Mantzoros, 2013). They also showed an important role of IL-1β in colon cancer. APN has been shown to reduce oxidative stress by the downregulation of Transforming Growth Factor β (TGF-β) through the activation of AMPK (Cheng et al., 2015). TGF-β alongwith β catenin has been shown to increase cellular proliferation and cell migration leading to epithelial to mesenchymal transition (EMT). Under the influence of β catenin, epithelial cells lose the tight junction or adherence and transit to more loose and mobile mesenchymal phenotype. During the EMT, epithelial cells lose the expression of proteins like ZO-1 and cadherin which are required for continued normal gut barrier and maintaining the integrity of the gut epithelium (Tian et al., 2011). Another important study by Moon at al., 2013 has shown that APN administration (5μg/mouse/day) for 28 days

reduced implanted tumor growth and angiogenesis and increased anti-inflammatory cytokines and improves insulin resistance in mice fed with high and low fat diet (Moon et al., 2013). All these studies have indicated the protective role of APN in inflammation and colon cancer.

In addition to medication, diet plays an important role in protection form diseases and ailments. Selenium (Se), a non-metal and a well-known anti-oxidant has been shown to have several potential benefits including anti-ageing, it boosts immunity, improves brain function, anti-heart disease, anti-diabetic, formation of many selenoenzymes, which plays an important role in hormone regulation and has anti-cancer properties (K. H. Lee & Jeong, 2012). Se has been implied in the treatment of breast cancer (Chen, Prabhu, Das, & Mastro, 2013), has been considered as a potential treatment in cancer metastasis (Chen, Prabhu, Das, et al., 2013), osteosarcoma (Wang et al., 2013) and widely studied in colon cancer (Gupta, Jaworska-Bieniek, Lubinski, & Jakubowska, 2013; Hu et al., 2013; Z. Li, Meng, Xu, Qin, & Zhou, 2013; Maseko, Howell, Dunshea, & Ng, 2014) and other gut related disorders (Nagy, Fulesdi, & Hallay, 2013). Colon cancer patients tend to have Se deficiency or lower Se level. A recent study by Li et al., 2013 on human colorectal carcinoma cell lines (HCT 116 and SW620) has shown that Se administration leads to the apoptosis of the colon cancer cells by Bcl_2 associated X protein (Bax) dependent pathway. Another study by Luo et al., 2013 has shown that supranutritional dosage of sodium selenite leads to the apoptosis of colon cancer cells by reactive oxygen species (ROS) modulation of phosphatase and tensin homolog (PTEN) mediated Phosphatidylinositol-4,5-bisphosphate 3-kinase/ Protein Kinase B/ Foxhead box O3 (PI3K/AKT/FoxO3a) signaling pathway. High and low dose of sodium selenite had showed a reduction in the

TGF-β1 signaling in diabetic rat kidney (Roy, Dontamalla, Mondru, Sannigrahi, & Veerareddy, 2011). A recent study by Bi et al., 2013 has shown that Se and sulindac synergistically act to suppress the Wnt/ β-catenin signaling by the induction of their inhibitor including p27 and p53. Although there are several publications defining the role of Se in the treatment of colon cancer but most of the studies are focused on cancer cells apoptosis on colon cancer cell lines rather than animal models of colon or intestinal cancer. Also, at the same time these studies are focused on studying a single mechanism that deals with the apoptotic pathway leading to colon cancer cell apoptosis. There is a need to expand research and explore several other pathways leading to protection mediated by Se rich diet.

Currently there are several therapies available for the treatment of colon cancer including chemotherapy, radiotherapy, radiofrequency ablation, cryosurgery, and target therapy. But all these have been associated with severe to mild side effects and there is a greater chance of recurrence. Also depending on the stage of the colon or intestinal cancer these therapies and medication may not produce desire effects and could permanently reduce the quality of the patient's life. In order to prevent these side effects, reoccurrence, improve recovery and the quality of life in colon or intestinal cancer patients, it is necessary to use alternative and complementary medicine, which might include the use of APN and Se rich diet. Alone or the combination of these might be effective in reducing the severity of colon cancer and may play an important role in recovery and prevent side effects. Although there is some published research indicating the role of Se and APN in the treatment of colon cancer but the mechanism of action of these remain unclear. Also, there is no published research that could indicate that the combination of these could be effective in the treatment of colon cancer. Based on our preliminary data and published studies by

several researchers around the globe it will be interesting to study the effect of Se rich diet and APN both alone and in combination in reducing the severity of intestinal and chronic inflammation induced colon cancer.

The overall purpose of this dissertation is to determine if chronic inflammation leading to colon and intestinal cancer are regulated by APN or Se rich diet or both.

AIM 1: To determine if chronic inflammation induced colon cancer (CICC) is regulated by APN.

Hypothesis: APN deficiency will exacerbate the pathology and the severity of CICC leading to greater inflammation and tumor load caused by reduction in goblet cell production and mucus secretion.

Rationale: APN is an adipocytokine secreted by adipocytes in response to various signals. It has been considered as an anti-inflammatory and anti-cancerous molecule. It works through the autocrine or paracrine and endocrine pathway (Ealey & Archer, 2009). Several epidemiological studies have linked lower APN levels with greater incidences of obesity related disorders including prostate, breast, endometrial and more aggressively with colon cancer (Dalamaga, 2013; Gulcelik et al., 2012; Wei, Giovannucci, Fuchs, Willett, & Mantzoros, 2005). APN has been shown to be involved in energy regulation, cycle of inflammation and remodeling (Brochu-Gaudreau et al., 2010). In vitro and clinical studies have indicated an inverse relationship of APN with colorectal cancer through mechanism involving inhibition of cancer cell growth and promoting cancer cell apoptosis (Byeon et al., 2010; A. Y. Kim et al., 2010). APN has been known to shown majority of its effect by activating AMPK. It also works by activating STAT-3, mitogen activated protein

kinase (MAPK), mammalian target of rapamycin (mTOR), PI3K/Akt and NF-κB (Obeid & Hebbard, 2012; Shackelford & Shaw, 2009). APN increased LKB expression in the breast cancer cell lines which resulted in AMPK activation leading to inhibition of tumor cell migration and adhesion (Moon & Mantzoros, 2013). Besides the above published evidences, our preliminary data indicated the protective role of APN in DMH induced colon cancer. Significantly higher clinical score including diarrhea, weight loss and fecal hemoccult was found in APNKO given DMH when compared to WT mice. Tumor number was also found be significantly higher in APNKO mice in comparison to WT mice. Although there have been published study indicating negative effects of APN deficiency Our preliminary data and the published research provides sufficient evidence to study the effect of APN deficiency in chronic inflammation and CICC.

AIM 1.1 To study the effect of APN deficiency on clinical score and tumor load in CICC.

Hypothesis: APNKO mice will have greater clinical score and tumor load when compared to WT mice given the same treatment.

AIM 1.2 To determine the effect of APN deficiency on goblet cell production and mucus secretion.

Hypothesis: APN deficiency will exacerbate CICC through reduced production of goblet cell production and mucus secretion.

AIM 1.3 To study how APN administration could affect goblet cell production and epithelial to goblet cell transition with mucin production in goblet cell lines.

Hypothesis: APN administration to the goblet cell line will decrease the apoptosis of goblet cells and will increase mucin secretion leading to greater protection from colon cancer.

AIM 2: To determine if Se rich diet can interact with APN to alleviate CICC.

Hypothesis: Se rich diet can interact with APN to significantly reduce the severity of CICC by reducing oxidative stress and increasing goblet cell mediated protection and cancer cell apoptosis.

Rationale: Selenium has been shown to be useful in the treatment of inflammation and several types of cancers including prostate (Hurst et al., 2012), breast (Jiang, Ganther, & Lu, 2000), fibrosarcoma (Yoon, Kim, & Chung, 2001), melanoma (Yan, Yee, Li, McGuire, & Graef, 1999), lung (Yan & DeMars, 2012; Zhuo, Smith, & Steinmaus, 2004) and colon cancer (Nolfo et al., 2013; C. F. Tsai, Ou, Liang, & Yeh, 2013). Our preliminary data indicate that the administration of selenium rich diet was effective in reducing the clinical score that is diarrhea, weight loss and blood in stools of both APNKO and WT mice in DMH induced colon cancer. We also observed a reduction in the tumor number and tumor area of APNKO and WT mice administered Se rich diet with significant reduction in the APNKO mice. In this aim we will study the effect of Se rich diet on chronic inflammation induced by DSS, DMH induced colon cancer and CICC induced DSS+DMH. This study will also delineate the different mechanism of action of Se in reducing tumor load in all the three treatment groups. Several *in vitro* and *in vivo* (J. H. Kim et al., 2011) studies have shown that Se administration could upregulate antioxidant selenoproteins which could be one of the major mechanism of action of Se in reducing the severity of

CICC. Luo et al., 2013 has shown that selenite induced the apoptosis of the human colorectal cancer cell lines HTC 116 and SW480 through the activation of caspase 9 with the involvement of AKT/FoxO3a/Bim/PTEN axis (Luo et al., 2013). Although there have been several studies depicting the role of Se in different types of cancers, there are limited publications indicating the protective role of Se in the treatment of colon cancer and delineating the mechanism of action of Se in reducing the severity of colon cancer. By the means of this aim, we are trying to provide an explanation for the protective role of Se in reducing the clinical score and tumor load in DMH induced colon cancer. The focus of this aim lies in determine the preventive effect of Se rich diet on chronic inflammation and colon cancer. This aim will study the different mechanism of action of Se including how Se could reduce inflammation by overexpression of antioxidant selenoproteins in the colon and reducing the expression of pro-inflammatory cytokines and proteins. It will also study the effect of Se rich diet on colon cancer cells apoptosis and goblet cell renewal leading to greater mucus secretion, which could provide protection against colon insult.

AIM 2.1 To study the effect of selenium rich diet and APN deficiency on clinical score and tumor load in CICC.

Hypothesis 2.1 Se rich diet and APN will significantly reduce clinical score and tumor load associated with CICC leading to reduced pathology and severity of disease.

AIM 2.2 To determine the effect of Se rich diet and APN deficiency on selenoproteins expression and oxidative stress.

Hypothesis 2.2 Se rich diet with APN will significantly increase the expression of selenoproteins leading to reduced oxidative stress resulting in lower inflammation and CICC.

AIM 2.3 To study the effect of Se rich diet and APN deficiency on colon cancer cell apoptosis and goblet cell production.

Hypothesis 2.3 Se rich diet and APN will significantly increase the expression of pro-apoptotic markers leading to the colon cancer cell apoptosis and simultaneously increase the production of goblet cells leading to reduced severity of CICC.

AIM 3: To study the combined effects of Adiponectin and Selenium administration on the genetic model of intestinal cancer.

Hypothesis: Adiponectin administration in addition to Se rich diet will reduce the severity of intestinal cancer by cancer cell apoptosis, increased goblet cells production and by the modulation of inflammatory marker.

Rationale: Adiponectin, an adipocytokine secreted by the adipose tissue has been implicated as an anti-inflammatory and anti-cancerous protein. Our published data clearly indicate that APNKO mice are at increased risk of developing DMH induced colon cancer with higher clinical score and more tumor number when compared to the WT counterparts. Otani et al., 2010 has shown that intraperitoneal injection of APN (1.5mg/kg/week) 10 times from age 6 weeks to age 15 weeks significantly reduced adenomatous polyps in small intestines. However, this study failed to identify any mechanistic and physical attributes of colon cancer except polyp count. Another recent study by Moon and Mantzoros 2013, have shown that co-administration of APN and Metformin, an anti-diabetic drug reduced

malignant potential in STAT3 and LKB1/AMPK dependent manner. Another important study by Moon at al., 2013 has shown that APN administration (5μg/mouse/day) for 28 days reduced implanted tumor growth and angiogenesis and increased anti-inflammatory cytokines and improves insulin resistance in mice fed with high and low fat diet. Also, APN treatment in HT29 colon cancer cell lines shows an increase expression of Muc2 in a dose dependent manner. APN has also been shown to inhibit goblet cell apoptosis via modulation of Bax/Bcl_2 ratio and is dependent on APN R1 and R2 receptors (Saxena et al., 2013). Adiponectin administration increased the expression of p21, p27 and p53 in mouse MCA 38 and human HT29 colon cancer cell lines leading to colon cancer cell apoptosis (Moon, et al., 2013). Although these studies provided evidences for the protective role of APN administration in colon cancer but failed to study mechanism of action in animal models of colon and intestinal cancer rather focused more on *in vitro* studies.

Our preliminary data has also shown that Se administration was effective in reducing the severity of clinical score and tumor number in both WT and APNKO mice with CICC. Recent study by Bi et al., 2013 has shown that the combination of Se and sulindac significantly increase the expression of p27, p53 and c-Jun N-terminal kinases (JNK) 1 phosphorylation leading to suppression of β catenin and its downstream signaling resulting in decreased intestinal tumorigenesis (Bi, Pohl, Dong, & Yang, 2013). Our preliminary data indicates that $APC^{Min/+}$ mice have significantly reduced serum APN when compared with the WT mice. On the basis of this preliminary and published data, we would want to study the effect of administration of APN alone and in addition with Se diet in $APC^{Min/+}$ mice model of intestinal cancer. This study will provide another proof of the use of Se as anti-inflammatory and anti-cancerous dietary supplement. In this aim, we will study the

preventive role of both APN and Se rich diet in reducing the severity of intestinal cancer by increasing goblet cell production in both SI and colon and hence producing more mucus. The co-administration of both APN and Se rich diet may increase the apoptosis of the cancer cells and at the same time reduce apoptosis of the colon epithelial cells.

AIM 3.1 To study the combined effect of APN administration and Se rich diet on clinical score and tumor load in $APC^{Min/+}$ mice model of intestinal cancer.

Hypothesis 3.1 APN administration alone and in addition to Se rich diet will significantly reduce the severity of intestinal cancer by reducing clinical score, inflammation and tumor load.

AIM 3.2 To study the combined effect of APN administration and Se rich diet on goblet cell production and cancer cell apoptosis.

Hypothesis 3.2 APN administration alone and in addition to Se rich diet will significantly increase goblet cell production, mucin expression and will lead to apoptosis of cancer cells in small intestine.

AIM 3.3 To determine the combined effect of APN administration and Se rich diet on oxidative stress.

Hypothesis 3.3 APN administration in addition to Se rich diet will reduce oxidative stress leading by downregulating Nitrotyrosine and 4HNE expression and increasing Gpx-2 protein expression.

Working Model

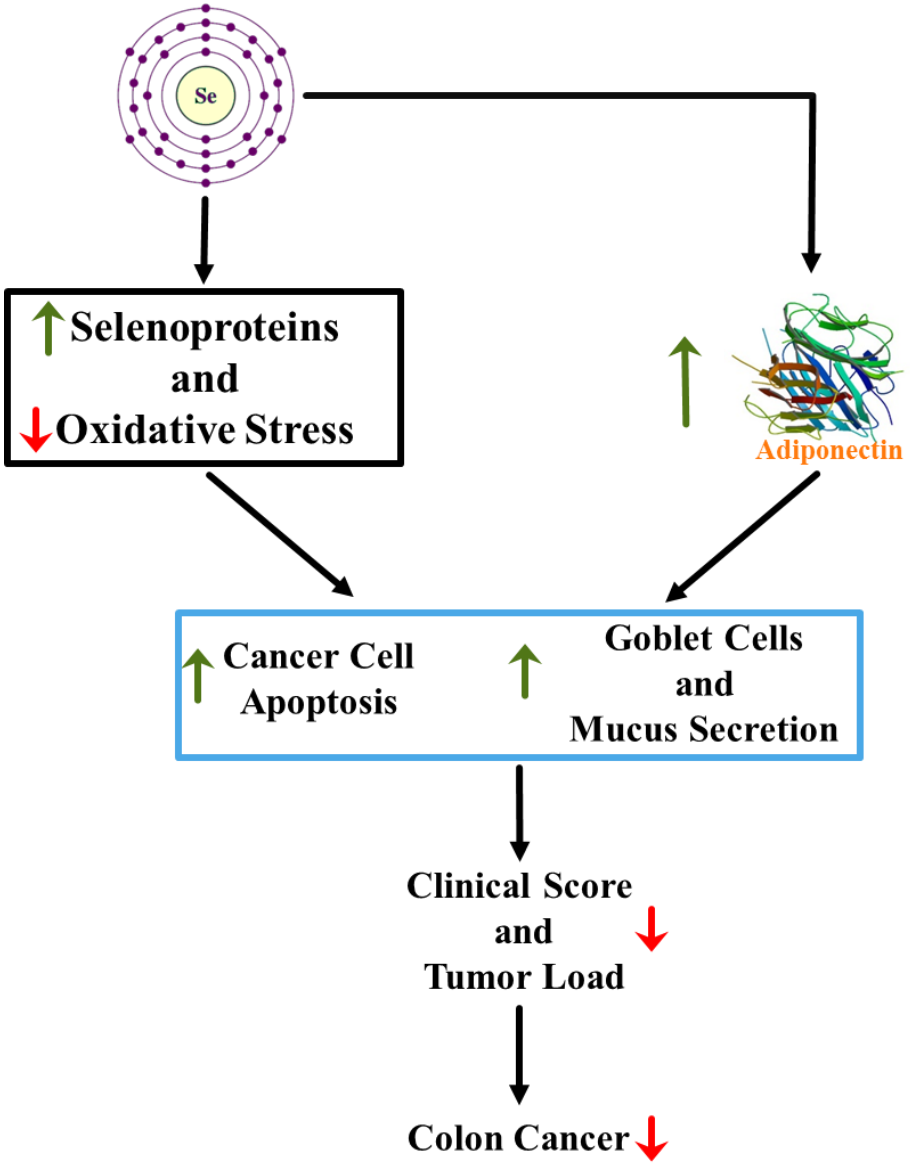

Figure 1.1. Working Model

Central idea of this dissertation is to study the protective effect of APN and Se rich diet on intestinal cancer and CICC and delineate the mechanism for this protection. To achieve this, we will be using the inducible (DSS+DMH) model for studying CICC and $APC^{Min/+}$ mice model for studying intestinal cancer. DMH+DMH and $APC^{Min/+}$ mice models are very widely used model for studying colon and intestinal cancer respectively (Tong, Yang, & Koeffler, 2011). Colon cancer in most of the cases is preceded by cycles of chronic inflammation and exposure to carcinogen sparking the formation of colon polyp. Colon and intestinal cancer at the clinical level is marked by blood in stools, diarrhea, weight loss, nausea, vomiting, constipation and constant fatigue. At the molecular level, colon and intestinal cancer is marked by increase in pro-inflammatory marker and proteins and suppression of anti-inflammatory response. Earlier stage pathology of the colon and intestine indicates pre-cancerous lesion and inflammation, which later on develops into colon tumors of varying size and shape. Our model of CICC is very near to mimic human stage II and III of colon cancer progression. Additionally, $APC^{Min/+}$ mutation accounts for majority of the intestinal and colon cancer cases along with a large similarity in the symptoms with human condition. There have been published study indicating the role of Se rich diet and APN administration in colorectal or intestinal cancer but these studies are limited in explaining the mechanism of action and most of the studies are *in vitro*. Also the combination of the above intervention has never been used in colon or intestinal cancer related studies.

This thesis is divided in to 3 different aims, where the 1^{st} aim is based on our preliminary experiment, which indicate that APNKO mice showed a significantly higher clinical score when compared to WT mice treated with DMH to induce colon cancer. We

also found a significant increase in the tumor number in APNKO mice when compared to WT mice given DMH to induce colon cancer. On the basis of our preliminary data, we are trying to study whether CICC is regulated by APN deficiency. APN has been considered as an anti-inflammatory, antidiabetic and anti-cancer molecule secreted by the adipose tissue. However, in obese individuals, a reduction in serum APN has been reported (Nigro et al., 2014). APN has been shown to decrease inflammation by the activation of AMPK (A. Y. Kim, et al., 2010). Our first aim will study the effect of APN deficiency on chronic inflammation induced colon cancer. In this aim, we will determine the effect of APN on clinical score, tumor load and inflammatory markers associated with chronic inflammation and CICC. Aim 1.2 will study the effect of APN through AMPK and STAT3 activation and Cyclooxygenase (Cox) -2 mediated chronic inflammation and cancer. In addition to this we will study the effect of APN on hairy and enhancer of split (Hes)-1 and mouse atonal homolog (Math)-1 mediated goblet cell production and mucus secretion. The last part of this aim will study the how APN administration on goblet cell lines could affect goblet cell production and mucin secretion.

Our second aim is also based on our preliminary data where we found that Se rich diet (0.75ppm) was effective in reducing the clinical score and tumor number of mice with colon cancer. Se has been widely studied for it benefits in reducing inflammation, oxidative stress and to some extent leads to the reduction in cancer pathology. Se has been found to cause apoptosis of the colon cancer cells *in vitro* (Luo, et al., 2013). In this aim, we will study the role of Se and APN in reducing the severity of chronic inflammation and colon cancer by administering Se rich diet to APNKO and WT mice model with chronic inflammation, colon cancer and CICC. Aim 2.1 will study the reduction in tumor and

clinical score through the mechanism leading to colon cancer cell apoptosis in the response to Se rich diet and serum APN. Since Se is a well-known antioxidant and anti-inflammatory non-metal, it could be easily derived that Se rich diet might be increasing the production of antioxidant selenoproteins like Glutathione peroxidase (Gpx) I and II which could reduce overall oxidative stress in the state of CICC and hence reducing inflammation leading to reduce pathology of CICC (Aim 2.2). It could be possible that Se might play an important role in increasing the goblet cell production and the secretion of mucus from goblet cells providing protection form the DSS and DMH induced colon insult, which will be studied under aim 1.3.

There have been very limited studies indicating the protective role of APN administration on colon or intestinal cancer (Luo, et al., 2013). In aim 3 of this proposal will study the protective effect of both APN administration and Se rich diet on intestinal cancer. This will provide a reinforcement of our previous aims by studying a genetic model of intestinal and colon cancer ($APC^{Min/+}$) along-with exploring the effect of APN administration alone and in conjugation with Se rich diet on colon cancer. Aim 3.1 will study the clinical score, colon and intestinal tumor number and area, histopathology and inflammation and infiltration of immune cells; mainly concerning the physical attributes of intestinal and colon cancer in both colon and iliac part of small intestine. Sodium selenite has been shown to cause apoptosis of colon cancer cell *in vitro* by the activation of Bax dependent mitochondrial pathway (Z. Li, et al., 2013). APN treatment has also been shown to increase the apoptosis of the implanted colon cancer cells (Moon, et al., 2013). Aim 3.2 will determine the effect of both co-administration and individual effect of Se rich diet and APN administration on caspase 9 mediated apoptosis of the cancer cells in addition to

goblet cell production. This aim will also study the pathways leading to the change in the phenotype from epithelial to goblet cells (Hes1 and MATH1 expression) and mucin production (Muc2). Aim 3.3 will further study the in-depth mechanism providing an explanation for the protective effect of the Se rich diet and APN on reducing oxidative stress (Nitrosylation and Lipid Peroxidation) by increasing Gpx2 expression. By the means of this proposal will test the role Se rich diet and APN in murine model of intestinal and colon cancer.

CHAPTER 2

LITERATURE REVIEW

2.1 What is Colon Cancer?

Colon cancer is an uncontrolled growth of epithelial cell of the colon leading to inflammation and polyps formation. Repeated cycles of inflammation and colon insult leads to the formation of pre-cancerous lesions. As these lesion grows, gut bacteria and toxins present in the colon invades the inner layer of the colon leading to mutations in the epithelial cells of the colon which is translated into polyps. The small polyps if not detected at an early stage develops into tumors. In 2014, estimated new cases of colorectal cancer in United States were around 130,000 and estimated number of deaths were around 50,000 including both sexes (R. Siegel, Ma, Zou, & Jemal, 2014). Colon cancer is the second largest cause of cancer death in United States and is the third most commonly diagnosed cancer in the men and second in women worldwide (Baena & Salinas, 2015). Higher incidence of colon cancer is found in North America and European countries where the incidence has reached 44.8 cases per 100,000 men and 32.2 cases per 100,000 women population. However, the rates have been significantly low in Western African countries with only 4.5 and 3.8 cases per 100,000 men and women population respectively (Baena & Salinas, 2015). This variability in incidence indicates towards the difference in the environmental and dietary factors in the two population. Especially for CRC, diet is one of the most important risk factor besides sex, age and family history of the disease (Anand et al., 2008; Brenner, Kloor, & Pox, 2014).

Patients suffering from colon cancer tends shows symptoms including weight loss, diarrhea, blood in the stools, nausea, discomfort in bowel movement, abdominal pain and cramping, bloating, change in appetite and fatigue. One of the most common and more aggressive symptoms of colon cancer including weight loss, diarrhea and fecal hemoccult

are being used in animal models to determine the severity of the disease at various stages of colon cancer and other related diseases like IBD, Colitis and CD.

Etiology of colon cancer is widespread and diverse. Certain risk factors associated with colon cancer includes age greater than 50, history of polyps or colorectal cancer or inflammatory bowel disease (IBD), family history of familial adenomatous polyposis (FAP) and hereditary non-polyposis colorectal cancer (HNPCC), race and ethnic background, food choices, lack of exercise, obesity, smoking and alcohol use (Bardou, et al., 2013). There is a decrease in the incidence of the colon cancer since two decades but this decrease is attributed to increased awareness and early screening.

2.2 Chronic inflammation and Colon Cancer:

Inflammation is a very complex biological response to a harmful stimuli including allergen, pathogen, damage tissue and injury (Ferrero-Miliani, Nielsen, Andersen, & Girardin, 2007). Inflammation is a protective response of the immunovascular system which eliminate tissue injury, pathogen and allergen and initiate tissue repair process. The process of inflammation is regulated by the body where too little or excessive inflammation leads to injury and damage to the respective tissue or organ leading to disease and disorders. Acute phase of inflammation with respect to the condition or injury is helpful but chronic inflammation leads to permanent damage, cancer or disease. Rudolf Virchow in 186 hypothesized that the sited of chronic inflammation are same the sites for the origin of cancer (Virchow, 1989). It was based on the presence of "lymphoreticular infiltrate" in human tumors. Twenty five percent of all cancers have been linked with chronic

inflammation, environmental exposure or pathogen infection (Balkwill & Mantovani, 2010). It has been found that DNA damage is present during inflammation and its accumulation during chronic inflammation leads to mutation which culminates into colon cancer (Kidane et al., 2014). Chronic inflammation is marked by infiltration of the inflammatory cells including neutrophils, macrophage, platelets and lymphocytes. These cell provides signals for the production of pro-inflammatory or T helper -1 (T_H1) cytokines and markers including IL-6, TNF-α, INF-γ, IL-1β, lipid mediators and other related chemokines. On the other hand, they reduce the expression of anti-inflammatory or T_H2 cytokines including IL-4, IL-10, IL-11 and IL-13. During chronic inflammation this storm of cytokines produce more damage than repair leading to abundant accumulation of chemokines resulting in neovascularization, angiogenesis and finally tumor growth (Coussens & Werb, 2002). Tumor growth is complemented by the production of various cytokines and chemokines that attract leukocytes which in turn produced more cytokines and inflammatory mediators like matrix metalloproteinases (MMP), ROS, Interleukins and Interferons. All these factors further exacerbate the condition leading to the activation of inflammatory pathways including STAT3 and NFκB leading to the vicious cycle of chronic inflammation, tumor growth and metastasis.

2.3 Obesity and Colon cancer:

Obesity and higher visceral fat is associated with greater incidence of colon cancer, around 11% of the colorectal cases have been associated with overweight and obesity (Bardou, et al., 2013). According to world health organization (WHO), obesity is defined

as the body mass index (BMI) ≥ 30 and overweight as BMI ≥25. According to center for disease control and prevention (CDC), 16.9% of the adults were obese in 2011-2012 in United States. Increase incidence of CRC with higher BMI appears to be more consistent in men as compared to women. This sex difference could be attributed to the hormonal difference and the onset of metabolic syndrome. Visceral obesity has been suggested to promote metabolic changes culminating in to angiogenesis (Sarkanen et al., 2012). Adipose tissue though seems to provide all the detrimental effects but it also act an active endocrine organ secreting adipocytokines including APN, leptin, resistin, visfatin and cytokines including IL-10, IL-8, IL-6 and IL-1 receptor agonist and TNF-α. Although, adipose tissue act a source of these beneficial molecule but in obesity, secretion of these adipocytokines is altered leading to metabolic disorders which exacerbate chronic inflammation and CRC (Barb, Williams, Neuwirth, & Mantzoros, 2007).

2.4 Adiponectin, an anti-inflammatory and anti-cancer adipocytokine:

APN is a well-known insulin sensitizing adipocytokine whose serum levels has been inversely linked with obesity, chronic inflammation and colon cancer (Barb, et al., 2007). It is an abundant protein with the blood concentration of a healthy individual ranging from 5-20 µg/mL and accounts for 0.01% of the total blood protein (Fayad et al., 2007; J. Y. Kim & Scherer, 2004; Kishida, Funahashi, & Shimomura, 2014). It has a complex structure and is structurally homologous to TNF-α and C1q (complement factor). Its monomer is made of the globular and collagenous domain and could polymerize in to dimer, trimer and other higher molecular weight isomer (Waki et al., 2003). Greater levels

of polymerization leads to low, medium and higher molecular weight APN. Most of the APN levels in the serum are inversely related to the body's visceral fat content. The mechanism of this relationship remains unclear. Lower levels of APN is associated with several disease including hypertension, type-2 diabetes, dyslipidemia, coronary artery disease, stroke, sleep apnea, non-alcoholic fatty liver disease, inflammatory bowel disease, colon cancer, breast cancer, leukemia, prostate and gastric cancer (Kishida, et al., 2014). Higher APN levels or hyperadiponectinemia is associated with cardiac dysfunction, pulmonary and kidney diseases. APN exerts its function by binding to its receptors ADIPOR1 and ADIPOR2 (seven transmembrane domain receptors) which is located in the various cell types and tissue in the body. They act through multiple pathways including p38 mitogen activated proteins (MAP) kinase and adenosine monophosphate (Kadowaki & Yamauchi, 2005). APN can bind to several growth factors including platelet-derived growth factor (PDGF), fibroblast growth factor (bFGF) and heparin binding epidermal growth factor (HB-EGF) and differential binding of APN to these growth factors is precluded by the binding of these growth factors to their respective receptors leading to cessation of their DNA synthesis and cell proliferation (Wang et al., 2005). APN has been known to show several anti-inflammatory properties including inhibition of tumor necrosis factor alpha (TNF-α), STAT3 and NFκB resulting in the downregulation of pro-inflammatory cytokines like IL-6 and Il-1β and induction of several anti-inflammatory cytokines like IL-10 (Fantuzzi, 2005). High fat diet has been shown to increase the colon tumor number and area and APN treatment has been to significantly reduce tumor weight with larger center necrotic tumor area. It has also been shown to decrease cell proliferation in the human LoVo and mouse MCA38 colon cancer cell lines. Anti-proliferative effect of

APN has been shown to be mediated by the activation of AMPK. Administration of APN has been shown to increase the phosphorylation of AMPK in HT29 colon cancer cell lines. Higher doses of APN has been shown to inhibit the STAT3 phosphorylation in HT209 colon cancer cell lines (Moon, et al., 2013). APN has also been shown to downregulate Cox-2 and upregulate T-cadherin mRNA expression in human colon cancer HCT116 cell lines (Tae et al., 2014b). All the above data provides string evidence for the use of APN as an anti-inflammatory anti-cancerous compound for the treatment of chronic inflammation, colon cancer and CICC.

2.5 Role of AMPK, STAT3, NFκB and Cox-2 in inflammation and colon cancer

AMPK is the energy sensor of the body which is known to regulate lipid and glucose homeostasis, protein synthesis, insulin sensitivity and autophagy. It is a heterotrimeric complex composed of regulatory β and γ subunits and catalytic α subunit (Grahame Hardie, 2014). Its expression is found in almost all the tissue of the body and is activated by the increase in adenosine monophosphate (AMP) to adenosine triphosphate (ATP) ratio in addition to the modulating hormone levels (J. S. Tsai et al., 2014). Anti-tumor function of AMPK comes from the idea that AMPK might aid LKB1, which is known tumor suppresser (Lizcano et al., 2004). AMPK has the ability to inhibit all biosynthetic pathways that is required for growth and could cause cell cycle arrest. Chronically AMPK activation leads to the promotion of more energy efficient pathways that is oxidative metabolism and opposing aerobic glycolysis which is the primary tumor supporting mechanism (Vander Heiden, Cantley, & Thompson, 2009). Activators of

AMPK including metformin and phenformin delay the onset of tumor in tumor prone mice (X. Huang et al., 2008). Transgenic mice overexpressing the Myc oncogene showed accelerated development of lymphoma whole body AMPK-α1 knockout mice (Faubert et al., 2013). Besides the tumor suppressive function, AMPK is evidently know to show anti-inflammatory effects. Macrophages related studies have shown that AMPK activation attenuates the production of inflammatory cytokines (Sag, Carling, Stout, & Suttles, 2008).

STAT3 is mediator of the JAK/STAT signaling pathway and is an important member of the STAT family of transcription factors located in the cytoplasm in an inactive state. After the phosphorylation activation of STAT3 by extracellular signals including Janus Kinase (JAK), cytokines and hormones, it dimerizes and translocate to the nucleus leading to the expression of several critical genes required for proliferation, survival, migration, invasion and progression of cell cycle (Buettner, Mora, & Jove, 2002). STAT3 autocrine feedback loop functionally link inflammation and cancer where oncogenic events leads to the increased expression of intrinsic STAT3. NFκB and STAT3 are activated further in response to inflammatory cytokines like TNF-α, IL-6, IL-17 and IL-22 forming a vicious loop (Pandurangan & Esa, 2014). The phosphorylated STAT3 was found to be significantly elevated in patients with colorectal cancer; along with the activation of anti-apoptotic genes including Bcl_2 and Bcl_{xl} that are related with metastasis, tumor growth and bad prognosis. Therefore STAT3 pathway is suggested to be the target pathway for the treatment of colon cancer (Atreya & Neurath, 2008).

NFκB is a transcription factor that under basal conditions is present in the cytoplasm as a heterotrimer consisting of 3 subunits including p50, p65 and IκBα. It has an important role in the immune system to target and eliminate terraformed cells. However,

this is true only under acute inflammation where its activation leads to the attack of cytotoxic cells on cancer cells preventing tumor formation. In chronic condition, continued activation of NFκB leads to the certain pro-tumorigenic activity (Disis, 2010). Activation of NFκB leads to the phosphorylation, ubiquitination and degradation of IκBα protein and translocation of p50 and p65 subunit to the nucleus, initiating the transcription activation of several downstream target genes. These gene targets including genes responsible for inflammation, cytokine production like TNF-α, IL-1, IL-6 and IL-8, cell proliferation and survival, angiogenesis, neovascularization (upregulation of VEGF), invasion, epithelial to mesenchymal transition (EMT) and metastasis (upregulation of MMPs and loosening the extracellular matrix for the invasion of cancer cells). (Aggarwal, Vijayalekshmi, & Sung, 2009). Besides other inflammatory pathway, STAT3 and TNF-α is highly interconnected with the activation of NFκB. Mutation of NFκB signaling genes is directly associated with lymphoid malignancies. Studies on animal models have shown a correlation between increased expression of activated NFκB or its mutation with increase severity of hepatocellular carcinoma, breast cancer, melanoma, lung and even colon cancer. NFκB has also been shown to polarize the classic M1 macrophages towards M2 phenotype which instead of attacking tumor foster it for further growth and metastasis (Hoesel & Schmid, 2013). Due to the above mentioned reasons, NFκB pathway is one of the popular pathways to be targeted by chemotherapeutic agents. Inhibition of NFκB might be appropriate for reducing the severity of chronic inflammation and colon cancer.

Cyclooxygenase (COX) is an enzyme that catalyze the rate-limiting step of converting arachidonic acid to prostaglandin. There are 2 isoforms of COX: COX-1 and COX-2. COX-1 is expressed in several tissues in the body and is required to maintain

normal physiological functions like maintaining gastric mucosa, renal blood flow and platelet aggregation. Overexpression of COX-2 has been associated with several cancers (Miladi-Abdennadher et al., 2012) and is contributing factor in the development of colon cancer. 85% of the sporadic human colorectal cancer especially neoplastic epithelial cells have reportedly increased expression of COX-2. It may induce angiogenesis, metastasis, alter extracellular matrix adhesion and resistance to apoptosis. Overexpression of COX-2 has been determined in the carcinogenesis induced by mutation of APC gene leading to increased intestinal tumor. Celecoxib, a COX-2 inhibitor has been shown to reduce the incidence of AOM induced colon cancer by 93% and rofecoxib another COX-2 specific inhibitor significantly decreased the rectal polyp number and size in patients with familial adenomatous polyposis (Higuchi et al., 2003; Miladi-Abdennadher, et al., 2012). Besides these evidences it is still controversial to use COX-2 as a prognostic marker for the recurrence and survival of the patients with colorectal cancer (Petersen et al., 2002). Its be concluded form the above that the overexpression of COX-2 is directly related with increased severity of colorectal cancer and the reduced expression could a better outcome for the treatment of colon cancer.

2.6 Goblet cell and Mucus Secretion

Colon epithelial tissues is the one of the tissues with highest turnover and is proliferative in nature. Colon and intestinal tissue composed of four different cell types: 3 belongs to the secretory lineages: enteroendocrine cells (endocrine in nature), goblet cells (mucus secretion) and Paneth cells (antimicrobial) and one enterocytes (absorptive in

nature). These cell are derived from the multipotent stem cells located at the base of the Crypts of Liberkühn (Shroyer, Wallis, Venken, Bellen, & Zoghbi, 2005). The mechanism which leads to the formation of the crypts and fates of these cells to the respective lineage is not completely understood. Several genes and factors are involved in the differentiation of these cells to their defined fate including Wnt β-catenin pathway, Notch signaling, Math-1, Hes-1 and KLF-4. Expression of Hes-1 in the progenitor cells leads to the absorptive enterocytes fate while those expressing Math-1 get committed to the secretory lineage which could then become goblet cells, enteroendocrine cells or Paneth cells. The section of the final fate of the secretory lineage still remains unclear (Schonhoff, Giel-Moloney, & Leiter, 2004). The colon is the home of millions of bacteria that under normal healthy condition are friendly and aid in the digestion of food. Bacteria in the colon doesn't directly lie on the epithelial cell layer but are separated by the protective mucus covering or it can be summed up in a two layer design where inner mucus layer is anchored to the colon epithelium and excludes the bacterium while the upper layer provides a thriving place for commensal bacteria (Johansson et al., 2008). The mucus scaffold primarily consist of MUC2 which is a prominent member of the mucin family. Mucins are high molecular weight *O*-linked glycoproteins which are distributed in different parts of the body and plat critical pathophysiological role. Twenty know mucin genes have been identified in humans, most of which are expressed in the gastrointestinal tract. MUC2 being the major mucus forming mucin is constitutively expressed by the goblet cells and its core is covered with glycans (almost 80% glycans in mature MUC2). These glycans are not destroyed by the host enzymes but they can degraded by the bacterial enzymes. However, the complexity of these glycans make degradation a time consuming process. Although, some parasitic

bacteria like Entamoeba histolytica produce proteases that could cleave the MUC2 in such a way that the whole complex structure falls apart but commensal bacteria including Lactobacilli and Bacteroidetes family don't produce any mucin that will degrade MUC2 (Johansson & Hansson, 2013). Goblet or mucus secreting cells of the colon were found to be significantly reduced in colon adenocarcinoma alongwith the significant reduction in the HATH1 mRNA expression in clinical samples. HATH1 expression was also downregulated in the various human colon cancer cell lines (Leow, Polakis, & Gao, 2005). Math-$1^{-/-}$ mice failed to develop the gastrointestinal secretory lineages including goblet cell, paneth cell and enteroendocrine cells (Q. Yang, Bermingham, Finegold, & Zoghbi, 2001). All the above provides an important role of goblet cell, Hes-1 and MATH-1 in reducing the pathogenesis of colitis and colorectal cancer. Secretion of mucus and especially MUC2 is very critical for the normal maintenance and working of the colon and prevention form toxins and gut bacterial invasion.

2.7 Selenium, an anti-oxidant and anti-cancer molecule

Selenium is an essential micronutrient and is widely accepted as an anti-oxidant non-metal (Maseko, et al., 2014). This micronutrient forms selenocysteine, which is the twenty-first amino acid and integrates into proteins to form 25 selenoproteins (Metanis & Hilvert, 2014). It has been shown to lay a wide physiological role including immune function, male fertility and thyroid function. Se can be obtained in the diet through several sources including Brazil nut, fish, liver, chicken, certain vegetables and meats (Maseko, et al., 2014). The recommended dietary allowance for Se is 55μg per day for human adults

and the upper safe limit is 400 μg/day. Beneficial effects of Se can be obtained at a dosage of 200 μg per day. Se has been shown to reduce the severity of cancers including prostate (Gerstenberger et al., 2014), breast (Arsenyan et al., 2014) and lung (Okuno, Honda, Arakawa, Ogino, & Ueno, 2014b) and has acted as a useful supplementation for several ailments including cystic fibrosis (Ciofu & Lykkesfeldt, 2014), male and female infertility (Balazs & Racz, 2013), glucose metabolism in type 2 diabetes (Mao & Teng, 2013), grave's disease (Kryczyk & Zagrodzki, 2013) and other related inflammatory and autoimmune diseases. A dosage of 200 μg/day of Se has been shown to decrease the total incidence of cancer by 25% (Reid et al., 2008). Higher intake or the overdose of Se is associated with severe toxicity. A dosage higher than 400 μg per day is associated with selenosis. Some of the symptoms associated include gastrointestinal disorders, fatigue, irritability, hair loss and neurological disorders. During extreme cases, it can result in liver cirrhosis, pulmonary edema and even death. An inverse association has been established between higher Se status and colorectal cancer (Hughes et al., 2014). The protective effect of the Se in various diseases and conditions is mostly due to the anti-oxidative property leading to an increase in the production of selenoproteins like glutathione peroxidases (Gpx), which neutralize or prevent the formation of reactive oxygen species (ROS) (Kosaric et al., 2014). Se metabolism is complex and most of the biological effects of elemental Se that is ingested are mediated by selenoproteins (Labunskyy, Hatfield, & Gladyshev, 2014). Gpx-1 and Gpx-2 are the most abundant selenoproteins present and mediate most of the protective effect of Se. Gpx-1 is ubiquitously presents in the cytosol and the mitochondria in all the tissues of the body, while Gpx-2 is mostly concentrated in the intestinal epithelium (Brigelius-Flohe & Maiorino, 2013). Gpx-1 or Gpx-2 knockout

mouse or double knockout mouse has shown to exhibit severe pathology of colorectal cancer (Krehl et al., 2012; D. H. Lee, Esworthy, Chu, Pfeifer, & Chu, 2006) and Se rich diet has been shown to increase Gpx activity in mice model of colorectal cancer. Increased activity of Gpx-1 and Gpx-2 has also been linked to the chemo preventive effect of Se supplementation (Hu, McIntosh, Le Leu, & Young, 2010).

A recent study by Li et al. 2013 on human colorectal carcinoma cells (HCT 116 and SW620) has shown that different dosages (1 μM, 5 μM and 10 μM) of Se lead to apoptosis of the colon cancer cells by Bax dependent pathway (Z. Li, et al., 2013) with 10 μM being the most effective. Another study by Luo et al. 2013 has shown that supranutritional dosage of sodium selenite (10 μM) lead to apoptosis of colon cancer cells by ROS modulation of phosphatase and tensin homolog (PTEN) mediated PI3K/AKT/FoxO3a signaling pathway in colon xenograft animal model (Luo, et al., 2013). Sodium selenite has also shown to reduce inflammation by downregulating the expression of nuclear factor kappa light-chain-enhancer of activated B cells (NFκB) and related cytokines (Pillai, Sugathan, & Indira, 2012). All the above mentioned evidence provide a strong case for the use of Se rich diet in the treatment of chronic inflammation and colorectal cancer.

2.8 Oxidative Stress and Cancer cell apoptosis

According to the 2014 statistics, cancer is the cause of one in four deaths in United States (R. Siegel, et al., 2014) and colorectal cancer is the major cause of cancer worldwide and accounts for 9% of total cancer incidence. Oxidative stress refers to the uncontrollable

overproduction of free radicle and their derivatives that interact with macromolecules like lipid, proteins and DNA and modulate their structure and function (Perse, 2013). Among the wide etiology of cancer, DNA damage by ROS is one of the main culprit for the onset and the development of cancer. Increase in oxidative byproducts of the normal metabolism leads to increase inflammation which in presence of an external stimulus including toxin or carcinogen leads to cancer. Studies have shown the protective role of antioxidants and phyochemicals including vitamin E, selenium, glutathione, resveratrol, catechins, sulforaphane, curcumin and genistein on inflammation and cancer (Shukla, Meeran, & Katiyar, 2014). ROS may oxidize polyunsaturated fatty acids (PUFA) and initiates the process of lipid peroxidation that leads to the formation of other free radicles and substances like hydroperoxides, lipoperoxides, conjugated dienes, aldehydes which are toxic in nature and malondialdehyde (MDA). This process of lipid peroxidation increase membrane permeability, results in the loss of gradient maintenance and inflammation (Finaud, Lac, & Filaire, 2006). MDA and 4-hydroxy-2-nonenal; products of lipid peroxidation can act at different levels and could modulate cell proliferation and gene expression leading to greater production of ROS which could further modify or oxidize protein and render them non-functional (Marnett, 2002). Oxidized protein are either catabolized to amino acids or rapidly degraded by proteasomes or in worst case scenario may accumulate in the cell leading to pathologies and inflammation (Grune, Merker, Sandig, & Davies, 2003). Nitrosylation is another consequence of the oxidative stress which leads to the production of Nitric Oxide (NO) that reacts with the cysteine residue of different proteins and could inhibit or promote the activity of those proteins. This process of nitrosylation shutdowns the activity of caspases which are responsible for apoptosis of

cancer cells. It may also inactivate certain DNA repair enzyme leading to the accumulation of mutations and DNA damage further promoting inflammation and cancer (Floyd, Chandru, He, & Towner, 2011). Therefore one of the mechanism for the treatment of colon cancer is the use of anti-oxidant such as Se which has been shown to increase activity of antioxidant protein like Gpx that can reduce oxidative stress and hence decrease the severity of inflammation and colon cancer.

Apoptosis or programmed cell death is an orchestrated process which includes a sequence of biochemical and morphological changes that eliminate the old and infected area and create space for new cell growth and repair (Huerta, Goulet, Huerta-Yepez, & Livingston, 2007). Se administration has been shown to increase the apoptosis of the human colorectal carcinoma cell lines (HCT 116 and SW620) by Bax dependent pathway (Z. Li, et al., 2013). Methylseleninic acid has been shown to cause the apoptosis of breast cancer cell by the activation of caspase 8 and 9 (Z. Li, Carrier, & Rowan, 2008). Another study by Luo et al., 2013 has shown that supranutritional dosage of sodium selenite leads to the apoptosis of colon cancer cells by reactive oxygen species (ROS) modulation of phosphatase and tensin homolog (PTEN) mediated PI3K/AKT/FoxO3a signaling pathway (Luo, et al., 2013). APN has been to know to act by the activation of AMPK which in turn play a critical role of in the suppression of cellular proliferation and cancer cell apoptosis by the activation of p53 and p21. APN has been shown to cause the apoptosis of the Barrett's adenocarcinoma cell line OE-19 by the upregulation of Bax and downregulation of Bcl_2. APN can induce apoptosis of the gastric, liver and endometrial carcinoma in Bax dependent manner along with the activation of caspase 3 (Dalamaga, Diakopoulos, &

Mantzoros, 2012). Both APN and Se has been known to cause apoptosis of the cancer cells and could be used alone or in conjugation for the treatment of colon and intestinal cancer.

2.9 Wnt Pathway, β catenin, TGF-β and ZO1

More than 80% of the colorectal cases are caused by the truncation of the Apc protein. Wnt signaling is one of the primary mechanism that is involved in cell proliferation, polarity and cellular differentiation during embryogenesis, development and homeostasis (Logan & Nusse, 2004). A slight mutation in the Wnt pathway result in birth defects, cancer and related diseases. There are 2 types of Wnt pathways: canonical and non- canonical. Canonical Wnt pathway is the most studied pathway and causes the accumulation of β catenin in the cytoplasm and final translocation in to the nucleus where it act as a transcription factor and leads to the activation of certain genes.

Colon and intestinal epithelium is one of the most dynamic and self-replenishing organ in the mammalian system which get renewed in 3-5 days along the crypt villus axis (Leblond & Stevens, 1948). Colon and small intestine is designed in a way to increase the surface area of the organ for maximum absorption. Several *in vivo* and *in vitro* studies have indicated the important role of Wnt signaling in maintaining the proliferative and pluripotent nature of the intestinal stem cells. In the absence of the Wnt signal, Apc/Axin complex or the destruction complex degrades the cytoplasmic β catenin by targeting it for ubiquitination which has a potential to go in the nucleus and activate the Wnt target genes (Burgess, Faux, Layton, & Ramsay, 2011). However in the presence of Wnt ligand and following its binding to the Frizzled (Fzd) receptor and low density lipoprotein, disheveled

(Dvl) protein is phosphorylated and it inactivates glycogen synthase kinase-3-β (GSK3-β) which leads to the disruption of destruction complex and β catenin accumulates in the cytoplasm leading to its translocation to the nucleus. In the nucleus, β catenin forms a complex with the TCF/LEF transcription factor and leads to the transcription of Wnt target genes which further leads to cell proliferation, inflammation, cell migration and carcinogenesis (Sebio, Kahn, & Lenz, 2014). β catenin is also the part of the complex that forms the adherence junctions and plays an important role in embryogenesis and EMT. β catenin is also considered as a proto-oncogene and its mutation is common in several cancers including liver cancer, ovarian cancer, breast cancer, lung and colon cancer (Forbes et al., 2011).

β catenin is responsible for several morphogenetic changes in the epithelial cells of the colon. Under the influence of β catenin, epithelial cells lose the tight junction or adherence and transit to more loose and mobile mesenchymal phenotype. During the EMT, epithelial cells lose the expression of proteins like ZO-1 and cadherin which are required for continued normal gut barrier and maintaining the integrity of the gut epithelium (Tian, et al., 2011). TGF-β is a 25 kDa cytokines that plays a critical role in carcinogenesis, homeostasis, cell proliferation, migration, apoptosis, fibrosis, differentiation of cell and wound healing. TGF-β signaling pathway is one of the most common altered signaling. It can play a dual role as a tumor suppressor and as a cancer promotor. During the progression of the human colon TGF-β1 switches form being inhibitor to tumor cell growth promotor. Higher TGF-β protein levels is associated with an increased incidence of tumor reoccurrence (Friedman et al., 1995). TGF-β alongwith β catenin has been shown to enhance EMT and angiogenesis leading to greater severity of colon cancer (Lampropoulos

et al., 2012). APN and Se administration independently has been to reduce the expression of TGF-β and β catenin. Therefore studying the role of APN and Se on Wnt mediated β catenin activation and TGF-β will provide conclusive evidence for the protective role of APN and Se in cancer, inflammation and CICC.

2.10 Mouse Model of colon cancer

Development of colon cancer is a sequential process involving the genetic changes or toxic exposure in the colon epithelium leading to the formation of pre-cancerous lesions. These lesions then develop in to adenomatous polyp which finally progress in to invasive tumors which invade the different layers of the colon epithelium depending on the stage of the colon cancer. The survival rate of the colon cancer various depending on the stage of colon cancer with 92% 5 year survival at stage I and only 11% survival at stage IV.

2.11 Chemically induced colon cancer mouse models:

Induction of colon cancer by carcinogen and inflammatory chemicals is rapid in mice and very reproducible which marks the conversion from adenoma to adenocarcinoma that overlaps with the sequence of events that occurs in human colorectal cancer. Commonly used carcinogen include the following: 1,2 Dimethylhydrazine (DMH), azoxymethane (AOM), 2-amino-1-methyl-6-phenylimidazo [4,5-b]pyridine (PhIP), 2-amino-33-methylimidazo [4,5-f], 3,2′-dimethyl-4-aminobiphenyl (DMAB) and N-methyl-N′-nitro-N-nitrosoguanidine (MNNG). Repeated exposure to DMH intraperitoneally

produces colon tumors that leads to severe pathology which is very similar to the human disease. This makes DMH as one of the most commonly used carcinogen along with AOM which serve the same function as DMH. Several studies have successfully indicated the use of DMH in developing pre-cancerous lesions and tumor associated with colon and rectal cancer. Our preliminary data indicated that intraperitoneal DMH injection (20mg/kg mouse body weight) once a week for 12 weeks was effective in producing tumor in both APNKO and WT mice (Tong, et al., 2011).

DMH can also be complemented by DSS which is a sodium salt that is effective in producing both chronic and acute inflammation depending on the amount, duration and frequency of exposure. DSS alone is commonly used in acute and chronic model of murine colitis (Okayasu et al., 1990). DSS is usually administered in drinking water and the concentration usually varies with the study duration and exposure time. 1.5 to 3% DSS in the drinking water has been reported in studies relating to colitis and colon cancer. In the DSS+DMH model, dysplasia could be observed initially after DMH administration followed by the first DSS cycle in the colon mucosa. Mutation of the β catenin in the later stage of the colon cancer could be observed in 80-100% of the DSS+DMH induced CICC. Similar result could be obtained by using AOM instead of DMH (Seril, Liao, Yang, & Yang, 2003; Tong, et al., 2011).

2.12 Genetic model of Intestinal Cancer: $APC^{Min/+}$

Adenomatous polyposis coli (APC) is a human gene that is commonly associated with tumor suppression by downregulating the canonical pathway of Wnt signaling as

discussed above. It acts by binding to β catenin as a part of the destruction complex resulting in its degradation. Loss of APC impairs the degradation of β catenin leading to its accumulation in the cytoplasm, followed by its translocation to the nucleus where it activates the LEF/TCF transcription factors. These transcription factor further activates the Wnt target genes which is one of the common pathway in tumorigenesis of the colorectal cancer and shows a similar pathology observed in the human subjects (Korinek et al., 1997). APC mutation is the truncating mutation of the APC gene at codon 850. Homozygous $APC^{Min-/-}$ mutation are lethal at the early embryonic stages but the heterozygous $APC^{Min/+}$ mutation on the C57BL/6 background survives and develops around 30 tumors at an age of 16 weeks with more than 50 tumors at an age of 20 weeks in the intestine. Most of the tumors are concentrated in the small intestine with few tumor invading the colon. In both small intestine and the colon, tumors are located more towards the distil end that is in the iliac part of the small intestine and the descending part of the colon (Tong, et al., 2011). Abnormal intestinal epithelial and goblet cell morphology is also observed in the $APC^{Min/+}$ mice model of intestinal cancer. There are several mutants of the APC gene including mutations at 716 (truncating mutation), 1638N (neomycin insertion at codon 15 resulting in truncation of codon 1638), 1638T (hygromycin insertion at codon 15 resulting in truncation of codon 1638) and frameshift of 580 and 474 codon (Colnot et al., 2004; Moser, Pitot, & Dove, 1990; Pretlow, Edelmann, Kucherlapati, Pretlow, & Augenlicht, 2003; Sasai, Masaki, & Wakitani, 2000). These difference in the mutation sites results in different number of polyps in the small intestine but the colon polyps remains the same. In addition to tumor development these mice show loss of both mature and immature thymocytes with a complete regression of thymus at an age of 18

weeks (Coletta et al., 2004). Bone marrow shows depletion of immature and progenitor B cells. IL-6 levels have been reported to increase 10 fold as compared to the C57BL/6 mice which causes the development of cachexia that is accompanied by the loss of fat and muscle mass leading to extreme weight loss (Baltgalvis et al., 2008). Due to these complication, the maximum lifespan of these $APC^{Min/+}$ mice is 24 weeks with and average lifespan of 16-20 weeks depending on the degree of cachexia (Tong, et al., 2011).

Due to the above mentioned reasons and on the basis of our preliminary data we will be using DSS+DMH model of CICC and $APC^{Min/+}$ mice model of intestinal cancer in our colon cancer prevention studies.

CHAPTER 3

ADIPONECTIN DEFICIENCY: ROLE IN CHRONIC INFLAMMATION INDUCED COLON CANCER[1]

[1] Arpit Saxena, Alexander Chumanevich, Emma Fletcher, Bianca Larsen, Kirby Lattwein, Kamaljeet Kaur, and Raja Fayad. Accepted by Biochim Biophys Acta. 2012 Apr; 1822(4): 527–536. Reprinted here with the permission of publisher.

3.1 Abstract

Adiponectin (APN), an adipokine, exerts an anti-inflammatory and anti-cancerous activity with its role in glucose and lipid metabolism and its absence related to several obesity related malignancies including colorectal cancer. The aim of this study is to determine the effect of APN deficiency on the chronic inflammation-induced colon cancer. This was achieved by inducing inflammation and colon cancer in both APN knockout (KO) and C57B1/6 wild type (WT) mice. They were divided into four treatment groups (n= 10): 1) control (no treatment); 2) treatment with three cycles of dextran sodium sulfate (DSS); 3) weekly doses of 1,2-dimethylhydrazine (DMH) (20 mg/kg of mouse body weight) for twelve weeks; 4) a single dose of DMH followed by 3 cycles of DSS (DMH+ DSS). Mice were observed for diarrhea, stool hemoccult, and weight loss and were sacrificed on day 153. Tumor area and number were counted. Colonic tissues were collected for Western blot and immunohistochemistry analyses. APNKO mice were more protected than WT mice from DSS induced colitis during first DSS cycle, but lost this protection during the second and the third DSS cycles. APNKO mice had significantly severe symptoms and showed greater number and larger area of tumors with higher immune cell infiltration and inflammation than WT mice. This result was further confirmed by proteomic study including pSTAT3, pAMPK and Cox-2 by western blot and Immunohistochemistry. Conclusively, APN deficiency contributes to inflammation-induced colon cancer. Hence, APN may play an important role in colorectal cancer prevention by modulating genes involved in chronic inflammation and tumorigenesis.

Keywords: Adiponectin, Inflammation, Colon, Cancer

3.2 Introduction

Patients with inflammatory bowel disease, such as Crohn's and ulcerative colitis (UC), are at increased risk for developing colorectal cancer (Guthrie et al., 2002; Itzkowitz & Yio, 2004). UC patients, in particular, have ten to forty fold increased risk of developing cancer, compared with the general population (Munkholm, 2003; Whelan, 1991). The pathogenesis of colitis-associated colorectal cancer is thought to be related to an increased rate of epithelial cell proliferation associated with the repetitive cycles of inflammation, damage and regeneration (Eaden, Abrams, & Mayberry, 2001; Seril, et al., 2003). In addition, obesity, an established risk factor for colorectal cancer, is characterized by the accumulation of excessive adipose tissue, which is the source of a variety of biologically active substances, collectively referred to as adipokines (Berg, Combs, & Scherer, 2002; Giovannucci et al., 1995). Adiponectin (APN), an adipokine secreted by the adipose tissue, has been found at low levels in obese subjects (Wei, et al., 2005; Weiss et al., 2003). Obesity and APN have been linked to colon cancer by various studies (Bianchini, Kaaks, & Vainio, 2002; Birmingham, Busik, Hansen-Smith, & Fenton, 2009; Calle & Kaaks, 2004; Gunter & Leitzmann, 2006; Larsson & Wolk, 2007). Furthermore; obesity is associated with a heightened inflammatory response in Crohn's disease (CD) patients who have typical alterations of mesenteric fat deposits (Blain et al., 2002). Adiponectin exerts its activity through its receptors. Two receptors, AdipoR1 and AdipoR2, had been identified for APN and were found to mediate glucose and fatty acid metabolism by Adenosine mono-phosphate kinase (AMPK) activation, although no mechanism has been devised for its activation (A. Y. Kim, et al., 2010; Yamauchi et al., 2003; Yamauchi et al.,

2002; Yamauchi et al., 2007). AMPK is a serine threonine kinase, which is activated by phosphorylation, in the presence of cellular stress (Carling, 2004; Shaw et al., 2004). AMPK has anti-inflammatory effects and has been considered as a potential therapeutic target for cancer (Grossmann, Nkhata, Mizuno, Ray, & Cleary, 2008; Hwang, Ha, & Park, 2005; Masferrer et al., 2000; Ouchi et al., 2004). APN increases the rate of phosphorylation of AMPK and suppresses cell growth by inhibiting the mammalian target of rapamycin (mTOR) (Ouchi, et al., 2004). AMPK activity also inhibits the activity of Cyclooxygenase (Cox)-2, an enzyme that is upregulated in the presence of various stimuli like inflammation, tumorigenesis, metastasis, and growth factors (Grossmann, et al., 2008; Masferrer, et al., 2000). More importantly, APN has been linked to reduce expression of Cox-2 in APNKO mice treated with azoxymethane (Hwang, et al., 2005).

Signal transducer and activator of transcription (STAT)-3 is overexpressed in many cancers and is a potent indicator of inflammation (Bowman, Garcia, Turkson, & Jove, 2000). It plays a critical role in tumor progression and metastasis through transcriptional activation of anti-apoptotic genes like Bcl-x_L, Mcl-1 and survivin, cell-cycle regulators (e.g. cyclin D1 and c-Myc) and inducers of angiogenesis (e.g. vascular endothelial growth factor) (Darnell, 2005; Miyazaki, Bub, Uzuki, & Iwamoto, 2005).

In this paper, we have used dextran sodium sulphate (DSS), a potent inducer of inflammation and promoter of colorectal carcinogenesis. It was administered in mice for three cycles to induce chronic inflammation, while dimethylhydrazine (DMH) was injected intraperitoneally to induce cancer. APN knockout (KO) and the C57Bl/6 wild type (WT)

mice were given different treatments to elucidate the role of APN deficiency in chronic inflammation-induced colon cancer (CICC).

We hypothesized that APNKO mice are more susceptible to CICC as compared to their WT counterpart, which could be deduced by greater weight loss, bloody stools, diarrhea, larger number and size of the tumors. It is also evident by the up-regulation of pro-cancerous and downregulation of anti-cancerous and inflammatory genes.

3.3 Methods

Animals and experimental groups: Six to eight week old male APNKO (n=24) and male C57BL/6 (WT, n=24) were housed in conventional animal room and treated in the animal facility at the University of South Carolina. All APNKO mice were homozygous for APN deficiency $^{(-/-)}$. The mice were on a 12:12 h light–dark cycle in a low stress environment (22 °C, 50% humidity and low noise) and had access to food (Purina Chow) and water *ad libitum*. All animal care followed institutional guidelines under a protocol approved by the Institutional Animal Care and Use Committee at the University of South Carolina. APNKO and WT mice were randomly assigned to 4 different groups of equal number (n=6 mice per group): 1) DMH+DSS; 2) DMH; 3) DSS and 4) Control or no treatment. The body weight of both APNKO and WT mice showed no significant difference at the beginning of the study.

Induction of chronic inflammation and cancer: Chronic inflammation was induced in the WT and APNKO mice assigned to the DSS treatment group. These mice received 2% dextran sodium sulfate (DSS) (MP Biochemicals, MW: 36,000–50,000) dissolved in their drinking water for five days, followed by five days of regular drinking water, this represented single cycle and DSS was administrated for three cycles on days 4, 27 and 50. To establish chronic inflammation induced colon cancer, another group of mice received 3 cycles of DSS and a single injection of DMH intraperitoneally (i.p) (SIGMA ALDRICH) (20 mg/kg body weight) administered at the beginning of the DSS treatment. Cancer was induced in the WT and APNKO mice assigned to DMH treatment group by administering weekly dose of DMH i.p. for twelve weeks and the mice were sacrificed on day 153.

Monitoring animal health: Mice were observed daily for clinical signs of disease attributed by weight loss, fecal hemoccult and diarrhea during all treatments and till day 153. Ranking for the weight loss was based on the following scale: 0 = 0–5% weight loss; 1 = 6–10% weight loss; 2 = 11–15% weight loss; 3 = 16–20% weight loss; and 4 = >20% weight loss. The appearance of diarrhea was scored as: 0 = well-formed pellets, 2 = pasty and semi-formed stools that do not adhere to the anus, 4 = liquid stools that adhere to the anus. Appearance of blood in the stools was assessed using a hemoccult kit (BECKMAN COULTER) and scored as: 0 = no blood, 2 = positive hemoccult, 4 = gross bleeding. The clinical score was then determined by totaling the weight loss, hemoccult, and diarrhea scores with the highest score being twelve.

Tissue collection and tumor quantification: The mice were euthanized by cervical dislocation. The colon was removed and flushed with PBS containing 5000 IU/mL and 5000 IU/mL penicillin and streptomycin (CELLGRO) respectively. Two 2 mm^2 sections of the descending colon were dissected and stored at −80 °C for Western blot analysis and at 37 °C, 5% $CO_2$with overnight incubation for tissue culture. The remaining colon was fixed in 10% formalin (AZER SCIENTIFIC) for a day. It was then stained with 0.2% methylene blue (FISHER SCIENTIFIC) to count tumors and measure tumor area followed by its swiss roll and sectioning it for immunohistochemistry and Hematoxylin and Eosin (H&E) staining. Tumor quantification was done in blinded condition by two individuals.

Colonic cytokines and serum APN measurement: The secreted concentrations (pg/mg of protein) of IL-6, IL-10, IL-1β and TNF-α in the tissue culture were determined by Enzyme Linked Immunosorbent Assay (ELISA) using BD OptEIA kit (BD BIOSCIENCES). Serum APN was determined in all the treatment groups at the beginning and at the end of the study. This was achieved by diluting the serum samples to 1:2000 and performing ELISA using DuoSet mouse/Acrp30 kit (R&D SYSTEMS).

Protein determination and western blot: Tissues frozen at −80 °C were thawed and homogenized in RIPA buffer (SIGMA) containing 1:1000 dilution of protease inhibitor solution (SIGMA). Concentration of the total protein in the solution of homogenized tissue was calculated by Bradford protein assay. Protein homogenate from each group was loaded and electrophoresed on 10% SDS-PAGE gels and transferred to a nitrocellulose membrane at constant voltage of 200 mA for 150 min at 4 °C. The membrane was then blocked with

5% non-fat dry milk (BIO-RAD) in DPBS (cellgro)+0.1% Tween 20 (BIO-RAD) for one hour at room temperature followed by overnight incubation at 4 °C with STAT3 and pSTAT3 (1:000) (CELL SIGNALING TECHNOLOGY), AMPK and pAMPK (1:1000) (SANTA CRUZ BIOTECHNOLOGY) and GAPDH (1:3000) (R&D SYSTEM) diluted in DPBS+0.1% Tween 20. Membrane was subsequently washed 5 times for 10 min with DPBS+0.1% Tween 20 with consequent incubation with anti-rabbit or anti goat secondary antibody conjugated with horseradish peroxidase enzyme (1:3000) (SANTA CRUZ BIOTECHNOLOGY) for 1 h. The membrane was washed and incubated for 5 min in Amersham ECL Plus Western blot detection system (GE HEALTHCARE) with subsequent detection on high performance chemiluminescence film (Amersham Hyperfilm ECL, GE HEALTHCARE). GAPDH was used as a loading control to normalize the protein expression by densitometry using Image J software (NCBI). Western blot for each protein was done thrice by using all samples from the same treatment group to determine statistical significance.

Immunohistochemical staining: Serial tumor and non tumor sections of mouse colon tissues were incubated with antibodies against cyclooxygenase-2 (Cox-2; rabbit polyclonal; diluted 1:5000; CAYMAN CHEMICAL). To ensure even staining and reproducible results, sections were incubated by slow rocking overnight in primary antibodies (4 °C) using the Antibody Amplifier (ProHisto, LLC). Following incubation with primary antibody, sections were processed using EnVision+System-HRP kit (DAKO CYTOMATION). The chromogen was 3,3′-diaminobenzidine and sections were

counterstained with 0.5% methyl green. The positive control tissue was colon cancer sections which were highly positive for iNOS, Cox-2, TNF-α, p53, and p53-phospho-Ser[15]. Stained tissues were examined for intensity of staining using a method similar to that previously described by Nishihara et al., 2008. Briefly, intensity of staining in colon sections was evaluated independently by two blinded investigators. For each tissue section, the summation of the intensity of staining and the percentage of the positively stained cells was analyzed and quantified on a scale of 4, where 0 represents no staining, 2 — 50–75% of moderately stained cells, and 4 indicates more than 75% of darkly stained cells. All the images were taken in 20X magnification with Nikon e600 microscope. The scale bar represents 120 µm.

Hematoxylin and Eosin staining and histological scoring: To determine the pathological state of the colon, a standard protocol for H&E staining was used. Quantification of severity of disease including inflammation and immune cell infiltration was done on the scale of 4 for both the parameters, where 0 = no infiltration or no inflammation; 2 = moderate infiltration or inflammation; and 4 = severe inflammation with distorted crypts or infiltration and formation of lymphatic follicles. All the images were taken in 20× magnification with Nikon e600 microscope. The scale bar represents 120 µm.

Aberrant crypt foci (ACF): The H&E stained slides for DSS treated groups for APNKO and WT were scanned by two investigators in the blinded conditions for aberrant crypt foci. The ratio of the number of ACF to normal crypts was calculated in the 2 mm^2 area

and was plotted on a graph. All the images were taken in 40× magnification with Nikon e600 microscope. The scale bar represents 60 µm.

Statistical analysis: Two-way analysis of variance (ANOVA), Two-way repeated measure ANOVA and One-way ANOVA was used to analyze the data with Tukey post hoc-analyses. A p value<0.05 was considered statistically significant. All the statistical analyses were done by using SigmaStat 3.5 (SPSS, Chicago, IL).

3.4 Results

Clinical manifestation of CICC in APNKO and WT mice

To study the role of APN deficiency in CICC, WT and APNKO mice were given three different treatments and were observed for weight loss, diarrhea and hemoccult for 153 days and during this time clinical score was calculated. After the first DSS cycle in DSS and DSS+DMH group, WT mice lost their protection from DSS in comparison to APNKO mice and showed a significantly higher clinical score on day 18 in DSS group (Fig. 1B and C). However, no significance was observed in DSS+DMH group. After the second DSS cycle, APNKO mice manifested significantly higher clinical score on days 32, 34 and 36 when treated with DSS alone, but in DSS+DMH treatment group, it was observed on day 29 (Fig. 1B and C). Following the third DSS cycle, there was a complete loss of protection from DSS in the DSS and DSS+DMH group resulting in a significantly

higher clinical score in APNKO mice as compared to WT mice (Fig. 1B and C). Mice in DSS+DMH group didn't recover from the treatment and the clinical score continued to remain significantly higher in APNKO mice till the date of sacrifice (Fig. 1C). DSS treated mice recovered after every DSS cycle but after the third cycle, APNKO mice showed a comparatively higher clinical score than WT (data not shown). In DMH treatment group, significantly higher clinical score was observed in APNKO mice when compared to WT mice on days 77, 105 and 128, after which the score continued to remain higher till the date of sacrifice (Fig. 1A).

Tumor development in APNKO and WT mice

Immediately following the sacrifice, mice colon was fixed and stained in methylene blue for tumor quantification (Fig. 2A). APNKO mice had a significantly greater tumor number than WT mice in all the treatment groups (Fig. 2A and B). The degree of significance was higher in DMH group, but the number of tumors was higher in DSS+DMH group as compared to others. In DSS+DMH group, APNKO mice showed a significantly larger tumor area as compared to the WT group (Fig. 2C). Most of the tumors were observed in the descending and the rectal part of the colon.

Colon morphology

To study the change in the colon morphology in CICC, H&E staining for all the treatment groups was done for both WT and APNKO mice and quantified on a scale of one

to four. It was observed that the APNKO mice treated with DSS+DMH showed a complete loss of structural integrity of the colon epithelium. Infiltration of the immune cells was also observed in addition to crypt destruction. Tumor growth was more prominent and the number of tumors was observed to be greater in APNKO mice than WT in DSS+DMH group (Fig. 3A). APNKO mice treated with DSS+DMH had significantly severe immune cell infiltration, inflammation and distorted crypts as compared to WT mice (Fig. 3B). Significance in the severity of inflammation and infiltration was also observed in APNKO mice treated with DMH (H&E not shown). DSS treated group showed no significant difference between the APNKO and WT mice (Fig. 3B). DSS treated group however showed a significantly higher ACF in the APNKO mice as compared to WT mice (Fig. 3C and D). Other treatment groups were observed for ACF, but neither showed ACF as they have developed tumors or the observed difference was not significant between the APNKO and WT mice.

Systemic APN in WT mice and secreted cytokine profiling for all the treatment groups

To determine the effect of different treatments on the systemic APN levels, sera were obtained from the WT mice at the beginning of the study or pre-treatment and at the time of sacrifice. It was observed that the serum APN concentration in DSS+DMH treated group was significantly less when compared to the WT mice treated with DSS or DMH alone and with the control group (Fig. 4E). DMH treated mice showed a significantly lower concentration of serum APN than the DSS alone and control group. Significant decrease in the serum APN level was observed in the DSS+DMH and DMH alone treated WT mice

on days 153 and 0 (Fig. 4E). However no significant difference was found in the mice treated with DSS and the control group (Fig. 4E).

The tissue culture media was then used to perform secreted cytokine profiling and the concentration of the secreted IL-6, IL-10, TNF-α and IL-1β was calculated in all the treatment groups by using ELISA. APNKO mice showed a significantly higher colonic IL-6 and TNF-α levels in DSS and DSS+DMH groups when compared to the WT mice (Fig. 4A and D). IL-1β, another pro-inflammatory cytokine was found to be secreted in significantly higher concentrations in APNKO mice in DMH and DSS+DMH group (Fig. 4C). IL-10, grouped as an anti-inflammatory cytokine was quantified and it was found that in all the treatment groups, was a significant decrease in APNKO mice with greater significance in the DSS+DMH group as compared to WT mice. IL-10 level in APNKO mice of DSS+DMH group was comparable to the baseline untreated control group (Fig. 4B).

Colonic STAT3, AMPK, and Cox-2 expression

We investigated the effect of APN deficiency on various pathways involved in inflammation and colon cancer in our different treatment groups. We observed significantly higher expression levels of pSTAT3^{Ser727} and Cox-2 in APNKO mice treated with DSS+DMH and DMH in comparison to WT mice. However, no significant difference was observed in the expression level of APNKO and WT mice administered with DSS alone (Fig. 5A, B and D). No to minimum expression of pSTAT3^{Ser727} was detected in control group (Fig. 5A and B). However, low expression of Cox-2 was observed in

APNKO mice in control group while there was no expression in WT mice (Fig. 5A and D). p-AMPK-α ½$^{Thr\ 172}$ was downregulated and significantly decreased expression in APNKO mice treated with DSS+DMH and DSS alone in comparison to the WT mice. Comparatively, higher expression of p-AMPK-α ½$^{Thr\ 172}$ was observed in control group (Fig. 5A and C). GAPDH was used as a loading control and was used to normalize all the protein density measurements (Fig. 5A). Ratio of the phosphorylated protein to full protein was represented on the graph.

Cox-2 localization

After proteomic study by Western blot, localization of Cox-2 was determined, by immunohistochemistry for Cox-2 antigen in the tumor and the non tumor area of the descending colon section of both APNKO and WT mice. This study revealed significantly higher expression of Cox-2 in the tumor area than the non tumor area of the mice treated with DSS+DMH, irrespective of mice genotype (Fig. 6A, B and C). APNKO mice also showed significantly higher expression of Cox-2 when compared with WT mice treated with DSS+DMH (Fig. 6A, B and C). Significant difference was also found in APNKO mice of the tumor and the non tumor group and most importantly between the APNKO and the WT mice treated with DSS+DMH in the tumor group (Fig. 6A, B and C). However, the Cox-2 expression level was insignificant between the WT and APNKO mice treated with DSS+DMH in the non tumor sections and other treatment group including DSS alone and DMH alone group with no expression in untreated groups (Fig. 6A, B and C).

3.5 Discussion

Protective role of APN in obesity, cancer and other disease models has been established but, in this paper, we have tried to delineate its function in the CICC, which is a common condition in patients suffering from IBD and have been the second leading cause of cancer death in the United States (R. Siegel, et al., 2014). This study was primarily designed to deduce the effect of APN deficiency on the physical and molecular attributes of CICC. Our results showed a significantly severe clinical manifestation in the APNKO mice treated with DSS+DMH after the third DSS cycle. It continued to remain severe till the date of sacrifice. However there was no significant difference observed after the first and second DSS cycles. This observation is in accordance with common diseased state observed during colon cancer and could be explained by the loss of protection in the colonic epithelium of APNKO mice treated with DSS and DMH in chronic conditions. Absence of APN made the mice more vulnerable to DSS induced colitis and DMH induced colon cancer. Our group has shown that in acute phase in WT mice, this effect was not prominent as APN binds to growth factors like HB-EGF, bFGF that prevents the renewal of the colonic epithelium and hence there was no significant difference between the clinical score of APNKO and WT mice treated with DSS+DMH (Fayad, et al., 2007). This paper adds another chapter in APN research on the much-debated topic of APN as an anti-inflammatory or pro-inflammatory adipokine. Our results show a peculiar behavior of APN deficiency that has an anti-inflammatory effect in acute phase and a pro-inflammatory entity in chronic condition and colon cancer. Nishihara et al. (Nishihara et al., 2008) showed significant weight loss in the APNKO mice treated with AOM than WT mice;

however we followed a more comprehensive approach and combined weight loss with diarrhea and hemoccult.

DSS+DMH treated group was found to show the highest number of tumors and tumor areas. A significant difference was found between the WT and APNKO mice for both area and number of tumors. This observation could be explained by the results of Brakenhielm et al. (Brakenhielm et al., 2004), where they proved APN to induce anti-angiogenesis and to perform anti-tumor activity involving caspase- mediated endothelial cell apoptosis. DSS and DMH alone groups also showed a significant difference in the tumor number between the WT and APNKO. Most of the tumors observed were in the descending and the rectal portion of the colon with greater tumor area in the descending colon. Spleen was also found to be enlarged and more number of tumors was observed in the APNKO mice as compared to WT (data not shown). However, no metastasis was found in the lungs and liver. These data are in agreement with our previous observations and provide an insight about the role of APN in tumor development with absence of APN being a risk factor for chronic colonic inflammation and colitis. It also follows the same pattern as counted by Nishihara et al. (Nishihara, et al., 2008).

Ferroni et al. (Ferroni et al., 2007) had regarded lower serum APN as an adjunctive prognosis for the risk of colorectal cancer. Likewise, we found significantly decreased level of serum APN in the DSS+DMH treated WT mice as compared to control and along the length of the experiment (days 0 and 153). This indicates an inverse relation between the APN and CICC and could be attributed to greater chronic inflammation and cancer growth

(Ishikawa et al., 2005). A study conducted by Karmiris et al. showed significantly elevated APN levels in UC patients (Karmiris et al., 2006). On the contrary, we observed no significant difference in the APN level of the WT mice treated with DSS and control and also during the length of the experiment. This disparity could be due to that most of the UC patients received 5-aminosalicylic acid, which has been shown to increase PPAR-γ expression, which in turn increases APN production (Westerink & Visseren, 2011). In addition, the DSS model that we used is not an ideal model for UC. This protective role of APN was further strengthen by our histological evidences which indicates significantly greater formation of ACF in APNKO mice treated with DSS as compared to WT mice, which has been debated by several pathologist as a diagnostic tool for colon cancer. We confirmed the results obtained by Fujisawa et al. (Fujisawa et al., 2008) indicating significantly higher ACF and aberrant crypt in APNKO under high fat diet condition. However, we obtained the same results under normal diet with DSS treatment. Further exploration was done by quantification of inflammation and immune cell infiltration in DSS+DMH group, which was found to be significantly higher in the APNKO mice. Tumors could be histologically observed in the APNKO mice treated with DSS+DMH. Higher infiltration of the immune cells and greater inflammation, epithelial cell disruption and formation of the primary and secondary lymphatic follicles were common sightings, which is a clear indication of greater colon epithelium insults in APNKO mice when compared to WT.

Adipose tissues have been linked to the secretion of several proinflammatory cytokines and APN has been proved to play an important role in regulating their secretion

by downregulating the autocrine release of adipose tissue derived pro-inflammatory cytokines like IL-6, IL-8 from macrophages (Bruun et al., 2003; Dietze-Schroeder, Sell, Uhlig, Koenen, & Eckel, 2005). Our results indicate similar finding with significantly higher secretions of pro-inflammatory cytokines like IL-6, IL-1β and TNF-α and reduced secretion of anti-inflammatory cytokines like IL-10 in the descending colon section of the APNKO mice treated with DSS+DMH as compared to WT mice. IL-6 and TNF-α was also found to show significantly higher level in the APNKO mice treated with DSS while IL-1β was found to show significantly higher level in APNKO mice treated with DMH while IL-10, an anti-inflammatory cytokine, level was significantly downregulated in the same group. Higher secretion of TNF-α was observed in the DSS-treated than DSS+DMH-treated APNKO mice, but the difference was not significant. This could be explained by the multifunctional roles of this cytokine in apoptosis, cell survival and inflammation (van Horssen, Ten Hagen, & Eggermont, 2006). Although some investigators argue that the higher TNF-α levels are associated with tumorigenesis but at the same time, TNF-α is a well-known pyrogen that induce apoptotic cell death and acts synergistically with cytostatic drugs in cancer treatments (Kapas et al., 1992; van Horssen, et al., 2006). Lower levels of TNF-α in DSS+DMH treated APNKO mice directly correlate with greater tumor number and size. Higher TNF-α production in DSS treated APNKO mice could be primarily due to the greater secretion of TNF-α by macrophages and lymphocytes due to chronic inflammation (Carswell et al., 1975; Trayhurn & Wood, 2004), delayed recovery from the third DSS cycle and the involvement of the gut microflora that may exacerbate the inflammatory condition (Gordon, Hooper, McNevin, Wong, & Bry, 1997). However, these mechanisms are remained to be investigated. These data provide a link between the

absence of APN and higher production of pro-inflammatory cytokines and decrease production of anti-inflammatory cytokines under the conditions including cancer, inflammation and CICC. This might be regarded as the first direct influence of the APN deficiency on CICC.

To further investigate the role of the APN deficiency in CICC, we searched deeper in to the protein expression especially targeting the key pathways involved in cancer and inflammation. Our main focus lies on the JAK/STAT signaling pathways, followed by phosphorylation of AMPK, which is directly correlated with the major protein synthesis, mTOR pathway. Phosphorylation of the STAT3 was found to be up-regulated in oppose of AMPK phosphorylation in the APNKO mice treated with DSS+DMH. This indicates higher inflammation and reduction in the energy state milieu and might be the reason for slower recovery. This up-regulation of JAK/STAT3 signaling pathway could be mediated by IL-6 and regulated by SOCS3 signaling (Y. Li et al., 2010; Shu et al., 2009). However, partial hepatectomy or liver regeneration studies showed reduced expression of phosphorylated STAT3 with the concomitant increase in SOCS3 mRNA in APN null mice (Shu, et al., 2009). This variability could be accounted to the variable SOCS3 mediated activation pattern of STAT3, during different time points along the length of the study. Another explanation could be the variable roles of APN that may play in different tissues and disease models. Higher STAT3 expression was observed in the control group as compared to DSS treated groups, which could be attributed to the constitutive expression of STAT3. However, only the activated or the phosophorylation of the protein could be affected by the diseased state. This was followed by another investigation of the Cox-2

expression, which plays multiple roles in oncogenesis, metastasis and inflammation related to cancer. Cox-2 was found to be over-expressed in the APNKO mice treated with DSS+DMH and DMH alone. However in heart ischemia model, APN was found to increase the expression of Cox-2 (Shibata et al., 2005). This provides another evidence of the multifaceted nature of adiponectin. By the means of Cox-2 expression studies, we confirmed the results of Nishihara et al. (Nishihara, et al., 2008), but in our CICC model we went a step further to investigate localized expression of Cox-2 in tumor and non-tumor area by immunohistochemistry. Cox-2 was found to be significantly over-expressed in tumor area of the colon as compared to non-tumor area, which could be due to the combined effect of the overexpression of cancer epithelial cells in addition to the localized secretion by inflammatory mononuclear cells, fibroblast and vascular endothelial cells. However the majority of the intensity and the extent of Cox-2 are due to the overexpression by cancer cells (Mikkelsen, Rumessen, & Qvortrup, 1991; Sano et al., 1995). In APNKO mice treated with DSS+DMH, Cox-2 expression was found to be the highest and significantly greater than WT mice in the tumor area. This approach was also instrumental in studying the histopathology of the colon, which was found to show a complete disruption of the tissue architecture in the tumor area along with the formation of the primary lymphoid follicle.

Although, our study established a link between the absence of APN and its effects on the molecular and physical attributes of CICC, with its absence linked with higher expression of pro-inflammatory and pro-cancerous markers, it did not illustrate the direct role of APN in CICC. To define the function of APN in our model system, our future work

will be to reconstitute APN in all the treatment groups and observe its role during the same timeline. It could also be suggested to further explore the role of APN in apoptotic pathways and establish the interplay of APN in other molecular and cellular pathways by the application of whole genome microarray. Further characterization of APN isoforms could also result in clinical applications.

Acknowledgements

The authors would like to acknowledge Alena P. Chumanevich, for her help in immunohistochemical analyses. We would also like to acknowledge Center of Biomedical Research Excellence (COBRE), NIH Center for Colon Cancer Research, USC for funding our study. The study sponsor has no personal and financial interest and involvement in any section of the manuscript.

3.6 Figure Legends

Figure 3.1. Clinical score of DSS and DMH treatments. (A–C) Clinical score for DMH, DSS and DSS+DMH was plotted against the different time point during the study. The arrows represent the days of DSS administration in DSS and DSS+DMH study groups. The score was calculated out of twelve points; four points for each weight loss, diarrhea and hemoccult. Two-way repeated measure analysis of variance (ANOVA) was applied to calculate the significant difference between the clinical score for APNKO and WT mice thought the length of the experiment. $^{**}p<0.05$, $^{\#}p<0.001$, $^{*}p<0.03$ (n=6).

Figure 3.2. Tumor development in APNKO and WT mice treated with DSS and DMH. (A) Colon of WT and APNKO mice treated with DSS+DMH and stained with 0.2% methylene blue. (B) Average number of tumors counted per mice per group for all the treatments in order of their severity. (C) Average tumor area in mm^2 counted for each mouse per group plotted in the order of their severity. One-way ANOVA was used to calculate significant difference between APNKO and WT mice given the same treatment for all the experimental groups.*$p<0.05$ and $^{\#}p<0.03$ (n=6).

Figure 3.3. Hematoxylin and Eosin staining and aberrant crypt foci. (A) H&E stained sections of the descending colon of KO and WT mice in DSS group with 20× magnification (scale bar=120μm). (B) Quantification of inflammation and immune cell infiltration in all the treatment groups on a scale of four. (C) H&E stained slides of the descending colon section of the APNKO and WT mice treated with DSS alone and observed and marked for Aberrant crypt foci with 40× magnification (scale bar = 60μm). (D) Quantification of the ACF by calculating the ratio of the aberrant crypts to the normal crypts. Degree of significance was calculated by One-way ANOVA between the KO and WT of the same treatment group. *$p<0.05$ and $^{\#}p<0.01$ (n=5).

Figure 3.4. Cytokine secretion from the colon of APNKO and WT mice. (A-D) Amount of IL-6, IL-10, Il-1 β and TNF- α secreted respectively from the colon of the APNKO and WT mice subjected to treatment of DSS, DMH and DSS + DMH and to the control group. (E) Serum adiponectin levels (μg/mL) in WT mice treated with DSS + DMH, DMH alone,

DSS alone and control group at days 0 and 153. Significant difference was observed in the serum adiponectin level of the WT mice treated with DSS + DMH and DMH alone, DSS alone and control group, and WT mice treated with DMH and DSS alone and control group. Significant difference was also observed within the DSS + DMH and DMH alone group at days 0 and 153. One way ANOVA was applied to calculate the significant difference between the secretion of cytokine from APNKO and WT mice belonging to the same group. *$p < 0.01$,**$p < 0.04$, ***$p < 0.02$, $^{\#}p < 0.05$ (n=6).

Figure 3.5. Protein expression of STAT3, pSTAT3, AMPK, pAMPK, COX-2 in APNKO and WT mice under different treatment conditions. A) Western blot representing the expression of STAT3, pSTAT3, AMPK, pAMPK, COX-2 and GAPDH. B‑D) Graphs showing the ratio of the relative density of the bands for pSTAT3/STAT3 (B), p-AMPK/AMPK (C) and COX-2 (D) being normalized by GAPDH, for control and three other treatments in the order of their severity in WT and APNKO mice. ANOVA was used to determine the significant difference between APNKO and its wild counter parts for all the treatments. *$p<0.03$, **$p<0.05$, $^{\#}p<0.02$ (n=5).

Figure 3.6. Cox-2 immunohistochemical staining and quantification. (A) Immunohistochemical staining for Cox-2 (brown) in the non-tumor area of the descending colon (2 mm^2) section of control, DSS, DMH and DSS + DMH treated groups in both WT and KO mice. (B) Immunohistochemical staining for Cox-2 (brown) in the tumor area of the descending colon (2 mm^2) section of DSS + DMH treated groups in both WT and KO

mice. (C) Quantification of the Cox-2 expression in the non-tumor descending colon 2 mm^2 section of the WT and KO mice treated with DSS, DMH, DSS + DMH and control group and DSS + DMH group in the tumor area. Two-way ANOVA was used for statistical significance. # versus ‡ ($p < 0.002$), † and * versus § and ** ($p < 0.002$), § versus **($p < 0.002$), *versus ** ($p < 0.002$) (n=5).

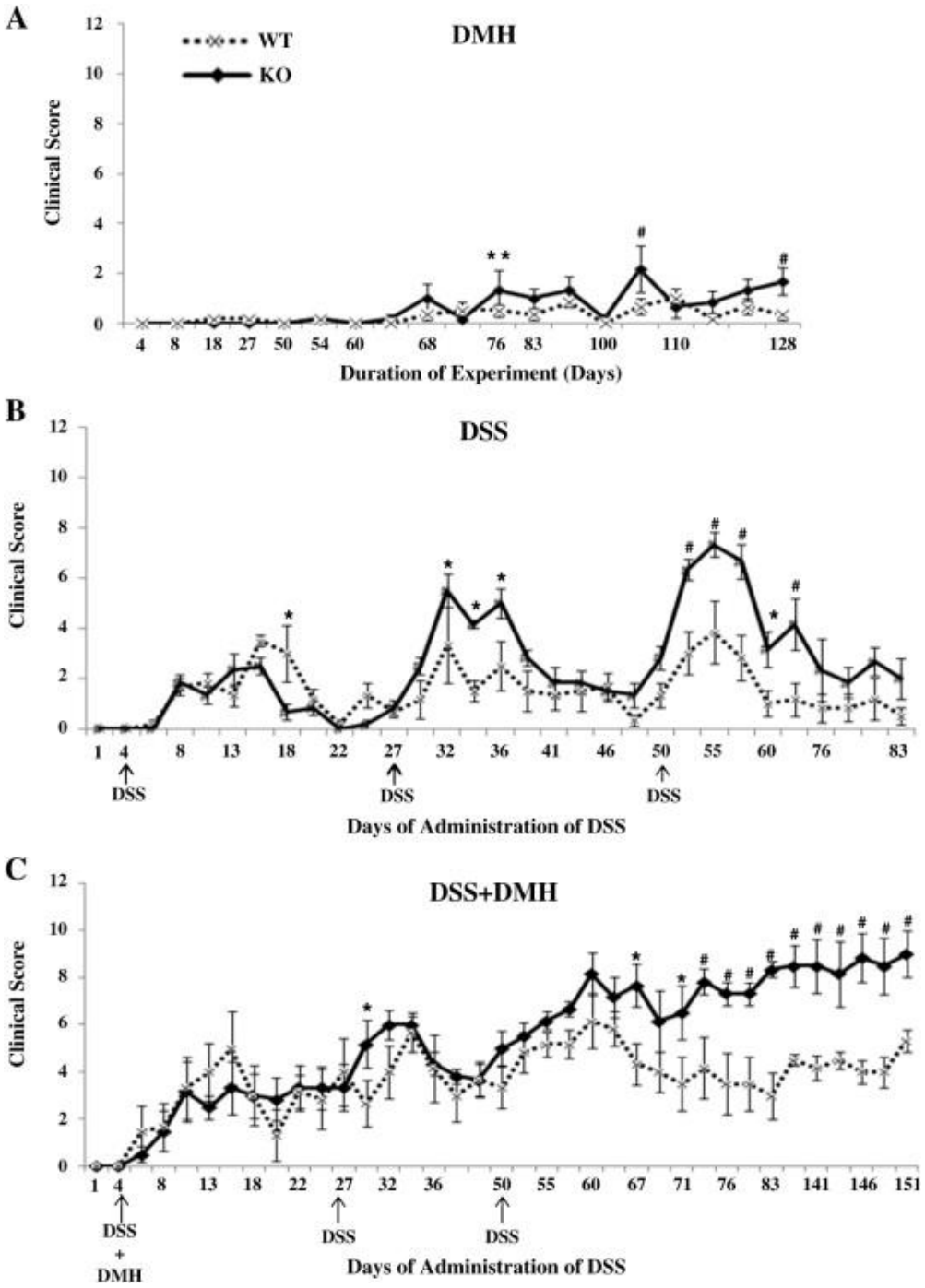

Figure 3.1. Clinical score of DSS and DMH treatments. (A–C) Clinical score for DMH, DSS and DSS+DMH was plotted against the different time point during the study. The arrows represent the days of DSS administration in DSS and DSS+DMH study groups. The score was calculated out of twelve points; four points for each weight loss, diarrhea and hemoccult. Two-way repeated measure analysis of variance (ANOVA) was applied to calculate the significant difference between the clinical score for APNKO and WT mice thought the length of the experiment given the same treatment. **$p<0.05$, $^{\#}p<0.001$, *$p<0.03$ (n=6).

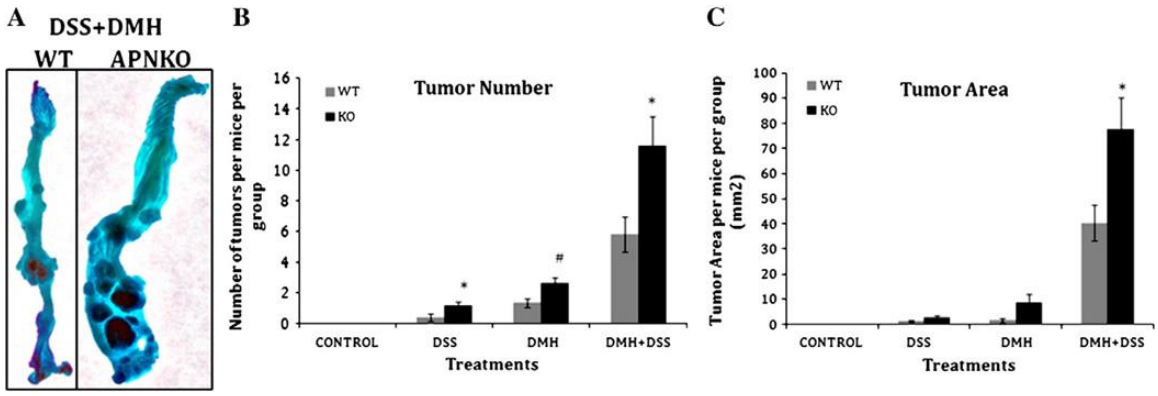

Figure 3.2. Tumor development in APNKO and WT mice treated with DSS and DMH. (A) Colon of WT and APNKO mice treated with DSS+DMH and stained with 0.2% methylene blue. (B) Average number of tumors counted per mice per group for all the treatments in order of their severity. (C) Average tumor area in mm^2 counted for each mouse per group plotted in the order of their severity. One-way ANOVA was used to calculate significant difference between APNKO and WT mice given the same treatment for all the experimental groups given the same treatment. *$p<0.05$ and $^{\#}$ $p<0.03$ (n=6).

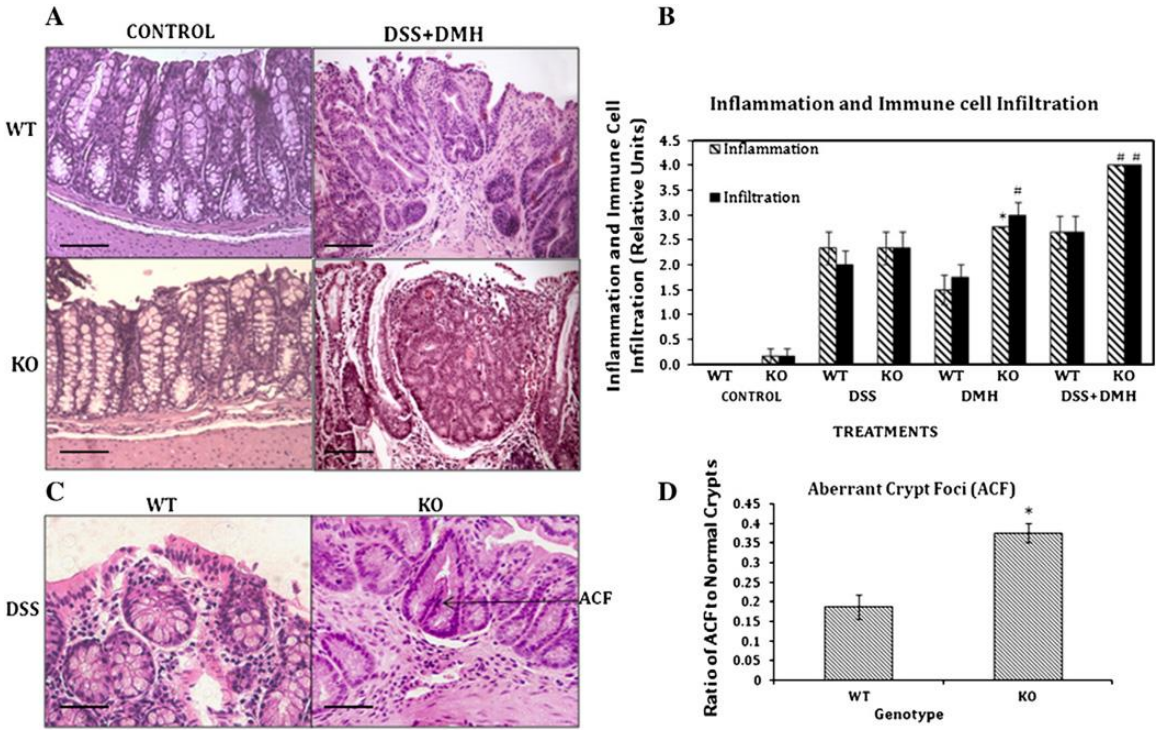

Figure 3.3. Hematoxylin and Eosin staining and aberrant crypt foci. (A) H&E stained sections of the descending colon of KO and WT mice in DSS group with 20× magnification (scale bar=120 µm). (B) Quantification of inflammation and immune cell infiltration in all the treatment groups on a scale of four. (C) H&E stained slides of the descending colon section of the APNKO and WT mice treated with DSS alone and observed and marked for Aberrant crypt foci with 40× magnification (scale bar=60 µm). (D) Quantification of the ACF by calculating the ratio of the aberrant crypts to the normal crypts. Degree of significance was calculated by One-way ANOVA between the KO and WT of the same treatment group given the same treatment. *$p<0.05$ and $^{\#}$ $p<0.01$ (n=5).

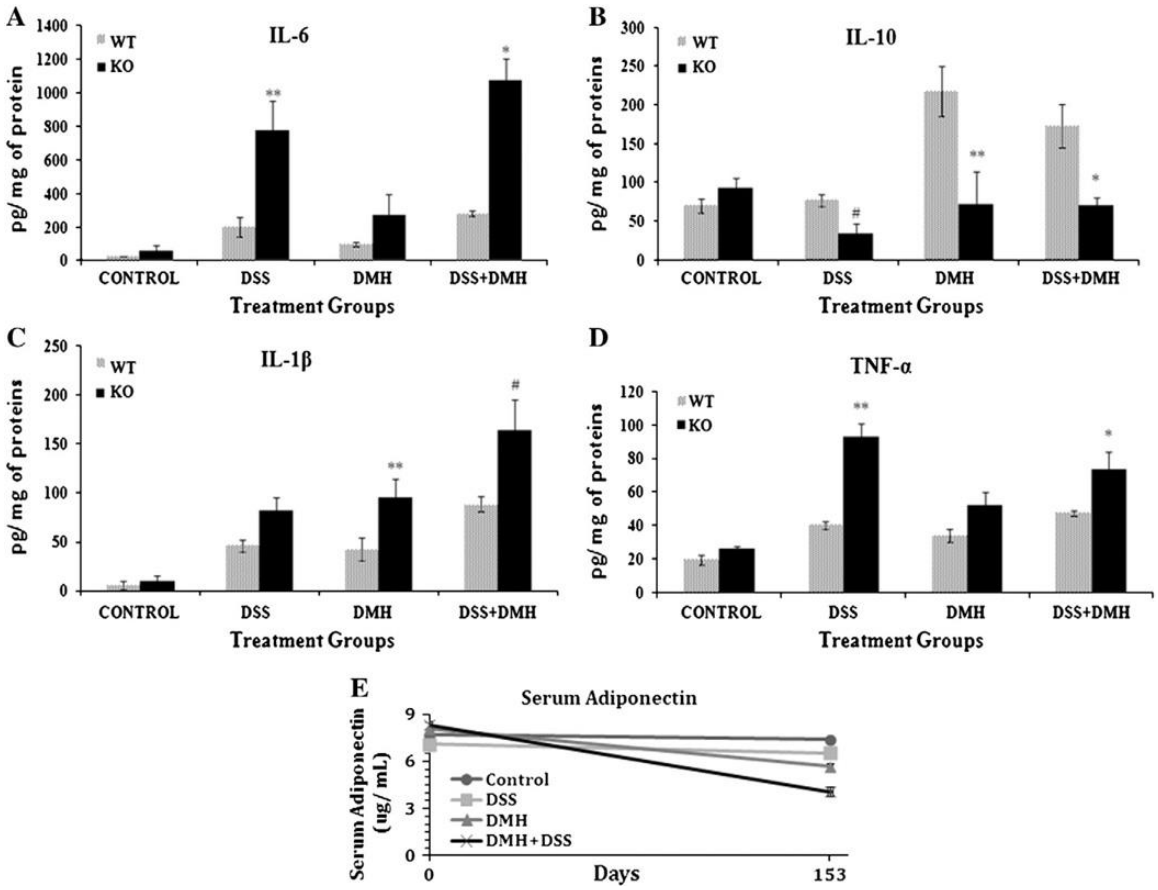

Figure 3.4. Cytokine secretion from the colon of APNKO and WT mice. (A-D) Amount of IL-6, IL-10, Il-1β and TNF-α secreted respectively from the colon of the APNKO and WT mice subjected to treatment of DSS, DMH and DSS+DMH and to the control group. (E) Serum adiponectin levels (µg/mL) in WT mice treated with DSS+DMH, DMH alone, DSS alone and control group at days 0 and 153. Significant difference was observed in the serum adiponectin level of the WT mice treated with DSS+DMH and DMH alone, DSS alone and control group, and WT mice treated with DMH and DSS alone and control group. Significant difference was also observed within the DSS+DMH and DMH alone group at days 0 and 153. One way ANOVA was applied to calculate the significant difference between the secretion of cytokine from APNKO and WT mice belonging to the same group given the same treatment. *$p<0.01$,**$p<0.04$, ***$p<0.02$, #$p<0.05$ (n=6).

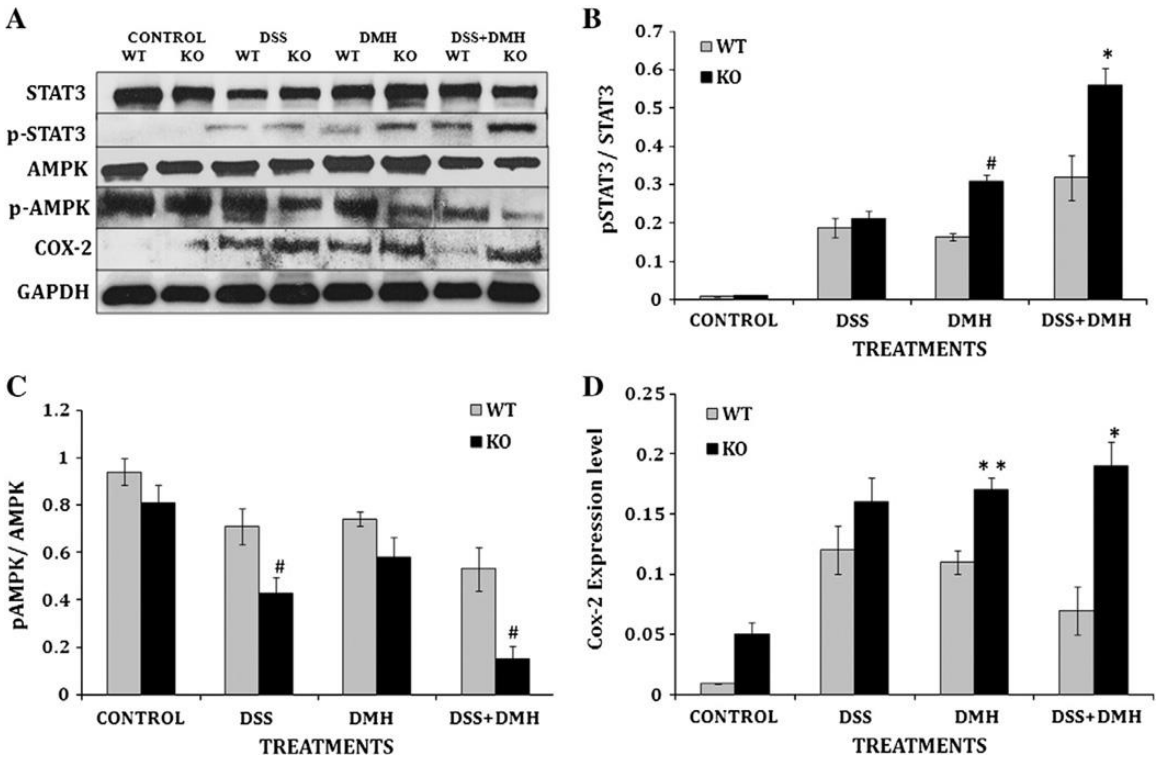

Figure 3.5. Protein expression of STAT3, pSTAT3, AMPK, pAMPK, COX-2 in APNKO and WT mice under different treatment conditions. A) Western blot representing the expression of STAT3, pSTAT3, AMPK, pAMPK, COX-2 and GAPDH. B–D) Graphs showing the ratio of the relative density of the bands for pSTAT3/STAT3 (B), p-AMPK/AMPK (C) and COX-2 (D) being normalized by GAPDH, for control and three other treatments in the order of their severity in WT and APNKO mice. ANOVA was used to determine the significant difference between APNKO and its wild counter parts given the same treatment. * $p<0.03$, ** $p<0.05$, # $p<0.02$ ($n=5$).

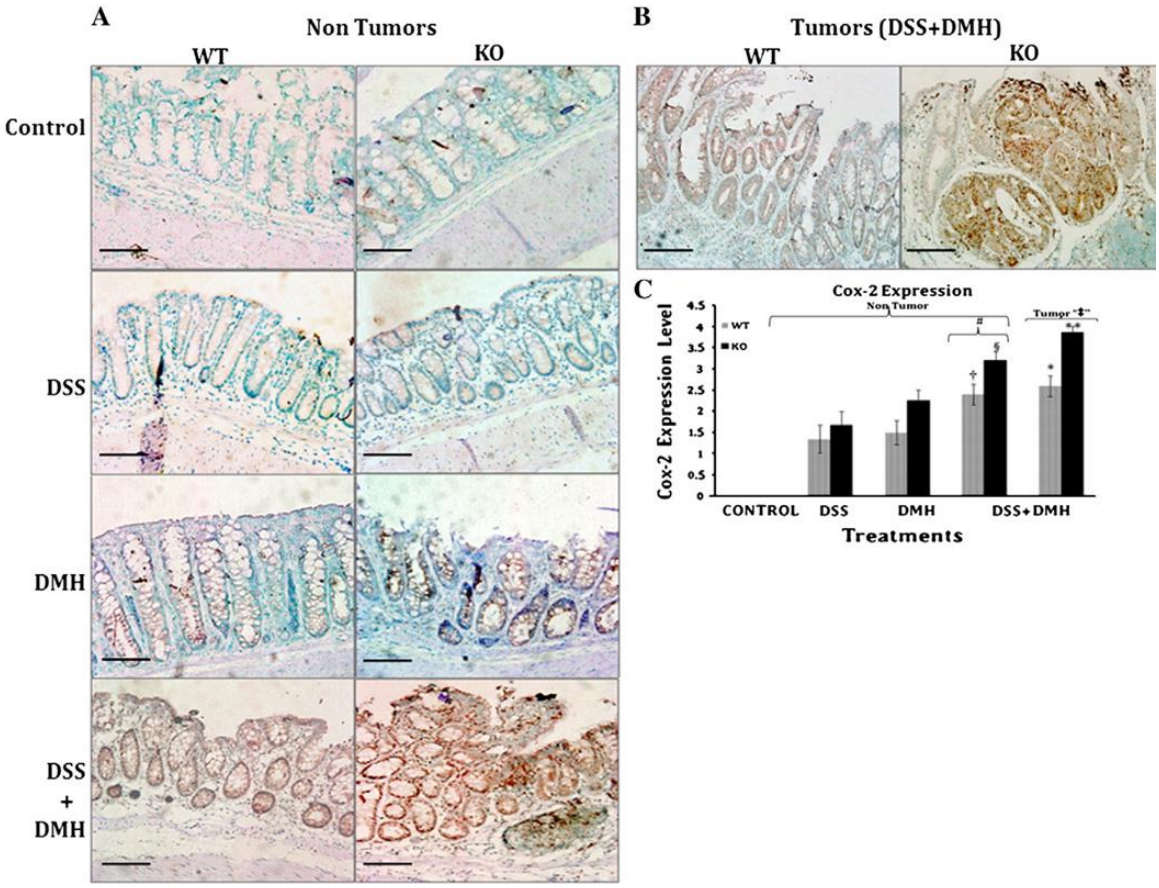

Figure 3.6. Cox-2 immunohistochemical staining and quantification. (A) Immunohistochemical staining for Cox-2 (brown) in the non-tumor area of the descending colon (2 mm^2) section of control, DSS, DMH and DSS+DMH treated groups in both WT and KO mice. (B) Immunohistochemical staining for Cox-2 (brown) in the tumor area of the descending colon (2 mm^2) section of DSS+DMH treated groups in both WT and KO mice. (C) Quantification of the Cox-2 expression in the non-tumor descending colon 2 mm^2 section of the WT and KO mice treated with DSS, DMH, DSS+DMH and control group and DSS+DMH group in the tumor area. Two-way ANOVA was used for statistical significance. # versus ‡ ($p<0.002$), † and * versus § and ** ($p<0.002$), § versus **($p<0.002$), * versus ** ($p<0.002$) (n=5).

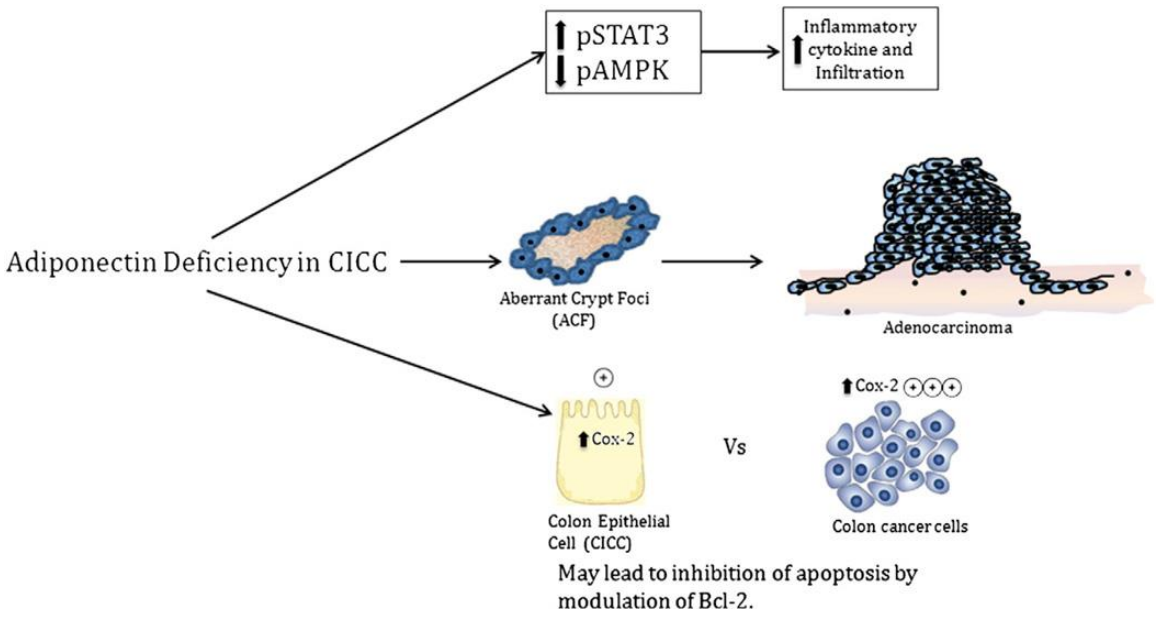

Figure 3.7. A hypothetical model showing the effect of APN deficiency in chronic inflammation induced colon cancer. In CICC, APN deficiency aggravates the inflammatory condition by increased expression of pro-inflammatory molecule like STAT3 and cytokines like IL-6, TNF-α and IL-1β and reduced production of anti-inflammatory molecules like pAMPK and cytokines like IL-10. It also results in higher ACF presence, which subsequently leads to adenocarcinoma. APN deficiency in CICC increased Cox-2 expression in the epithelial cells with the highest been found in the tumor area. This might be a potential mechanism of Cox-2, which inhibits apoptosis mediated by Bcl-2 that regulates the release of cytochrome c from mitochondria with further inhibition of caspases.

CHAPTER 4

MUCUS AND ADIPONECTIN DEFICIENCY: ROLE IN CHRONIC INFLAMMATION INDUCED COLON CANCER[2]

[2] Arpit Saxena, Manjeshwar Shrinath Baliga, Venkatesh Ponemone, Kamaljeet Kaur, Bianca Larsen, Emma Fletcher, Jennifer Greene and Raja Fayad. Accepted by Int J Colorectal Dis. 2013 Sep; 28(9): 1267–1279. Reprinted here with the permission of publisher.

4.1 Abstract

Purpose: This study aims to define the role of APN in preventing goblet cell apoptosis and in differentiation of epithelial cells to goblet cell lineage resulting in greater mucus production and hence greater protection from CICC. Methods: 6 to 8 weeks old male APNKO and C57BL/6 (WT) mice were randomly distributed to 3 treatment groups: DSS, DMH, DSS+DMH and control. Chronic inflammation was induced in DSS and DSS+DMH group by administrating 2 % DSS in drinking water for 5 days followed by 5 days of normal drinking water and this constitutes one DSS cycle. Three cycles of DSS were administered to induce chronic inflammation. Cancer was induced in both APNKO and WT mice in DMH and DSS+ DMH groups by intraperitoneal injections of DMH (20 mg/kg body weight) once for DSS+DMH group and once per week for 12 weeks for DMH group. On day 129, the colon tissue was dissected for mucus thickness measurements and for genomic studies. HT29-C1.16E and Ls174T cells were used for several genomic and siRNA studies. Results: APNKO mice have more tumors and tumor area in DSS+DMH group than WT mice. APN deficiency downregulated goblet to epithelial cell ratio and enhanced the colonic mucosal erosion with reduced mucus thickness. APN increases Muc2 production with no effect on Muc1 production. APN abated goblet cell apoptosis, while APN deficiency reduced epithelial to goblet cell differentiation. Conclusion: APN may be involved in reducing the severity of CICC by preventing goblet cell apoptosis and increasing epithelial to goblet cell differentiation.

Keywords: Adiponectin, Goblet cells, Colon cancer, mucus, inflammation

4.2 Introduction

Colorectal Cancer (CRC) is globally the third most commonly diagnosed cancer (Jemal et al., 2011). Several epidemiological studies have linked long standing inflammatory bowel disease (IBD) with 2 to 3 fold greater lifetime risk of developing colorectal cancer (Hartnett & Egan, 2012; Saxena et al., 2012). The development of chronic inflammation induced colon cancer (CICC) is thought to be multifaceted and the repetitive cycles of inflammation, damage, increase rate of epithelial cell proliferation and regeneration initiate and promote the process of CICC (Saxena, et al., 2012).

The intestinal homeostasis is a complex interplay of microbiota, intestinal epithelial cells (IECs) and the host immune system (Artis, 2008; Hooper & Macpherson, 2010; Kaser, Zeissig, & Blumberg, 2010a, 2010b). Mucus overlies epithelial cells of colon and acts as a physical barrier that prevents the invasion of colonic bacteria and thus inflammation (Kaser, et al., 2010b). The mucus-secreting goblet cells protect the epithelial layer and the depletion of these cells is a common characteristic of multiple models of murine intestinal inflammation (Hooper & Macpherson, 2010; Specian & Oliver, 1991), UC patients (Sheng, Xu, Tang, & Zhan, 2012), and colon cancer (Leow, et al., 2005). The goblet cells are derived from the multipotent stem cells and the Notch signaling pathway has been shown to play a major role in their differentiation (Q. Yang, et al., 2001). The basic helix-loop-helix (bHLH) transcription factor Math1 and a transcriptional repressor Hairy and Enhancer of split type 1 protein (Hes-1) are important downstream molecules in

the Notch signaling pathway and their interplay may determine the onset of goblet cell differentiation (Wong, 2004).

The viscoelastic, polymer-like properties of mucus are derived from the major gel-forming glycoprotein components called mucins (Deplancke & Gaskins, 2001; Lang, Hansson, & Samuelsson, 2007). Fifteen different mucin genes have so far been described of which Muc1, 2, 3, 12, 13, and 17 are found in the colon (Saeki et al., 2011). Muc2, the major colonic mucin (Tytgat et al., 1994; Van Klinken, Dekker, Buller, de Bolos, & Einerhand, 1997), creates a functional barrier between the host and the luminal contents and any alteration in this could act as a trigger for IBD (Johansson et al., 2010; Petersson et al., 2011), particularly in UC patients (Petersson, et al., 2011). Mucin has also been linked to colorectal cancer (Niv, Byrd, Ho, Dahiya, & Kim, 1992) and increased expression of Muc1 is associated with poor prognosis (Ahmed, 2003), while Muc2 is involved in the suppression of colorectal cancer (Sheng, et al., 2012; Van der Sluis et al., 2006; Velcich et al., 2002) and has a protective role in IBD (Artis, 2008; Hooper & Macpherson, 2010; Kaser, et al., 2010b).

Mounting evidence indicates a positive association between adiposity and colon cancer (Paz-Filho, Lim, Wong, & Licinio, 2011; Renehan, Tyson, Egger, Heller, & Zwahlen, 2008). Obesity is a chronic sub-inflammatory condition and adipocytokines, biologically active substances produced by the adipocytes, are crucial players in the process of CICC (Barb, et al., 2007; Saxena, et al., 2012). Obesity is also associated with a

heightened inflammatory response in people with CD (Blain, et al., 2002) and could result in a vicious cycle of localized inflammation that can expedite CICC.

Recent data suggest that the adipocytokine adiponectin (APN) has an important role in modulating the pathophysiology of the CICC. An inverse correlation has been established between APN plasma concentrations and Body Mass Index (BMI) (Arita et al., 1999), and with the risk of CICC (Wei, et al., 2005). The role of APN in carcinogenesis is not yet fully understood, but its anti-inflammatory, immune-modulatory and insulin-sensitizing effects are considered to be beneficial (van Kruijsdijk, van der Wall, & Visseren, 2009). Several clinical studies have shown lower APN levels being associated with colorectal carcinoma (Otake et al., 2005). APNKO mice have greater and larger colon lesions as compared to C57BL/6 WT mice in chronic inflammation induced colon cancer (CICC) model (Saxena, et al., 2012). APN modulates p53 and Bcl-2 gene expression (Mistry, Digby, Desai, & Randeva, 2008) and provides anti-carcinogenic effects, many of which are mediated through the AMP-activated Protein Kinase (AMPK) system via two receptors; the AdipoR1 and R2 (van Kruijsdijk, et al., 2009).

Recent studies from our laboratory have shown that APN deficiency contributes to CICC (Saxena, et al., 2012). In extension to our ongoing studies, this paper aims at understanding the role of APN in preventing the DSS, DMH and DSS+DMH induced mucus depletion. This study also aims at deciphering the role of APN in modulating Muc2 and its associated proteins. To achieve our goal, we used the human colonic goblet cell line HT29-Cl.16E (Augeron & Laboisse, 1984) as this clonal derivative of HT29 displays a

homogeneous and stable differentiated phenotype of mucus secreting cells. It is a validated model for determining the regulation of mucin secretion (Gaudier, Forestier, et al., 2004).We also used Ls174T cells, a well-established *in vitro* model to study mucus production (Wright, Ford-Hutchinson, Chadee, & Metters, 2000). In addition, the Muc gene expression profile of HT29-Cl.16E and Ls174T cells includes Muc1, Muc2 and Muc3, the major mucins expressed in the human colon (Augeron & Laboisse, 1984; Gaudier, Jarry, et al., 2004).

4.3 Materials and methods

Animals and experimental groups: Six- to eight-week-old male homozygous APNKO−/− and male C57BL/6 (WT) were housed in conventional animal room and treated in the animal facility at the University of South Carolina. The mice were on a 12:12 h light–dark cycle in a low stress environment (22 °C, 50 % humidity, and low noise) and had access to food (Purina Chow) and water *ad libitum*. All animal care followed institutional guidelines under a protocol approved by the Institutional Animal Care and Use Committee at the University of South Carolina. APNKO and WT mice were randomly assigned to four different groups of equal number (n=12 mice per group): (1) DMH+DSS; (2) DMH; (3) DSS, and (4) control or no treatment. The body weight of both APNKO and WT mice showed no significant difference at the beginning of the study.

Induction of chronic inflammation and cancer: Chronic inflammation was induced in mice assigned to the DSS treatment group. These mice received 2 % dextran sodium sulfate

(DSS) (MP BIOCHEMICALS, MW: 36,000–50,000) dissolved in their drinking water for 5 days, followed by 5 days of regular drinking water; this represented single cycle and DSS was administrated for three cycles on day 8, 23, and 38. To establish chronic inflammation-induced colon cancer, another group of mice received three cycles of DSS and a single injection of DMH intraperitoneally (i.p) (SIGMA ALDRICH) (20 mg/kg body weight) administered at the beginning of the DSS treatment. Cancer was induced in mice assigned to DMH treatment group by administering weekly dose of DMH i.p. for 12 and the mice were sacrificed on day 129.

Tissue collection and tumor quantification: Mice colon were harvested and sectioned (2 mm2) to confirm the mouse histopathology of the entire group (6 mice/group). The remainder of the colons was stored at −80 °C for gene and protein expression studies. The dissected tissues were stained with 0.5 % methylene blue (SIGMA ALDRICH) to count tumors and measured tumor area using a stereomicroscope followed by sectioning for Alcian blue staining. Tumor quantification was done in blinded condition by two individuals.

Mucus thickness: Mucus thickness was measured with micropipettes connected to a micromanipulator (LEITZ) with a digimatic indicator (IDC SERIES 543, Mitutoyo). The degraded luminal mucus layer was removed. Glass tubing (borosilicate tubing with 1.2 mm OD and 0.6 mm ID; Frederick Haer) was pulled with a pipette puller (pp-83; NARISHIGE SCIENTIFIC) to a tip diameter of 1–3 μm and to prevent mucus adhering to glass, the pipettes were siliconized by dipping the tip of the micropipette into a silicone solution followed by drying at 100 °C for 30 min. The luminal surface of the mucus gel was

visualized by placing graphite particles (activated charcoal, extra pure, Merck) on the gel, and the colonic epithelial cell surface was visible through the microscope. The micropipette was inserted into the mucus gel at an angle of ~30° (θ) to the surface. The distances traveled by the micropipette from the luminal surface of the mucus gel to the epithelial cell surface were measured with a digimatic indicator connected to the micromanipulator, and a mean value (A) was calculated. The mucus thickness (T) was calculated using the formula $T=A (\sin \theta)$. Mean of four to five different measurements was taken as one thickness value.

Alcian blue staining: Standard deparaffinization procedure was followed using xylene and gradation of ethanol. Alcian blue solution (1 %) of pH2.5 in 3 % acetic acid and nuclear fast red in aluminum sulfate was prepared. Tissues were stained with Alcian blue and counterstained with nuclear fast red solution. Goblet to epithelial cell ratio was counted per crypt with ten crypts per section and five sections per group.

Cell culture: HT29-Cl. 1 6E and Ls174T cells (ATCC) were seeded on porous nitrocellulose filters (MILLIPORE filters HAHY, porosity 0.45 μm; 2×106 cells per filter) to provide improved access to basolateral membrane of cells [37]. The cells were cultured in Dulbecco's modified Eagle's medium (DMEM) (GIBCO) supplemented with 10 % (v/v) heat inactivated fetal calf serum (FCS) (GIBCO). HT29-Cl.16E and Ls174T cells form at confluence homogeneous monolayer of differentiated goblet cells, secreting a mucus gel in the culture medium. HT29-C1.16E and Ls174T cells (106/well) were incubated at 37 °C and 5 % CO2 in the presence of different dosages of recombinant APN (0, 0.25, 0.5, 1.0,

1.5, 2.0 μg/mL) in one experiment and in other experiment APN (2 μg/mL), TNF-α (10 ng/mL), and APN+TNF-α (PROSPEC) for 24 h.

Muc1 and Muc2 measurement: Muc1 and Muc2 production was measured in HT29-Cl.16E and Ls174T cells treated with different dosages of APN for 24 h and cell supernatant was collected. A parallel experiment that was undertaken with the goal to determine the spontaneous production of Muc1 and Muc2 at different time points in the colonic epithelial cells of APNKO (n=40) and WT (n=40) mice each treated with three cycles of DSS on day 8, 23, and 38. Mice were sacrificed at different time points after the start of third DSS cycle on day 38, 44, 54, and 62 (n=10 each time point). Colonic epithelial cells were scraped and cultured in DMEM supplemented with 10 % heat-inactivated FCS for 24 h. Muc1 and Muc2 production was measured both in colonic epithelial cells and in HT29-Cl.16E and Ls174T cell supernatant by ELISA (USCN LIFE SCIENCE) using standard protocol.

Genes knockdown using siRNA: Small interfering RNA (siRNA) (40nM) targeting MUC2, Bax, APN R1 and R2 (QIAGEN), and Math-1 was transfected in HT29-Cl.16E and Ls174T cells (106) using lipofectamine 2000 reagent (Invitrogen) according to the manufacturer's instructions. Controls were transfected with unrelated siRNA (CsiRNA) (SANTA CRUZ, QIAGEN, and INVITROGEN). Reductions of cell-surface proteins were analyzed with flow cytometry. The efficacy of knockdowns was assessed by conventional semi-quantitative RT-PCR. Assays were performed 2 days after transfection.

Apoptosis detection by TUNEL: Terminal deoxynucleotidyl transferase (TdT)-mediated dUTP-biotin nick-end labeling (TUNEL) technique was used as per manufacturer instructions (R&D systems) to detect DNA strand breaks in situ. After treating cells with APN (2 μg/mL), TNF-α (10 ng/mL), and APN+TNF-α pelleted cells were rinsed with PBS and TUNEL staining procedure was performed. Cells were then counterstained with methyl green. Negative controls were performed by substituting PBS for TdT enzyme, which exhibited no immunostaining. Enumeration of apoptotic nuclei was made on ten slides per treatment, using a Zeiss light microscope with a 40× objective and a 10× eyepiece. All nuclei counted showing a brown labeling. The incidence of apoptotic nuclei was given as the percentage relative to total nuclei (apoptotic ratio). The data are representative of three repeated experiments, all displaying similar results.

Reverse transcription-polymerase chain reaction: Semi-quantitative reverse transcription-polymerase chain reaction (RT-PCR) was used to determine the efficacy of siRNA transfection and relative gene expression in HT29-Cl.16E and Ls174T cells and colonic epithelial cells. Total cellular RNAwas isolated using TRIzol reagent (Invitrogen) according to the manufacturer's instructions. A total of 2.5 mg extracted RNA was used as the template for complementary DNA (cDNA) synthesis using the Thermoscript reverse transcription-polymerase chain reaction system (Invitrogen). Semi-quantitative PCR was performed for Muc2, Bax, APN R1 and R2, Hes-1, and Math-1 using the following primer pairs: MUC2 forward primer (FP) (5-GACATTTGTCAT GTACTCGGC-3) and reverse primer (RP) (5-GCAAGGACTGAACAAAGACTC-3), Bcl-2 (FP-59-GACTTCGCCGA GATGTCCAG-39 and RP-5-TCACTTGTGGCTCAGATAGG-3), Bax (FP-59-GGTTTC

ATCCAGGATCGAGACGG-3 and RP-5-ACAAAGATGGTCACGGTCTGCC-3), GAPDH (HT29-Cl.16E cells) (FP-5 -GCAGGGGGGAGCCAAAAGGG-3 and RP- 5 -TGCCAGCCCCAGCGTCAAAG-3), Hes1 (FP-CAGCCAGTGTCAACACG ACAC and RPTCGTTCATGCACTCGCTGAG), Math1 (FPA GTGACGGAGAGTTTTCCCC and R P- CTGCAGCCGTCCGAAGTCAA), and GAPDH (colonic epithelial cells) (FP-GTCATCA TCTCCGCCCCTTCTGC and RP-GATGCCTGCTTCACCACC TTCTTG). The synthesized cDNA was amplified by RT-PCR assay; the PCR cycle consisted of 94 °C for 1 min, 56 °C for 2 min,and 72 °C for 1 min, with final extension at 72 °C for 10 min. Relative mRNA abundance of Math-1, Hes-1, and ratio of Bax/Bcl-2 was calculated using semiquantitative RT-PCR and Image J software (NCBI) for densitometry. GAPDH was used as a loading control and the gels were run thrice using different samples from the same group to calculate significant difference.

Statistical analysis: Two-way and one-way analysis of variance (ANOVA) was used to analyze the data with Tukey post hoc-analyses. A p value<0.05 was considered statistically significant. All the statistical analyses were done by using SigmaStat 3.5 (SPSS).

4.4 Results

Promotion of colorectal carcinogenesis in adiponectin-deficient mice

We investigated the role of APN in the progression of (CICC). No morphological differences in the colon were observed between the WT and the APNKO control mice (Fig.

1a) and an administration of three cycles of DSS alone did not induce tumors in both WT and APNKO mice. However, APNKO and WT mice receiving DMH and DSS+DMH developed tumors (Fig. 1a), with greater tumor number and size in APNKO mice treated with DMH+DSS when compared to WT mice (Fig. 1a). These were similar to the results obtained in our previous study (Saxena, et al., 2012). The tumors were observed mostly in the descending colon and the rectum. Moreover, shortening of the colon length (one of the macroscopic signs of colitis representing the severity of colitis) was more evident in DSS + DMH treated APNKO mice when compared to WT mice (Fig. 1a).

APN deficiency enhances colonic mucosal erosions and reduces goblet to epithelial cell ratio

One of the consistent features of both IBD and CICC is the denudation of the mucus layer coating the gastrointestinal tract. To evaluate the role of APN in preventing DSS, DMH and DSS+DMH induced mucosal erosions; we measured the colon mucosal thickness as well as the goblet to epithelial cell ratio in all the treated groups as described by Petersson et al., 2011 (Petersson, et al., 2011). No change in the mucus thickness was observed in untreated APNKO and WT mice (Fig. 1b). All DSS, DMH and DSS+DMH treated mice had a significant reduction in the mucus thickness as compared to untreated mice (Fig. 1c). APNKO mice treated with DSS, DMH and DSS+DMH had significantly decreased ($p < 0.04$) mucus thickness when compared to WT mice in the same treatment group (Fig. 1c). APNKO mice treated with DSS+DMH had the lowest mucosal thickness compared to other groups. Additionally, when compared with the concurrent controls in

the WT group, the number of goblet cells was reduced significantly in APNKO mice treated with DMH and DSS+DMH, thereby offering an explanation for the loss of mucus in these animals (Fig. 1d and 1e). The DSS treated WT and APNKO mice did not show any difference in the goblet cell number (data not shown).

Effect of APN on in vitro and in vivo Muc2 production and TNF-α induced apoptosis.

To elucidate the role of APN in the synthesis of Muc1 and Muc2 production, HT29-Cl.16E and Ls174T cells were cultured for 24 h with media containing various concentrations of APN. The results show a dose dependent increase in the Muc2 production with an increase in the APN concentration when compared to untreated cells (Fig 2a), suggesting that APN has a direct role in Muc2 production by goblet cells. Similar results were found in Ls174T cells exposed to the same treatment (data not shown). Data also show that APN did not have any effect on Muc1 production (Fig. 2a).

To characterize the effect of APN deficiency on Muc1 and Muc2 production by the primary epithelial cells, APNKO and WT mice treated with 3 cycles of DSS were sacrificed at various time points. The colonic epithelial cells were collected, cultured for 24h, and measured for Muc1 and Muc2 production by ELISA (Fig 2b). Muc2 level was significantly reduced on day 44, and was recovered by day 54 and 62 in WT mice without any changes in Muc1 production. However, in APNKO mice, Muc2 level was reduced dramatically and its production was consistent by day 62, indicating that APNKO mice are prone to

decreased Muc2 production or fewer goblet cells during and after chronic DSS administration (Fig 2b).

APNKO mice treated with DSS, DMH and DSS+DMH had lesser goblet cells as compared to WT mice, indicating that APN has an inhibitory role in goblet cell apoptosis. To validate this observation, the experiment was performed to assess the impact of APN (2μg/mL) on TNF-α (10 ng/mL) induced apoptosis in cultured HT29-CI.16E and Ls174T cells. The results showed that supplementing the HT29-CI.16E and Ls174T cells for two hours with media containing APN, decreased apoptosis by almost half when compared to untreated controls (no APN or TNF- α). TNF- α increased apoptosis by almost three folds (Fig 2c), however when these cells are co-treated with APN (APN + TNF-α), the goblet cell apoptosis is reduced, indicating that the APN inhibits TNF- α-induced apoptosis of the goblet cells (Fig 2c). To test whether APN inhibition of apoptosis is Muc2 dependent, we knocked down Muc2 expression (~60% reduction) using Muc2-siRNA (Tai et al., 2008). Muc2 knockdown resulted in a four-fold increase in the apoptosis in APN treated group and two fold increase in APN+TNF-α group as compared to siRNA controls ($p < 0.01$) (Fig 2c). APN plays an important role in inhibiting TNF-α induced apoptosis of goblet cells and is Muc2 mediated. Similar results were found in Ls174T cells exposed to the same treatment (data not shown).

APN inhibits TNF- α induced apoptosis of the goblet cell by modulating Bax/Bcl-2 through the activation of APN receptors

To analyze the Bax and Bcl-2 role in regulating TNF- α induced goblet cell apoptosis by APN, we quantified the Bax/Bcl-2 mRNA levels in cells treated with APN, TNF- α and APN + TNF-α. The results showed down-regulation of Bax expression with up-regulation of Bcl-2 in cells treated with APN alone (Fig. 3a-b). TNF-α treatment resulted in the up-regulation of Bax, while cells co-treated with APN (APN+TNF-α) reduced TNF-α induced up-regulation of Bax with increase in Bcl-2 expression (Fig. 3b). APN alone caused a reduction in Bax/Bcl-2 mRNA levels as compared to untreated controls ($p<0.01$), also APN reduced TNF-α induced Bax/Bcl-2 mRNA expression when compared to cells treated with APN+TNF-α ($p<0.04$) (Fig. 3b). The apoptosis ratio was measured in cells with various treatments and the results show that APN reduced TNF- α induced apoptosis ratio in control cells ($p<0.03$), but no significant difference was seen in Bax depleted cells (siRNA) cells ($p>0.05$) . However Bax depleted cells (Bax siRNA) has a higher apoptosis ratio in all treated groups compared to control (CsiRNA) cells (Fig. 3c-d), suggesting that APN inhibits goblet cell apoptosis via Bax/Bcl-2 modulation.

To evaluate the role APN R1 and R2 in mediating APN effect on goblet cell apoptosis by TNF- α, the HT29-Cl.16E and Ls174T cells were treated with APN, TNF-α and APN +TNF-α in APN R1 and R2 depleted cells. The data show that APN is able to inhibit TNF- α apoptosis ratio in control (CsiRNA) cells ($p<0.01$) (Fig. 3e-f), while APN is unable to inhibit TNF- α apoptosis ratio in cells deficient of APN receptors APN R1 and

R2 (Fig. 3g). Thus, it appears that APN may selectively inhibit TNF- α goblet cell apoptosis through adiponectin receptors.

APN deficiency modulates genes responsible for goblet cell differentiation.

Hes-1 and Math-1 genes play an important role in epithelial to goblet cell differentiation. We evaluated these genes expression in the colonic mucosa of WT and APNKO mice treated with DSS, DMH and DSS+DMH. Hes-1 gene expression is upregulated in APN deficient mice significantly (Fig. 4a), with concomitant reduction in the expression of Math-1 gene (Fig. 4b) in DMH and DSS+DMH treated group ($p<0.04$), as compared to WT mice, while DSS treated (data not shown) and untreated groups did not show any difference in the expression of Hes-1 and Math-1 genes. These results indicate that epithelial cells of the APN deficient mice express genes that reduce epithelial cell differentiation to goblet cells.

Increase in Muc2 by APN is Math-1 dependent and mediated by APN receptors.

In our previous experiments it has been shown that APN induces Math-1 expression *in vivo*. We detected Math-1 expression in HT29-Cl. 16E and Ls174T cells treated with various concentrations of APN. The results indicate a dose dependent increase in the Math-1 expression with an increase in APN concentration (Fig. 5a-b). In order to analyze if Math-1 gene is responsible for APN induced Muc-2 production, various concentrations of APN are treated with Math-1 deficient (by knocking down with Math-1 siRNA) cells. The results

show a dose dependent increase in Muc-2 production with an increase in APN concentration. There was a significant reduction in Muc-2 production in cells deficient of Math-1 gene (Math-1 siRNA), when treated with various concentrations of APN, as compared with control (CsiRNA) group ($p<0.01$) (Fig. 5c-d), suggesting that APN induced Muc-2 production, is mediated by Math-1 gene expression.

APN R1 and R2 were knocked down in HT29-Cl.16E (Fig. 5e) and Ls174T cells (data not shown), and were treated with APN and measured for Math-1 expression. The results show a significant reduction in the Math-1 expression in APN R1 and R2 deficient cells compared to control (CsiRNA) cells ($p<0.02$) (Fig. 5f-g), suggesting that APN R1 and R2 activation is required for Math-1 gene expression.

4.5 Discussion

Obesity and IBD are known factors that induce chronic inflammation and contribute to the colorectal carcinogenesis (Hartnett & Egan, 2012). Deregulation of adipose tissue derived adipokines may be directly involved in obesity-related carcinogenesis (van Kruijsdijk, et al., 2009). Adiponectin is arguably one of the highly investigated adipokine as its anti-inflammatory and insulin-sensitizing effects are reported to be beneficial in various health conditions including cancer (van Kruijsdijk, et al., 2009). The concentration of APN in plasma is reduced in obesity (Arita, et al., 1999), and an inverse relation between serum levels of adiponectin and risk of colorectal cancer has been established (Otake, et al., 2005; Wei, et al., 2005; Williams et al., 2008).

Chronic colonic inflammation is a prerequisite for colitis-associated colorectal carcinogenesis and our earlier studies have shown that APN deficiency contributes to inflammation-induced colon cancer (Saxena, et al., 2012). The present study plans to investigate the role of APN and goblet cells in preventing CICC by emphasizing on the mechanism/s responsible for the protective effects.

Tumor development was found to be similar in all the treatment groups when compared to our previous study (Saxena, et al., 2012), with significantly greater number of tumor and tumor size in APNKO mice treated with DSS+DMH in comparison to WT mice indicating that the absence of APN made the mice more vulnerable to DSS induced colitis and DMH induced colon cancer. This could be explained by the apoptotic effect of APN on tumor cells and decreased neovascularization in T241 mice fibrosarcoma (Brakenhielm, et al., 2004). It has also been found to decrease azoxymethane-induced intestinal carcinogenesis in $Apc^{min/+}$ and WT mice (Mutoh et al., 2011). It is quite possible that APN mediates the protective effects possibly by inhibiting chemokine production in intestinal epithelial cells and the following inflammatory responses, including infiltration of macrophages and release of proinflammatory cytokines (Nishihara et al., 2006; Saxena, et al., 2012).

The mucus layer has a crucial role in intestinal homeostasis and act as a hallmark of human IBD, particularly UC and in mice lacking the major mucin protein Muc2 that develop spontaneous colitis (Maloy & Powrie, 2011). The mucus layer produced by the goblet cells is part of the innate immunity and forms a physical barrier against mechanical

and chemical insults (Hollingsworth & Swanson, 2004; Hooper & Macpherson, 2010; Specian & Oliver, 1991). We therefore detected the role of APN deficiency in mucin depletion by quantifying mucus thickness in both APNKO and WT mice treated with DSS, DMH and DSS+DMH. The results indicates significant reduction in mucus thickness in both APNKO and WT mice, which are in agreement with earlier reports for IBD (Johansson, et al., 2010; Pelissier, Muller, Hill, & Morfin, 2006; Petersson, et al., 2011) and CICC (Femia, Dolara, Luceri, Salvadori, & Caderni, 2009). The depletion of mucus was significantly pronounced in the APNKO mice, indicating that APN could directly or indirectly modulate mucus production. We also a found a significant reduction in the goblet to epithelial cell ratio in the APNKO mice treated with DMH alone and DSS+DMH when compared to WT counterparts. Therefore, a positive correlation is achieved between APN deficiency and decrease mucus production with a concomitant decrease in goblet cells.

The mucus composed of secretory (Muc2, Mic5AC, Muc5B, and Muc6) and transmembrane proteins (Muc1, Muc3A, Muc3B, Muc4, Muc12, Muc17) that form a semi-permeable barrier between the intestinal lumen and the underlying epithelium (Corfield, Carroll, Myerscough, & Probert, 2001; Sheng, et al., 2012). Several lines of evidence point towards a biological role of mucin in preventing colorectal cancer (Byrd & Bresalier, 2004) with Muc2 being an active player (Velcich, et al., 2002). Muc2 may act as a trigger for intestinal tumorigenesis as Muc2 deficient mice develop small and large intestinal and rectal tumors (Andrianifahanana, Moniaux, & Batra, 2006; Velcich, et al., 2002). Experiments with cultured HT29-Cl.16E and Ls174T cells have clearly shown that APN increased the synthesis of Muc2, but not of Muc1. Similar results were obtained in the

animal model with reduced Muc2 production in APNKO mice when compared to WT mice. Altered Muc2 and Muc1 expression is a hallmark of IBD and colon cancer and we provided substantial evidence that APN may participate in modulating the expression of these two proteins and might contribute to the reduction in the symptoms associated with CICC.

To further explore the protective role of APN, we hypothesized that APN inhibition of goblet cell apoptosis is Muc2 dependent. To validate this hypothesis, Muc2 expression was knocked down (~60% reduction) using siRNA (Tai, et al., 2008) and the goblet cells (siRNA against Muc2 and controls) were investigated for the anti-apoptotic effects of APN. We observed that Muc2 knockdown resulted in a significant increase in apoptotic ratio in all the treatment groups with a fourfold increase in APN treated group and twice in APN+TNF-α group when compared to CsiRNA treated cells, thereby strengthening our hypothesis.

To further explore the mechanism of APN mediated goblet cell protection, we calculated the relative ratio of Bax (pro-apoptotic) and Bcl-2 (anti-apoptotic) mRNA abundance in all the treatment groups (untreated, APN, TNF-α and APN+TNF-α) and found that administration of APN decreased Bax, but increased Bcl-2 expression and attenuated the pro-apoptotic effect of TNF-α. Additionally, using siRNA Bax, we were able to observe that APN neither reduced apoptosis nor inhibited the pro-apoptotic effect of TNF-α in partially depleted Bax (siRNA) in HT29-Cl.16E and Ls174T cells (Fig. 5C), which indicates that APN reduces goblet cell apoptosis by regulating Bax/Bcl-2 ratio. To

the best of our knowledge, this is the first study that demonstrates APN inhibiting goblet cell apoptosis via Bax/Bcl-2 modulation.

Adiponectin has been shown to exert some of its protective effects through adiponectin receptors (AdipoR1 and AdipoR2) (Kadowaki & Yamauchi, 2005; A. Y. Kim, et al., 2010). The upregulation of both adiponectin receptors in tumor cells may be a cellular response to lower circulating adiponectin levels in patients with colorectal cancer and/or a compensatory response of their malignant cells (Williams, et al., 2008). To examine whether the anti-apoptotic effect of APN in goblet cells is mediated through adiponectin receptors, we repressed the expression of AdipoR1 or AdipoR2 via siRNA technique. The results indicated that the presence of APN treatment decreased apoptosis ratio in CsiRNA HT29-Cl.16E and Ls174T cells treated with TNF-α, but no change in the apoptotic ratio was observed in the cells deficient in APN R1 and R2. This study provides conclusive evidence that APN may prevent goblet cell apoptosis through the activation of its two receptors R1 and R2 and its downstream effecters, which could further modulate Bax/Bcl-2 ratio and up-regulate Muc2 expression.

Notch signaling pathway is essential in regulating the differentiation of colonic goblet cells and stem cells/progenitor cells (Katoh, 2007; Qiao & Wong, 2009). Canonical activation of the Notch signaling leads to Hes1 upregulation and Atoh1/Hath1/Math1 down-regulation (Leow, et al., 2005). Suppression of Notch signaling by depletion of Hes-1 was associated with a significant increase in the secretory lineage of intestinal epithelial cells and vice-versa (Jensen et al., 2000; Stanger, Datar, Murtaugh, & Melton, 2005).

The Hes family of genes functions as transcriptional repressors of further downstream targets like Math-1, which defines the secretory epithelial lineages (Shroyer et al., 2007). Recent studies also indicate that Math1 possess tumor suppressor function in colorectal neoplasia and its function is lost in some patients with colorectal cancer (Bossuyt et al., 2009).

To further explore the role of APN in goblet cell differentiation, we quantified the expression of Hes-1 and Math-1. We found a significant increase in the expression of Hes-1 and decrease Math-1 expression in mice treated with DMH alone and DSS+DMH when compared to WT counterpart. We further pursue this path by studying the expression of Math-1 with the exogenous APN dose response in HT-29-Cl.16 E and Ls174T cells and found an increase in the Math-1 mRNA expression with increasing APN dosage. This was followed by another set of experiments where we demonstrated that the expression of Muc2 by the goblet cell is Math-1 dependent, which could be further regulated by APN. It was also found that the expression of Math-1 is dependent on the presence of APN receptors R1 and R2, which was achieved by silencing receptors expression and quantifying Math-1 mRNA abundance in CsiRNA and siRNA APN R1 and R2 treated groups. These results clearly demonstrate that APN is governing the overall expression of both Muc2 and Math-1 in a dose dependent manner in the presence of both APN R1 and R2 receptors and directing the pathway of intestinal cell differentiation towards the formation of goblet cells, which secrete mucus to form a protective layer to prevent colonic epithelial cells from luminal factors that may induce inflammation and cancer.

4.6 Conclusion

By the means of this study, we have established the protective role of APN and its receptors in CICC that is depicted in our hypothetical model (Fig. 6). APN can down-regulate the expression of Hex-1 with the concomitant up-regulation of Math-1 expression leading to the differentiation of epithelial cell to goblet lineage. Also, APN can modulate the ratio of Bax and Bcl-2, which could be a contributing factor in reducing goblet cell apoptosis, which is Muc2 dependent. APN has also been shown to increase the production of Muc2, which is dependent on Math-1. All these data point towards the common observation of the protective role of APN in reducing the severity of CICC.

Although this study provided evidences of the protective role of APN in CICC, but reconstituting APN in the same model system is crucial in defining the role of APN in mucus production. This will be the framework for our future studies.

Acknowledgements

We would like to acknowledge Dr. Bob Price, Medical School, University of South Carolina for technical support with the microscope and other instrumentation. This work was funded and supported by Grant P20 RR-017698, the National Center for Research Resources, Center for Colon Cancer Research, Center of Biomedical Research Excellence (COBRE) Program, University of South Carolina, Columbia SC.

4.7 Figure Legends

Figure 4.1. Tumor incidence and decrease in mucus thickness and goblet to epithelial cell ratio with adiponectin deficiency in different treatment groups: (A) Representative of methylene blue-stained colonic tissues of WT and APNKO mice treated with DMH, DSS+DMH and control group. Measurement of mucus thickness in untreated (B), DSS, DMH and DSS+DMH (C) treated APNKO and WT mice (n=10). (D) Graph representing goblet to epithelial cell ratio in control, DMH and DSS+DMH groups. (E) Descending colon, 2 mm^2 sections of the mice stained with Alcian Blue dye representing goblet cells (blue). The data are representative of two independent experiments, all displaying similar results. (n=8) *$p<0.04$ (APNKO versus WT in the same group)

Figure 4.2. Effect of APN on Muc2 production and goblet cell apoptosis. (A) Graph representing the dose dependent relationship of Muc1 and 2 productions (ng/mL) by HT29-CI.16E cells (10^6) and APN (µg/mL) treatments. (B) Spontaneous Muc1 and Muc2 production from mucosal tissue obtained from WT and APNKO mice respectively and treated with DSS (third cycle). They were measured in different time points. (C) The gel picture represents the Muc2-siRNA knockdown in HT29-CI.16E cells (10^6). The cells with CsiRNA and Muc2-siRNA were treated with TNF- α (10ng/mL) or globular APN (2µg/mL) or both for 2h (the peak effect of TNF-α in cell apoptosis) and the apoptosis ratio was determined using TUNEL assay. The data are representative of two independent experiments, all displaying similar results. The data are representative of two independent experiments, all displaying similar results. (n=5) *$p< 0.01$ (treated versus untreated cells,

TNF-α versus APN+TNF-α at 2 h time point), #p<0.04 (Muc2 levels on day 38 versus 44 in WT mice). **p<0.05 (Muc2 levels on day 38 versus 44, 54, and 62 in KO mice).

Figure 4.3. APN inhibits goblet cell apoptosis via Bax/Bcl-2 modulation and is APN R1 and R2 dependent. (A and B) Bax and Bcl-2 expressions were measured in HT29-Cl.16E treated with TNF- α (10ng/mL) or globular APN (2µg/mL) or both. (C and D) Apoptosis ratio in CsiRNA and siRNA-Bax HT29-Cl.16E cells that were treated with TNF-α (10ng/mL) or globular APN (2µg/mL) or both. (E) Gel representing the APN R1 and R2 knocked-down using siRNA. (F and G) Apoptosis ratio in CsiRNA and APN R1 and R2 siRNA injected HT29-Cl.16E cells treated with TNF- α (10ng/mL) or globular APN (2µg/mL) or both. The data are representative of two independent experiments, all displaying similar results. (n=5) *p<0.01 (control versus APN treated), **p<0.03 (APN versus APN+TNF-α treated), #p< 0.04 (APN versus APN+TNF-α treated).

Figure 4.4. APNKO mediated alteration of gene expression reduction of epithelial to goblet cell differentiation. (A) Graph and the gel picture showing the relative Hes-1 expression to GAPDH in the non-tumor colonic tissue of WT and APNKO mice treated with DMH and DSS+DMH and control group. (B) Graph and the gel picture showing the relative Math-1 expression to GAPDH in the non-tumor colonic tissue of WT and APNKO mice treated with DMH and DSS+DMH and control group (n=5 mice/ group).*p<0.04 (APNKO versus WT in the same group).

Figure 4.5. APN induces math-1 expression and an increase of Muc2 is Math-1 dependent which requires APN receptors. (A and B) Relative Math-1 mRNA abundance in HT29-CI.16E cells (106/ml) incubated with different doses of APN (0, 0.5, 1 and 2 µg/mL). (C) Gel representing knockdown Math-1 expression using Math-1-siRNA. (D) Graph showing APN dose dependent (µg/mL) Muc2 production (ng/mL) in HT29-CI.16E cells (10^6/ml) treated with CsiRNA and math-1 siRNA. **(**E) Gel showing knockdown expression of APN R1 and R2 receptors. (F and G) Math-1 expression in HT29-CI.16E cells CsiRNA and siRNA APN R1 and R2 and treated with APN (2µg/mL). The data are representative of two independent experiments, all displaying similar results. (n=5) *$p<0.01$ (0 vs 1 and 2 µg/mL APN dosage and CsiRNA and siRNA APN R1 and R2 given the same treatment), **$p<0.01$(CsiRNA vs Math-1 siRNA with same dosage).

Figure 4.6. A hypothetical model showing the effect of APN on epithelial to goblet cell differentiation, goblet cell apoptosis and Muc-2 production. In CICC, APN may play a protective role by reducing the expression of Hes-1 and Bax with a concomitant increase in the production of Math-1 and Bcl-2 leading to greater epithelial to goblet differentiation and reduction in goblet cell apoptosis. APN also increases the expression of Muc-2 leading which affects goblet cell differentiation. All the above pathways lead to an increase in goblet cell number and hence greater mucus secretion. This enhances the protection from luminal factors that invade the colon epithelium and hence reducing the incidence of CICC.

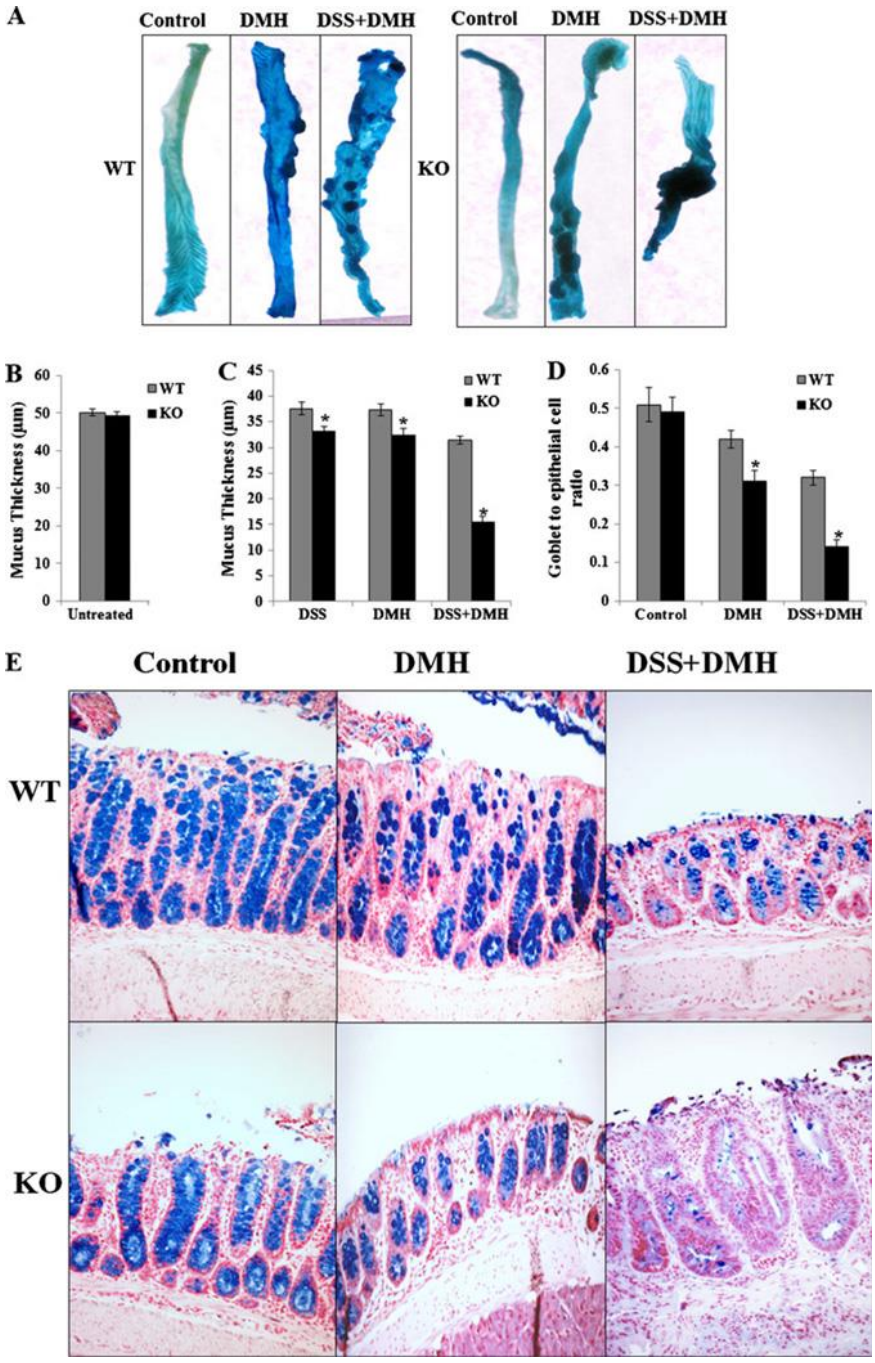

Figure 4.1. Tumor incidence and decrease in mucus thickness and goblet to epithelial cell ratio with adiponectin deficiency in different treatment groups: (a) Representative of methylene blue-stained colonic tissues of WT and APNKO mice treated with DMH, DSS+DMH, and control group. Measurement of mucus thickness in (b) untreated, (c) DSS-, DMH-, and DSS+ DMH-treated APNKO and WT mice (n=10). (d) Graph representing goblet to epithelial cell ratio in control, DMH, and DSS+DMH groups. (e) Descending colon, 2 mm^2 sections of the mice stained with Alcian blue dye representing goblet cells (blue). The data are representative of two independent experiments, all displaying similar results. (n=8) *p<0.04 (APNKO versus WT in the same group)

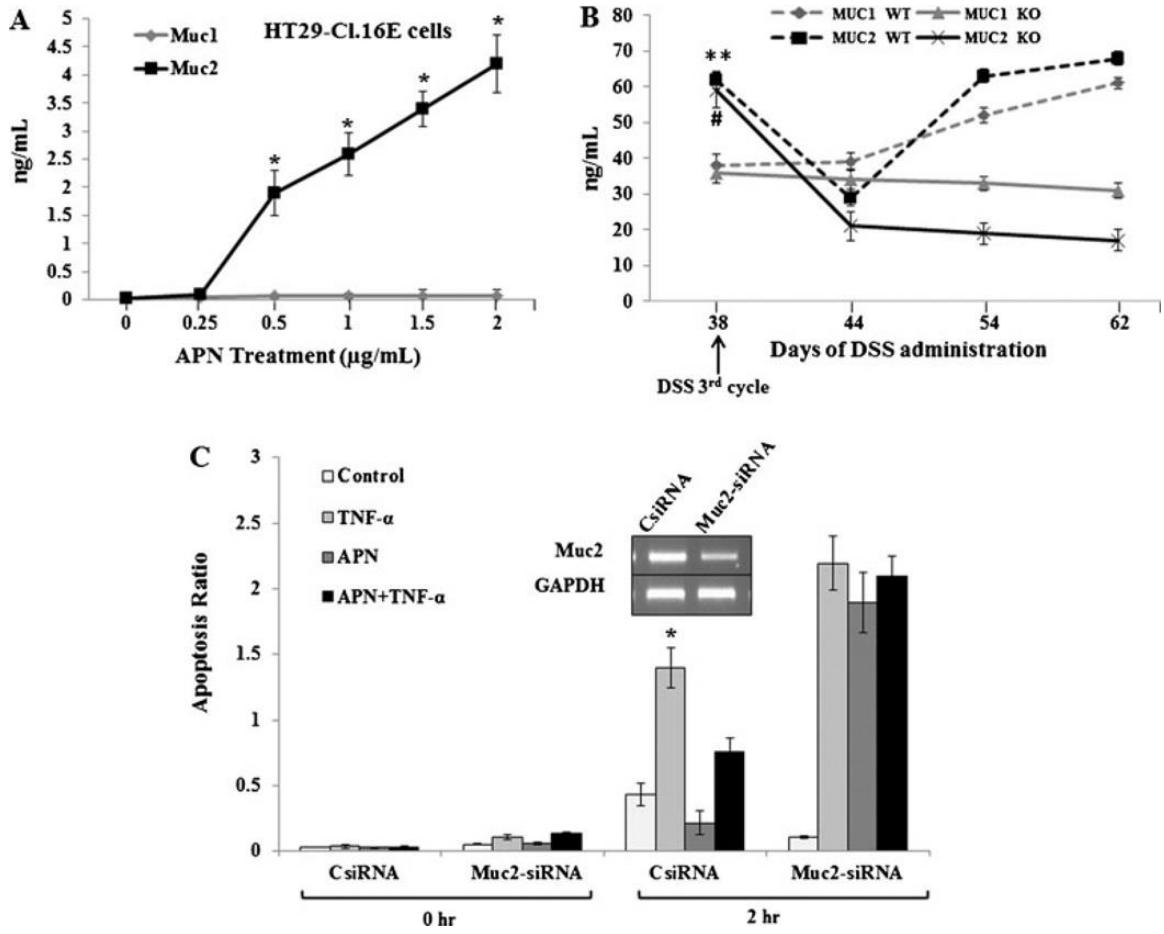

Figure 4.2. Effect of APN on Muc2 production and goblet cell apoptosis. a Graph representing the dose-dependent relationship of Muc1 and 2 productions (nanogram per milliliter) by HT29-CI.16E cells (10^6) and APN (microgram per milliliter) treatments. b Spontaneous Muc1 and Muc2 production from mucosal tissue obtained from WT and APNKO mice, respectively, and treated with DSS (third cycle). They were measured in different time points. c The gel picture represents the Muc2-siRNA knockdown in HT29-CI.16E cells (10^6). The cells with CsiRNA and Muc2-siRNA were treated with TNF-α (10 ng/mL) or globular APN (2 µg/mL) or both for 2 h (the peak effect of TNF-α in cell apoptosis), and the apoptosis ratio was determined using TUNEL assay. The data are representative of two independent experiments, all displaying similar results. (n=5) *p< 0.01 (treated versus untreated cells, TNF-α versus APN+TNF-α at 2 h time point), $^{\#}p$<0.04 (Muc2 levels on day 38 versus 44 in WT mice). **p<0.05 (Muc2 levels on day 38 versus 44, 54, and 62 in KO mice).

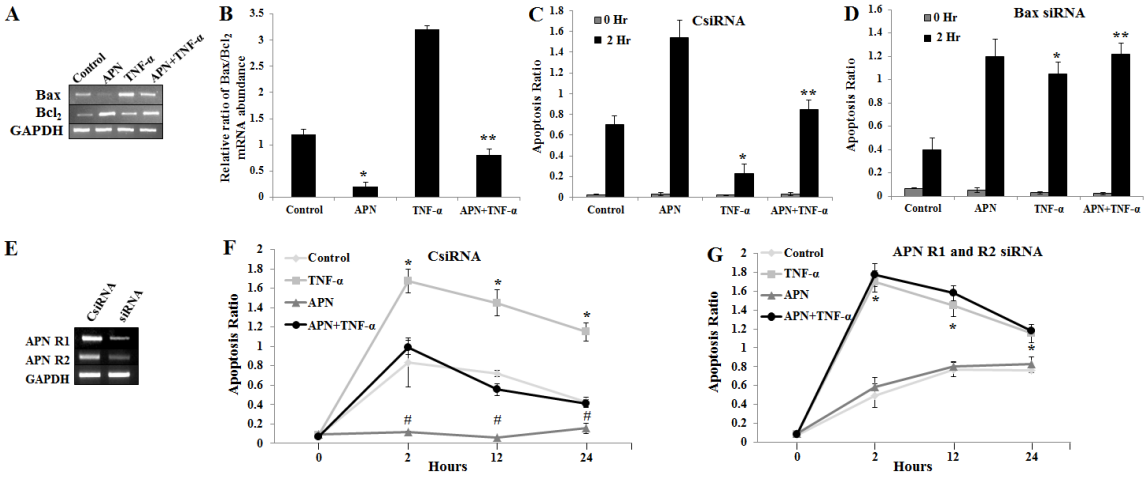

Figure 4.3. APN inhibits goblet cell apoptosis via Bax/Bcl-2 modulation and is APN R1 and R2 dependent. (A) and (B) Bax and Bcl-2 expressions were measured in HT29-Cl.16E treated with TNF-α (10ng/mL) or globular APN (2 µg/mL) or both and the ratio of their RNA abundance was calculated. c and d Graph showing Apoptosis ratio in CsiRNA and siRNA-Bax HT29-Cl.16E cells that were treated with TNF-α (10 ng/mL) or globular APN (2 µg/mL) or both. e Gel representing the APN R1 and R2 knocked-down using siRNA. f and g Graph representing Apoptosis ratio in CsiRNA and APN R1 and R2 siRNA injected HT29-Cl.16E cells treated with TNF-α (10 ng/mL) or globular APN (2 µg/mL) or both. The data are representative of two independent experiments, all displaying similar results. (n=5) *p<0.01 (control versus APN treated), **p<0.03 (APN versus APN+TNF-α treated), $^{\#}p$< 0.04 (APN versus APN+TNF-α treated).

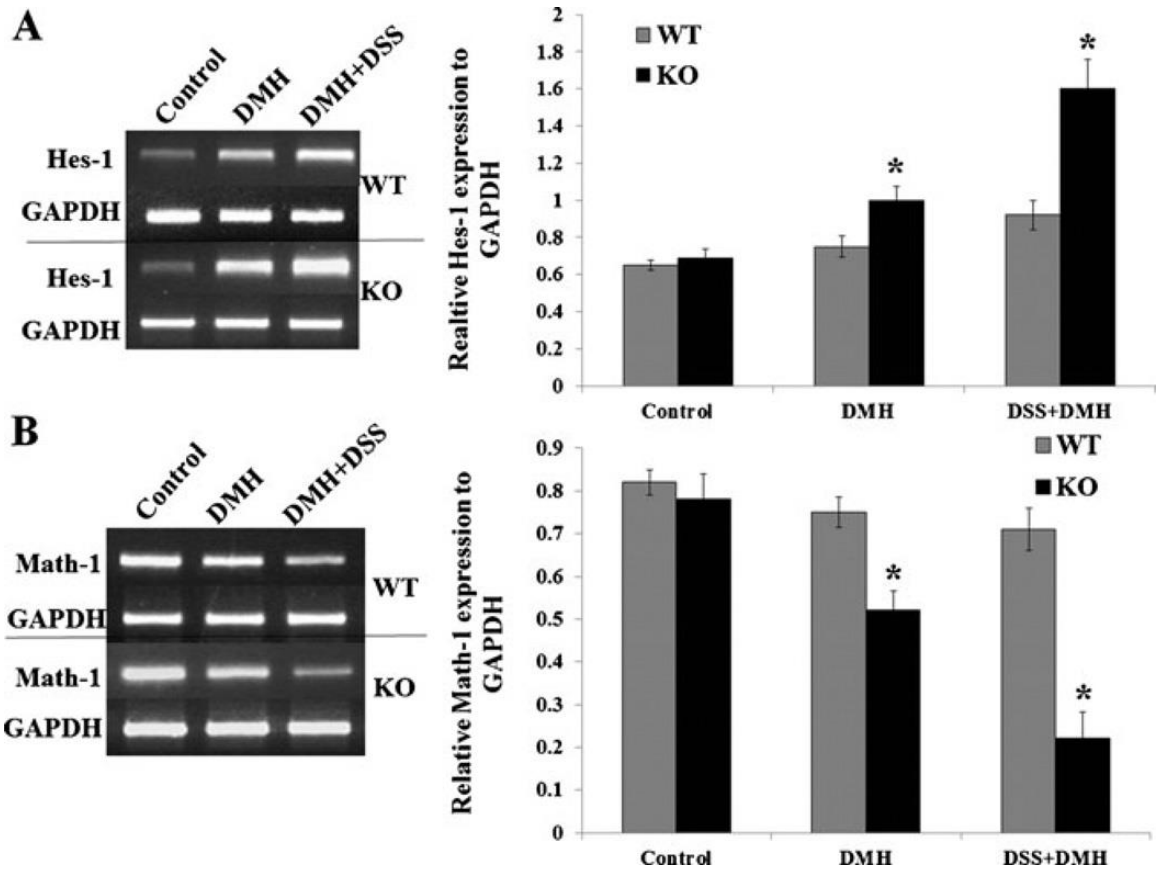

Figure 4.4. APNKO mediated alteration of gene expression reduction of epithelial to goblet cell differentiation. (A) Graph and the gel picture showing the relative Hes-1 expression to GAPDH in the non-tumor colonic tissue of WT and APNKO mice treated with DMH and DSS+DMH and control group. (B) Graph and the gel picture showing the relative Math-1 expression to GAPDH in the non-tumor colonic tissue of WT and APNKO mice treated with DMH and DSS+DMH and control group (n=5 mice/ group).*$p<0.04$ (APNKO versus WT in the same group).

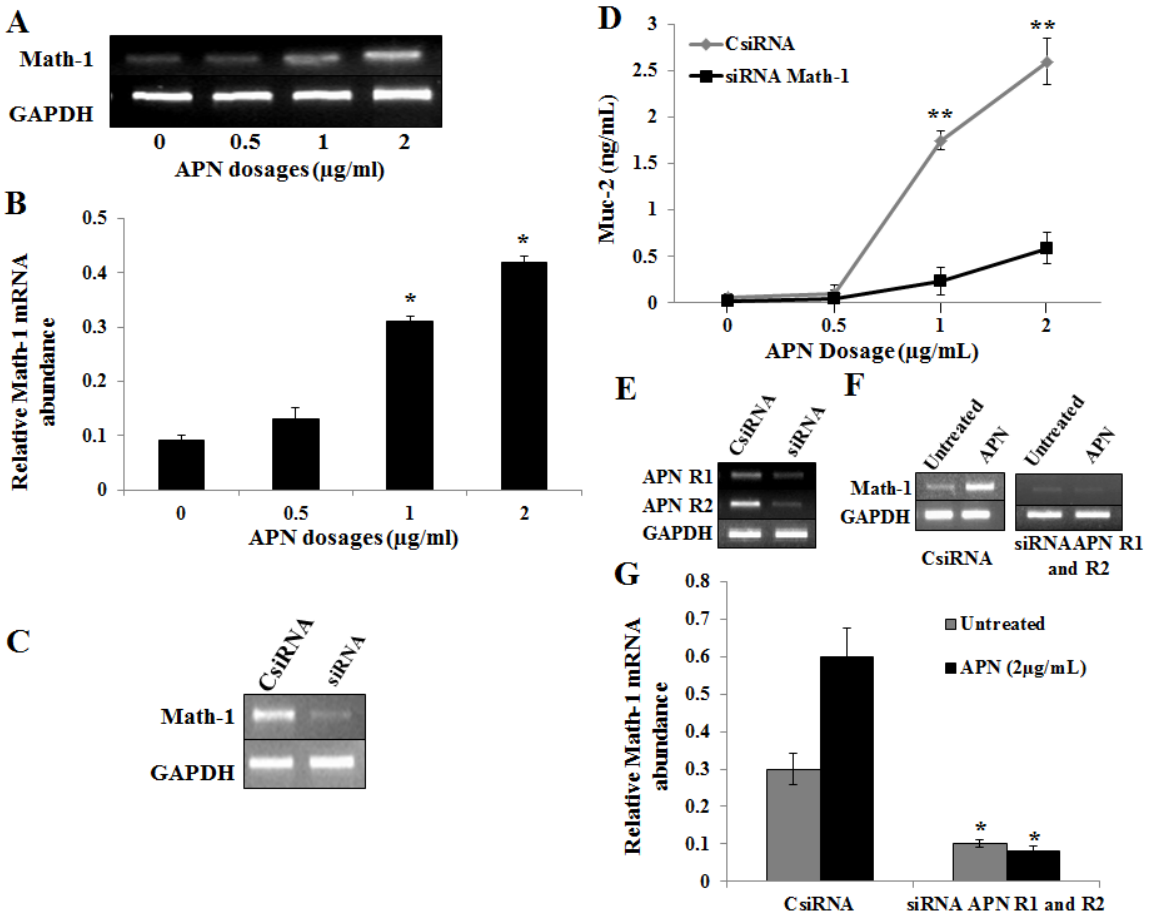

Figure 4.5. APN induces math-1 expression and an increase of Muc2 is Math-1 dependent which requires APN receptors. (A and B) Relative Math-1 mRNA abundance in HT29-CI.16E cells (106/ml) incubated with different doses of APN (0, 0.5, 1 and 2 µg/mL). (C) Gel representing knockdown Math-1 expression using Math-1-siRNA. (D) Graph showing APN dose dependent (µg/mL) Muc2 production (ng/mL) in HT29-CI.16E cells (10^6/ml) treated with CsiRNA and math-1 siRNA. **(**E) Gel showing knockdown expression of APN R1 and R2 receptors. (F and G) Math-1 expression in HT29-CI.16E cells CsiRNA and siRNA APN R1 and R2 and treated with APN (2µg/mL). The data are representative of two independent experiments, all displaying similar results. (n=5) *p<0.01 (0 vs 1 and 2 µg/mL APN dosage and CsiRNA and siRNA APN R1 and R2 given the same treatment), **p<0.01(CsiRNA vs Math-1 siRNA with same dosage).

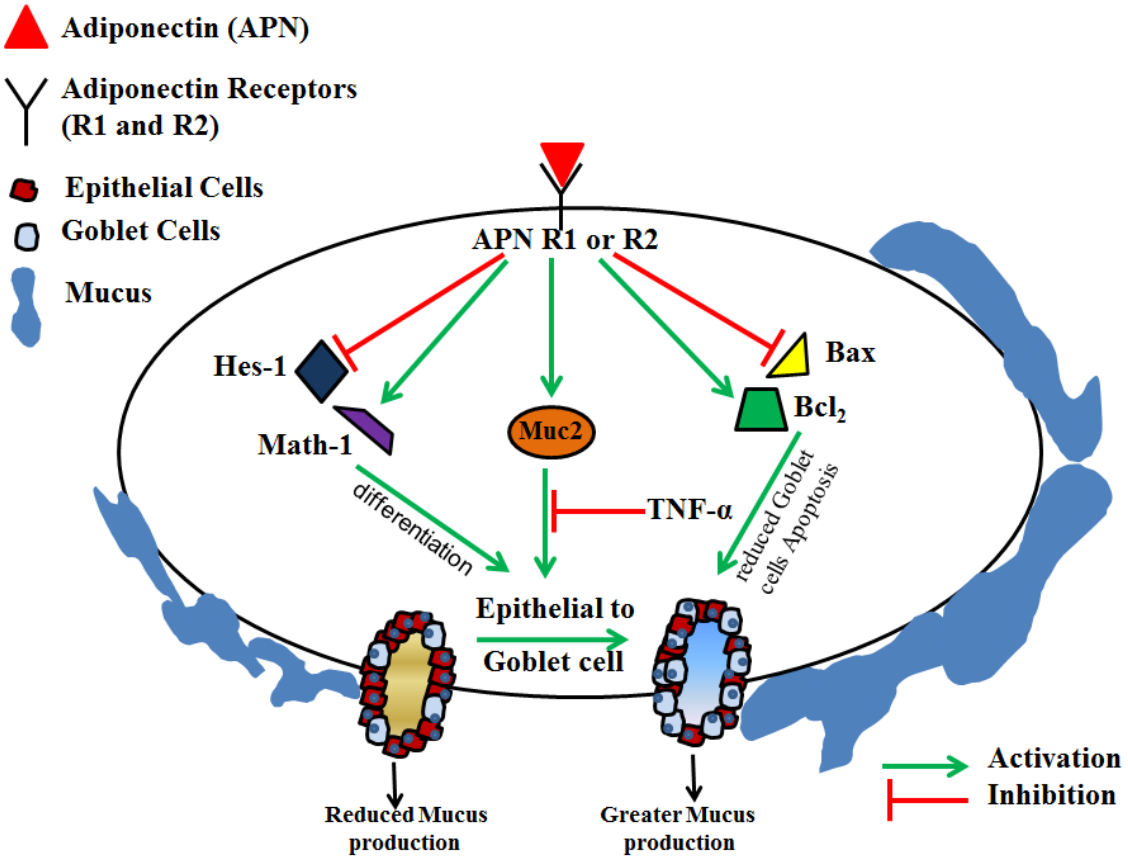

Figure 4.6. A hypothetical model showing the effect of APN on epithelial to goblet cell differentiation, goblet cell apoptosis and Muc-2 production. In CICC, APN may play a protective role by reducing the expression of Hes-1 and Bax with a concomitant increase in the production of Math-1 and Bcl-2 leading to greater epithelial to goblet differentiation and reduction in goblet cell apoptosis. APN also increases the expression of Muc-2 leading which affects goblet cell differentiation. All the above pathways lead to an increase in goblet cell number and hence greater mucus secretion. This enhances the protection from luminal factors that invade the colon epithelium and hence reducing the incidence of CICC.

CHAPTER 5

SELENIUM RICH DIET CAN BE PROTECTIVE IN THE TREATMENT OF CHRONIC INFLAMMATION INDUCED COLON CANCER[3]

[3] Arpit Saxena, Kamaljeet Kaur, Samantha Truman, Matthew Rorro, Bianca Larsen, Emma Fletcher, Alexander Chumanevich and Raja Fayad. To be submitted

5.1 Abstract

Background: Colon cancer is the second largest cause of cancer deaths and ranks third in the number of new cases every year in both sexes in the United States. Repeated cycles of chronic inflammation that are found in inflammatory bowel disease (IBD), crohn's disease and ulcerative colitis, have been be linked to colon cancer. Obesity is a risk factor associated with colon cancer and increased adiposity leads to reduced production of certain adipokines including Adiponectin (APN). It is secreted by the adipose tissue and found to have anti-inflammatory and anti-cancerous effects. Selenium (Se) is a well-known antioxidant non-metal which has been shown to reduce inflammation and induce cancer cell apoptosis by the modulation of Bax and Bcl_2 in colon cancer cell lines. Purpose: The purpose of this publication is to study the effect of Se rich diet and APN deficiency on chronic inflammation induced colon cancer. Methods: C57BL/6 and APNKO mice were randomly assigned to 6 different treatment groups including: C57BL/6 (WT) + Control Diet, WT+Se Diet, APNKO+Control Diet, APNKO+Se Diet, WT+DSS+ Control Diet, WT+DSS+Se Diet, APNKO+DSS+Control Diet, APNKO+DSS+Se Diet, WT+DMH+ Control Diet, WT+DMH+Se Diet, APNKO+DMH+ Control Diet, APNKO+DMH+Se Diet, WT+DSS+DMH+ Control Diet, WT+DSS+DMH+Se Diet, APNKO+DSS+DMH+ Control Diet and APNKO+DSS+DMH+Se. Inflammation and cancer was induced by DSS and DMH respectively and Se rich diet (0.75 ppm) or control diet (0.02 ppm) were administered to respective group on day 25. Mice were monitored for clinical score and were sacrificed on day 194 and colon tissue was collected for differential analysis. Results: Se rich diet was found to reduce clinical score, tumor load and inflammation in both

APNKO and WT mice with CICC. Se rich diet was found to increase the serum APN in WT mice with CICC when compared with control diet. Colon cancer cell apoptosis was found to be significantly higher with Se rich diet as compared to control group. Se rich was found to increase Gpx activity and the expression of selenoproteins including Gpx-1 and Gpx-2 in normal colon tissue while higher oxidative stress in the colon tumor tissue. Se rich diet was also found to increase goblet cell production and increase the expression of Math-1 and Muc-2. Conclusion: Se and APN might be effective in reducing the severity of CICC by suppressing inflammation and tumor burden and increasing cancer cell apoptosis and goblet cell production.

Keywords: Selenium, oxidative stress, Adiponectin, colon cancer, apoptosis

5.2 Introduction

Colon cancer is the second largest cause of cancer deaths and ranks third in the number of new cases every year in both sexes in the United States (R. Siegel, et al., 2014). Repeated cycles of chronic inflammation that are found in inflammatory bowel disease (IBD), crohn's disease and ulcerative colitis, have been be linked to colon cancer(Rubin, Shaker, & Levin, 2012). Clinical signs and symptoms of colon cancer include hematochezia, fecal hemocult, diarrhea, weight loss, nausea, constipation and constant fatigue(Korsgaard, et al., 2006). Etiology of colon cancer is very complex and heterogeneous and ranges from dietary and lifestyle factors to genetic abnormalities(Fearon, 2011). Obesity has been considered an established risk factor for

colon cancer patients (Hull & Lagergren, 2014). Reduced secretion of adiponectin (APN), an adipocytokines secreted by adipose tissue, has been linked with increased obesity and severity of colorectal cancer (Saxena, et al., 2012). Our published report indicated that APN deficient mice developed more tumors and showed an increase in the pathology of chronic inflammation induced colon cancer (CICC)(Saxena, et al., 2012). Serum selenium (Se) levels were found to be 25-30% lower in cancer patients(Gorozhanskaia, Sviridova, Dobrovol'skaia, Zybrikhina, & Kashnia Sh, 2013). Nutritional deficiencies or malnutrition is one of the major concern with the colon cancer patients received chemotherapy (Du et al., 2012; Hebuterne et al., 2014). Downregulation of several selenoproteins have been also identified in IBD(Andoh et al., 2005).There are several treatment strategies available for colon cancer including chemotherapy and radiotherapy, but these have severe side effects with increased morbidity and reduced quality of life. Complimentary medicine including the use of micronutrients and phytochemicals has been gaining popularity as they aid in reducing these side effects and lower the severity of the disease(Baliga et al., 2012; W. L. Lee, Huang, & Shyur, 2013).

Selenium is an essential micronutrient and is widely accepted as an anti-oxidant element (Maseko, et al., 2014). This micronutrient forms selenocysteine, which is the twenty-first amino acid and integrates into proteins to form 25 selenoproteins (Metanis & Hilvert, 2014). Se can be obtained in the diet through several sources including Brazil nut, fish, liver, chicken, certain vegetables and meats (Maseko, et al., 2014). The recommended dietary allowance for Se is 55µg per day for human adults and the upper safe limit is 400 µg/day. Beneficial effects of Se can be obtained at a dosage of 200 µg per day. Se has been

shown to reduce the severity of cancers including prostate(Gerstenberger, et al., 2014), breast (Arsenyan, et al., 2014) and lung (Okuno, et al., 2014b) and has acted as a useful supplementation for several ailments including cystic fibrosis (Ciofu & Lykkesfeldt, 2014), male and female infertility(Balazs & Racz, 2013), glucose metabolism in type 2 diabetes (Mao & Teng, 2013), grave's disease (Kryczyk & Zagrodzki, 2013) and other related inflammatory and autoimmune diseases. A dosage of 200 μg/day of Se has been shown to decrease the total incidence of cancer by 25% (Reid, et al., 2008). An inverse association has been established between higher Se status and colorectal cancer (Hughes, et al., 2014). The protective effect of the Se in various diseases and conditions is mostly due to the anti-oxidative property leading to an increase in the production of selenoproteins like glutathione peroxidases (Gpx), which neutralize or prevent the formation of reactive oxygen species (ROS)(Kosaric, et al., 2014). Se metabolism is complex and most of the biological effects of elemental Se that is ingested are mediated by selenoproteins (Labunskyy, et al., 2014). Gpx-1 and Gpx-2 are the most abundant selenoproteins present and mediate most of the protective effect of Se. Gpx-1 is ubiquitously presents in the cytosol and the mitochondria in all the tissues of the body, while Gpx-2 is mostly concentrated in the intestinal epithelium (Brigelius-Flohe & Maiorino, 2013). Gpx-1 or Gpx-2 knockout mouse or double knockout mouse has shown to exhibit severe pathology of colorectal cancer (Krehl, et al., 2012; D. H. Lee, et al., 2006) and Se rich diet has been shown to increase Gpx activity in these animals. Increased activity of Gpx-1 and Gpx-2 has also been linked to the chemo preventive effect of Se supplementation (Hu, et al., 2010).

A recent study by Li et al. 2013 on human colorectal carcinoma cells (HCT 116 and SW620) has shown that different dosages (1 μM, 5 μM and 10 μM) of Se lead to apoptosis of the colon cancer cells by Bax dependent pathway(Z. Li, et al., 2013) with 10 μM being the most effective. Another study by Luo et al. 2013 has shown that supranutritional dosage of sodium selenite (10 μM) lead to apoptosis of colon cancer cells by ROS modulation of phosphatase and tensin homolog (PTEN) mediated PI3K/AKT/FoxO3a signaling pathway in colon xenograft animal model(Luo, et al., 2013). Sodium selenite has also shown to reduce inflammation by downregulating the expression of nuclear factor kappa light-chain-enhancer of activated B cells (NFκB) and related cytokines (Pillai, et al., 2012). In this study, we used dextran sodium sulphate (DSS) that is widely used chemical to induce acute and chronic inflammation. In addition, we will be using dimethylhydrazine (DMH), which is a potent carcinogen and has been used to induce colon cancer in numerous published animal studies (Femia, et al., 2009; Saxena, et al., 2012).

Although there are few studies indicating the protective role of Se in chronic inflammation and colon cancer, most of these studies used *in vitro* approach and lacked the mechanism of action of Se in reducing the severity of chronic inflammation and colon cancer. Also, as indicated by our published data, APN has been implicated in reducing the severity of chronic inflammation and colon cancer. Se could either be used in the prevention or as a treatment for colon cancer. In this study we have used Se as a prevention by administering Se on the same day as DSS or DMH.

In this report, we studied the role of Se rich diet administration in reducing CICC severity in C57BL/6 (WT) mice and APN knock out (KO) mice and how Se exerts such mechanism.

5.3 Material and Methods:

Animal Model: Four week-old C57BL/6 and APNKO mice were obtained from Jackson Laboratories and bred in the animal facility at the University of South Carolina under the Institutional Animal Care and Use Committee guidelines. APNKO mice were homozygous with the absence of APN expression confirmed by serum protein expression. Mice were fed regular chow and *ad libitum*. Mice were then randomized into 16 different treatment groups with n=10/group. The mice were then acclimatized to the animal facility for 24 days in a low stress environment (22°C, 50% humidity and low noise) with 12:12 hours of light-dark cycle. The first DSS or DMH administration was performed on day 25 of the start of the study. The groups include: C57BL/6 (WT) + Control Diet, WT+Se Diet, APNKO+Control Diet, APNKO+Se Diet, WT+DSS+ Control Diet, WT+DSS+Se Diet, APNKO+DSS+Control Diet, APNKO+DSS+Se Diet, WT+DMH+ Control Diet, WT+DMH+Se Diet, APNKO+DMH+ Control Diet, APNKO+DMH+Se Diet, WT+DSS+DMH+ Control Diet, WT+DSS+DMH+Se Diet, APNKO+DSS+DMH+ Control Diet and APNKO+DSS+DMH+Se Diet. Mice were monitored throughout the study period by measuring the clinical score that includes weight loss, diarrhea and fecal hemoccult. Mice were sacrificed by cervical dislocation under anesthesia on day 194.

There was no significant difference in the body weight of APNKO and WT mice at the beginning of the study.

Chronic Inflammation and Colon Cancer: Depending on the treatment group, mice were either administered DSS or DMH or both. DSS was administered alone to induce chronic inflammation. DMH was injected to induce cancer while the combination of both was given to induce CICC. DSS was administered in 3 cycles where one cycle constitutes 2% DSS (MP Biochemicals, MW: 36,000-50,000) in drinking water for 5 days followed by 5 days of normal drinking water. DSS was administered on day 25, 50 and 75 to induce chronic inflammation. DMH (Sigma Aldrich) was injected intraperitoneally at a concentration of 20mg/kg either once for DSS+DMH treatment group on day 25 or once a week for 12 weeks for DMH alone group. These concentration and model have been well established to study chronic inflammation and colon cancer (Saxena, et al., 2012).

Selenium Diet Administration: Selenium rich diet containing 0.75 ppm of Se per kg was administered to 8 groups on day 25 simultaneously with the administration of DSS, DMH, or both or to the Control group. The diet was administered till the day of sacrifice that is day 194. Control diet contains all the components of the Se rich diet except that the Se content is 0.02 ppm per kg of diet.

Clinical Score: Clinical score was measured for each mouse in each group from day 25 to day 194. Mice were sacrificed after the last clinical score measurement. Score for the weight loss is based on the following published scale where 0 = 0–5% weight loss; 1 = 6–10% weight loss; 2 = 11–15% weight loss; 3 = 16–20% weight loss; and 4 = >20% weight loss. Scoring of diarrhea is as follows: 0 = well-formed pellets, 2 = pasty and semi-formed stools that do not adhere to the anus, 4 = liquid stools that adhere to the anus. Detection of blood in the stools was determined using hemoccult kit (BECKMAN COULTER). The higher intensity of blue color indicates greater bleeding. The followings are the score rates for the fecal hemoccult: 0 = no blood, 2 = positive hemoccult, 4 = gross bleeding. The total clinical score was the summation of the individual score of weight loss, diarrhea and fecal hemoccult. The maximum score a mouse could get is 12. The clinical score was calculated and plotted against days of DSS administration. Higher clinical score indicates more severity of colon cancer development in animals.

Colon Tissue and Serum Collection: Blood was collected before sacrifice through retro-orbital puncture and was spun down at 10,000 rpm for 18 minutes and serum was obtained and stored at -20°C to measure APN. Mice colon was excised and flushed clean with PBS. $2mm^2$ colon tissue section with tumor and non-tumor area was fixed in 10% formalin. 24 hours later, tissues was submerged with with 70% Ethanol followed by paraffin embedding and sectioning to obtain 5 µm thin section on glass slide. Sections with tumor and non-tumor areas were snap frozen on dry ice and stored at -80°C for protein analysis. Another $2mm^2$ colon tissue section was incubated in RPMI medium containing 5000 IU/mL and 5000 IU/mL penicillin and streptomycin (CELLGRO) respectively at 37°C and 5% CO_2

for 24 hours. This was followed by centrifugation at 2500 rpm for 15 minutes. Supernatant was obtained and stored at -20°C to measure secreted cytokine levels.

Tumor Number and Tumor Area and Histopathology: Mice colon was excised and flushed with PBS. Tumor number and area were counted under the microscope in all mice of different groups and significant different was calculated between different groups.

Hematoxylin and Eosin staining was used to determine the morphology of mice colon. Histopathology was quantified based on the scoring system indicating the severity of disease and constituting inflammation, immune cell infiltration and degree of tumor. This was on the scale of 12 where highest score of 4 was given for each parameter, where 0 = no infiltration or no inflammation or no cancer; 2 = moderate infiltration or inflammation or pre-cancerous lesions; and 4 = severe inflammation with distorted crypts or infiltration and formation of lymphatic follicles or visible tumors. All the images were taken in 20X magnification with Nikon e600 microscope. The score was measured by two investigators in blinded fashion.

TUNEL Assay: Degree of apoptosis was measured in the tumor and non-tumor tissue sections of the colon by TUNEL assay. TUNEL assay (EMD Millipore) was used to determine the number of TUNEL positive cells and total number of epithelial cells of the colon in $2mm^2$ tissue cross-sectional tissue area. 5 sections were randomly selected from

each tissue section and 10 tissue sections were randomly selected from each group. The ratio of TUNEL positive cell to total epithelial cell were used to determine the ratio of apoptosis and plotted as a graph for different treatment groups. All the images were taken in 20X magnification with Nikon e600 microscope.

Alcian blue staining: Standard deparaffinization procedure was followed using xylene and gradation of ethanol. Alcian blue solution (1 %) of pH 2.5 in 3 % acetic acid and nuclear fast red in aluminum sulfate was prepared. Tissues were stained with Alcian blue and counterstained with nuclear fast red solution. Goblet to epithelial cell ratio was counted per crypt with ten crypts per section and five sections per group.

Protein determination using Western Blot: Colon tissue frozen at -80°C was homogenized in RIPA buffer added to protease and phosphatase inhibitors (SIGMA). It was then centrifuged at 10,000 rpm for 15 minutes and supernatant was obtained for protein analysis. Protein concentration in the supernatant was determined by using Bradford protein assay. This was followed by loading equal amounts of protein (50 µg) in each well for a 10% Sodium Dodecyl Sulphate (SDS) gel electrophoresis. The protein from the gel was then transferred to a nitrocellulose membrane (Pall Scientific) and blocked with 5% non-fat dry milk (Biorad) in phosphate buffer saline (PBS) (cellgro) with 0.1% Tween 20. The membrane was incubated overnight with the primary antibody. The -primary antibodies include Gpx-1, Gpx-2 and GAPDH obtained from Genetex. phospho-NFκB p65, NFκB p65, cleaved caspase 9, MDA and Nitrotyrosine were obtained from cell

signaling technology. Membrane was washed by PBS containing 0.1% Tween 20 (Biorad). The membrane was then incubated with secondary antibody (Santa Cruz) followed by another washing step. The last step includes incubating the membrane in ECL substrate (Western Bright, Advansta). The film was developed using by using a developer (SRX-101A, Konica Minolta Medical & Graphic, INC.) in the dark room. Finally the film was scanned and the density of the protein bands obtained was analyzed using Image J software.

Enzyme Linked Immunosorbent Assay (ELISA): Spontaneous secreted cytokines were measured from the tissue incubated in the RPMI medium for 24 hours at 37°C. The media were collected and centrifuged at 2500 rpm for 16 minutes. Pellet was discarded and the supernatant was isolated. Cytokines IL-6, TNF-α, IL-1β and IL-10 levels were measured by using BD OptEIA ELISA kit obtained from BD biosciences and normalized by total protein content estimated by using standard Bradford assay procedure.

Immunofluorescence: Colon tumor tissue sections were deparaffinzed by xylene and dehydrated by different concentration of ethanol. The sections then underwent heat mediated antigen retrieval step with 10nM citrate buffer (Prohisto), 0.05% Tween 20, pH 6.0 in an autoclave at 121°C, 15 psi for 20 minutes. The tissues were then blocked with 10% goat anti-rabbit serum with PBS. Tissues were then incubated in a primary antibody that is cleaved caspase 9 (Cell Signaling Technology) for overnight incubation. This was followed by 5 washing steps and 2 hour- incubation with anti-rabbit secondary antibody (Aexa Flour 488) (Cell Signaling Technology). Finally the tissue section was mounted with a DAPI based mounting media (Genetex) and covered with a coverslip. 10 random 20X

magnification, 2x2 images of the 8 slides per group belonging to different mice were taken and quantified by using Image J software.

Mass Spectrometry: Colon tissues were frozen-dried using lyophilizer and weight prior to be used for mass spectrometry. The tissue was then digested using aqua regia (1 mL of optima grade nitric acid plus 3 mL of optima grade hydrochloric acid) at 140°C and the final volume was brought to 10 ml. The samples were analyzed for Selenium using the Finnigan ELEMENT2 double focusing magnetic sector field inductively coupled plasma-mass spectrometer (ICP-MS). Iridium was used as the internal standard. The instrument was calibrated for element ^{82}Se. The calibration range was from 1.0 to 60 ppb. The R squared value for the initial calibration curve was greater than 0.99. The samples were analyzed immediately after the initial calibration, and the target element results were within the calibration range. The samples were then diluted (5X) and the instrument blank contained 0.31 ppb of Se. The ending continuing calibration verification recovery for Se standard was 112%. The results were then converted to the amount in nanomolar per gram of the colon tissue and plotted on a graph.

Statistical analysis: Two-way and one-way analysis of variance (ANOVA) was used to analyze the data with Tukey post hoc-analyses. A p value<0.05 was considered statistically significant. All the statistical analyses were done by using SigmaStat 3.5 (SPSS).

5.4. RESULTS

Clinical Score:

All the treatment groups were monitored for the changes in the clinical score, which is a combination of weight loss, diarrhea and hemoccult, thrice a week till day 194. Control and Se rich diet were administered on day 25 to all treatment and control groups. WT mice administered control diet in the DSS alone group showed severe clinical manifestation characterized by a significantly higher clinical score when compared to WT mice administered Se rich diet (figure 1a). APNKO mice showed lower clinical score as compared to WT mice after the first DSS cycle in the same treatment group. APNKO mice administered Se rich diet showed a lower clinical score with significance on day 40 after the first DSS cycle when compared to control diet. APNKO and WT mice fed control diet showed significantly higher clinical score as compared to the APNKO and WT mice given Se rich diet. After the third DSS cycle administartion (day 96-194), the difference in the clinical score became even more significant between the Se rich diet and control diet in both WT and APNKO mice and continued to remain high till the date of sacrifice (figure 1a). APNKO mice also showed a higher clinical score than WT given both control and Se rich diet. In the DMH alone group, APNKO and WT mice given control diet showed significantly higher clinical score as compared to the same phenotypic mice given Se rich diet, towards the end of this study (day 185-194). APNKO mice were found to have a higher clinical score as compared to their WT counterparts (figure 1b). In the DSS+DMH

group, no significant difference in the clinical score was found in the WT and APNKO administered control and Se rich diet after the first and the second DSS cycle. However, after the third DSS cycle (day 85-194), both APNKO and WT mice given control diet showed significantly higher clinical score as compared to APNKO and WT mice given Se rich diet. APNKO mice fed either control or Se rich diet showed higher clinical score when compared to WT mice fed the same diet. DSS+DMH treatment group showed the highest clinical score as compared to DSS alone and DMH alone group. Both APNKO and WT mice received control diet continued to show higher clinical score as compared to mice given Se rich diet and APNKO mice showed higher score than WT mice till the date of sacrifice (figure 1c).

Tumor Quantification:

After sacrificed on day 194, mice colon was resected and washed with PBS. Colon was then cut longitudinally and flattened to count tumor number and area (figure 2a). No significant difference in the colon tumor number was found in DSS group with control or Se rich diet. APNKO mice given Se rich diet and treated with DMH alone was found to have significantly lower tumor number as compared to the APNKO mice received control diet in the same group. No significant difference was observed between the WT mice fed control diet and Se rich diet in the DMH group. Significant reduction in tumor number was observed in WT and APNKO mice administered Se rich diet in the DSS+DMH group as compared to the WT and APNKO mice given control diet in the same group. No significant

difference was found in the tumor number of APNKO and WT mice given control or Se rich diet in DSS+DMH group, however APNKO mice received control diet showed greater tumor number as compared to WT counterparts (figure 2b). Tumor area in the DMH group showed no significant difference either phenotypically or between diets. However, APNKO mice with control diet showed larger tumor area as compared to the APNKO mice fed Se rich diet. In DSS+DMH group, significant difference was observed between APNKO and WT mice given the same diet. WT and APNKO mice in DSS+DMH group fed control diet showed significantly larger tumor area as compared to mice given Se rich diet (figure 2c).

Colon Selenium Content:

Mice colon Se content (per gram of tissue) was detected by mass spectrometry using the lyophilized mice colon. The content of the Se was measured in the control and the DSS+DMH group. A significant increase in the content of Se with Se administration was found in both APNKO and WT mice. Control group showed more Se content and APNKO mice showed a decrease in the Se content irrespective of Se rich diet administration (figure 3).

Oxidative stress in tumor and non-tumor colon tissues:

Nitrotyrosine and 4HNE protein expression studies were conducted to determine the degree of oxidative stress in the tumor and non-tumor tissue frozen at -80 ºC. No significant difference was found in the expression of Nitrotyrosine and 4HNE in the colon tumor tissue section of both WT and APNKO mice in DSS+DMH group given control and Se rich diet. Significant decrease in the expression of Nitrotyrosine was found in the colon tissue section of the WT mice given Se rich diet in the DSS+DMH treatment group when compared to WT mice given control diet (figure 4). No significance was observed in the expression of 4HNE in the colon tissue section of WT mice with Se rich or control diet. Significant decrease was also observed in the protein expression of both Nitrotyrosine and 4HNE of colon tissue section of the APNKO mice given Se rich diet when compared to the APNKO mice given control diet (figure 4).

Selenoproteins Activity and Expression:

Colon tissue that was snapped frozen and stored at -80°C was utilized to determine the total Gpx activity in all the treatment groups in addition to Gpx 1 and 2 protein expression. Total Gpx activity was decreased with an increase in severity of the inflammation and cancer. Control group shows the highest Gpx activity with a significant increase in the activity in Se rich diet when compared to control diet in both APNKO and WT mice. APNKO mice

tend to show lower Gpx activity when fed Se rich diet as compared to WT mice given the same diet. In DSS group, no significant difference was found in the GPX activity between Se rich diet and the control diet in APNKO and WT mice (figure 5a). DMH group showed a lower Gpx activity than control and DSS groups. In DMH group, there is a significant increase in the Gpx activity in animals fed Se rich diet as compared to control diet in both APNKO and WT mice (figure 5a). DSS+DMH group showed the least Gpx activity with a significant increase in the Gpx activity with Se rich diet in both APNKO and WT mice in comparison to control diet. There is a significant decrease in the Gpx activity in APNKO mice when compared to WT mice fed Se rich diet. No significant difference was found in the Gpx activity of APNKO and WT mice given control diet (figure 5a). This was followed by more specific approach of identifying the particular selenoproteins including Gpx-1 and Gpx-2. A significant increase in Gpx1 expression was observed with Se rich diet for both APNKO and WT mice, when compared to control diet in control group. No significant difference in the Gpx-1 expression was found in the Se rich and control diet in APNKO mice in DSS alone group. However, we found a significant decrease in Gpx-1 expression with Se rich diet in WT mice as compared to control diet in DSS alone group. In DMH group, no significance was observed in the Gpx-1 expression between the Se rich and control diet in WT mice, but APNKO mice showed a significant increase in Gpx-1 expression with Se rich diet. In DSS+DMH group significant increase in the Gpx-1 expression was observed with Se rich diet in both APNKO and WT mice given Se rich diet when compared to control diet (figure 5b and 5c). Gpx-2 expression was also measured by using Western blot. We found a significant increase in Gpx-2 expression in the control group fed Se rich diet when compared to control diet. In DSS group, APNKO mice given

Se rich diet showed a significant increase in the Gpx-2 expression while WT mice showed a significant decrease in the Gpx-2 expression as compared to the control diet (figure 5b and 5d). No significant difference was obtained in DMH alone group (figure 5b and 5c). DSS+DMH group, with highest severity of chronic inflammation and colon cancer manifestation, showed a significant increase in the Gpx-2 activity with Se rich diet for both APNKO and WT mice when compared to control diet. GAPDH was used as a loading control (figure. 5b and 5c).

Histopathology:

Tissues were stained with Hematoxylin and Eosin (H&E) and analyzed for inflammation, immune cell infiltration and cancer pathology. Colon tissues in the control group showed normal appearing histology with well-formed crypts in mucosal layer without any sign of immune cell infiltration or inflammation (figure 6a). DSS alone group showed infiltration of the immune cells in the lamina propria of the colon of APNKO mice given control diet and to a lesser extent in the WT mice. Se administration was shown to reduce the inflammation and immune cells infiltration in the colon of both the APNKO and WT mice (figure 6a). DMH alone group given control diet showed inflammation and cell infiltration in the lamina propria with aberrant crypts. Se diet administration seems to reduce the severity of the inflammation in both APNKO and WT mice (figure 6a). Finally, mice in DSS+DMH group showed highest degree of inflammation, infiltration and tumorous growth as opposed to animals fed Se rich diet. In DSS+DMH group fed control Se diet,

lamina propria is fully infiltrated with immune cells with a complete changes of the morphology of the muscularis and submucosa layers. WT mice given Se rich diet in the DSS alone group showed a significant decrease in the histopathology score as compared to the WT mice fed control diet in the same group (figure 6b). No significant difference was observed in the APNKO mice between the two diets in DSS alone group, but the APNKO mice had a greater score than WT mice. In addition, DMH group had a higher histopathology score as compared to the DSS group. In DMH alone group, WT mice given Se rich diet showing significantly lower score as compared to the WT mice administered control diet. No significance was obtained between the control and Se rich diet in APNKO mice in DMH alone group, however these mice showed a higher histopathology score than WT mice (figure 6b). DSS+DMH group showed the highest pathological score as compared to other groups. Both WT and APNKO mice with Se rich diet showed a significant reduction in the histopathology score when compared to the same phenotypic mice with control diet. Interestingly, APNKO mice showed a significantly higher clinical score when compared to WT mice given the control diet, but no significance was observed between these groups with Se rich diet (figure 6b).

Cytokine and pshospho-p65 NFκB expression:

To measure the degree of inflammation, spontaneously secreted pro-inflammatory and anti-inflammatory cytokines were measured from the colonic tissue samples incubated at 37 ºC and 5% CO_2 in RPMI medium. This was followed by the study of phosphor-p65

NFκB protein expression. Pro-inflammatory cytokine expression shows no significant difference in the expression of IL-6, TNF-α and IL-1β in the control, DSS alone and DMH alone groups between the Se rich and control diet given to APNKO and WT mice. However, a significant reduction in IL-6, TNF-α and IL-1β levels was observed in APNKO mice given Se rich diet when compared to control diet. WT mice showed no significant difference in the level of IL-6, TNF-α and IL-1β. In general DSS+DMH group showed an increased level of all the pro-inflammatory cytokines including IL-6, TNF-α and IL-1β. APNKO mice showed a significant increase in the expression of anti-inflammatory cytokine IL-10 with Se rich diet when compared to control diet in DSS alone, DMH alone and DSS+DMH group. However no significance was observed in WT mice. A general trend of an increase of the IL-10 and a decrease in IL-6 and TNF-α levels in mice fed Se rich diet was observed in both APNKO mice and WT mice in all the treatment groups.

Colon Epithelial and Tumor Cell Apoptosis:

Colonic tissue sections were prepared to perform TUNEL assay for quantification of apoptosis. No significant difference in colonic epithelial apoptotic cells was observed between Se rich and control diet in WT and APNKO mice in DSS alone and control groups. In DMH group, both APNKO and WT mice fed Se rich diet showed a significant decrease in the TUNEL positive epithelial cells when compared to control diet. APNKO mice showed a significant decrease in TUNEL positive cells when compared to WT mice given control diet in DMH alone group. In DSS+DMH group, highest number of apoptotic cells

was found in all the treatment groups. Significant reduction in the number of apoptotic cells were observed in Se rich fed diet for both APNKO and WT mice when compared to control diet. APNKO mice showed significant decrease in the apoptotic cells when compared to WT mice given both Se rich and control diet. In DSS+DMH group, both APNKO and WT mice showed a significant increase in the TUNEL positive cell in the colon tumor tissue section with Se rich diet as compared to control diet.

Cleaved Caspase 9 and phospho-p53 Expression:

TUNEL assay was followed by the mechanistic search for the molecule(s) responsible for Se mediated apoptosis of the cancer cells. Colon tumor tissue was collected after sacrificing the mice at the end of the study at day 194. Florescence staining and Western blot analyses were performed on the sectioned and frozen colon tumor tissue respectively. Significant increase in cleaved caspase 9 protein expression in the tumor tissue was observed in Se rich diet in comparison to control diet in DSS+DMH group of both the WT and APNKO mice by florescence study and Western blot. Both techniques indicated a significant decrease in the cleaved caspase 9 protein expression in APNKO mice when compared to WT mice given Se rich diet (figure 7). Phospho p53 expression was also determined in the tumor tissue by Western blot indicating a significant increase in phospho-p53 with Se rich diet in both WT and APNKO mice when compared to control diet in the same group (figure 7).

Goblet Cell Production and Muc 2 Expression:

Alcian blue staining was performed in the colon tissue section of the mice belonging to all treatment groups and control group. Ratio of goblet to epithelial cell was calculated and a graph was plotted to determine the effect of Se on goblet cell production. Control group showed the highest ratio of goblet to epithelial cells with DSS group showing the lowest ratio. Significant increase in the ratio was found in the WT mice given Se rich diet when compared to WT mice with control diet belonging to DSS treatment group. No significant difference in the ratio was observed between APNKO mice Se rich and control diet. In DMH group, APNKO mice given Se rich diet showed a significant increase in goblet cell production when compared to APNKO mice given control diet. However, no significance was observed in the WT mice given Se rich and control diet. In DSS+DMH treatment group, both APNKO and WT mice showed a significant increase in goblet to epithelial cell ratio with Se rich diet when compared with control diet belonging to the same genotype and treatment group. Significant reduction in goblet to epithelial cell ratio was found in the in all the treatment groups when compared to the control group. This was further followed by studying the protein expression for Hes-1 and Math-1 in the colon tissue section by using western blot in DSS+DMH treatment group. No significant difference in the expression of Hes-1 was found in the both APNKO and WT mice given control and Se rich diet. However, significant increase in the expression of Math-1 was found in the APNKO and WT mice given Se rich diet when compared to control diet.

This was followed by studying the expression of major mucus protein Muc-2. Muc-2 expression was measured in APNKO and WT mice belonging to DSS+DMH treatment group and significant increase in the protein expression of Muc-2 was found in the APNKO and WT mice given Se rich diet when compared to mice given control diet.

Serum Adiponectin:

To establish a link between Se and APN, serum APN was determined in the WT mice belonging to all treatment group. There was a significant decrease in the levels of serum APN in WT mice belonging to DSS, DMH and DSS+DMH group when compared to control group. In DSS+DMH group, WT mice given Se rich diet showed a significant increase in level of serum APN when compared to WT mice given control. No other group showed any significant increase with Se rich diet administration.

5.5. Discussion:

Colon cancer is one of the major causes of cancer deaths in United States (R. Siegel, et al., 2014). There are several treatments available for patients with colon cancer, but most of the treatment methods have mild to severe side effects depending on the stage of colon cancer and the mode of treatment(Chatterjee et al., 2014; Law, Rogers, & Eng, 2014). Therefore, it's imperative to develop alternative treatment methods or provide

complementary medications that could prevent potential side effects or aid in the treatment of cancer without severe adverse effects. Our previous study indicated that APNKO mice showed increased pathology of CICC (Saxena, et al., 2012). APN administration has been shown to reduce intestinal tumor in $APC^{Min/+}$ mice model of intestinal cancer (Otani et al., 2010). Several studies have reported APN as an anti-inflammatory and anti-cancer adipocytokine (Nagaraju, Aliya, & Alese, 2014; Tae, et al., 2014b). Se has also been used in the treatment of several diseases including autoimmune disease (Kryczyk & Zagrodzki, 2013; Wimmer, Hartmann, Brustbauer, Minear, & Dam, 2014), different types of cancer and disorders like diabetes(Rayman, 2012). Although there have been few studies indicating the protective role of Se in colon cancer, but most of these studies are *in-vitro* or lack the mechanism of action of Se in reducing the severity of colon cancer and chronic inflammation (Barrett et al., 2013; Z. Li, et al., 2013). Other studies have observed an acute effect of Se administration on colon cancer. In this project, we studied the effect and different mechanisms of action of Se rich diet on both APNKO and WT mice with chronic inflammation, cancer and CICC. Se has been used as a prevention in the colon cancer and not as a potential treatment as the Se rich diet was administered to the mice on the same day as DSS or DMH or DSS+DMH.

This study has utilized three different treatment groups including DMH alone, which is a carcinogen and can induce pre-cancerous lesions and colon cancer, DSS alone group to study chronic inflammation and DSS+DMH, which mimics CICC. In order to study the physical attributes of the disease progression clinical score including hemoccult, diarrhea and weight loss was calculated from day 1 till the date of sacrifice (day 194) for

all the treatment groups and control groups. We found a significant reduction in the clinical score with Se rich diet in both APNKO and WT mice given DSS alone in all the three DSS cycle. Decrease in the clinical score was more significant in the second and the third DSS cycle with mice given Se rich diet showing greater protection from DSS insult when compared to the control diet. APNKO mice given control diet showed highest clinical score in the second and third DSS cycle (Clinical Score=8) with an average score of 6. This score was contributed by diarrhea and fecal hemoccult as the APNKO and WT mice didn't show significant weight reduction. APNKO mice tends to have a higher clinical score as APN has been shown to act as an anti-inflammatory and anti-cancerous molecule which prevents colon goblet cells apoptosis and aids in the differentiation of epithelial to goblet cells(Saxena, et al., 2013). This prevents colon from DSS insults leading to lower clinical score of WT mice as compared to APNKO mice. After the third DSS cycle, both APNKO and WT mice given control diet continue to show a significantly higher clinical score as compared to the mice given Se rich diet. This Se mediated protection could be due to the anti-inflammatory role of Se, which protected colon from DSS insult by negatively modulating inflammatory cytokines and proteins in DSS alone and DSS+DMH group(Turanov et al., 2014). DMH alone group showed significance only at the end of the study as DMH is not a very potent carcinogen to induce the pathology required for a higher clinical score (Saxena, et al., 2012). However, a significant reduction in the clinical score was found in the DMH alone group from day 185 till day 194 in APNKO mice given Se rich diet when compared to the control diet. This could be attributed to the antioxidant potential of Se which in turns relates to the reduction in the pre-cancerous lesions induced by DMH (Ghadi, Malhotra, Ghara, & Dhawan, 2013). No significance in the clinical score

was obtained in the WT mice given DMH treatment as our published data indicate that APNKO mice are at increased risk of developing colon cancer as compared to WT mice (Saxena, et al., 2012). Presence of APN provides an additional benefit to WT mice by preventing precancerous lesions and hence lowering the clinical score when compared to APNKO mice. DSS+DMH group is an ideal model for studying chronic inflammation induced colon cancer. Clinical score pattern in this group was very similar to DSS alone group for the first and the second DSS cycle. However, after the third DSS cycle, clinical score remained high around 10, till the date of sacrifice (day 194). Significant reduction in the clinical score was found in both WT and APNKO mice with Se rich diet when compared to control diet. In this group, Se mediated protection is not only restricted to the anti-inflammatory and the anti-oxidant potential, but to the ability of Se leading to the apoptosis of the colon cancer cells causing reduction in tumor size and number and resulting in decreased fecal hemoccult and diarrhea. Significant reduction in the tumor number and area was found in the DSS+DMH treatment group with Se rich diet in both APNKO and WT mice when compared to the control diet. This provided a strong evidence for the Se mediated protection and an explanation for the lower clinical score with Se rich diet. These result could also be explained by the published work of Li et al. 2013 that provided evidence that sodium selenite induces apoptosis of the colorectal cancer cells: HCT116 and SW620 cells via Bax dependent pathway(Z. Li, et al., 2013). No significance was found in the tumor number and area of WT and APNKO mice given Se rich and control diet in DMH alone group except for the tumor number of the APNKO mice. APN has been considered both as pro-apoptotic and anti-apoptotic molecule depending on the disease condition. A recent study by Xing et al., 2015 has shown APN to induce apoptosis in

hepatocellular carcinoma(Xing et al., 2015) while Gao et al, 2014 has published APN to cause no apoptosis of PC-3; human prostate cell line but inhibits proliferation(Gao & Zheng, 2014). Another study by Kato et al., 2014 has shown APN to inhibit cellular proliferation alongwith increased apoptosis with increased caspase-3 and caspase-7 expression(Kato et al., 2014). DMH alone has been known as a mild carcinogen as shown by our previous publication. Although some APNKO mice with control diet show increased tumor area, but the variability in the groups lead to no significant difference. This was followed by an investigation to determine the Se content in the colon tissue supporting our hypothesis that colon Se content was higher in mice given Se rich diet (figure 3).

After mass spectrometry study, the colon tissue was investigated for the markers of oxidative stress. Significant reduction in the oxidative stress was found with Se rich diet in DSS+DMH treatment group as indicated by Nitrotyrosine and 4HNE protein expression studies (figure 4). These data add support to our hypothesis that Se content in the colon is inversely related to oxidative stress. Oxidative stress study in AOM/DSS murine model by Barrett et al. 2013 also indicated that the mice given Se rich diet showed a reduced F_2-isoprostanes (marker of lipid peroxidation and oxidative stress) and DNA damage in response to DSS injury(Barrett, et al., 2013). Se has also been shown to reduce oxidative stress and lipid peroxidation in DMH treated rats(Ghadi, Malhotra, Ghara, & Dhawan, 2012) and its deficiency is associated with higher levels of iNOS and MDA expression in chickens(Yu et al., 2014). We went a step further to determine the selenoproteins responsible for this Se mediated oxidative stress protection by determining the Gpx activity and protein expression. Gpx activity was found to be significantly higher with Se rich diet

with an exception of DSS group. Control group showed the highest while the DSS+DMH has the lowest Gpx activity, but we found a significant increase in the Gpx activity with Se rich diet when compared to control diet. APNKO mice showed lower Gpx activity, which could be due to higher oxidative stress as a result of higher degree of inflammation and cancer pathology. Gpx being a well know antioxidant and major selenoprotein is considered as an anti-inflammatory marker, which was found to be reduced with greater inflammation and cancer(Chen, Prabhu, & Mastro, 2013). To further investigate specific selenoproteins, Gpx-1 and Gpx-2 protein expression were determined as these selenoproteins have been considered as the major selenoproteins of the gut and has been widely studied in colon cancer. Our results indicated an increase in both Gpx-1 and Gpx-2 protein expression with Se rich diet with significance in DSS+DMH group indicating the potential benefit of Se rich diet. Gpx-2 has been shown to be upregulated in colorectal cancer(Chen, Prabhu, & Mastro, 2013; Florian et al., 2001; Murawaki et al., 2008) and is considered both protective and detrimental based on stage of cancer(Chen, Prabhu, & Mastro, 2013). Krehl et al 2011 has shown that Gpx-2 and Se (0.65=4 mg/kg diet) reduced inflammation and tumor in inflammation associated carcinogenesis, which overlaps with our model of CICC (Krehl, et al., 2012).

Above results provide an indication of the protective role of Se and APN in CICC, which lead to further in depth investigation by Hematoxylin and Eosin staining to determine histopathology scoring of colon tissue section. DSS group showed little inflammation and infiltration of the immune cells, however increased inflammation, immune cell infiltration and cancerous lesions along with some visible tumors were found

in DMH alone group. Significant reduction in the pathology scoring was obtained with Se rich diet in WT mice given DMH or DSS alone. DSS+DMH group showed the highest histopathology scoring with severe inflammation and immune cell infiltration along with severe lesions and abundant tumor regions. Significant reduction in the histopathology scoring was obtained with Se rich diet and APNKO mice showed increased pathology when compared to WT mice. APN has been implicated as an anti-cancerous and anti-inflammatory adipocytokine leading to APNKO mice at an increased risk of inflammation and infiltration by immune cells (Saxena, et al., 2012). Lower Se levels has been found in IBD patients indicating the potential use of Se as an anti-inflammatory and anti-cancerous compound(Nagy, et al., 2013).

The above results were supported by studying the expression of phospho-NFκβ p65 and related cytokine including IL-6, TNF-α, IL-1β and IL-10. phospho-NFκβ p65 expression was found to be significantly decreased with Se rich diet in DSS+DMH treatment group. Se has been shown to downregulate NFκβ expression in diabetic rats (Pillai, et al., 2012). Pro-inflammatory secreted IL-6, TNF-α and IL-1β expression was also significantly decreased with Se rich diet in APNKO mice with DSS+DMH treatment. Se deficiency has been shown to increase pro-inflammatory and pro-tumorigenic cytokines with increase DNA damage in AOM/DSS induced colon tumorigenesis (Barrett, et al., 2013). No significance was obtained in WT mice and other treatment groups. APN administration has been shown in APC mice to reduce tumor burden and inflammation (Otani, et al., 2010). These result were similar to the results of our previous publication where APNKO mice showed a heightened pro-inflammatory cytokine response than WT

mice(Saxena, et al., 2012). Full length APN has been shown to reduce the production of inflammatory markers including TNF-α, IL-8 and IL-6. In addition, it was shown to suppress NFκB p65 activation with decreased intracellular ROS levels in OE19 esophageal adenocarcinoma cells.

To further investigate the mechanism of action of Se leading to reduce tumor number and area, TUNEL assay was performed in both the tumor and the non-tumor regions of the colon tissue sections. The degree of apoptosis was quantified by counting the TUNEL positive cells to the total epithelial cells. No significance was obtained in the control and DSS treatment group. Significant reduction in the TUNEL positive cells were obtained in the normal colon tissue section given Se rich diet when compared to the control diet in both WT and APNKO mice in DMH and DSS+DMH treatment group. These data provide an inclination towards the anti-apoptotic role of Se in the non-tumor region of the colon tissue section indicating towards faster epithelial cell removal or the termination of the apoptotic pathway which in turn prevents colon from DSS and DMH insult preventing inflammation, infiltration and cancer pathology. However the data were completely reversed when the tumor region of the same tissue section was analyzed. There was a significant increase in the TUNEL positive cell with Se rich diet in the colon tumor tissue sections of the WT and APNKO mice in the DSS+DMH. Higher apoptosis was also observed in the WT mice when compared to the APNKO mice. These data provide a proof to the *in –vitro* study published by Li et al. 2013 in HCT116 and SW620 colorectal cancer cells proposing the pro-apoptotic role of sodium selenite on cancer cells (Z. Li, et al., 2013). It was also found that APNKO mice had lower degree of apoptosis when compared to WT

in both tumor and non-tumor region of colon tissue section. APN, as previously mentioned, has been shown to be both pro and anti-apoptotic depending on the disease condition. To determine the mode of action of Se and APN as a pro-apoptotic and anti-oxidant, expression of cleaved caspase-9 and phospho-p53 were determined in the tumor tissue section. Significant increase in both cleaved caspase-9 and phospho-p53 expression was found in the tumor tissue section of both WT and KO mice in DSS+DMH treatment groups. Cleaved caspase-9 expression was also determined by immunofluorescence indicating the significantly increased expression and localization of cleaved caspase-9 in tumor region of colon tissue section of both APNKO and WT mice in DSS+DMH group. A recent publication by Gandhi et al. 2014 has shown that supraphysiologic dosage of selenium lead to the apoptosis of cancer stem-like cells derived from chronic or acute myelogenous leukemias by the activation of ATM-p53 dependent apoptotic pathway(Gandhi et al., 2014). Sodium selenite has also been shown to increase the expression of Bax, Bad, Bim and activated caspase-9 alongwith the downregulation of Bcl-xL in xenografted human colorectal carcinoma SW480 cell lines (Y. Yang et al., 2009). We also found a reduction in the expression of cleaved caspase -9 in APNKO mice but no significant changes in phospho-p53 expression indicating that APN may lead to the apoptosis of colon cancer cell by activation of cleaved capase-9. However, *in vitro* siRNA studies are warranted to provide conclusive evidence.

After this we also studied the effect of Se rich diet on goblet cell production and mucus secretion. This was accomplished by using Alcian blue staining and then determining the ratio of goblet to epithelial cells. This study provide the first evidence of

the effect of Se rich diet and APN deficiency on goblet cell production in WT and APNKO mice with CICC. Our study indicated a significant increase in the goblet to epithelial cell ratio with Se administration in both WT and APNKO mice with CICC. WT mice showed higher goblet cells than APNKO. This was followed by the molecular investigation to determine the mechanism for increased goblet cell production. We found a significant increase in Math-1 protein expression with Se rich diet. Math-1 is a basic helix loop helix transcription factor involved in the determination of cell fate in multiple tissues including colon where higher expression of Math-1 is linked with secretory fate of pluripotent colon stem cells (van Es, de Geest, van de Born, Clevers, & Hassan, 2010). Higher expression of Math-1 is linked with increase goblet cell phenotype. Muc-2 mucin expression was determined by using western blot and we found a significant increase in Muc-2 production with Se rich diet in both APNKO and WT mice with CICC. Muc-2 is one of the major secretory mucin of the colon and forms the main component of the protective mucus layer. Suppression of Muc-2 is associated with higher secretion of IL-6 and has been found to aid in tumor growth (Shan et al., 2014). Muc-2 has also been shown to suppress inflammation of the intestinal tract and inhibit intestinal tumorigenesis (Van der Sluis, et al., 2006; Velcich, et al., 2002). Our study provided evidence that the Se rich diet is effective in increasing goblet cell production and mucin secretion which might be protective in itself by shielding the colon from toxic insults and gut bacterial infiltration. Further studies could be required to define the expression of other mucins which forms a part of the colon mucus to define other mechanism by which Se could enhance colon mucus secretion.

5.6. Conclusion:

Although there have been several studies indicating the protective role of Se and APN in colon cancer, but most of these studies are *in-vitro*, xenograft or lack the mechanism of action. Our study used a chronic model of inflammation induced colon cancer and compared it with the just chronic inflammation induced by DSS and pre-cancerous lesion by DMH. CICC by DSS+DMH is one of the most accepted model of colorectal cancer as it mimics most of the condition associated with human colorectal cancer. APNKO mice were also used in this study, which indicated a possibility of using both APN and Se as a complementary treatment for colorectal cancer. Our study has indicated a dual nature of Se as a pro-apoptotic molecule for cancer cells and at the same time providing protection to normal colon epithelial cells leading to faster epithelial cell renewal which lead to further reduction in the inflammation, immune cell infiltration and colon insult. It also provided evidence for the preventive nature of Se by increasing goblet cell production and mucus secretion. Absence of APN has also been related with severe pathology, increased inflammation and reduction of colon cancer cell apoptosis culminating in to higher degree of CICC. This study although providing several important conclusions has some limitations. Se was given in the form of food pellets which leads to unequal intake of Se by mice depending on their food consumption. DSS was administered through water which again result in differential consumption of DSS by different mice in the same which could be one of the cause of higher variability in the tumor size in DSS+DMH treatment group.

This study provided sufficient evidence to further investigate the role of Se and APN as an anti-tumor and anti-inflammatory protective non-metal antioxidant and adipocytokine respectively. Further studies exploring the role of Se and APN in other models of colon and intestinal cancer and their effect on goblet cell and mucus production, changes in gut permeability and the diversity in the gut microbiome may provide further indication of the mechanism of action of both of these anti-inflammatory and anti-cancer molecule in inflammation and colorectal cancer.

5.7. Figure Legends:

Figure 5.1. Clinical Score: The 3 graph represents clinical score for 3 different treatment groups including DSS, DMH and DSS+DMH. Clinical score is a culmination of hemoccult, diarrhea and weight loss. One way and two way Analysis Of Variance (ANOVA) was used to calculate significant difference between different groups. Significant difference was calculated between Se rich and control diet with in the same phenotype and between APNKO and WT mice either given Se rich or control diet. *$p<0.05$ and $^{\#}p<0.01$. (n=10).

Figure 5.2. Tumor Quantification: (A) Colon tissue stained with 2% Methylene blue to represent tumor number and tumor in APNKO and WT mice give Se rich and control diet. **(B)** Graph representing the tumor number in APNKO and WT in DSS, DMH and

DSS+DMH treatment group given Se rich and control diet. **(C)** Graph representing the tumor area (mm^2) of the APNKO and WT mice in DMH and DSS+DMH treatment group given Se rich and control diet. Significant difference was calculated using one way (ANOVA) was used to calculate significant difference between different groups. *$p<0.05$ between WT and WT+Se in DSS+DMH treatment group and KO and KO +Se in DMH alone treatment group. $^{\#}p<0.01$ between KO and KO+Se in DSS+DMH treatment group. **$p<0.04$ between control and Se rich diet given to WT mice in DSS+DMH treatment group. $^{€}p<0.05$ between WT+Se and KO+Se in DSS+DMH treatment group. $^{¥}p<0.05$ between WT control diet and KO control diet in DSS+DMH treatment group. $^{‡}p<0.05$ between the KO Se rich diet vs WT Se rich diet in DSS+DMH treatment group. (n=10).

Figure 5.3. Mass Spectrometry: Bar graph showing the Se content of the colon tissue in control and DSS+DMH treatment group administered control and Se rich diet. One way ANOVA was used to determine the significant difference between the control diet and Se rich diet belonging to the same treatment and genotype. *$p<0.05$. (n=5).

Figure 5.4. Oxidative Stress: (A) Western blot and ponceau staining for 4HNE and Nitrotyrosine expression representing oxidative stress in DSS+DMH colon tissue section. **(B)** The graph represents the expression level of 4HNE and Nitrotyrosine in APNKO and WT mice give control and Se rich diet in DSS+DMH treatment groups. One way ANOVA was used to determine the significant difference. *$p<0.05$ represents the significant difference between the Se rich and control diet within same genotype. (n=5).

Figure 5.5. Selenoproteins Activity and Expression: (A) Graph representing the Gpx activity (nmol/min/mg protein) in the colon tissue section of the APNKO and WT mice given Se rich and control diet in DSS+DMH, DMH, DSS and control group. **(B)** Western blot images for Gpx-1 and Gpx-2 protein expression in the colon tissue section of WT and APNKO mice give Se rich and control diet belonging to Control, DSS, DMH and DSS+DMH treatment groups. **(C)** Graph showing the expression of Gpx-1 protein in the colon tissue section of both APNKO and WT mice given Se rich and control diet in control, DSS, DMH and DSS+DMH treatment group. **(D)** Graph showing the expression of Gpx-2 protein in the colon tissue section of both APNKO and WT mice given Se rich and control diet in control, DSS, DMH and DSS+DMH treatment group. One way ANOVA was used to determine the significant difference between the Se rich diet and control diet within the same treatment group with same genotype. *$p<0.05$ between Se rich and control diet with same treatment group and genotype. **$p<0.03$ between Se rich and control diet with same treatment group and genotype. $^{\#}p<0.01$ between Se rich and control diet with same treatment group and genotype. $^{\#}p<0.01$ between Gpx activity of KO+Se and WT+Se given DSS+DMH treatment. (n=5).

Figure 5.6. Histopathology Staining and Scoring: (A) The images represents the hematoxylin and eosin stained colon tissue section of both APNKO and WT mice belonging to control, DSS, DMH and DSS+DMH treatment groups. These indicate pathology including inflammation, infiltration of immune cells and tumor associated with

the genotype, diet and treatment. **(B)** Graph representing the histopathology scoring performed after hematoxylin and eosin staining of the colon tissue section. The scoring was performed by 2 investigators in the blinded conditions. One way ANOVA was used to determine the significant difference. *$p<0.05$ between Se rich and control diet with in the same genotype and treatment group. $^{\#}p<0.03$ between WT+control diet and KO+control diet in DSS+DMH treatment group. **$p<0.04$ between WT+control diet and WT+Se rich diet in DSS+DMH treatment group. ***$p<0.01$ KO+control diet and KO+Se rich diet in DSS+DMH treatment group. (n=5).

Figure 5.7. Markers of Inflammation: (A) The image and the graph represents the western blot image and the expression levels of phospho-NFκB p65 and total NFκB p65 in both APNKO and WT mice given control and Se rich diet in control, DSS, DMH and DSS+DMH treatment groups. (n=5) **(B)** Graph representing the levels of secreted cytokines from the colon tissue section, incubated in RPMI media at 37ºC overnight. One way ANOVA was used to determine the significant difference. (n=10) *$p<0.05$ between the Se rich and control diet within the same genotype given the same treatment. $^{\#}p<0.01$ between the Se rich and control diet within the same genotype given the same treatment.

Figure 5.8. TUNEL Assay and Apoptosis: (A) Images showing the TUNEL positive epithelial cells (brown color) in the non-tumor colon tissue section of APNKO and WT mice with Se rich and control diet in control, DSS, DMH and DSS+DMH treatment group. The tissue was counterstained with methyl green. **(B)** Graph representing ratio of the

number of TUNEL positive cells to the total epithelial cells (degree of apoptosis) in APNKO and WT colon tissue section given Se rich and control diet in control, DSS, DMH, DSS+DMH treatment group. **(C)** Figure depicting TUNEL positive colon tumor cells (brown color) in the tumor area of colon tissue section of APNKO and WT mice with Se rich and control diet in DSS+DMH treatment group. **(D)** Graph showing the ratio of the number of TUNEL positive colon tumor cells to the total epithelial cells (degree of apoptosis) in APNKO and WT mice tumor colon tissue section given Se rich and control diet in DSS+DMH treatment group. The scoring was performed by 2 investigators in the blinded conditions. One way ANOVA was used to determine the significant difference. $^{\#}p<0.04$ between the Se rich and control diet within the same genotype and treatment group. ***$p<0.01$ between WT and WT+Se in DMH treatment group. **$p<0.05$ between the Se rich and control diet within the same genotype and treatment group. *$p<0.05$ between WT+Se and KO+Se in DSS+DMH treatment group. (n=5).

Figure 5.9. Cleaved caspase-9 and phospho-p53 expression: (A) Figure shows the fluorescent expression of cleaved caspase-9 (red and pink) in tumor tissue colon section of the APNKO and WT mice given Se rich and control diet in DSS+DMH treatment group. DAPI (blue) is used to stain nucleus of the tumor cells. **(B)** Graph showing the quantification of the fluorescent expression of cleaved caspase-9 in the tumor colon tissue section of the APNKO and WT mice given Se rich and control diet in DSS+DMH treatment group. **(C)** Western blot images showing the expression of cleaved caspase-9, phospho p53 and GAPDH in tumor colon tissue section of the APNKO and WT mice given Se rich and control diet in DSS+DMH treatment group. Bar graphs showing cleaved caspase-9 and

phospho p53 protein expression quantification using Image J software and one way ANOVA was used to determine the significant difference. *$p<0.05$ between Se rich and control diet within the same genotype in DSS+DMH treatment group. **$p<0.05$ between KO+Se and WT+Se in DSS+DMH treatment group. $^{\#}p<0.02$ cleaved capase-9 protein expression in WT+Control Diet and WT+Se diet in DSS+DMH treatment group. (n=5).

Figure 5.10. Goblet Cell production: (A) Figure indicates Alcian blue staining for the colon tissue section of the both APNKO and WT mice in different treatment groups. Blue staining indicates goblet cells while the pink stained cells by neutral red are colon epithelia cells. (B) Graph showing goblet to epithelial cell ratio per view per group. One way ANOVA was used to determine the significant difference. *$p<0.05$ between Se rich and control diet belonging to same phenotype and same treatment group. (n=5).

Figure 5.11. Molecular pathway for goblet cell production and Mucin expression in DSS+DMH treatment group: (A) Western blot image indicating protein expression of Muc-2, Math-1, Hes-1 and GAPDH. (B) Graph showing Muc-2 expression normalized by GAPDH expression in DSS+DMH treatment group. (C) Graph showing Math-1 expression normalized by GAPDH expression in DSS+DMH treatment group. (D) Graph showing Hes-1 expression normalized by GAPDH expression in DSS+DMH treatment group. One way ANOVA was used to determine the significant difference. *$p<0.05$ between Se rich and control diet belonging to same phenotype in DSS+DMH treatment group. (n=5).

Figure 5.12. Serum Adiponectin: Graph showing the level of serum APN in WT mice belonging to all the treatment group and control group with either Se rich or control diet. One way ANOVA was used to determine the significant difference. *$p<0.05$ between Se rich and control diet belonging to same phenotype in DSS+DMH treatment group. (n=10).

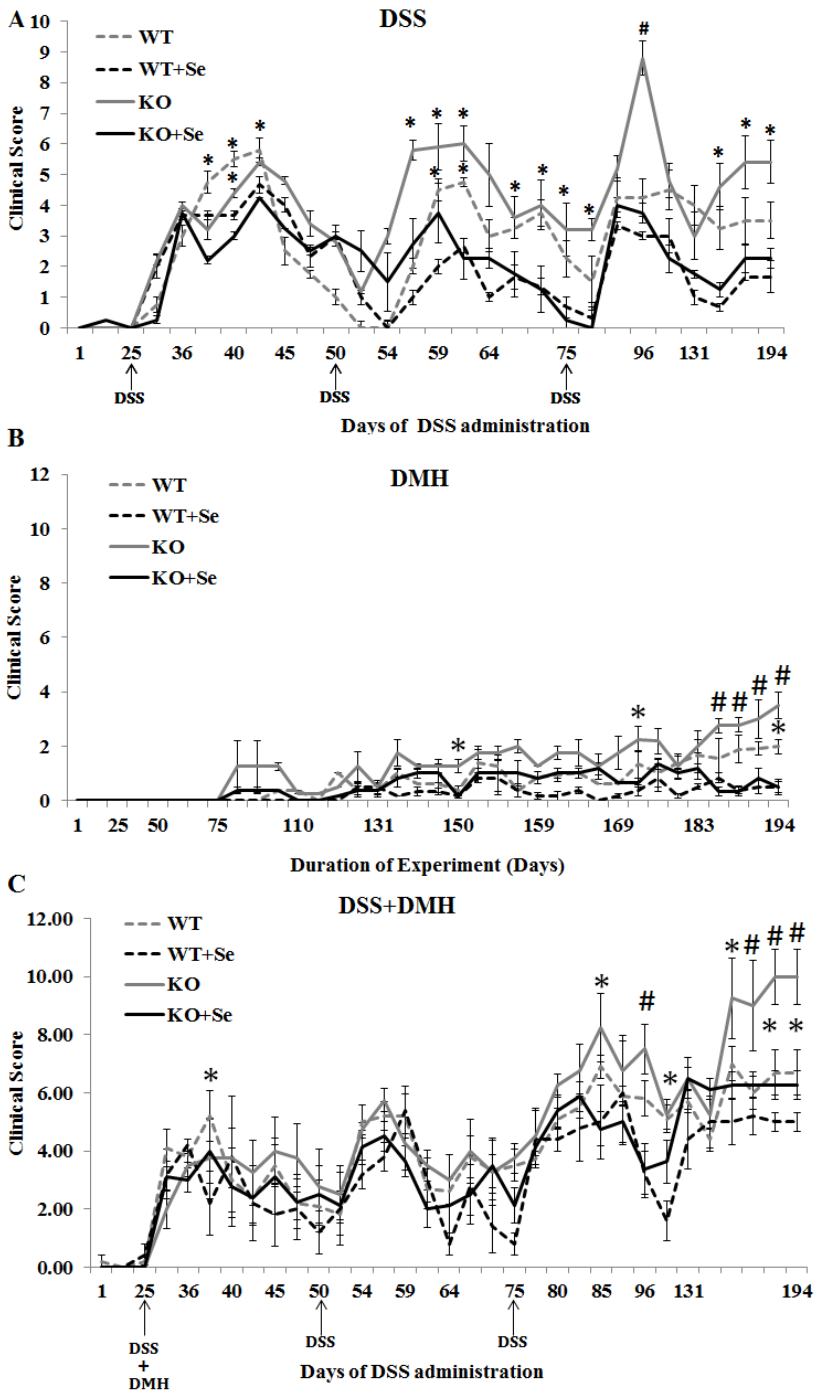

Figure 5.1. Clinical Score: The 3 graph represents clinical score for 3 different treatment groups including DSS, DMH and DSS+DMH. Clinical score is a culmination of hemoccult, diarrhea and weight loss. One way and two way Analysis Of Variance (ANOVA) was used to calculate significant difference between different groups. Significant difference was calculated between Se rich and control diet with in the same phenotype and between APNKO and WT mice either given Se rich or control diet. *$p<0.05$ and $^{\#}p<0.01$. (n=10).

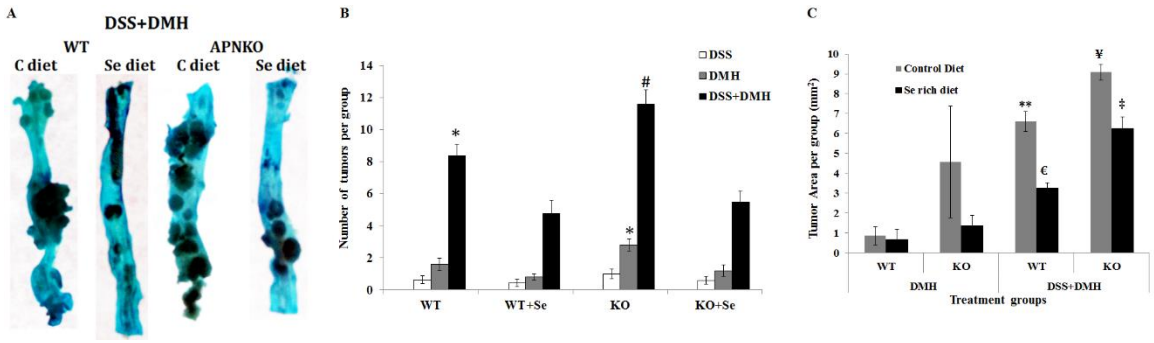

Figure 5.2. Tumor Quantification: (A) Colon tissue stained with 2% Methylene blue to represent tumor number and tumor in APNKO and WT mice give Se rich and control diet. **(B)** Graph representing the tumor number in APNKO and WT in DSS, DMH and DSS+DMH treatment group given Se rich and control diet. **(C)** Graph representing the tumor area (mm^2) of the APNKO and WT mice in DMH and DSS+DMH treatment group given Se rich and control diet. Significant difference was calculated using one way (ANOVA) was used to calculate significant difference between different groups. *$p<0.05$ between WT and WT+Se in DSS+DMH treatment group and KO and KO +Se in DMH alone treatment group. $^{\#}p<0.01$ between KO and KO+Se in DSS+DMH treatment group. **$p<0.04$ between control and Se rich diet given to WT mice in DSS+DMH treatment group. $^{€}p<0.05$ between WT+Se and KO+Se in DSS+DMH treatment group. $^{¥}p<0.05$ between WT control diet and KO control diet in DSS+DMH treatment group. $^{‡}p<0.05$ between the KO Se rich diet vs WT Se rich diet in DSS+DMH treatment group. (n=10).

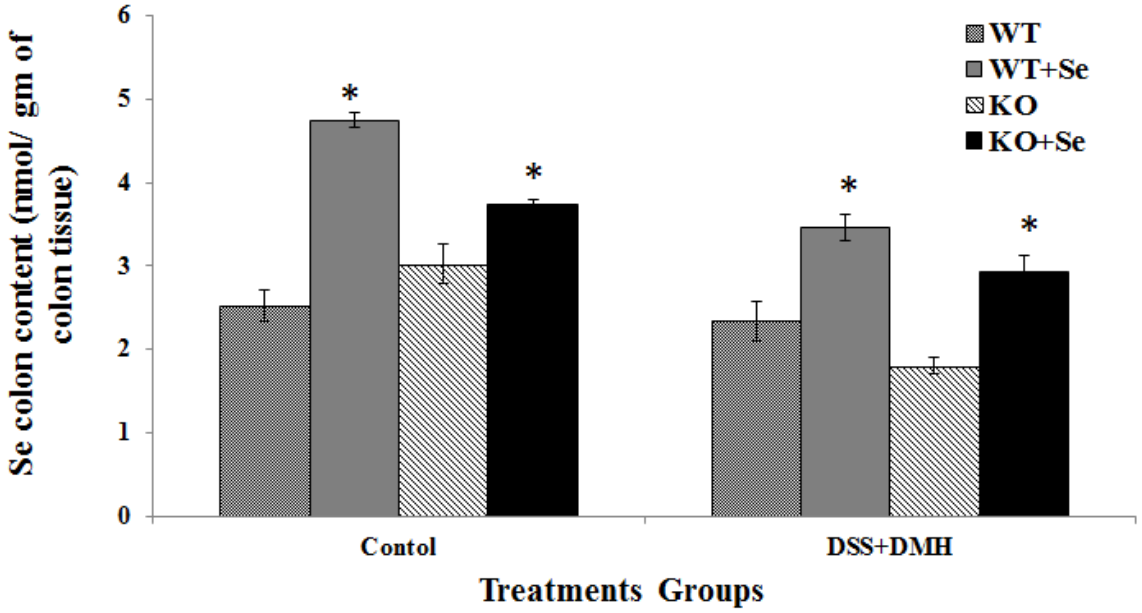

Figure 5.3. Mass Spectrometry: Bar graph showing the Se content of the colon tissue in control and DSS+DMH treatment group administered control and Se rich diet. One way ANOVA was used to determine the significant difference between the control diet and Se rich diet belonging to the same treatment and genotype. *$p<0.05$. (n=5).

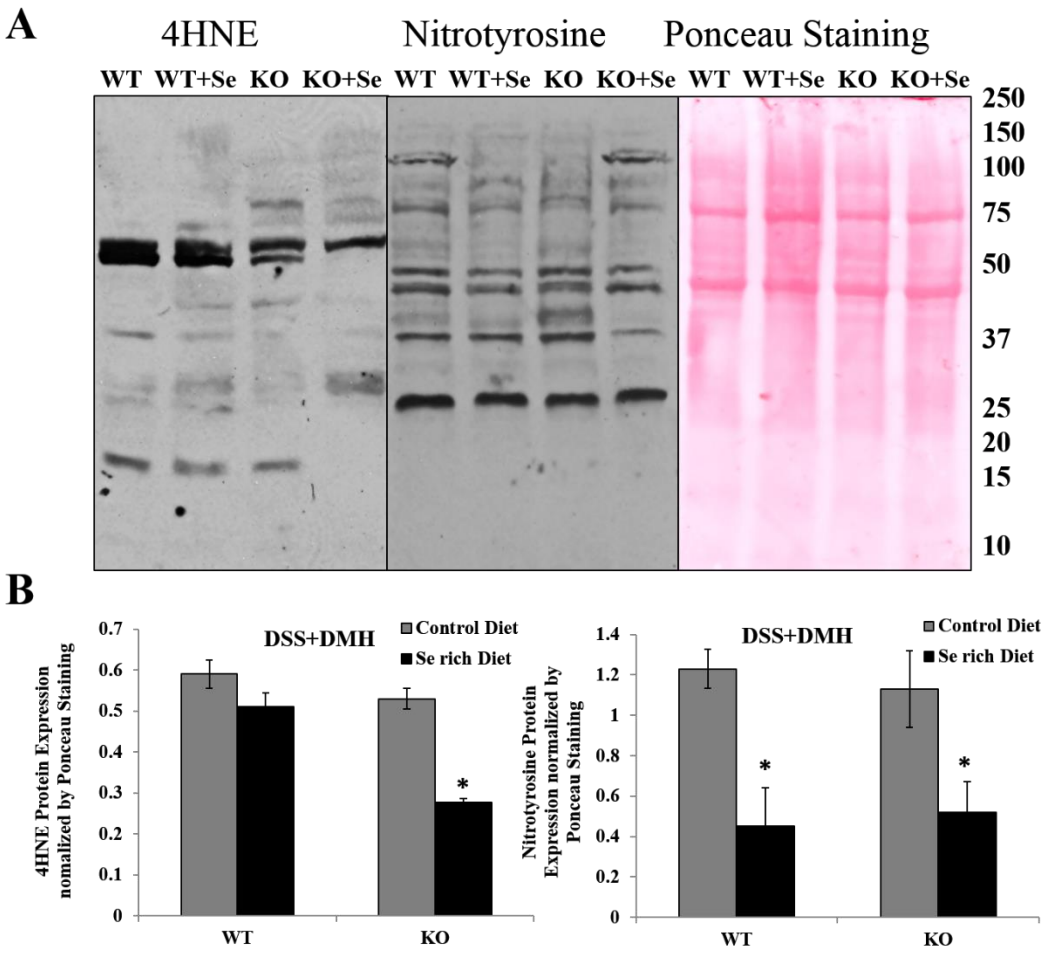

Figure 5.4. Oxidative Stress: (A) Western blot and ponceau staining for 4HNE and Nitrotyrosine expression representing oxidative stress in DSS+DMH colon tissue section. **(B)** The graph represents the expression level of 4HNE and Nitrotyrosine in APNKO and WT mice give control and Se rich diet in DSS+DMH treatment groups. One way ANOVA was used to determine the significant difference. *$p<0.05$ represents the significant difference between the Se rich and control diet within same genotype. (n=5).

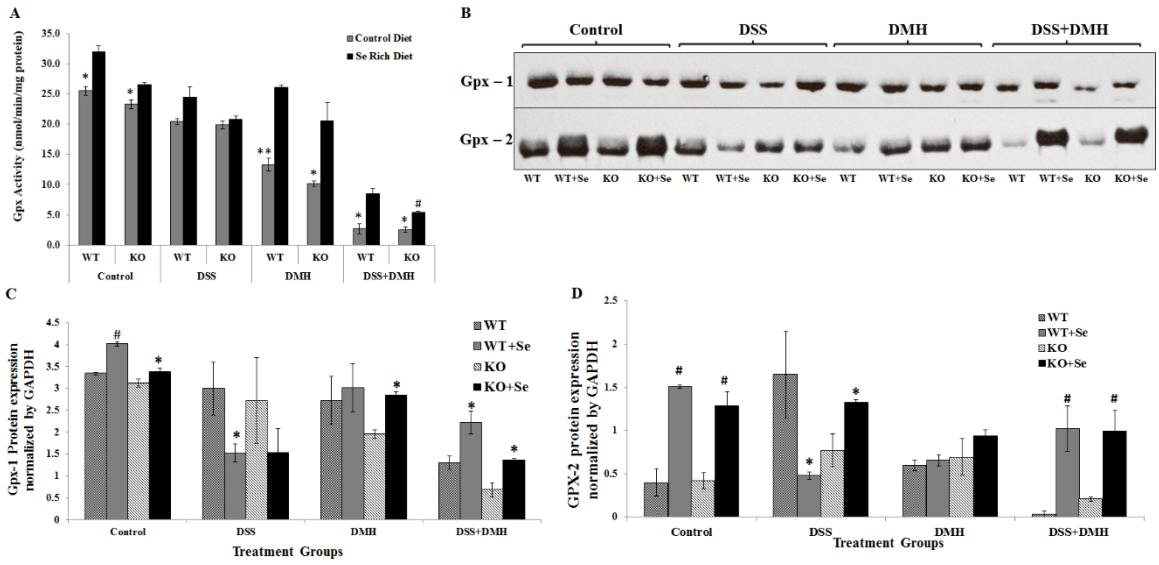

Figure 5.5. Selenoproteins Activity and Expression: (A) Graph representing the Gpx activity (nmol/min/mg protein) in the colon tissue section of the APNKO and WT mice given Se rich and control diet in DSS+DMH, DMH, DSS and control group. **(B)** Western blot images for Gpx-1 and Gpx-2 protein expression in the colon tissue section of WT and APNKO mice give Se rich and control diet belonging to Control, DSS, DMH and DSS+DMH treatment groups. **(C)** Graph showing the expression of Gpx-1 protein in the colon tissue section of both APNKO and WT mice given Se rich and control diet in control, DSS, DMH and DSS+DMH treatment group. **(D)** Graph showing the expression of Gpx-2 protein in the colon tissue section of both APNKO and WT mice given Se rich and control diet in control, DSS, DMH and DSS+DMH treatment group. One way ANOVA was used to determine the significant difference between the Se rich diet and control diet within the same treatment group with same genotype. *$p<0.05$ between Se rich and control diet with same treatment group and genotype. **$p<0.03$ between Se rich and control diet with same treatment group and genotype. $^{\#}p<0.01$ between Se rich and control diet with same treatment group and genotype. $^{\#}p<0.01$ between Gpx activity of KO+Se and WT+Se given DSS+DMH treatment. (n=5).

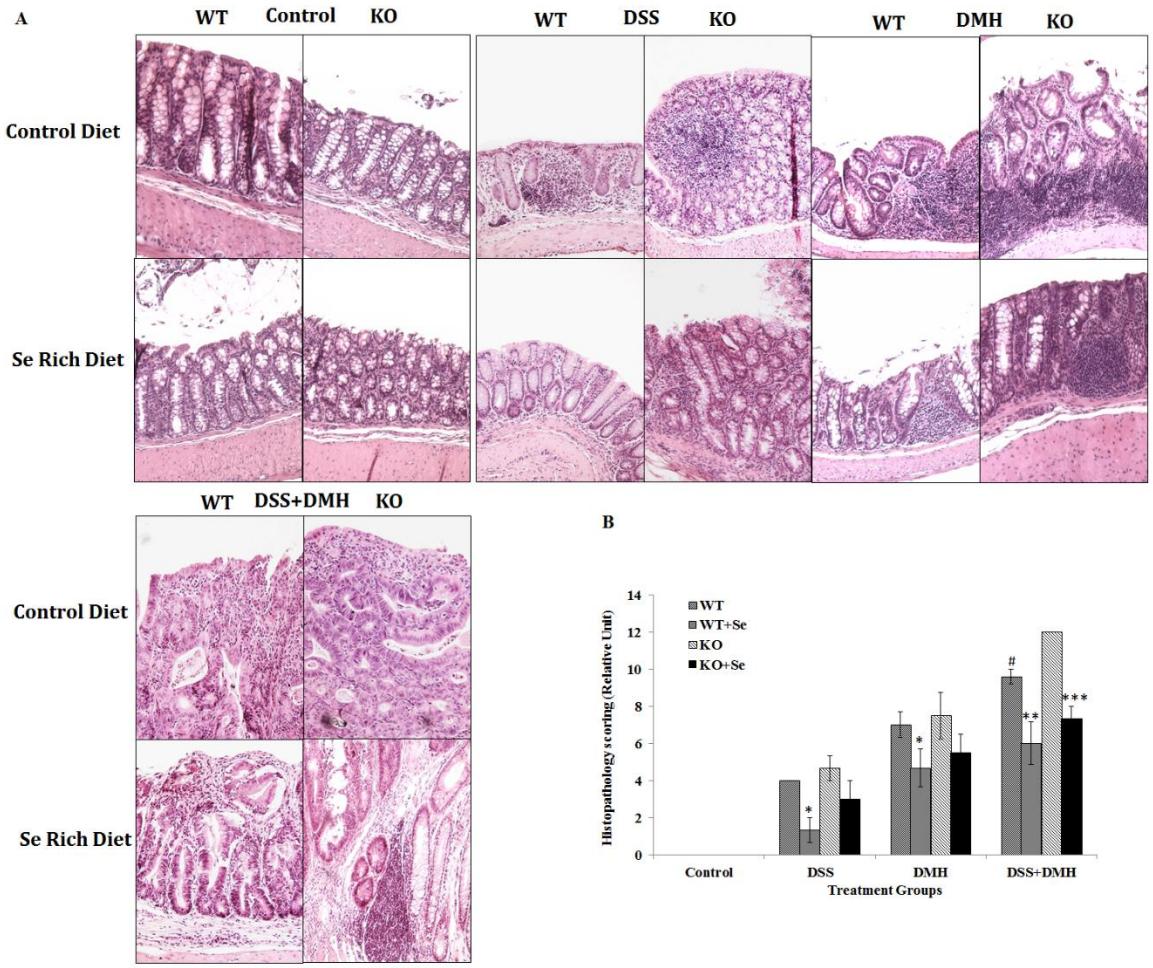

Figure 5.6. Histopathology Staining and Scoring: (A) The images represents the hematoxylin and eosin stained colon tissue section of both APNKO and WT mice belonging to control, DSS, DMH and DSS+DMH treatment groups. These indicate pathology including inflammation, infiltration of immune cells and tumor associated with the genotype, diet and treatment. (B) Graph representing the histopathology scoring performed after hematoxylin and eosin staining of the colon tissue section. The scoring was performed by 2 investigators in the blinded conditions. One way ANOVA was used to determine the significant difference. *$p<0.05$ between Se rich and control diet with in the same genotype and treatment group. $^{\#}p<0.03$ between WT+control diet and KO+control diet in DSS+DMH treatment group. **$p<0.04$ between WT+control diet and WT+Se rich diet in DSS+DMH treatment group. ***$p<0.01$ KO+control diet and KO+Se rich diet in DSS+DMH treatment group. (n=5).

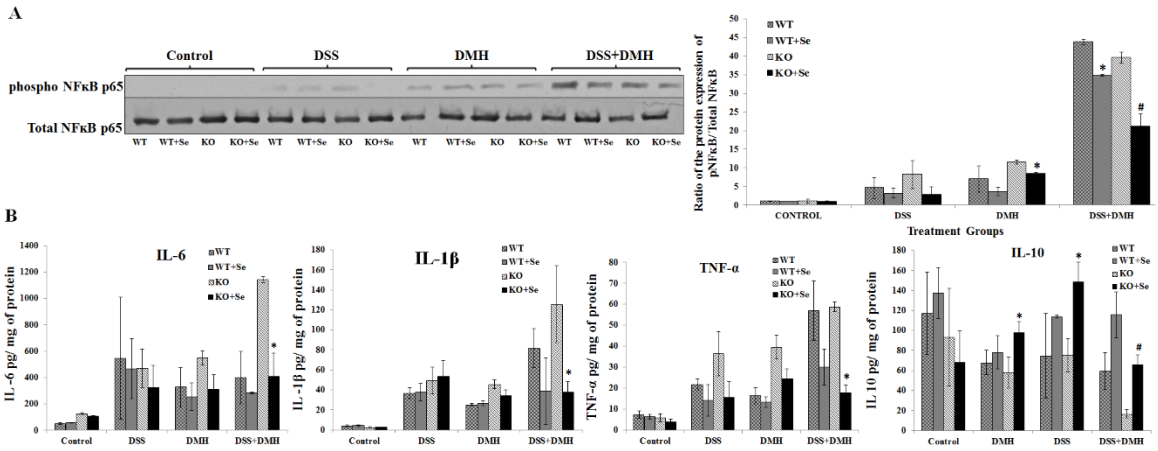

Figure 5.7. Markers of Inflammation: (A) The image and the graph represents the western blot image and the expression levels of phospho-NFκB p65 and total NFκB p65 in both APNKO and WT mice given control and Se rich diet in control, DSS, DMH and DSS+DMH treatment groups. (n=5). **(B)** Graph representing the levels of secreted cytokines from the colon tissue section, incubated in RPMI media at 37ºC overnight. One way ANOVA was used to determine the significant difference. (n=10).*$p<0.05$ between the Se rich and control diet within the same genotype given the same treatment. $^{\#}p<0.01$ between the Se rich and control diet within the same genotype given the same treatment.

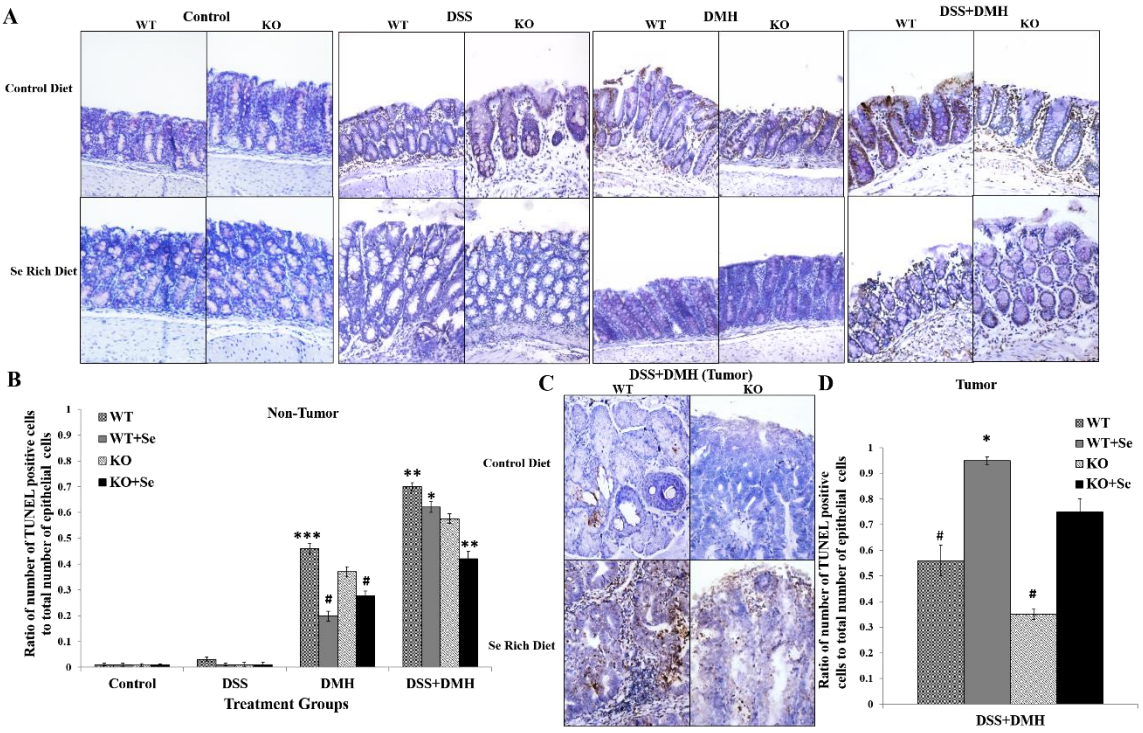

Figure 5.8. TUNEL Assay and Apoptosis: (A) Images showing the TUNEL positive epithelial cells (brown color) in the non-tumor colon tissue section of APNKO and WT mice with Se rich and control diet in control, DSS, DMH and DSS+DMH treatment group. The tissue was counterstained with methyl green. **(B)** Graph representing ratio of the number of TUNEL positive cells to the total epithelial cells (degree of apoptosis) in APNKO and WT colon tissue section given Se rich and control diet in control, DSS, DMH, DSS+DMH treatment group. **(C)** Figure depicting TUNEL positive colon tumor cells (brown color) in the tumor area of colon tissue section of APNKO and WT mice with Se rich and control diet in DSS+DMH treatment group. **(D)** Graph showing the ratio of the number of TUNEL positive colon tumor cells to the total epithelial cells (degree of apoptosis) in APNKO and WT mice tumor colon tissue section given Se rich and control diet in DSS+DMH treatment group. The scoring was performed by 2 investigators in the blinded conditions. One way ANOVA was used to determine the significant difference. $^{\#}p<0.04$ between the Se rich and control diet within the same genotype and treatment group. ***$p<0.01$ between WT and WT+Se in DMH treatment group. **$p<0.05$ between the Se rich and control diet within the same genotype and treatment group. *$p<0.05$ between WT+Se and KO+Se in DSS+DMH treatment group. (n=5).

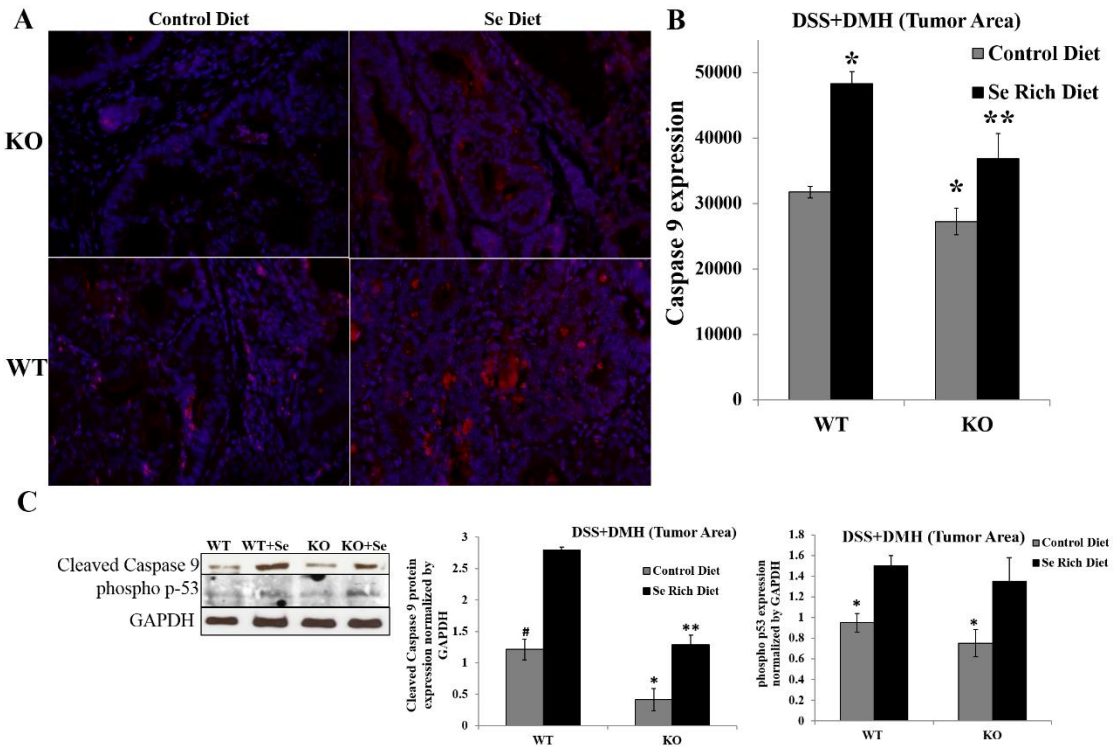

Figure 5.9. Cleaved caspase-9 and phospho-p53 expression: (A) Figure shows the fluorescent expression of cleaved caspase-9 (red and pink) in tumor tissue colon section of the APNKO and WT mice given Se rich and control diet in DSS+DMH treatment group. DAPI (blue) is used to stain nucleus of the tumor cells. **(B)** Graph showing the quantification of the fluorescent expression of cleaved caspase-9 in the tumor colon tissue section of the APNKO and WT mice given Se rich and control diet in DSS+DMH treatment group. **(C)** Western blot images showing the expression of cleaved caspase-9, phospho p53 and GAPDH in tumor colon tissue section of the APNKO and WT mice given Se rich and control diet in DSS+DMH treatment group. Bar graphs showing cleaved caspase-9 and phospho p53 protein expression quantification using Image J software and one way ANOVA was used to determine the significant difference. *$p<0.05$ between Se rich and control diet within the same genotype in DSS+DMH treatment group. **$p<0.05$ between KO+Se and WT+Se in DSS+DMH treatment group. $^{\#}p<0.02$ cleaved capase-9 protein expression in WT+Control Diet and WT+Se diet in DSS+DMH treatment group. (n=5).

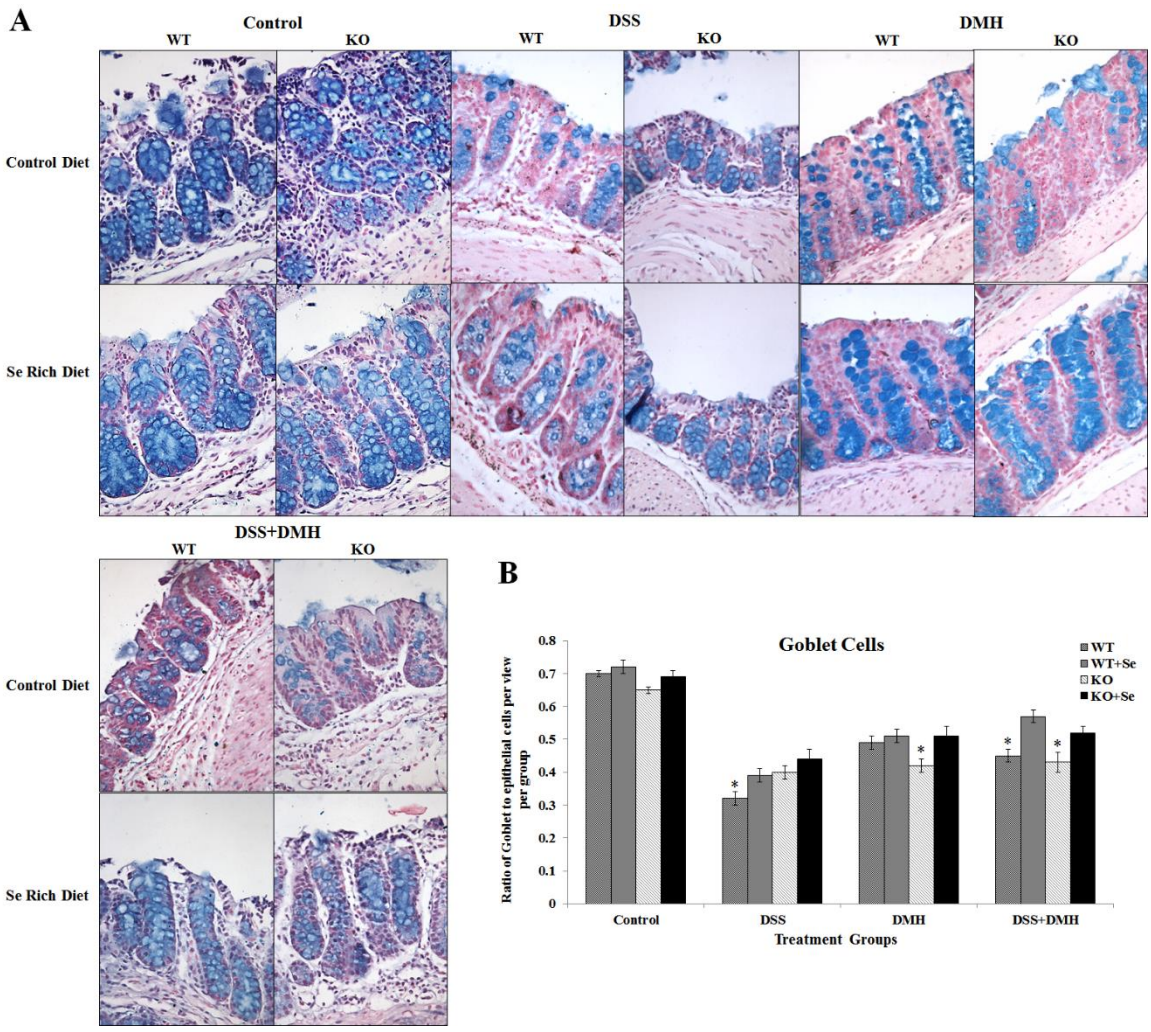

Figure 5.10. Goblet Cell production: (A) Figure indicates Alcian blue staining for the colon tissue section of the both APNKO and WT mice in different treatment groups. Blue staining indicates goblet cells while the pink stained cells by neutral red are colon epithelia cells. (B) Graph showing goblet to epithelial cell ratio per view per group. One way ANOVA was used to determine the significant difference. *$p<0.05$ between Se rich and control diet belonging to same phenotype and same treatment group. (n=5).

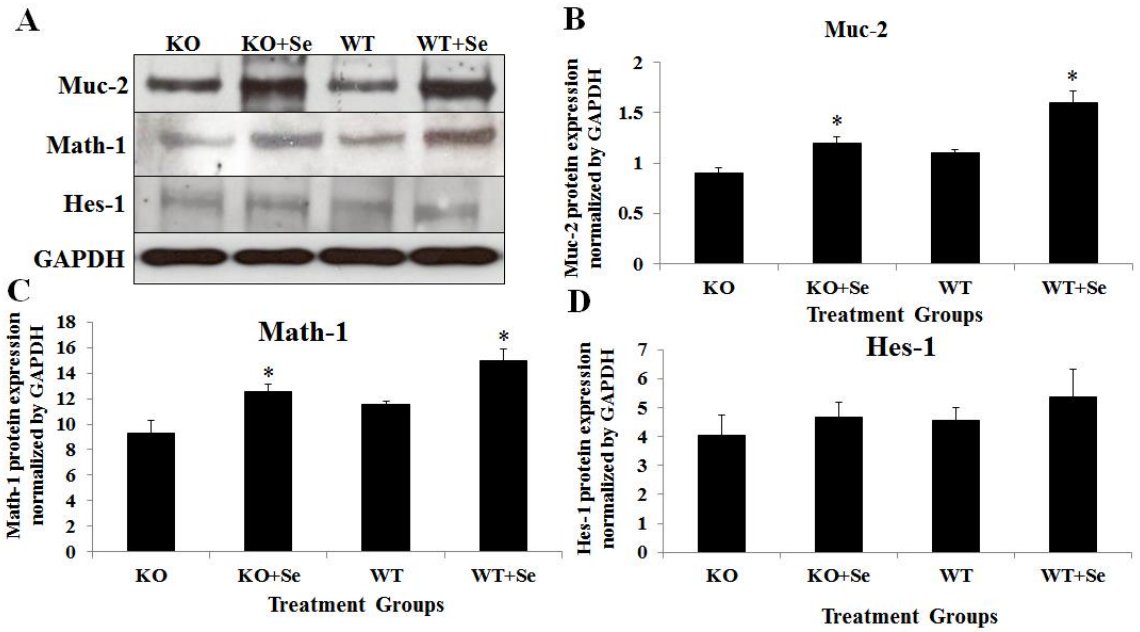

Figure 5.11. Molecular pathway for goblet cell production and Mucin expression in DSS+DMH treatment group: (A) Western blot image indicating protein expression of Muc-2, Math-1, Hes-1 and GAPDH. (B) Graph showing Muc-2 expression normalized by GAPDH expression in DSS+DMH treatment group. (C) Graph showing Math-1 expression normalized by GAPDH expression in DSS+DMH treatment group. (D) Graph showing Hes-1 expression normalized by GAPDH expression in DSS+DMH treatment group. One way ANOVA was used to determine the significant difference. *$p<0.05$ between Se rich and control diet belonging to same phenotype in DSS+DMH treatment group. (n=5).

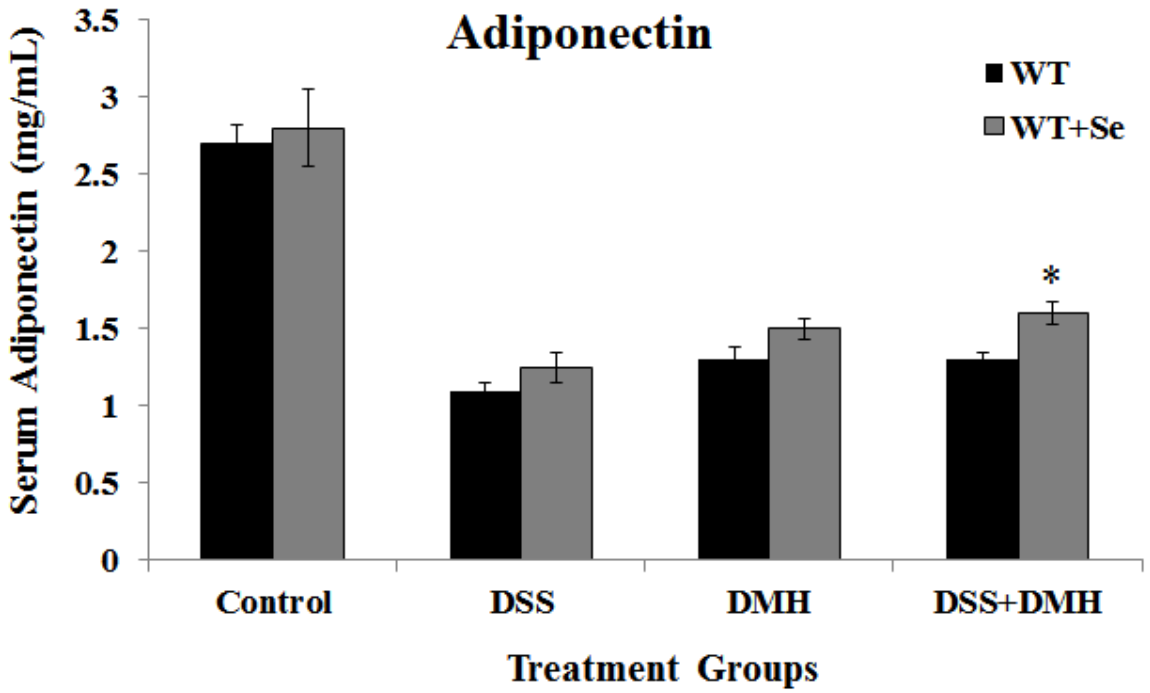

Figure 5.12. Serum Adiponectin: Graph showing the level of serum APN in WT mice belonging to all the treatment group and control group with either Se rich or control diet. One way ANOVA was used to determine the significant difference. *$p<0.05$ between Se rich and control diet belonging to same phenotype in DSS+DMH treatment group. (n=10).

CHAPTER 6

SELENIUM RICH DIET AND ADIPONECTIN ADMINISTRATION ACTS AS A PROTECTIVE AGENTS IN THE TREATMENT OF INTESTINAL CANCER[4]

[4] Arpit Saxena, Kamaljeet Kaur, Samantha Truman, Matthew Rorro, Bianca Larsen, Emma Fletcher, Alexander Chumanevich and Raja Fayad. To be submitted.

6.1 Abstract

Background: Cancer of the digestive tract is the second largest cause of cancer death in United States. Repeated cycles of inflammation or chronic inflammation has been considered as an underlying cause of intestinal cancer and patients suffering from IBD is at an increased risk of developing colon and intestinal cancer. Adiponectin (APN) is an adipocytokine secreted by the adipocyte and absence of APN has been linked with increase severity of chronic inflammation induced colon cancer. Selenium (Se) is a non-metal required by the body as the 21st amino acid selenocysteine and reduces the oxidative stress by increased production of antioxidant selenoproteins. Purpose: The purpose of this publication is to study the effect of Se and APN administration on intestinal cancer. Methods: 4 weeks old APC$^{Min/+}$ mice were randomly assigned to 4 different treatment groups including: Min, Min+APN, Min+Se and Min+APN+Se. Mice were fed either Se rich diet (0.75 ppm) or Se deficient diet (0.02 ppm). Mice were either administered APN or were given PBS once a week intraperitoneally for a period of 15 weeks. Mice were monitored for the clinical score throughout the length of this study. Mice were sacrificed on day 106 and tumor number was counted in both colon and small intestine and tissue was collected for staining and protein expression studies. Result: Mice administered Se or APN or both showed a significant decrease in the clinical score, tumor number and tumor area. Se and APN administration showed a decrease in inflammation but increased cancer cell apoptosis and goblet cell production. Conclusion: APN and Se rich diet might be used as a complementary medicine for the treatment of intestinal cancer.

Keywords: Selenium, Adiponectin, APC$^{Min/+}$, cancer, Goblet cells.

6.2 Introduction

Cancer of the digestive tract is the second largest cause of cancer death in United States. These include the cancer of the colon, rectal and small intestine which contributed to 50,960 deaths in 2015 besides other parts of the digestive tract (R. L. Siegel, Miller, & Jemal, 2015). Repeated cycles of inflammation or chronic inflammation has been considered as an underlying cause of intestinal cancer and patients suffering from IBD is at an increased risk of developing colon and intestinal cancer (E. H. Huang et al., 2006). High fat diet (HFD) is often linked with increased incidence of intestinal cancer and inflammation. HFD has been shown to result in two-fold increase in the colonic tumors when compared with the normal diet (Park, Kim, Seo, & Sung, 2012). Adiponectin (APN) is an adipocytokine secreted by the adipocyte and absence of APN has been linked with increase severity of chronic inflammation induced colon cancer (Saxena, et al., 2012). Serum APN levels is inversely related to obesity and insulin resistance. Epidemiological study has linked lower levels of APN with increased risk of colon cancer in men (Wei, et al., 2005). APN administration (1.5 mg/kg weight of mice) has also been shown to decrease the tumor number in the $Apc^{Min/+}$ mice model of intestinal cancer (Otani, et al., 2010).

Selenium (Se) is a non-metal required by the body as the 21^{st} amino acid selenocysteine and reduces the oxidative stress by increased production of antioxidant selenoproteins. Epidemiological studies had linked lower level of Se with increased risk of cancer and higher intake of Se resulted in the reduced risk for colon, prostate, lung and liver cancer (Combs, 2005; Meyer et al., 2005; Whanger, 2004). Se supplementation at the

supranutritional dosages has been shown to prevent mammary tumor (L'Abbe, Fischer, Campbell, & Chavez, 1989). Methylseleninic acid (MSeA) supplementation has been shown to increase the Se content in intestine, muscle and plasma has been shown to reduce 61% tumor growth. Se has been known to produce selenoproteins in the body which acts as an antioxidant in reducing inflammation and cancer. There are around 30 selenoproteins associated with the mammalian system. Se supplementation has been shown to increase blood glutathione peroxidases (Gpx) activity which is further associated with reduced inflammation and colon cancer (Zeng & Wu, 2015). Gpx2 is the most commonly associated selenoproteins with the gut and has been shown to reduce colon cancer incidence. Se supplementation in humans has been reported to significantly increase Gpx-1 and Gpx-2 protein expression. DMH induced carcinogenesis has been shown to significantly reduce the expression of superoxide dismutase, catalase and Gpx (Ghadi, Ghara, Bhattacharyya, & Dhawan, 2009). Selenium has also been shown to increase the apoptosis of the cancer cells. Sodium selenite induces cell cycle arrest (G2) and apoptosis in the SW620 and HCT116 colon cancer cell line in a dose dependent manner with the increased expression of Bax and downregulation of Bcl_2 (Z. Li, et al., 2013).

Morphology of colon and small intestine changes with inflammation and induction of cancer. Intestine consist of absorptive epithelial cells and secretory goblet cells. Goblet cells secrete mucus that forms a protective layer over the epithelial cell layer of the intestine preventing from harmful toxin and invasion by the gut bacteria which otherwise can lead to severe inflammation and gut related diseases and disorders. Goblet cells like other cells of the intestine are derived from the multipotent stem cells. The fate of the stem cells to

form goblet or epithelial cell lineage depends on the interplay of the genes involved in the Notch signaling pathways including a transcriptional repressor Hairy and Enhancer of split type 1 protein (Hes-1) and basic helix-loop-helix transcription factor Math1 (Wong, 2004; Q. Yang, et al., 2001). Ulcerative colitis is associated with the depletion of goblet cells induced by the suppression of Math1. Math1 is in turn regulated by Hes- 1 expression and Notch signaling (Zheng et al., 2011).

Mucus produced by the goblet cells is a viscous polymer formed by glycoproteins called mucins. There are 15 different mucins genes discovered so far and Muc2 is one of the major mucin found in the colon mucus. $Muc2^{-/-}$ (knockout) mice has been found to develop spontaneous colitis leading to the infiltration of the epithelial cell layer by the gut bacteria (Johansson et al., 2014; Johansson, et al., 2008). Defects in the mucus layer has also been observed in IL-10 knockout mice, which is an ideal model for the study of spontaneous colitis (Hasnain et al., 2013).

$Apc^{Min/+}$ with C57BL/6 background mouse model provides an ideal model of inflammation induced spontaneous intestinal cancer. $Apc^{Min/+}$ mice model has been widely studied for inflammation, cachexia and intestinal cancer. Our earlier publications have provided conclusive evidences of the protective role of Se rich diet in inflammation and colon cancer. Besides this our publications indicate that the absence of APN is related with increased severity of CICC. Colon cancer patients are not only given medication but complimentary treatment including exercise and dietary intervention. Combination of exercise, diet and medication is believed to be the most effective treatment for colon cancer

treatment. On the basis of this idea we hypothesize that the combination of APN administration and Se rich diet alone and in combination will be effective in reducing the tumor burden and severity of intestinal cancer. Se and APN has been used as a prevention for intestinal cancer.

6.3 Material and Methods:

Animal Model: Four week-old $APC^{Min/+}$ and C57BL/6 mice were obtained from Jackson Laboratories and bred in the animal facility at the University of South Carolina under the Institutional Animal Care and Use Committee guidelines. Mice were fed either Se rich diet (0.75 ppm) or Se deficient diet (0.02 ppm). Mice were either administered APN or were given PBS once a week intraperitoneally for a period of 15 weeks. 4 weeks old $APC^{Min/+}$ mice were then randomized into 4 different treatment groups with n=8/group. APN and Se were administered at Day 1 of the experiment (4 weeks $APC^{Min/+}$ and C57BL/6 of age). The groups includes: C57BL/6, $APC^{Min/+}$, $APC^{Min/+}$+APN, $APC^{Min/+}$+Se and $APC^{Min/+}$+APN+Se. Mice were monitored throughout the length of the study for clinical score that includes weight loss, diarrhea and fecal hemoccult. Mice were sacrificed by cervical dislocation under anesthesia on day 106. There was no significant difference in the body weight of $APC^{Min/+}$ and C57BL/6 mice at the beginning of the study.

Selenium Diet Administration and Food Consumption: Selenium rich diet containing 0.75 ppm of Se per kg were administered to 2 groups on day 1 simultaneously with the administration of APN or PBS. The diet was administered till the day of sacrifice that is

day 106. Control diet contains all the components of the Se rich diet except that the Se content is 0.02 ppm per kg of diet. Food consumption was administered throughout the length of the study and average food consumption per mice per group was calculated and a graph was plotted.

Adiponectin Administration: APN was administered intraperitoneally (1.5mg/kg/mice) once a week for total of 16 weeks to $APC^{Min/+}$+APN and $APC^{Min/+}$+APN+Se groups.

Clinical Score: Clinical score was measured for each mouse in each group from day 1 to day 106. Mice were sacrificed after the last clinical score measurement. Clinical score is a combination of diarrhea and hemoccult. Scoring of diarrhea is as follows: 0 = well-formed pellets, 2 = pasty and semi-formed stools that do not adhere to the anus, 4 = liquid stools that adhere to the anus. Detection of blood in the stools was determined using hemoccult kit (BECKMAN COULTER). The higher intensity of blue color indicates greater bleeding. The followings are the score rates for the fecal hemoccult: 0 = no blood, 2 = positive hemoccult, 4 = gross bleeding. The total clinical score was the summation of the individual score of weight loss, diarrhea and fecal hemoccult. The maximum score a mouse could get is 8. The clinical score was calculated and plotted against days of DSS administration. Higher clinical score indicates more severity of colon cancer development in animals.

Colon Tissue and Serum Collection: Blood was collected before sacrifice through retro-orbital puncture and was spun down at 10,000 rpm for 18 minutes and serum was obtained and stored at -20°C to measure APN. Mice colon was excised and flushed clean with PBS. $2mm^2$ colon tissue section with tumor and non-tumor area was fixed in 10% formalin. 24 hours later, tissues was submerged with with 70% Ethanol followed by paraffin embedding and sectioning to obtain 5 µm thin section on glass slide. Sections with tumor and non-tumor areas were snap frozen on dry ice and stored at -80°C for protein analysis. Another $2mm^2$ colon tissue section was incubated in RPMI medium containing 5000 IU/mL and 5000 IU/mL penicillin and streptomycin (CELLGRO) respectively at 37°C and 5% CO_2 for 24 hours. This was followed by centrifugation at 2500 rpm for 15 minutes. Supernatant was obtained and stored at -20°C to measure secreted cytokine levels.

Tumor Number and Tumor Area and Histopathology: Mice colon was excised and flushed with PBS. Tumor number and area were counted under the microscope in all mice of different groups and significant different was calculated between different groups.

Hematoxylin and Eosin staining was used to determine the morphology of mice colon. Histopathology was quantified based on the scoring system indicating the severity of disease and constituting inflammation, immune cell infiltration and degree of tumor. This was on the scale of 12 where highest score of 4 was given for each parameter, where 0 = no infiltration or no inflammation or no cancer; 2 = moderate infiltration or inflammation or pre-cancerous lesions; and 4 = severe inflammation with distorted crypts or infiltration and formation of lymphatic follicles or visible tumors. All the images were

taken in 20X magnification with Nikon e600 microscope. The score was measured by two investigators in blinded fashion.

TUNEL Assay*:* Degree of apoptosis was measured in the tumor and non-tumor tissue sections of the colon by TUNEL assay. TUNEL assay (EMD Millipore) was used to determine the number of TUNEL positive cells and total number of epithelial cells of the colon in $2mm^2$ tissue cross-sectional tissue area. 5 sections were randomly selected from each tissue section and 10 tissue sections were randomly selected from each group. The ratio of TUNEL positive cell to total epithelial cell were used to determine the ratio of apoptosis and plotted as a graph for different treatment groups. All the images were taken in 20X magnification with Nikon e600 microscope.

Alcian blue staining: Standard deparaffinization procedure was followed using xylene and gradation of ethanol. Alcian blue solution (1 %) of pH 2.5 in 3 % acetic acid and nuclear fast red in aluminum sulfate was prepared. Tissues were stained with Alcian blue and counterstained with nuclear fast red solution. Goblet to epithelial cell ratio was counted per crypt with ten crypts per section and five sections per group.

Protein determination using Western Blot: Colon tissue frozen at -80°C was homogenized in RIPA buffer added to protease and phosphatase inhibitors (SIGMA). It was then centrifuged at 10,000 rpm for 15 minutes and supernatant was obtained for protein

analysis. Protein concentration in the supernatant was determined by using Bradford protein assay. This was followed by loading equal amounts of protein (50 µg) in each well for a 10% Sodium Dodecyl Sulphate (SDS) gel electrophoresis. The protein from the gel was then transferred to a nitrocellulose membrane (Pall Scientific) and blocked with 5% non-fat dry milk (Biorad) in phosphate buffer saline (PBS) (cellgro) with 0.1% Tween 20. The membrane was incubated overnight with the primary antibody. The primary antibodies include Muc-2, Gpx-2 and GAPDH obtained from Genetex. cleaved caspase 9, 4HNE and Nitrotyrosine were obtained from cell signaling technology. Hes-1 and Math1 were obtained from abcam. Membrane was washed by PBS containing 0.1% Tween 20 (Biorad). The membrane was then incubated with secondary antibody (Santa Cruz) followed by another washing step. The last step includes incubating the membrane in ECL substrate (Western Bright, Advansta). The film was developed using by using a developer (SRX-101A, Konica Minolta Medical & Graphic, INC.) in the dark room. Finally the film was scanned and the density of the protein bands obtained was analyzed using Image J software.

Enzyme Linked Immunosorbent Assay (ELISA): Spontaneous secreted cytokines were measured from the tissue incubated in the RPMI medium for 24 hours at 37°C. The media were collected and centrifuged at 2500 rpm for 16 minutes. Pellet was discarded and the supernatant was isolated. Cytokines IL-6, TNF-α, IL-1β and IL-10 levels were measured by using BD OptEIA ELISA kit obtained from BD biosciences and normalized by total protein content estimated by using standard Bradford assay procedure.

Serum Adiponectin: Serum APN was determined in all the treatment groups at the end of the study. This was achieved by diluting the serum samples to 1:2000 and performing ELISA using DuoSet mouse/Acrp30 kit (R&D SYSTEMS).

Statistical analysis: Two-way and one-way analysis of variance (ANOVA) was used to analyze the data with Tukey post hoc-analyses. A p value<0.05 was considered statistically significant. All the statistical analyses were done by using SigmaStat 3.5 (SPSS).

6.4 Results

Effect of Se and APN on clinical score, body weight and average food consumption:

Clinical score is a combination of diarrhea and hemoccult. Mice were administered either Se rich diet or control diet (Se deficient diet) on day 1 with simultaneous administration of either APN or PBS depending on the treatment group. Greater clinical score is associated with higher degree of severity of intestinal cancer. Clinical score is compared between 4 different groups including Min, Min+APN, Min+Se and Min+APN+Se. Min group showed the highest clinical score while Min+APN+Se showed the lowest score. Min+APN and Min+Se showed similar pattern of clinical score and showed very less to no significant difference. Min+APN+Se showed zero clinical score till day 50 and was significantly lower when compared to Min, Min+APN and Min+Se. Min group showed significantly higher clinical score on day 12, 17, 26, 33,38, 57, 78, 87, 94, 101 and 108 when compared with other treatment groups including Min+APN, Min+Se

and Min+APN+Se. In addition to clinical score, body weight was also monitored throughout the length of this study. All the mice in different groups including control has the same starting body weight. No significant changes in the body weight were observed till day 52. After day 54, changes in the body weight began to appear between different treatment groups. Body weight continue to increase till day 50, followed by a decrease in body weight of Min and Min+APN. However body weight of mice in control, Min+Se and Min+APN+Se continue to increase till day 108. Body weight of mice in Control, Min+Se and Min+APN+Se was found to be significantly higher than the Min and Min+APN on day 78, 87, 94. 96, 101 and 108. No significant difference in the food consumption was found during the length of the study between different treatment groups.

Colon and small intestine tumor load:

Colon and small intestine polyp count was determined by staining the colon and small intestine with 2% methylene blue and counting the tumor under a microscope. Min group has the highest number of tumor in both colon and small intestine with an average around 5 and 65 for colon and small intestine respectively. Significant reduction in the number of colon and small intestine tumor was found in Min+APN, Min+Se and Min+APN+Se when compared with Min ($^{*}p<0.05$). Significant reduction in tumor number in both colon and small intestine was also found in the Min+APN+Se group when compared with Min+APN ($^{\#}p<0.05$).

Se and APN administration reduces histopathology score:

Hematoxylin and Eosin staining is used to study the mouse small intestine histology to assess inflammation, immune cell infiltration and degree of cancer. Severity of each is measured as defined in the method section and histopathology score was assigned to each group. Control group showed no sign of inflammation, infiltration or any tumor pathology. Min group showed the highest histopathology score ranging from 8 to 12 while Min+APN+Se showed the lowest histopathology score with the score ranging from 4 to 6. This group either showed very less or no tumor and hence the maximum score could not have exceeded 8. Significant difference was calculated between different treatment groups in comparison to each other. Both Min+Se and Min+APN+Se showed significant reduction in the histopathology score ($p<0.05$) as compared to Min. Min+APN showed no significant decrease in the histopathology score when compared to Min, however it was significantly higher in comparison to Min+Se and Min+APN+Se ($^{\#}p<0.05$).

Cytokine Production:

Secreted cytokine production was measured for different treatment groups in the RPMI medium solution obtained by incubating $2mm^2$ small intestine tissue at 37°C for 24 hours. Four different secreted cytokines were measured for all treatment groups and control. IL-6, IL-1β and TNF-α levels were found to be highest in the Min treatment group and lowest in the Min+APN+Se. Min+Se showed significantly lower IL-6 when compared to Min, however no significant reduction was found in comparison to Min+APN and

Min+APN+Se. Min+APN+Se was found to have significantly lower secreted IL-6, IL-1β and TNF-α in comparison to Min. Significant reduction in secreted TNF-α was also observed in Min+APN+Se when compared to Min+APN. No significance in any of the pro-inflammatory or TH_1 secreted cytokines was observed between Min+Se and Min+APN+Se. However reduction in the secreted pro-inflammatory cytokines was observed in Min+APN+Se when compared with Min+Se. IL-10, being an anti-inflammatory cytokine or a TH_2 cytokine showed different secretion pattern in different treatment groups. Highest level of IL-10 was found in Min+APN+Se treatment groups while the lowest level was found in Min. Significant decrease in secreted IL-10 was found in the Min and Min+APN when compared to the control group ($^{*}p<0.05$). Significant increase in the IL-10 secretion was also detected in the Min+APN+Se when compared with Min, Min+APN and Min+APN+Se ($^{\#}p<0.05$). No significance was observed in the Min, Min+APN and Min+Se when compared amongst each other. No significance was also observed when comparing IL-10 secretion between control and Min+Se.

Serum Adiponectin:

APN was measured in the serum of all the treatment groups. Min and Min+APN group showed a significant reduction in the serum APN when compared with control group ($^{**}p<0.05$). Min+Se and Min+APN+Se showed a significantly higher serum APN when compared with Min and Min+APN ($^{\#}p<0.05$) treatment groups. Min+Se showed a significantly higher APN in comparison to control group ($^{*}p<0.05$). No significant increase in the serum APN was observed in the Min+APN+Se when compared to control group.

Goblet Cell Production and Muc 2 expression:

Goblet cell production was measured using Alcian blue staining and counting the ratio of the goblet to epithelial cell. Goblet to epithelial cell ratio was found to be significantly reduced in Min group when compared to control group ($^{\#}p<0.05$). The ratio was found to be significantly higher in Min+APN, Min+Se and Min+APN+Se when compared with Min ($*p<0.05$). There was no significant difference in the ratio between control, Min+APN, Min+Se and Min+APN+Se.

After studying goblet cell production, protein expression of Muc-2, Hes-1 and Math-1 was determined using western blot. We found a significantly higher Muc-2 expression in Min+APN, Min+Se and Min+APN+Se when compared with Min ($*p<0.05$), however no significant increase was observed when compared with control group. Min showed a significant decrease in expression of Muc-2 when compared with other groups ($^{\#}p<0.05$). All the treatment groups including control showed no significant change in the expression of Hes-1 when compared with each other. Math-1 expression followed the same pattern as Muc-2, where we found a significant increase in expression of Math-1 in Min+APN, Min+Se and Min+APN+Se when compared to Min.

Cancer Cell Apoptosis:

Cancer cell apoptosis was measured by using TUNEL assay where TUNEL positive cells and epithelial cells were counted and ratio of the TUNEL positive cells to epithelial cell was calculated and used to determine the significant difference in cancer cell apoptosis

in different treatment groups. Control group was included to indicate the pathology of the colon and to show the degree of apoptosis that is observed in the normal colon tissue section in comparison to the cancer tissue section. Min showed the lowest degree of cancer cell apoptosis and Min+Se showed the highest degree of apoptosis. Significant increase in the cancer cell apoptosis was observed in Min+APN and Min+Se group when compared to Min (*$p<0.05$). Significant decrease in the apoptosis was observed in the normal tissue section of Min+APN+Se in comparison to Min+APN and Min+Se (**$p<0.05$). No significance in the apoptosis was observed between Min+APN+Se and Control and Min treatment groups. This was followed by cleaved Caspase-9 protein expression studies where we found a significant increase in cleaved Caspase-9 expression in Min+APN+Se when compared with Min and Min+APN.

Oxidative Stress:

To calculate the degree of oxidative stress, Gpx-2 (anti-oxidant expression), nitrosylation and lipid peroxidation (4HNE) was measured. No significant changes in the protein expression of Gpx-2 and 4HNE was observed among the 4 treatment group. However, a significant reduction in the protein expression of nitrotyrsosine was observed in Min+Se group (*$p<0.05$).

6.5 Discussion

Gastrointestinal cancer remains in the top 3 causes of cancer deaths in United States and the world. National cancer institute has estimated that the number of new cases to be 142,110 in the United States in the year 2015. There had been a decline in the number of new cases and cancer deaths in the recent years due to the early screening but still it continue to cause a significantly higher number of cancer death. The etiology of this cancer is very wide and range from genetic pre-disposition to toxic exposure and bad lifestyle (nutrition and exercise). There are several therapies available for the treatment of intestinal cancer but each therapy is associated with its side effects ranging from mild to severe including relapse of the tumor and pain. To ameliorate these side effects and to improve the prognosis and prevent reoccurrence complimentary medicine and therapy need to utilized in addition to the already know treatment. By the means of this publication, we hypothesize that APN administration and Se rich diet can act either alone or in conjugation to reduce the severity of intestinal cancer by acting through several different mechanism discussed in the publication. Se and APN has been used in this study as a prevention of intestinal cancer as these were administered at 4 week of age prior to the development of tumors which is assumed to be at 12 weeks of age.

One the primary outcome of this study is the clinical score and the tumor load which shows the physical manifestation of intestinal cancer and the efficacy of the treatment. We found a significant decrease in the clinical score which was a combination of diarrhea and hemoccult with APN, Se or their combination at several time points during the length of

the study. Min+APN and Min+Se followed a similar clinical score curve and showed significant decrease in the clinical score during several points in the study and at the end of this study. However, mice in Min+APN+Se treatment groups showed a significant reduction in the clinical score till day 61 starting from day 6 and then significantly lower clinical score at the end of the study. This pattern could be attributed to the protective role of both APN and Se in intestinal cancer. Our lab had already provided published evidences of the increase severity of CICC in APNKO mice when compared to WT mice. Se has been regarded as anti-inflammatory non-metal with anti-oxidant properties which could have provided protection form the invasion of immune cell in the colon and delayed the process of inflammation leading to small intestinal tumors. Combination of both APN and Se might have provided added protection form inflammation, infiltration and intestinal cancer polyp formation leading to delayed onset of diarrhea and fecal hemoccult.

After the mice were sacrificed, tumor number in both colon and small intestine was calculated and significant reduction in the tumor number were found in both with different treatment. Min+APN+Se was found to have the lowest number of tumors in both colon and small intestine. Se was found to be more effective in reducing tumor number when compared with APN alone, however the combination provide the highest decrease in the tumor number. This decrease in the tumor number could be due to higher degree of cancer cell apoptosis or could be due to the protection provided by the Se and APN in reducing inflammation and hence reducing tumor number. Otani et al., 2010 published that APN administration showed a significant decrease in adenomatous polyp when compared to the $APC^{Min/+}$ mice without APN administration (Otani, et al., 2010). Another study by Finley

JW., 2003 proved that Se obtained from high-Se broccoli decreased ACF incidence rats with chemically induced colon cancer. Tumor number and volume was also found to be decreased in $APC^{Min/+}$ mice with Se administration (Finley, 2003).

This physical measurements were followed by a more in depth investigation by studying the impact of these treatments on histopathology of the small intestine. This is a more comprehensive approach to study the manifestation of inflammation, infiltration of the immune cells and cancer pathology. Histology of the small intestine is rather more complex than colon in having microvilli at its surface for greater absorption of the nutrition than waster absorption in colon. $APC^{Min/+}$ mice without any treatment showed highest histopathology score with highest level of inflammation, cancer and infiltration of the immune cells. APN administration alone didn't have a significant effect on the reduction of the histopathology score. Se administration either alone or in combination with APN showed a significant decrease in the histopathology score when compared to the $APC^{Min/+}$ mice. Min+APN+Se didn't show greater cancer pathology as it has the lowest tumor number and hence has the lowest score. $APC^{Min/+}$ mice with either Se or APN alone showed lower score due to less inflammation and cancer pathology. This histological data supported the physical outcomes of the experiment leading to lower tumor load and clinical score with different treatment.

Another method of measuring inflammation and severity of disease is by studying the expression of secreted TH_1 and TH_2 cytokines including IL-6, IL-1β, TNF-α and IL-10. We found a significant decrease in the secretion of TH_1: pro-inflammatory cytokines

including IL-6, IL-1β and TNF-α with APN and Se administration and significant increase in the secretion of TH_2 cytokines including IL-10. This indicate a shift in the inflammatory phenotype to anti-inflammatory phenotype providing another proof of protective effect of APN and Se administration. This shift could be useful in reducing the severity of intestinal cancer and related inflammation. Our previous publication indicated that the absence of APN is linked with an increase in secreted pro-inflammatory cytokines and a decrease in anti-inflammatory cytokines.

Another important outcome of this study lies in the relationship between APN and Se rich diet. We found a significant increase in the serum APN with Se rich diet administration when compared to $APC^{Min/+}$ mice without any treatment. Min+Se also showed a significantly higher serum APN when compared with control group. No significant difference was observed in Min+Se and Min+APN+Se groups indicating that Se rich diet is sufficient enough to raise serum APN and could maintain higher levels of serum APN over a period of time. Intraperitoneal injection of APN might prove to be counterproductive in raising APN levels as they might trigger a negative feed loop in Min+Se+APN group leading to reduce secretion of indigenous APN. APN administration in Min+APN group might be effective in raising APN levels significantly higher than Min group but showed a significant reduction in the serum APN levels when compared with control group and might not be as effective in raising serum APN level as Se rich diet. These data provide a proof that Se rich diet might act to increase either APN directly or reducing inflammation and cancer pathology in $APC^{Min/+}$ mice leading to higher levels of

serum APN. Higher levels of serum APN is associated with reduced insulin resistance, lower degree of inflammation and colon cancer (Obeid & Hebbard, 2012).

To further investigate the mechanism of reduction in tumor count, TUNEL assay was performed in the small intestine paraffinized tissue sections in all the treatment group and control group. This was followed by protein expression study of cleaved caspase 9 in tumor tissue section of all the treatment group and normal intestinal tissue of the control group. TUNEL assay showed a significant increase in cancer cell apoptosis in the small intestine tumor region of Min+APN and Min+Se group when compared with Min group. Se administration showed greater cancer cell apoptosis than APN administration. Since Min+APN+Se group showed the least number of tumor therefore no tumor tissue section was obtained in this group and hence the cancer cell apoptosis was not observed in this group. However we observed normal epithelial cell apoptosis which showed no significant difference when compared with control group. To further decipher the mechanism leading to cancer cell apoptosis expression of cleaved capase-9 was studied in tumor tissue section of all the treatment groups and control group. We found a significant increase in the protein expression of cleaved caspase 9 in the tumor tissue section of Min+APN+Se group when compared with Min, Min+APN and control group. We also found an increase in the expression of cleaved caspase 9 in Min+Se group in comparison to Min, Min+APN and control group. This data provide evidence that Se leading to the apoptosis of intestinal cancer cells might be governed by the increased expression of cleaved caspase 9 while APN mediated apoptosis of the intestinal cancer cell may be governed by an alternative apoptotic pathway excluding cleaved caspase 9.

Cancer cell apoptosis was followed by studying goblet cell production and Muc-2 protein expression. Goblet cells are secretory cells of the gut and mainly present in the colon and small intestine. They secrete mucus which forms a protective layer over the intestine and protect it from intestinal insult including toxins and gut bacterial invasion. Reduced mucus production has been linked with increase inflammation and cancer.

Ratio of goblet to epithelial cell was determined using Alcian blue staining and we found a significant increase in the ratio with both Se and APN administration. Min group showed a significant decrease in the ratio when compared with control group pointing towards the protective role of APN and Se in intestinal cancer. However, no significance in the goblet cell production was found among the different treatments. To study the molecular mechanism behind this effect expression of Muc-2, Math-1 and Hes-1 was determined which revealed an increased expression of Math-1 indicating higher conversion of colon stem cell to secretory phenotype. Muc-2 expression was also significantly higher with Se and APN administration indicating an increased mucus secretion which forms a protective layer over the colon and preventing from toxic exposure and gut bacterial invasion.

This study provided conclusive evidence for the protective role of APN and Se in intestinal cancer and identify different mechanism by which Se and APN may act to reduce the severity of intestinal cancer.

6.6 Figure Legends

Figure 6.1. Clinical Score and Body Weight: (A) The graph represents the differences in the clinical score between different treatment groups and control. Significant difference was calculated between the different treatment groups and the control group. *$p<0.05$ between Min and Min+APN, Min+Se and Min+APN+Se. **(B)** The line graph represents the change in the body weight throughout the length of the study. **(C)** Line graph showing average food consumption per mice per day. Significant difference was calculated between different treatment groups. *$p<0.05$ represents the significant difference between Min vs Min+APN, Min vs Min+Se and Min vs Min+APN+Se. Student TTEST was used to determine significant difference between different treatment groups. (n=8).

Figure 6.2. Colon and Small Intestine Tumor Load: (A) The graphs shows difference in colon tumor number in all the treatment groups. *$p<0.05$ shows significant difference in the tumor number between Min vs Min+APN, Min vs Min+Se and Min vs Min+APN+Se. $^{\#}p<0.05$ showed significant decrease in the tumor number between Min+APN+Se vs Min+APN and Min+APN+Se vs Min+Se. **(B)** The graphs shows difference in small intestine tumor number in all the treatment groups. *$p<0.05$ shows significant difference in the tumor number between Min vs Min+APN, Min vs Min+Se and Min vs Min+APN+Se. $^{\#}p<0.05$ showed significant decrease in the tumor number between Min+APN+Se vs Min+APN and Min+APN+Se vs Min+Se. Student TTEST was used to determine significant difference between different treatment groups. (n=8).

Figure 6.3. Histopathology: (A) This figure shows the Hematoxylin and Eosin staining for the small intestine tissue section for the different treatment groups and control. (B) The graph shows histopathology score out of 12 for the treatment groups and control group. *p<0.05 Min+Se and Min+APN+Se vs Min. #p<0.05 Min+Se and Min+APN+Se vs Min+APN. Student TTEST was used to determine significant difference between different treatment groups. (n=5).

Figure 6.4. Secreted Cytokines: (A) Graph represent the differential expression of secreted IL-6 in different treatment groups. *p<0.05 significant difference between Min+Se and Min+APN+Se vs Min. **(B)** Graph represent the differential expression of secreted IL-1β in different treatment groups. *p<0.05 significant difference between Min and Min+APN+Se **(C)** Graph represent the differential expression of secreted TNF-α in different treatment groups. *p<0.05 significant difference between Min+APN+Se vs Min. #p<0.05 significant difference between Min+APN+Se vs Min+APN **(D)** Graph represent the differential expression of secreted IL-10 in different treatment groups. *p<0.05 significant difference between Min and Min+APN vs Control. #p<0.05 significant difference between Min+APN+Se vs Min, Min+APN and Min+Se. Student TTEST was used to determine significant difference between different treatment groups. (n=8).

Figure 6.5. Serum Adiponectin: The graph shows the levels of serum APN (mg/ml) in different treatment groups. *p<0.05 significant difference between Min+Se vs Control. **p<0.05 significant difference between Min vs Control and Min+Se vs Control. #p<0.05 significant difference between Min+Se and Min+APN+Se vs Min and Min+APN. Student

TTEST was used to determine significant difference between different treatment groups. (n=8).

Figure 6.6. Goblet cell production: (A) This figure shows the Alcian blue staining for the small intestine tissue section for the different treatment groups and control. (B) The graph shows the ratio of goblet to epithelial cell for the treatment groups and control group. *p<0.05 Min+APN Min+Se and Min+APN+Se vs Min. $^{\#}$p<0.05 Min vs control. Student TTEST was used to determine significant difference between different treatment groups. (n=5).

Figure 6.7. Change in goblet cell phenotype and Mucin Secretion: (A) Representative Western blot images showing the protein expression of Muc-2, Hes-1 and Math-1 in the small intestine. **(B)** Graph showing the expression of Muc-2 in all the treatment group and control. *p<0.05 significant difference between Min+APN, Min+Se and Min+APN+Se vs Min. $^{\#}$p<0.05 significant difference between Min vs control. **(C)** Graph showing the expression of Math-1 in all the treatment group and control. *p<0.05 significant difference between Min+APN, Min+Se and Min+APN+Se vs Min. $^{\#}$p<0.05 significant difference between Min vs control. **(D)** Graph showing the expression of Hes-1 in all the treatment group and control. No significant difference was found between in any treatment groups and control. Student TTEST was used to determine significant difference between different treatment groups. (n=5).

Figure 6.8. Cancer Cell apoptosis: (A) This figure shows the representative 20X images of TUNEL assay marking cancer cell apoptosis and counterstained with methyl green. The cells of the tumor undergoing apoptosis range from light to dark brown in color. **(B)** Graph representing the quantification of the degree of apoptosis determined by calculating the ratio of the TUNEL positive cell and total number of epithelial cells in a 20X microscopic view. 5 views per slide and 8 animals per group were used to calculate significant difference between different groups. *$p<0.05$ Min+APN vs Min and Min+Se vs Min. **$p<0.05$ Min+APN+Se vs Min+Se Student TTEST was used to determine significant difference between different treatment groups. (n=5).

Figure 6.9. cleaved Caspase 9 expression: Western blot and bar graph represents the differential expression of cleaved caspase 9 in different treatment groups. *$p<0.05$ Min+APN+Se vs Min +APN and $^{\#}p<0.05$ Min+APN+Se vs Min+APN. Student TTEST was used to determine significant difference between different treatment groups. (n=5).

Figure 6.10. Oxidative Stress: This figure shows the protein expression of 4HNE and Nitrotyrosine in Min, Min+APN (MA), Min+Se (MS) and Min+APN+Se (MAS) treatment groups using western blot and the protein expression was normalized by ponceau staining. *$p<0.05$ Min+Se vs Min, Min +APN and Min+APN+Se. Student TTEST was used to determine significant difference between different treatment groups. (n=5).

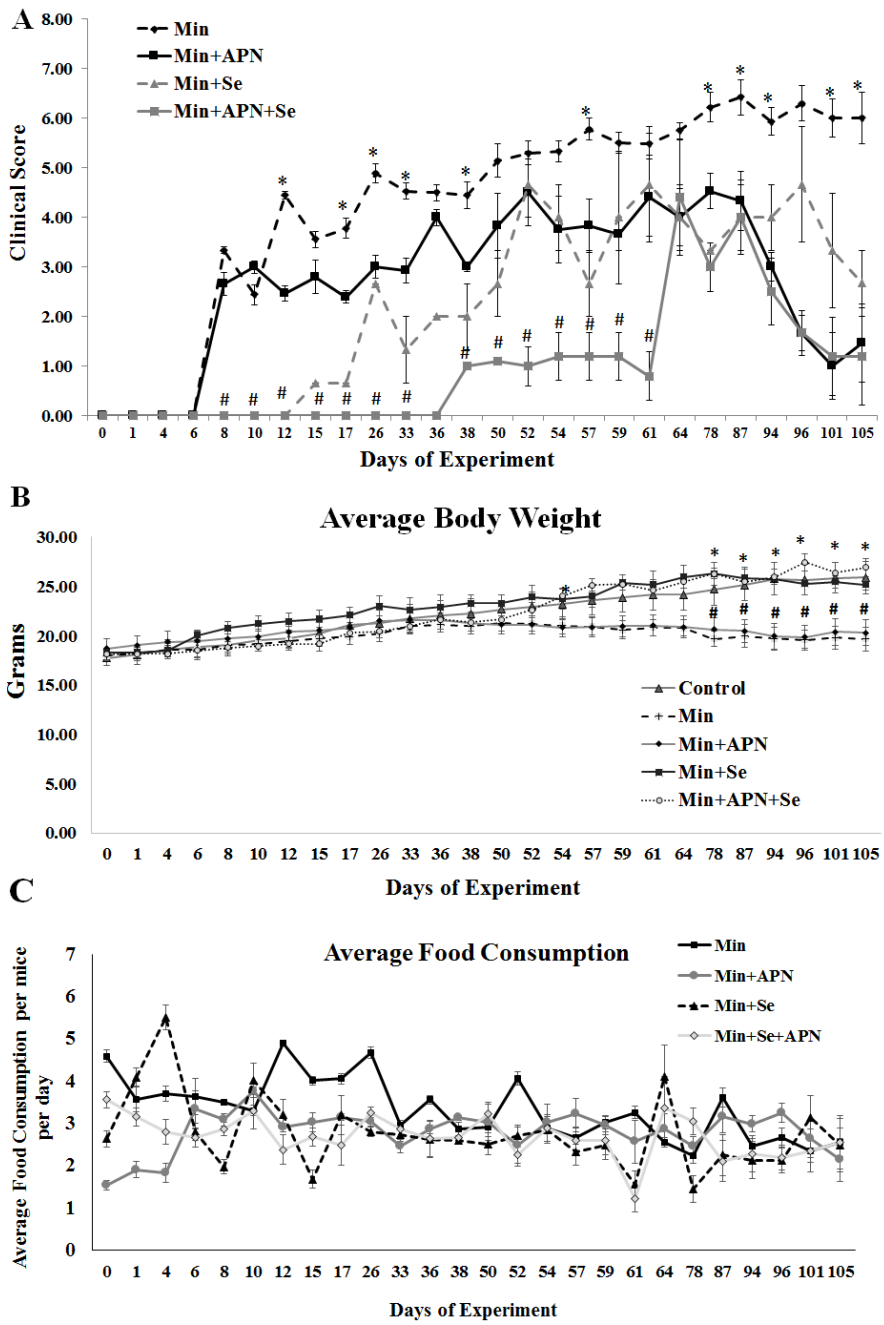

Figure 6.1. Clinical Score and Body Weight: (A) The graph represents the differences in the clinical score between different treatment groups and control. Significant difference was calculated between the different treatment groups and the control group. *p<0.05 between Min and Min+APN, Min+Se and Min+APN+Se. **(B)** The line graph represents the change in the body weight throughout the length of the study. **(C)** Line graph showing the average food consumption per mice per day for the length of the study. Significant difference was calculated between different treatment groups. *p<0.05 represents the significant difference between Min vs Min+APN, Min vs Min+Se and Min vs Min+APN+Se. Student TTEST was used to determine significant difference between different treatment groups. (n=8).

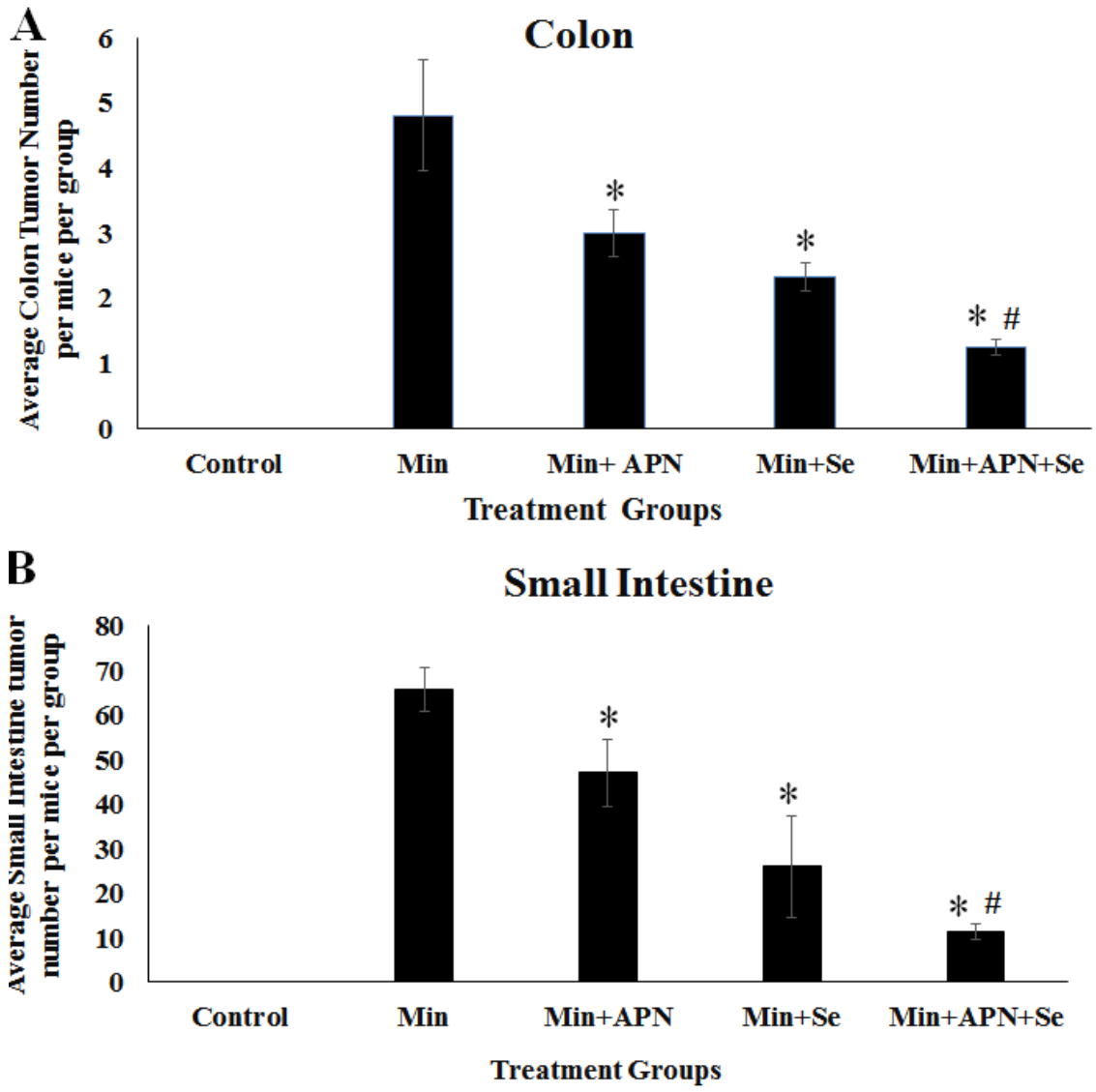

Figure 6.2. Colon and Small Intestine Tumor Load: (A) The graphs shows difference in colon tumor number in all the treatment groups. *$p<0.05$ shows significant difference in the tumor number between Min vs Min+APN, Min vs Min+Se and Min vs Min+APN+Se. $^{\#}p<0.05$ showed significant decrease in the tumor number between Min+APN+Se vs Min+APN and Min+APN+Se vs Min+Se. **(B)** The graphs shows difference in small intestine tumor number in all the treatment groups. *$p<0.05$ shows significant difference in the tumor number between Min vs Min+APN, Min vs Min+Se and Min vs Min+APN+Se. $^{\#}p<0.05$ showed significant decrease in the tumor number between Min+APN+Se vs Min+APN and Min+APN+Se vs Min+Se. Student TTEST was used to determine significant difference between different treatment groups. (n=8).

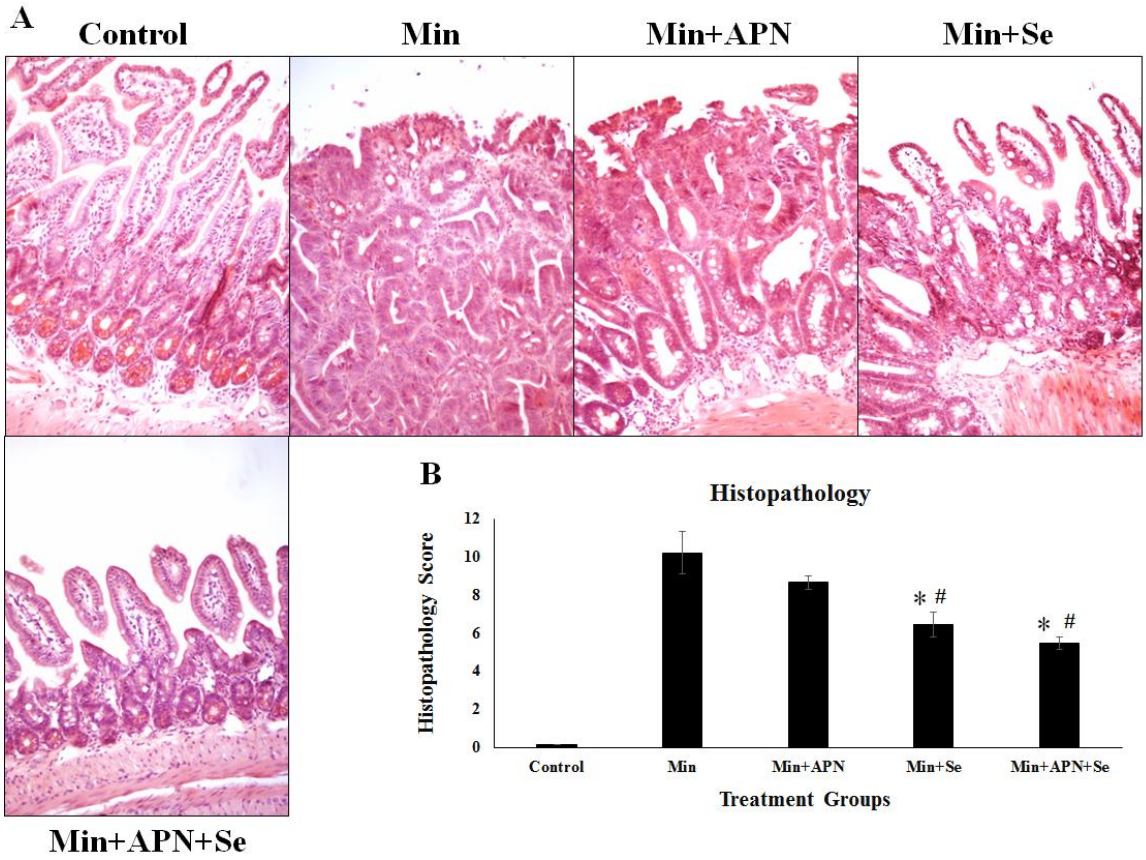

Figure 6.3. Histopathology: (A) This figure shows the Hematoxylin and Eosin staining for the small intestine tissue section for the different treatment groups and control. **(B)** The graph shows histopathology score out of 12 for the treatment groups and control group. *$p<0.05$ Min+Se and Min+APN+Se vs Min. $^{\#}p<0.05$ Min+Se and Min+APN+Se vs Min+APN. Student TTEST was used to determine significant difference between different treatment groups. (n=5).

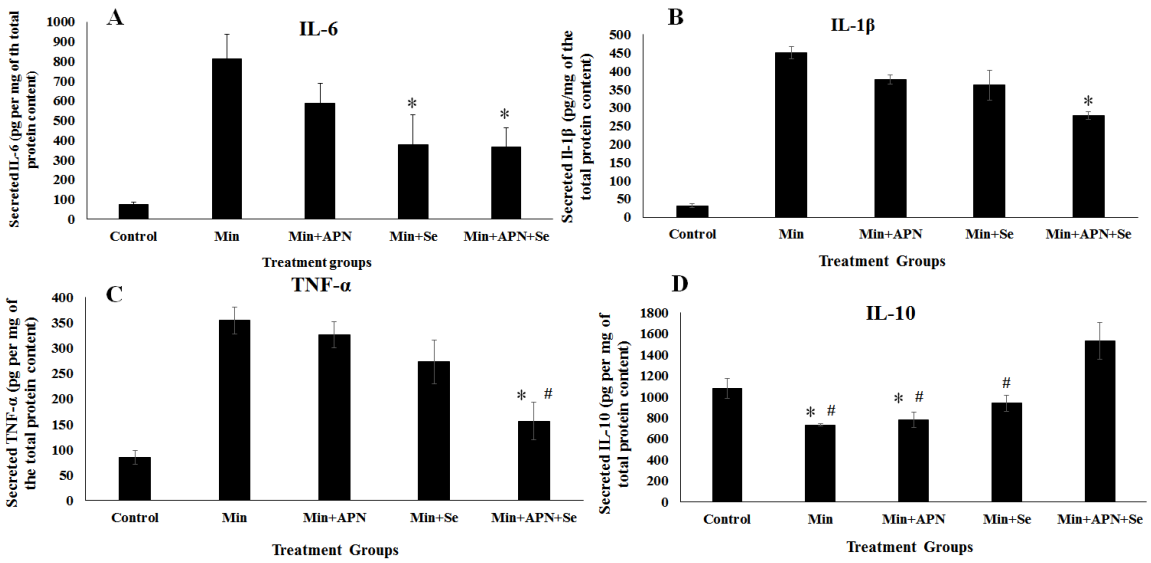

Figure 6.4. Secreted Cytokines: (A) Graph represent the differential expression of secreted IL-6 in different treatment groups. *p<0.05 significant difference between Min+Se and Min+APN+Se vs Min. **(B)** Graph represent the differential expression of secreted IL-1β in different treatment groups. *p<0.05 significant difference between Min and Min+APN+Se **(C)** Graph represent the differential expression of secreted TNF-α in different treatment groups. *p<0.05 significant difference between Min+APN+Se vs Min. #p<0.05 significant difference between Min+APN+Se vs Min+APN **(D)** Graph represent the differential expression of secreted IL-10 in different treatment groups. *p<0.05 significant difference between Min and Min+APN vs Control. #p<0.05 significant difference between Min+APN+Se vs Min, Min+APN and Min+Se. Student TTEST was used to determine significant difference between different treatment groups. (n=8).

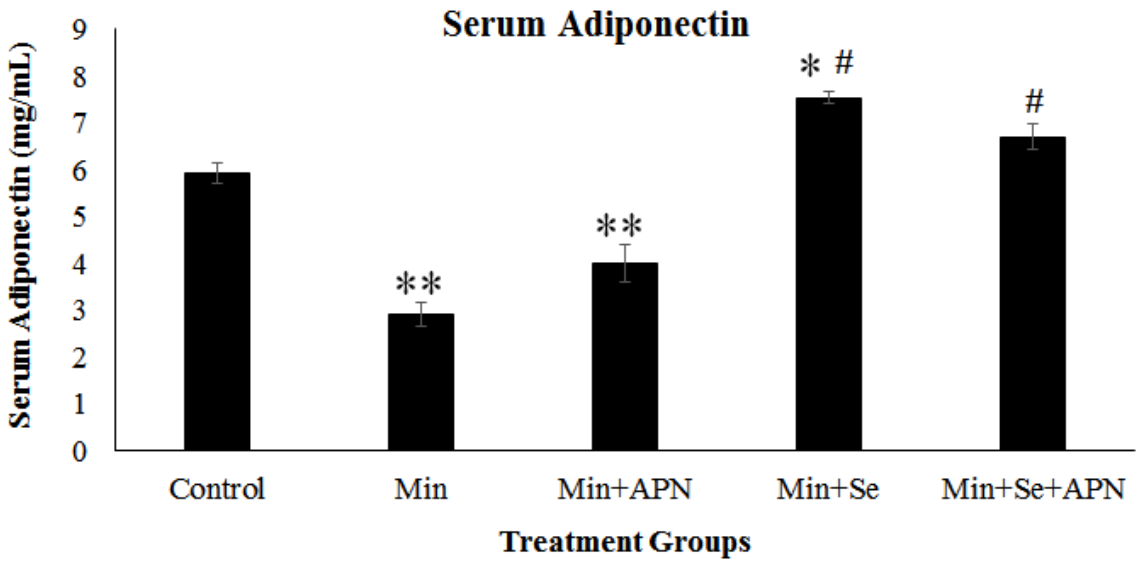

Figure 6.5. Serum Adiponectin: The graph shows the levels of serum APN (mg/ml) in different treatment groups. *p<0.05 significant difference between Min+Se vs Control. **p<0.05 significant difference between Min vs Control and Min+Se vs Control. $^{\#}$p<0.05 significant difference between Min+Se and Min+APN+Se vs Min and Min+APN. Student TTEST was used to determine significant difference between different treatment groups. (n=8).

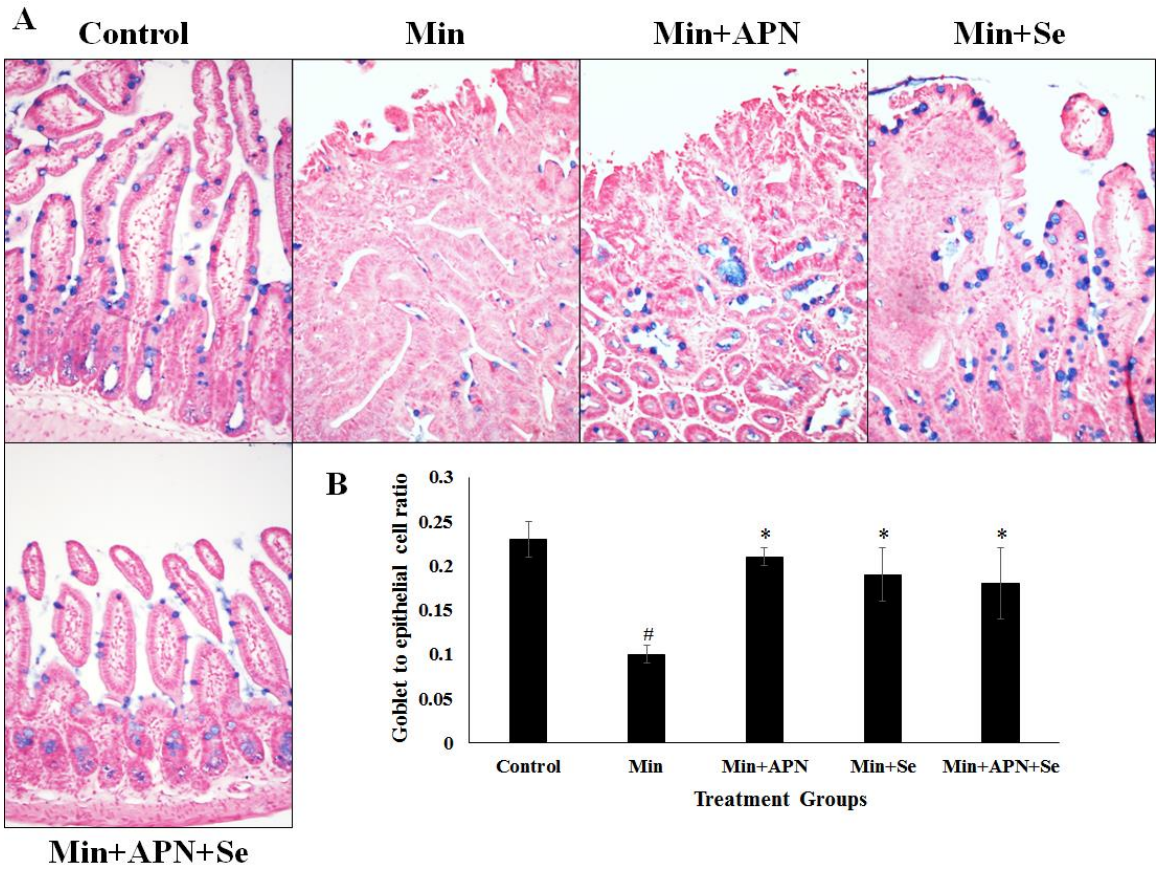

Figure 6.6. Goblet cell production: (A) This figure shows the Alcian blue staining for the small intestine tissue section for the different treatment groups and control. (B) The graph shows the ratio of goblet to epithelial cell for the treatment groups and control group. *$p<0.05$ Min+APN Min+Se and Min+APN+Se vs Min. $^{\#}p<0.05$ Min vs control. Student TTEST was used to determine significant difference between different treatment groups. (n=5).

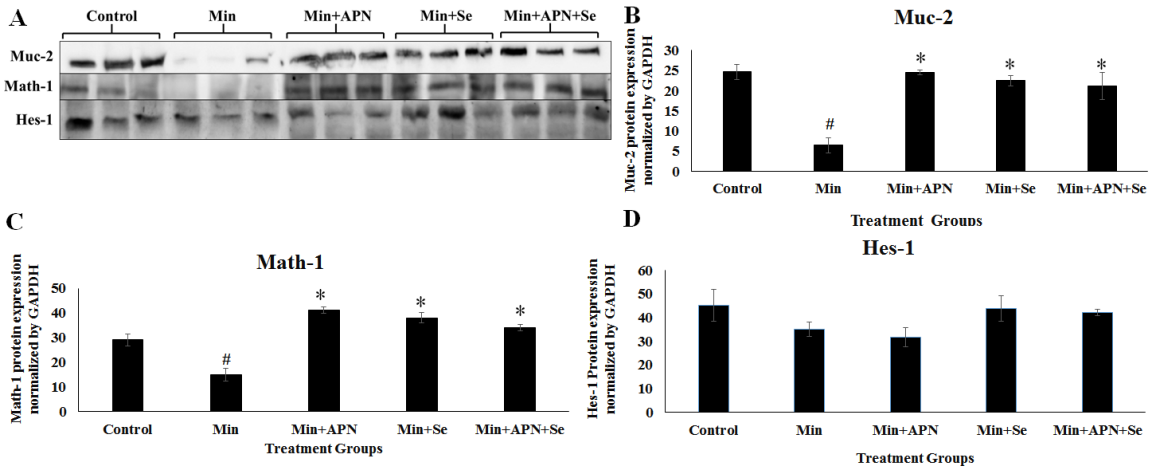

Figure 6.7. Change in goblet cell phenotype and Mucin Secretion: (A) Representative Western blot images showing the protein expression of Muc-2, Hes-1 and Math-1 in the small intestine. **(B)** Graph showing the expression of Muc-2 in all the treatment group and control. *p<0.05 significant difference between Min+APN, Min+Se and Min+APN+Se vs Min. #p<0.05 significant difference between Min vs control. **(C)** Graph showing the expression of Math-1 in all the treatment group and control. *p<0.05 significant difference between Min+APN, Min+Se and Min+APN+Se vs Min. #p<0.05 significant difference between Min vs control. **(D)** Graph showing the expression of Hes-1 in all the treatment group and control. No significant difference was found between in any treatment groups and control. Student TTEST was used to determine significant difference between different treatment groups. (n=5).

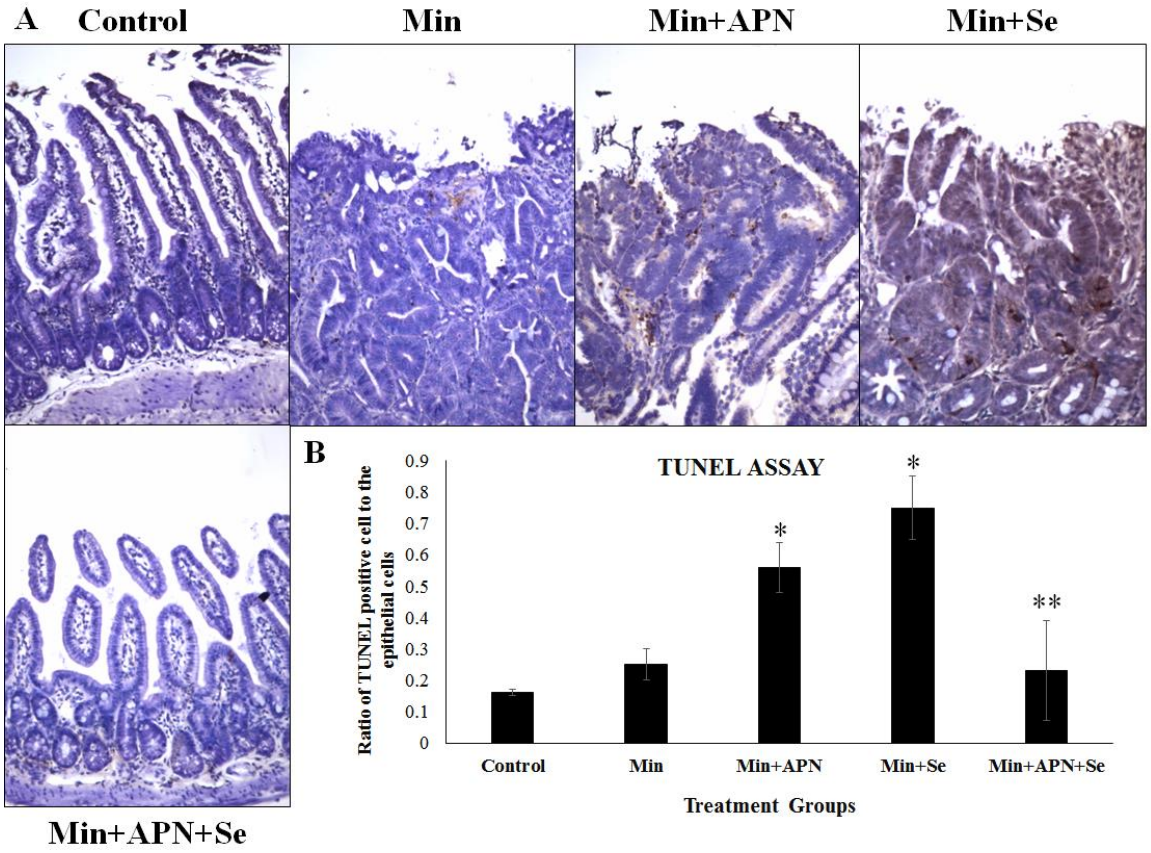

Figure 6.8. Cancer Cell apoptosis: (A) This figure shows the representative 20X images of TUNEL assay marking cancer cell apoptosis and counterstained with methyl green. The cells of the tumor undergoing apoptosis range from light to dark brown in color. **(B)** Graph representing the quantification of the degree of apoptosis determined by calculating the ratio of the TUNEL positive cell and total number of epithelial cells in a 20X microscopic view. 5 views per slide and 8 animals per group were used to calculate significant difference between different groups. *$p<0.05$ Min+APN vs Min and Min+Se vs Min. **$p<0.05$ Min+APN+Se vs Min+Se Student TTEST was used to determine significant difference between different treatment groups. (n=5).

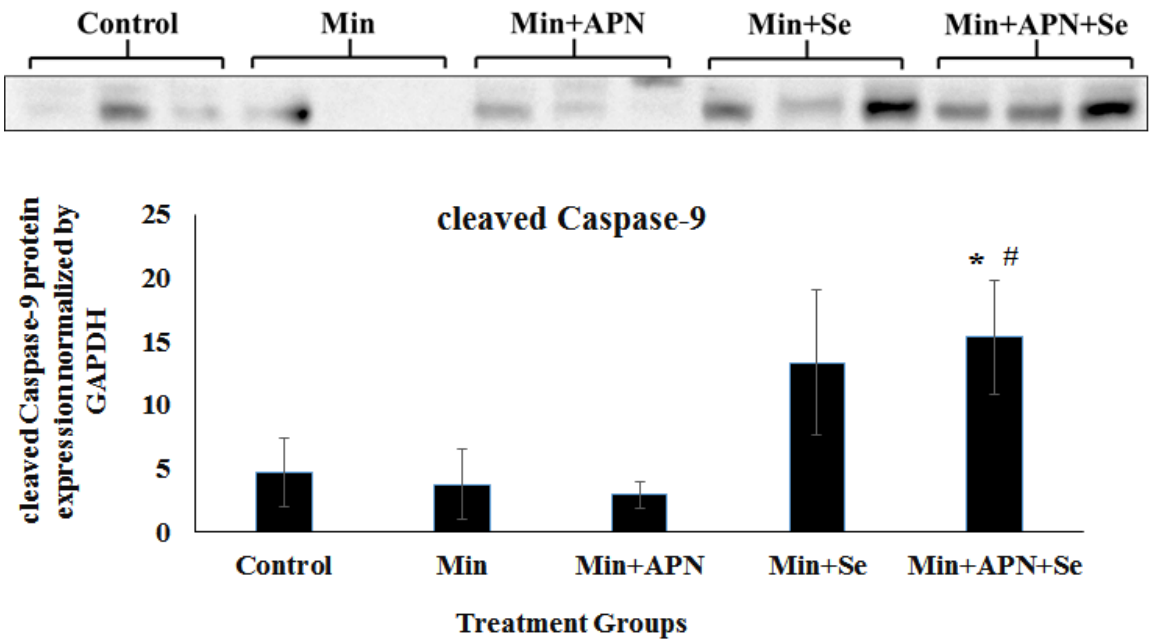

Figure 6.9. cleaved Caspase 9 expression: Western blot and bar graph represents the differential expression of cleaved caspase 9 in different treatment groups. *p<0.05 Min+APN+Se vs Min +APN and $^{\#}$p<0.05 Min+APN+Se vs Min+APN. Student TTEST was used to determine significant difference between different treatment groups. (n=5).

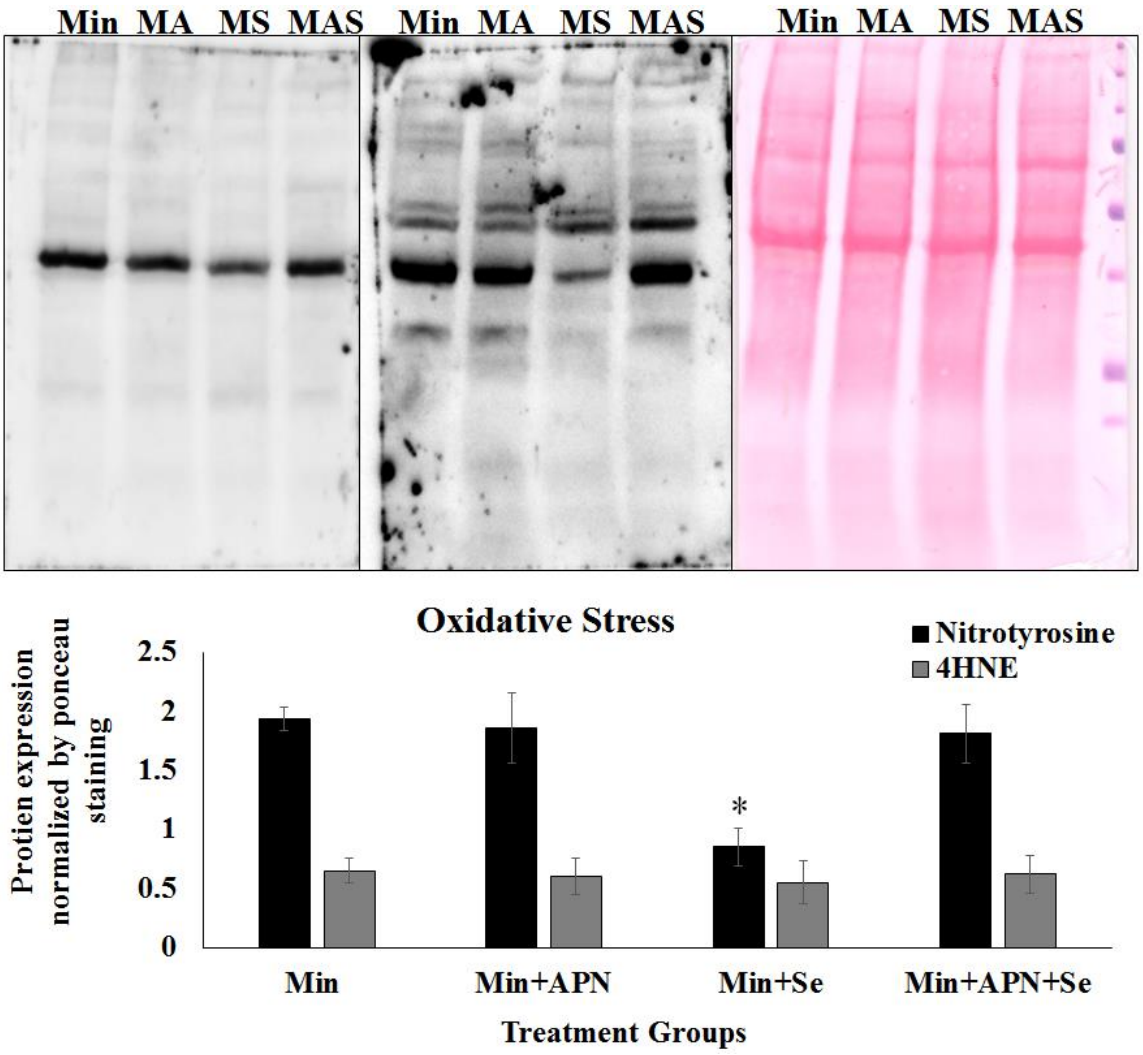

Figure 6.10. Oxidative Stress: This figure shows the protein expression of 4HNE and Nitrotyrosine in Min, Min+APN (MA), Min+Se (MS) and Min+APN+Se (MAS) treatment groups using western blot and the protein expression was normalized by ponceau staining. *p<0.05 Min+Se vs Min, Min +APN and Min+APN+Se. Student TTEST was used to determine significant difference between different treatment groups. (n=5).

CHAPTER 7

OVERALL DISCUSSION

Colorectal Cancer (CRC) is globally the third most commonly diagnosed cancer and it is the second largest cause of cancer death in United States and ranks fourth in the estimated new cases every year (R. Siegel, et al., 2014). Cancer of the colon, rectal and small intestine will contribute to 50,960 deaths in 2015 besides other parts of the digestive tract (R. L. Siegel, et al., 2015). Repeated cycles of inflammation or chronic inflammation has been considered as an underlying cause of intestinal cancer and patients suffering from IBD is at an increased risk of developing colon and intestinal cancer (E. H. Huang, et al., 2006). The etiology of this cancer is very wide and range from genetic pre-disposition to toxic exposure and bad lifestyle (nutrition and exercise). There are several therapies available for the treatment of colon and intestinal cancer but each therapy is associated with its side effects ranging from mild to severe including relapse of the tumor and pain. To ameliorate these side effects and to improve the prognosis and prevent reoccurrence complimentary medicine and new therapy needed to be developed and utilized in addition to the already know treatment. Therefore the purpose of this dissertation was to study the effect of APN and Se rich diet on reducing the severity of colon and intestinal cancer and decipher their mechanism of action. These two could be later used a complimentary medicine in the treatment of colorectal and intestinal cancer. We hypothesize that APN and Se could act either alone or complement each other in reducing tumor load and inflammation by downregulating pro-inflammatory proteins and cytokines and upregulating anti-inflammatory cytokines and proteins and by increasing cancer cell apoptosis. In addition to this we hypothesize that APN and Se either alone or in conjugation could also have an effect on goblet cell production and hence mucus secretion. Mucus can form a protective layer of the gut providing protection against tumor insult.

The data published in this dissertation provide conclusive evidence for the use of APN and Se alone in the treatment of colorectal and intestinal cancer but needed further experimentation to prove the use of the combination of both in the treatment of intestinal and colon cancer. Se rich diet has also been shown to increase the production of serum APN in both the models of spontaneous intestinal cancer and chemically induced colon cancer. APN administration alone might not be effective in bringing the level of serum APN comparable to the control group. Administration of APN in addition to Se rich diet was found to have lower serum APN levels than Se rich diet alone in $APC^{Min/+}$ model of intestinal cancer. This could be due to the negative feedback loop activated in response to excess of APN in the serum or due to the faster removal or breakdown of APN from the blood (Bauche et al., 2006)**.**

Role of Adiponectin in reducing the severity of colon and intestinal cancer.

Adiponectin is an adipocytokine secreted by the adipose tissue. Adipose tissue is an active source of several cytokines, hormones and proteins and APN is one of the anti-inflammatory compound secreted by it. With Obesity or increased adipose tissue volume, APN secretion is reduced due to the activation of a negative feedback loop. In addition, there is an increase necrosis of the adipose tissue leading to invasion by macrophages and their conversion from M2 to M1 phenotype leading to the vicious cycle of inflammation (Martinez & Gordon, 2014). During chronic inflammation, there is an increase secretion of Th_1 cytokines including IL-6, IL1 and reduced production of Th_2 cytokines including

IL-10. Besides cytokines there is a complete shift in the inflammatory mediators from being anti-inflammatory to pro-inflammatory. Repeated cycle of chronic inflammation leads to pre-cancerous lesion and aberrant crypts in both small and large intestine. This if untreated can lead to the development of tumors. The 5 year relative survival rate for colon cancer ranges from 92% at stage I to 11% at stage IV (Brenner, et al., 2014).

APN is an abundant protein with the blood concentration of a healthy individual ranging from 5-20 µg/mL and accounts for 0.01% of the total blood protein (Fayad, et al., 2007; J. Y. Kim & Scherer, 2004). It has a complex structure and is structurally homologous to TNF-α and C1q (complement factor). Its monomer is made of the globular and collagenous domain and could polymerize in to dimer, trimer and other higher molecular weight isomer. Greater levels of polymerization leads to low, medium and higher molecular weight APN. Most of the APN levels in the serum are inversely related to the body's visceral fat content. The mechanism of this relationship remains unclear (Waki, et al., 2003). Lower levels of APN is associated with several disease including hypertension, type-2 diabetes, dyslipidemia, coronary artery disease, stroke, sleep apnea, non-alcoholic fatty liver disease, inflammatory bowel disease, colon cancer, breast cancer, leukemia, prostate and gastric cancer (Kishida, et al., 2014). Our data indicated that the absence of APN is associated with increased severity of CICC as indicated by higher clinical score and greater tumor number when compared to WT mice given the same treatment. Histopathology of the colon tissue section was studied which provided another support to our data indicating high degree of inflammation, greater infiltration and tumors associated with APNKO mice in comparison to WT mice. DSS alone group showed

significantly higher aberrant crypts and several pre-cancerous lesions in APNKO mice. Our study indicated a link between APN deficiency and greater secretion of pro-inflammatory cytokines including IL-6, TNF-α, IL-1β and reduced secretion of anti-inflammatory cytokine including IL-10. IL-6 has been shown to modulate JAK/STAT3 signaling which in turn is regulated by SOCS (Y. Li, et al., 2010). Our further investigation indicated a significantly higher expression of Cox-2 and reduced expression of pAMPK in APNKO mice. APN has been shown to increase the phosphorylation of AMPK and suppresses the cell growth by inhibiting mTOR (Ouchi, et al., 2004), which could provide an explanation for higher tumor number in APNKO mice as they showed significantly reduced activation of AMPK leading to greater tumor cell growth in contrast to WT mice. Cox-2 was found to be significantly overexpressed in the tumor area, majority of this be attributed to the overexpression in cancer epithelial cells in addition to the localized secretion by inflammatory mononuclear cells, fibroblast and vascular endothelial cells. We also found a significant reduction in serum APN in WT mice with CICC indicating the colon cancer is linked with reduced secretion of APN. All the above outcome points towards the deleterious effect of APN deficiency which in the presence of outside stimulus like carcinogen could instigate the cycle of inflammation which if remain untreated for a long time could result in tumor formation.

The above stated mechanism directly deals with inflammation and cancer protein expression, however there might be other alternative pathways leading to protection from CICC. Goblet cell production and mucus secretion pathways may provide more insight about the protective role of APN. Goblet cells are the secretory cells of the colon secreting

mucus which forms a protective layer over the colon and the intestine preventing them from outside insult and gut bacterial invasion. We found a significant reduction in both goblet cell number and mucus secretion in APNKO mice with CICC. Direct effect of APN on mucus secretion was determined by studying mucin production including Muc-1 and Muc-2; major mucins of the colon using goblet cell lines HT29-CI.16E. APN administration was found to increase secretion of Muc-2 but not Muc-1 in HT29-CI.16E goblet cell line. APN administration also reduced the apoptosis of HT29-CI.16E goblet cells in the presence of Muc-2 through the downregulation of Bax and upregulation of Bcl_2. APN was also found to increase the expression of Math-1 gene through the activation of its receptor R1 and R2 which is required for increased goblet cell production.

This experiment only provide evidence for the absence of APN and could study the effect of APN administration on goblet cells through in vitro experimentation. To further study the direct effect of APN on intestinal cancer APN was administered intraperitoneally to $APC^{Min/+}$ mice. Administration of APN resulted in the significant reduction in fecal hemoccult and diarrhea followed by increased apoptosis of small intestine tumor cells which culminated in decreased tumor count providing proof for another mechanism by which APN could reduce the severity intestinal cancer. APN administration also resulted in greater protein expression of Math-1 which resulted in increased goblet cell production and higher Muc-2 secretion.

Both the absence of APN and APN administration has shown the protective role of APN in reducing the severity of both colon and intestinal cancer. To assertion this

observation, we used 2 different model of colon and intestinal cancer that is both inducible and genetic. We reached the same conclusion that APN is protective for CICC and intestinal cancer through reduction of inflammation, increased cancer cell apoptosis and goblet cell production.

Selenium act as protective antioxidant for colon and intestinal cancer.

Selenium is an essential micronutrient and is widely accepted as an anti-oxidant non-metal (Maseko, et al., 2014). This micronutrient forms selenocysteine, which is the twenty-first amino acid and integrates into proteins to form 25 selenoprotein (Metanis & Hilvert, 2014). It has been shown to play a wide physiological role including immune function, male fertility and thyroid function. Se can be obtained in the diet through several sources including Brazil nut, fish, liver, chicken, certain vegetables and meats (Maseko, et al., 2014). The recommended dietary allowance for Se is 55μg per day for human adults and the upper safe limit is 400 μg/day. Beneficial effects of Se can be obtained at a dosage of 200 μg per day. Se has been shown to reduce the severity of cancers including prostate (Gerstenberger et al., 2015), breast (Arsenyan, et al., 2014) and lung (Okuno, Honda, Arakawa, Ogino, & Ueno, 2014a) and has acted as a useful supplementation for several ailments including cystic fibrosis (Ciofu & Lykkesfeldt, 2014), male and female infertility (Balazs & Racz, 2013), glucose metabolism in type 2 diabetes (Mao & Teng, 2013), grave's disease (Kryczyk & Zagrodzki, 2013) and other related inflammatory and autoimmune diseases. A dosage of 200 μg/day of Se has been shown to decrease the total incidence of cancer by 25% (Reid, et al., 2008). An inverse association has been established

between higher Se status and colorectal cancer (Hughes, et al., 2014). The protective effect of the Se in various diseases and conditions is mostly due to the anti-oxidative property leading to an increase in the production of selenoproteins like glutathione peroxidases (Gpx), which neutralize or prevent the formation of reactive oxygen species (ROS) (Kosaric, et al., 2014). Although there are few studies indicating the protective role of Se in chronic inflammation and colon cancer, most of these studies used *in vitro* approach and lacked the mechanism of action of Se in reducing the severity of CICC and intestinal cancer. To achieve this we have used two different model of intestinal cancer both inducible and the genetic model of colon and intestinal cancer and has used Se as a prevention for both these conditions.

Our study indicated a reduction in the clinical score, tumor number and tumor area in both the APNKO and WT mice with CICC given Se rich diet. This indicated an improvement in the physical manifestation of colon cancer and led to further investigation to study major mechanism of colon cancer prevention. Se rich diet showed an increase in the production of serum APN in CICC. To check whether dietary Se was able to increase the total Se content of the colon, mass spectrometry was used which indicated an increase in the colon Se content in both APNKO and WT mice administered Se rich diet. Gpx activity was found to be significantly increased with Se rich diet and it lead to an increase in Gpx-1 and Gpx-2 protein expression. Gpx-2 is more localized in the gut and could be a major player in reducing oxidative stress in the colon tissue section of both APNKO and WT mice with Se rich diet. Colon tissue section was analyzed for histopathology which indicated a reduction in inflammation, infiltration of the immune cells and cancer

pathology. To decipher the mechanism of action of Se in reducing inflammation, NFκB mediated cytokine expression was studied. A significant decrease in the protein expression of p-NFκB followed by the reduction in the secreted pro-inflammatory cytokines like IL-6, TNF-α and Il-1β and increased expression of anti-inflammatory was observed with Se rich diet in both APNKO and WT mice with CICC.

Cancer cell apoptosis and goblet cell production are two other important mechanisms by which Se could reduce tumor count and could affect physical manifestation of colon cancer. Se was found to increase the apoptosis of colon cancer cells and simultaneously reduce colon epithelial cell apoptosis preventing colon damage and reducing tumor number and size. This protection rendered by Se leading to reduced apoptosis of colon epithelial cells could be due to the anti-oxidant nature of Se, lowering ROS in the epithelial cells and preventing them from oxidative damage. We also found increased degree of apoptosis in WT mice when compared to APNKO mice indicating that APN might play an important role in the cancer cell apoptosis. cleaved caspase-9 and phospho-p53 protein expression was significantly higher in the colon tumor tissue section of both APNKO and WT mice given Se rich diet indicating a possible mechanism of action of Se in increasing colon cancer cell apoptosis.

Goblet cells are the secretory cells of the colon which produce mucus and protect colon from toxic insult. Significantly higher goblet to epithelial cell ration was found in the colon tissue section of the both APNKO and WT mice with Se rich diet. WT mice had

higher goblet cell number than APNKO. In addition to this, Math-1 and Muc-2 protein expression was also found to be significantly higher with Se rich diet in both APNKO and WT mice with CICC.

All these findings point towards the protective role of Se rich diet in CICC. We have showed 3 different mechanism of action of Se in reducing the severity of CICC that includes lower inflammation and inflammatory marker, increase cancer cell apoptosis and higher goblet cell production. All these 3 pathways works together to reduce the severity of CICC by lowering clinical score, tumor number and tumor area.

Selenium and APN may work together to reduce the severity of intestinal cancer

To further prove the effectiveness of both APN and Se rich diet in reducing the severity of colon cancer; $APC^{Min/+}$ mouse model of spontaneous intestinal cancer was used in addition to APN and Se rich diet administration either alone or in combination. Both Se and APN was used as prevention of colon and intestinal cancer. We hypothesize that the combination of APN and Se rich diet will be more effective in reducing the severity of intestinal cancer than the individual treatment. Our result confirmed our hypothesis partially as we found a reduction in clinical score, tumor number and tumor area with combination of Se and APN administration but the difference was not significant in comparison to Se rich diet alone. However we found a significant difference in comparison

to APN administration alone. We also found a significant reduction in the histopathology score and pro-inflammatory cytokines production in small intestine tissue section obtained from mice belonging to Min+APN+Se groups when compared with Min groups but we failed to find a significance difference between Min+APN, Min+Se and Min+APN+Se. They tend to produce similar effect Min+Se almost mimicking Min+APN+Se group.

Intestinal cancer cell apoptosis was also significantly increased with APN and Se administration alone but we fail to obtain the tumor tissue section in the Min+APN+Se group and hence only epithelial cell apoptosis was observed which was found to be similar to control group. However, cleaved caspse-9 protein expression was determined in the intestinal cancer tissue sections and we found a significant increase in the expression with the combination of Se and APN. This provide an indirect measure that the combination is effective in increasing of intestinal cancer cell apoptosis. Goblet cell production was also found to be significantly higher in with APN, Se or APN+Se administration. However, again we failed obtain any added advantage of the combination treatment for Math-1 and Muc-2 protein expression and goblet cell production. Contrarily the combination showed a decreased in the serum APN levels when compared with Se rich diet alone. This could be explained by the negative feedback loop for APN which might have been active and could have reduced serum APN levels.

Our study didn't indicate any significant advantage of Se and APN combination treatment but proved that Se rich diet was the most effective in reducing the severity of intestinal cancer.

Summary

In summary, by the means of this dissertation, we have demonstrated the protective role of APN, Se and their combination in the treatment of CICC and intestinal cancer. Se or APN or both were effective in reducing clinical score, tumor number and tumor area in both CICC and intestinal cancer. They might act by reducing inflammation and infiltration of the immune cells which will prevent the transition from pre-cancerous lesions to tumor formation and might even prevent the formation of aberrant crypts. Another mechanism of their action is by the increasing cancer cell apoptosis which resulted in reduced tumor number and tumor size. They might also improve the production of goblet cells by activation of Math-1 and increase mucus secretion by increased production of gut specific mucin Muc-2. Se in addition to all these protective effect is a well-known anti-oxidant and was effective in reducing oxidative stress by the upregulation of selenoprotein antioxidants like Gpx-1 and Gpx-2 and hence might be protective to the colon epithelial cells. We also found a relationship between APN and Se and showed that Se rich diet was effective in increasing serum APN.

Future Direction

This study provided some novel insight about the role of Se and APN and their combination in reducing the severity of colon and intestinal cancer and established a relationship between the two. However, there might still be some gaps in understanding the complete action of Se and APN in cancer cell apoptosis and goblet cell production. It

would be interesting to study other mechanism of action of Se and APN in increasing cancer cell apoptosis especially by modulation of protein expression of Bax and Bcl_2. Selenoprotein expression was only studied in the normal colon tissue, it will interesting to study the expression of Gpx-1 and Gpx-2 in colon tumor tissue. Besides Gpx, no other selenoproteins were studied and there are total 25 selenoproteins known which might put light on the dual nature of Se where Se is protective for normal colon epithelial cells and pro-apoptotic to colon tumor cells. Also the protective effect of Se and APN on reducing colon epithelial cell apoptosis remained unclear and need more mechanistic investigation in addition to proliferation assay. Although the combination of Se and APN was most effective in reducing tumor but none of the mechanism shown in the dissertation provided a complete justification of the outcome, pointing towards the need to study other mechanism of action. The inflammatory cytokine study were restricted to secreted cytokines but studying serum cytokine may provide a better outcome and might reveal novel pathways. $APC^{Min/+}$ mice model of intestinal cancer is a result of a mutation in the APC gene leading to uncontrolled expression of β Catenin. Higher expression of β Catenin is associated with greater inflammation and higher tumor load. Therefore one of the future direction will be to study the effect of APN and Se rich diet administration on the expression of β Catenin which could provide evidence for the reduction in the tumor load and clinical score. Most of the molecular study for the last aim was done with small intestine and might be a reason for non-significance in APN+Se treatment. Colon tissue study might result in a better outcome for this aim.

Both of the studies implicating the role of Se in the treatment of colon and intestinal cancer studied Se as the prevention by administering Se before the development of the tumor. One of the future direction for this dissertation could be to study the effect of Se as a treatment by administering Se after 12 weeks of age in $APC^{Min/+}$ mice model of intestinal cancer. Tumor have already been formed by 12 weeks of age and Se could be used as a treatment for intestinal cancer. Also, Se could also be administered in the DSS+DMH inducible model of colon cancer after the second DSS administration as tumor might have been developed by that time and Se could be used as a treatment. Using a treatment approach might provide a better insight about the mechanism of action on Se in the treatment of colon and intestinal cancer.

Any treatment given for colon or intestinal cancer have an effect on gut bacteria which might provide another avenue for future research. Exercise has been shown to be effective in reducing the incidence of several cardiovascular diseases and cancer. Medium intensity exercise might provide complimentary benefits in reducing the severity of symptoms associated with colorectal cancer and could be studied in conjugation with Se rich diet. Since we have already shown that Se is effective in reducing the severity of CICC and intestinal cancer, it will be intuitive to study the effect of individual selenoproteins on colorectal cancer. Using non-conventional therapies and complementary medicine might provide a reduction in the symptoms and reoccurrence associated with colorectal cancer and might lead to the development of novel pharmacological interventions for colon cancer treatment.

REFERENCES

Aggarwal, B. B., Vijayalekshmi, R. V., & Sung, B. (2009). Targeting inflammatory pathways for prevention and therapy of cancer: short-term friend, long-term foe. *Clin Cancer Res, 15*(2), 425-430.

Ahmed, F. E. (2003). Colon cancer: prevalence, screening, gene expression and mutation, and risk factors and assessment. *J Environ Sci Health C Environ Carcinog Ecotoxicol Rev, 21*(2), 65-131.

Anand, P., Kunnumakkara, A. B., Sundaram, C., Harikumar, K. B., Tharakan, S. T., Lai, O. S., et al. (2008). Cancer is a preventable disease that requires major lifestyle changes. *Pharm Res, 25*(9), 2097-2116.

Andoh, A., Hirashima, M., Maeda, H., Hata, K., Inatomi, O., Tsujikawa, T., et al. (2005). Serum selenoprotein-P levels in patients with inflammatory bowel disease. *Nutrition, 21*(5), 574-579.

Andrianifahanana, M., Moniaux, N., & Batra, S. K. (2006). Regulation of mucin expression: mechanistic aspects and implications for cancer and inflammatory diseases. *Biochim Biophys Acta, 1765*(2), 189-222.

Arita, Y., Kihara, S., Ouchi, N., Takahashi, M., Maeda, K., Miyagawa, J., et al. (1999). Paradoxical decrease of an adipose-specific protein, adiponectin, in obesity. *Biochem Biophys Res Commun, 257*(1), 79-83.

Arsenyan, P., Paegle, E., Domracheva, I., Gulbe, A., Kanepe-Lapsa, I., & Shestakova, I. (2014). Selenium analogues of raloxifene as promising antiproliferative agents in treatment of breast cancer. *Eur J Med Chem, 87*, 471-483.

Artis, D. (2008). Epithelial-cell recognition of commensal bacteria and maintenance of immune homeostasis in the gut. *Nat Rev Immunol, 8*(6), 411-420.

Atreya, R., & Neurath, M. F. (2008). Signaling molecules: the pathogenic role of the IL-6/STAT-3 trans signaling pathway in intestinal inflammation and in colonic cancer. *Curr Drug Targets, 9*(5), 369-374.

Augeron, C., & Laboisse, C. L. (1984). Emergence of permanently differentiated cell clones in a human colonic cancer cell line in culture after treatment with sodium butyrate. *Cancer Res, 44*(9), 3961-3969.

Awazawa, M., Ueki, K., Inabe, K., Yamauchi, T., Kubota, N., Kaneko, K., et al. (2011). Adiponectin enhances insulin sensitivity by increasing hepatic IRS-2 expression via a macrophage-derived IL-6-dependent pathway. *Cell Metab, 13*(4), 401-412.

Baena, R., & Salinas, P. (2015). Diet and colorectal cancer. *Maturitas, 80*(3), 258-264.

Balazs, C., & Racz, K. (2013). [The role of selenium in endocrine system diseases]. [Review]. *Orv Hetil, 154*(41), 1628-1635.

Baliga, M. S., Joseph, N., Venkataranganna, M. V., Saxena, A., Ponemone, V., & Fayad, R. (2012). Curcumin, an active component of turmeric in the prevention and treatment of ulcerative colitis: preclinical and clinical observations. [Review]. *Food Funct, 3*(11), 1109-1117.

Balkwill, F., & Mantovani, A. (2010). Cancer and inflammation: implications for pharmacology and therapeutics. *Clin Pharmacol Ther, 87*(4), 401-406.

Baltgalvis, K. A., Berger, F. G., Pena, M. M., Davis, J. M., Muga, S. J., & Carson, J. A. (2008). Interleukin-6 and cachexia in ApcMin/+ mice. *Am J Physiol Regul Integr Comp Physiol, 294*(2), R393-401.

Barb, D., Williams, C. J., Neuwirth, A. K., & Mantzoros, C. S. (2007). Adiponectin in relation to malignancies: a review of existing basic research and clinical evidence. *Am J Clin Nutr, 86*(3), s858-866.

Bardou, M., Barkun, A. N., & Martel, M. (2013). Obesity and colorectal cancer. [Review]. *Gut, 62*(6), 933-947.

Barresi, V., Tuccari, G., & Barresi, G. (2009). Adiponectin immunohistochemical expression in colorectal cancer and its correlation with histological grade and tumour microvessel density. *Pathology, 41*(6), 533-538.

Barrett, C. W., Singh, K., Motley, A. K., Lintel, M. K., Matafonova, E., Bradley, A. M., et al. (2013). Dietary selenium deficiency exacerbates DSS-induced epithelial injury and AOM/DSS-induced tumorigenesis. [Research Support, N.I.H., Extramural

Research Support, U.S. Gov't, Non-P.H.S.]. *PLoS One, 8*(7), e67845.

Bauche, I. B., Ait El Mkadem, S., Rezsohazy, R., Funahashi, T., Maeda, N., Miranda, L. M., et al. (2006). Adiponectin downregulates its own production and the expression of its AdipoR2 receptor in transgenic mice. *Biochem Biophys Res Commun, 345*(4), 1414-1424.

Berg, A. H., Combs, T. P., & Scherer, P. E. (2002). ACRP30/adiponectin: an adipokine regulating glucose and lipid metabolism. *Trends Endocrinol Metab, 13*(2), 84-89.

Bi, X., Pohl, N., Dong, H., & Yang, W. (2013). Selenium and sulindac are synergistic to inhibit intestinal tumorigenesis in Apc/p21 mice. *J Hematol Oncol, 6*, 8.

Bianchini, F., Kaaks, R., & Vainio, H. (2002). Overweight, obesity, and cancer risk. *Lancet Oncol, 3*(9), 565-574.

Birmingham, J. M., Busik, J. V., Hansen-Smith, F. M., & Fenton, J. I. (2009). Novel mechanism for obesity-induced colon cancer progression. *Carcinogenesis, 30*(4), 690-697.

Blain, A., Cattan, S., Beaugerie, L., Carbonnel, F., Gendre, J. P., & Cosnes, J. (2002). Crohn's disease clinical course and severity in obese patients. *Clin Nutr, 21*(1), 51-57.

Bossuyt, W., Kazanjian, A., De Geest, N., Van Kelst, S., De Hertogh, G., Geboes, K., et al. (2009). Atonal homolog 1 is a tumor suppressor gene. *PLoS Biol, 7*(2), e39.

Bowman, T., Garcia, R., Turkson, J., & Jove, R. (2000). STATs in oncogenesis. *Oncogene, 19*(21), 2474-2488.

Brakenhielm, E., Veitonmaki, N., Cao, R., Kihara, S., Matsuzawa, Y., Zhivotovsky, B., et al. (2004). Adiponectin-induced antiangiogenesis and antitumor activity involve caspase-mediated endothelial cell apoptosis. *Proc Natl Acad Sci U S A, 101*(8), 2476-2481.

Brenner, H., Kloor, M., & Pox, C. P. (2014). Colorectal cancer. *Lancet, 383*(9927), 1490-1502.

Brigelius-Flohe, R., & Maiorino, M. (2013). Glutathione peroxidases. [Research Support, Non-U.S. Gov't

Review]. *Biochim Biophys Acta, 1830*(5), 3289-3303.

Brochu-Gaudreau, K., Rehfeldt, C., Blouin, R., Bordignon, V., Murphy, B. D., & Palin, M. F. (2010). Adiponectin action from head to toe. *Endocrine, 37*(1), 11-32.

Bruun, J. M., Lihn, A. S., Verdich, C., Pedersen, S. B., Toubro, S., Astrup, A., et al. (2003). Regulation of adiponectin by adipose tissue-derived cytokines: in vivo and in vitro investigations in humans. *Am J Physiol Endocrinol Metab, 285*(3), E527-533.

Buettner, R., Mora, L. B., & Jove, R. (2002). Activated STAT signaling in human tumors provides novel molecular targets for therapeutic intervention. *Clin Cancer Res, 8*(4), 945-954.

Burgess, A. W., Faux, M. C., Layton, M. J., & Ramsay, R. G. (2011). Wnt signaling and colon tumorigenesis--a view from the periphery. *Exp Cell Res, 317*(19), 2748-2758.

Byeon, J. S., Jeong, J. Y., Kim, M. J., Lee, S. M., Nam, W. H., Myung, S. J., et al. (2010). Adiponectin and adiponectin receptor in relation to colorectal cancer progression. *Int J Cancer, 127*(12), 2758-2767.

Byrd, J. C., & Bresalier, R. S. (2004). Mucins and mucin binding proteins in colorectal cancer. *Cancer Metastasis Rev, 23*(1-2), 77-99.

Calle, E. E., & Kaaks, R. (2004). Overweight, obesity and cancer: epidemiological evidence and proposed mechanisms. *Nat Rev Cancer, 4*(8), 579-591.

Carling, D. (2004). The AMP-activated protein kinase cascade--a unifying system for energy control. *Trends Biochem Sci, 29*(1), 18-24.

Carswell, E. A., Old, L. J., Kassel, R. L., Green, S., Fiore, N., & Williamson, B. (1975). An endotoxin-induced serum factor that causes necrosis of tumors. *Proc Natl Acad Sci U S A, 72*(9), 3666-3670.

Chatterjee, D., Roy, S., Hazra, A., Dasgupta, P., Ganguly, S., & Das, A. K. (2014). Variation of adverse drug reaction profile of platinum-based chemotherapy with body mass index in patients with solid tumors: an observational study. *Indian J Pharmacol, 46*(2), 222-224.

Chen, Y. C., Prabhu, K. S., Das, A., & Mastro, A. M. (2013). Dietary selenium supplementation modifies breast tumor growth and metastasis. [Research Support, Non-U.S. Gov't]. *Int J Cancer, 133*(9), 2054-2064.

Chen, Y. C., Prabhu, K. S., & Mastro, A. M. (2013). Is selenium a potential treatment for cancer metastasis? *Nutrients, 5*(4), 1149-1168.

Cheng, J. Y., Wang, M. J., Ma, H., Li, H. Y., Ren, J. B., & Wang, R. L. (2015). [Adiponectin inhibits oxidative stress and modulates TGF-b1 and COL-1 expression via the AMPK pathway in HSC-T6 cells]. *Zhonghua Gan Zang Bing Za Zhi, 23*(1), 69-72.

Ciofu, O., & Lykkesfeldt, J. (2014). Antioxidant supplementation for lung disease in cystic fibrosis. [Meta-Analysis

Research Support, Non-U.S. Gov't

Review]. *Cochrane Database Syst Rev, 8*, CD007020.

Coletta, P. L., Muller, A. M., Jones, E. A., Muhl, B., Holwell, S., Clarke, D., et al. (2004). Lymphodepletion in the ApcMin/+ mouse model of intestinal tumorigenesis. *Blood, 103*(3), 1050-1058.

Colnot, S., Niwa-Kawakita, M., Hamard, G., Godard, C., Le Plenier, S., Houbron, C., et al. (2004). Colorectal cancers in a new mouse model of familial adenomatous polyposis: influence of genetic and environmental modifiers. *Lab Invest, 84*(12), 1619-1630.

Combs, G. F., Jr. (2005). Current evidence and research needs to support a health claim for selenium and cancer prevention. *J Nutr, 135*(2), 343-347.

Corfield, A. P., Carroll, D., Myerscough, N., & Probert, C. S. (2001). Mucins in the gastrointestinal tract in health and disease. *Front Biosci, 6*, D1321-1357.

Coussens, L. M., & Werb, Z. (2002). Inflammation and cancer. *Nature, 420*(6917), 860-867.
Dalamaga, M. (2013). Interplay of adipokines and myokines in cancer pathophysiology: Emerging therapeutic implications. *World J Exp Med, 3*(3), 26-33.
Dalamaga, M., Diakopoulos, K. N., & Mantzoros, C. S. (2012). The role of adiponectin in cancer: a review of current evidence. *Endocr Rev, 33*(4), 547-594.
Darnell, J. E. (2005). Validating Stat3 in cancer therapy. *Nat Med, 11*(6), 595-596.
Deplancke, B., & Gaskins, H. R. (2001). Microbial modulation of innate defense: goblet cells and the intestinal mucus layer. *Am J Clin Nutr, 73*(6), 1131S-1141S.
Dietze-Schroeder, D., Sell, H., Uhlig, M., Koenen, M., & Eckel, J. (2005). Autocrine action of adiponectin on human fat cells prevents the release of insulin resistance-inducing factors. *Diabetes, 54*(7), 2003-2011.
Disis, M. L. (2010). Immune regulation of cancer. *J Clin Oncol, 28*(29), 4531-4538.
Du, Y. P., Li, L. L., He, Q., Li, Y., Song, H., Lin, Y. J., et al. (2012). [Nutritional risk screening and nutrition assessment for gastrointestinal cancer patients]. [Research Support, Non-U.S. Gov't]. *Zhonghua Wei Chang Wai Ke Za Zhi, 15*(5), 460-463.
Eaden, J. A., Abrams, K. R., & Mayberry, J. F. (2001). The risk of colorectal cancer in ulcerative colitis: a meta-analysis. *Gut, 48*(4), 526-535.
Ealey, K. N., & Archer, M. C. (2009). Elevated circulating adiponectin and elevated insulin sensitivity in adiponectin transgenic mice are not associated with reduced susceptibility to colon carcinogenesis. *Int J Cancer, 124*(9), 2226-2230.
Fantuzzi, G. (2005). Adipose tissue, adipokines, and inflammation. *J Allergy Clin Immunol, 115*(5), 911-919; quiz 920.
Faubert, B., Boily, G., Izreig, S., Griss, T., Samborska, B., Dong, Z., et al. (2013). AMPK is a negative regulator of the Warburg effect and suppresses tumor growth in vivo. *Cell Metab, 17*(1), 113-124.
Fayad, R., Pini, M., Sennello, J. A., Cabay, R. J., Chan, L., Xu, A., et al. (2007). Adiponectin deficiency protects mice from chemically induced colonic inflammation. *Gastroenterology, 132*(2), 601-614.
Fearon, E. R. (2011). Molecular genetics of colorectal cancer. [Review]. *Annu Rev Pathol, 6*, 479-507.
Femia, A. P., Dolara, P., Luceri, C., Salvadori, M., & Caderni, G. (2009). Mucin-depleted foci show strong activation of inflammatory markers in 1,2-dimethylhydrazine-induced carcinogenesis and are promoted by the inflammatory agent sodium dextran sulfate. *Int J Cancer, 125*(3), 541-547.
Ferrero-Miliani, L., Nielsen, O. H., Andersen, P. S., & Girardin, S. E. (2007). Chronic inflammation: importance of NOD2 and NALP3 in interleukin-1beta generation. *Clin Exp Immunol, 147*(2), 227-235.
Ferroni, P., Palmirotta, R., Spila, A., Martini, F., Raparelli, V., Fossile, E., et al. (2007). Prognostic significance of adiponectin levels in non-metastatic colorectal cancer. *Anticancer Res, 27*(1B), 483-489.
Finaud, J., Lac, G., & Filaire, E. (2006). Oxidative stress : relationship with exercise and training. *Sports Med, 36*(4), 327-358.
Finley, J. W. (2003). Reduction of cancer risk by consumption of selenium-enriched plants: enrichment of broccoli with selenium increases the anticarcinogenic properties of broccoli. *J Med Food, 6*(1), 19-26.

Florian, S., Wingler, K., Schmehl, K., Jacobasch, G., Kreuzer, O. J., Meyerhof, W., et al. (2001). Cellular and subcellular localization of gastrointestinal glutathione peroxidase in normal and malignant human intestinal tissue. *Free Radic Res, 35*(6), 655-663.

Floyd, R. A., Chandru, H. K., He, T., & Towner, R. (2011). Anti-cancer activity of nitrones and observations on mechanism of action. *Anticancer Agents Med Chem, 11*(4), 373-379.

Forbes, S. A., Bindal, N., Bamford, S., Cole, C., Kok, C. Y., Beare, D., et al. (2011). COSMIC: mining complete cancer genomes in the Catalogue of Somatic Mutations in Cancer. *Nucleic Acids Res, 39*(Database issue), D945-950.

Friedman, E., Gold, L. I., Klimstra, D., Zeng, Z. S., Winawer, S., & Cohen, A. (1995). High levels of transforming growth factor beta 1 correlate with disease progression in human colon cancer. *Cancer Epidemiol Biomarkers Prev, 4*(5), 549-554.

Fujisawa, T., Endo, H., Tomimoto, A., Sugiyama, M., Takahashi, H., Saito, S., et al. (2008). Adiponectin suppresses colorectal carcinogenesis under the high-fat diet condition. *Gut, 57*(11), 1531-1538.

Gandhi, U. H., Kaushal, N., Hegde, S., Finch, E. R., Kudva, A. K., Kennett, M. J., et al. (2014). Selenium suppresses leukemia through the action of endogenous eicosanoids. *Cancer Res, 74*(14), 3890-3901.

Gao, Q., & Zheng, J. (2014). Adiponectin-induced antitumor activity on prostatic cancers through inhibiting proliferation. *Cell Biochem Biophys, 70*(1), 461-465.

Gaudier, E., Forestier, L., Gouyer, V., Huet, G., Julien, R., & Hoebler, C. (2004). Butyrate regulation of glycosylation-related gene expression: evidence for galectin-1 upregulation in human intestinal epithelial goblet cells. *Biochem Biophys Res Commun, 325*(3), 1044-1051.

Gaudier, E., Jarry, A., Blottiere, H. M., de Coppet, P., Buisine, M. P., Aubert, J. P., et al. (2004). Butyrate specifically modulates MUC gene expression in intestinal epithelial goblet cells deprived of glucose. *Am J Physiol Gastrointest Liver Physiol, 287*(6), G1168-1174.

Gerstenberger, J. P., Bauer, S. R., Van Blarigan, E. L., Sosa, E., Song, X., Witte, J. S., et al. (2014). Selenoprotein and antioxidant genes and the risk of high-grade prostate cancer and prostate cancer recurrence. *Prostate*.

Gerstenberger, J. P., Bauer, S. R., Van Blarigan, E. L., Sosa, E., Song, X., Witte, J. S., et al. (2015). Selenoprotein and antioxidant genes and the risk of high-grade prostate cancer and prostate cancer recurrence. *Prostate, 75*(1), 60-69.

Ghadi, F. E., Ghara, A. R., Bhattacharyya, S., & Dhawan, D. K. (2009). Selenium as a chemopreventive agent in experimentally induced colon carcinogenesis. *World J Gastrointest Oncol, 1*(1), 74-81.

Ghadi, F. E., Malhotra, A., Ghara, A. R., & Dhawan, D. K. (2012). Selenium as a modulator of membrane stability parameters and surface changes during the initiation phase of 1,2-dimethylhydrazine induced colorectal carcinogenesis. *Mol Cell Biochem, 369*(1-2), 119-126.

Ghadi, F. E., Malhotra, A., Ghara, A. R., & Dhawan, D. K. (2013). Chemopreventive effects of selenium on cancer marker indices and ultrastructural changes during 1,2 dimethylhydrazine-induced colon carcinogenesis in rats. *J Gastrointest Cancer, 44*(1), 54-59.

Giovannucci, E., Ascherio, A., Rimm, E. B., Colditz, G. A., Stampfer, M. J., & Willett, W. C. (1995). Physical activity, obesity, and risk for colon cancer and adenoma in men. *Ann Intern Med, 122*(5), 327-334.

Gordon, J. I., Hooper, L. V., McNevin, M. S., Wong, M., & Bry, L. (1997). Epithelial cell growth and differentiation. III. Promoting diversity in the intestine: conversations between the microflora, epithelium, and diffuse GALT. *Am J Physiol, 273*(3 Pt 1), G565-570.

Gorozhanskaia, E. G., Sviridova, S. P., Dobrovol'skaia, M. M., Zybrikhina, G. N., & Kashnia Sh, R. (2013). [Selenium and oxidative stress in cancer patients]. [Clinical Trial]. *Biomed Khim, 59*(5), 550-562.

Grahame Hardie, D. (2014). AMP-activated protein kinase: a key regulator of energy balance with many roles in human disease. *J Intern Med, 276*(6), 543-559.

Grossmann, M. E., Nkhata, K. J., Mizuno, N. K., Ray, A., & Cleary, M. P. (2008). Effects of adiponectin on breast cancer cell growth and signaling. *Br J Cancer, 98*(2), 370-379.

Grune, T., Merker, K., Sandig, G., & Davies, K. J. (2003). Selective degradation of oxidatively modified protein substrates by the proteasome. *Biochem Biophys Res Commun, 305*(3), 709-718.

Gulcelik, M. A., Colakoglu, K., Dincer, H., Dogan, L., Yenidogan, E., & Gulcelik, N. E. (2012). Associations between adiponectin and two different cancers: breast and colon. *Asian Pac J Cancer Prev, 13*(1), 395-398.

Gunter, M. J., & Leitzmann, M. F. (2006). Obesity and colorectal cancer: epidemiology, mechanisms and candidate genes. *J Nutr Biochem, 17*(3), 145-156.

Gupta, S., Jaworska-Bieniek, K., Lubinski, J., & Jakubowska, A. (2013). Can selenium be a modifier of cancer risk in CHEK2 mutation carriers? [Research Support, Non-U.S. Gov't]. *Mutagenesis, 28*(6), 625-629.

Guthrie, E., Jackson, J., Shaffer, J., Thompson, D., Tomenson, B., & Creed, F. (2002). Psychological disorder and severity of inflammatory bowel disease predict health-related quality of life in ulcerative colitis and Crohn's disease. *Am J Gastroenterol, 97*(8), 1994-1999.

Hartnett, L., & Egan, L. J. (2012). Inflammation, DNA methylation and colitis-associated cancer. *Carcinogenesis, 33*(4), 723-731.

Hasnain, S. Z., Tauro, S., Das, I., Tong, H., Chen, A. C., Jeffery, P. L., et al. (2013). IL-10 promotes production of intestinal mucus by suppressing protein misfolding and endoplasmic reticulum stress in goblet cells. *Gastroenterology, 144*(2), 357-368 e359.

Hebuterne, X., Lemarie, E., Michallet, M., de Montreuil, C. B., Schneider, S. M., & Goldwasser, F. (2014). Prevalence of malnutrition and current use of nutrition support in patients with cancer. [Research Support, Non-U.S. Gov't]. *JPEN J Parenter Enteral Nutr, 38*(2), 196-204.

Higuchi, T., Iwama, T., Yoshinaga, K., Toyooka, M., Taketo, M. M., & Sugihara, K. (2003). A randomized, double-blind, placebo-controlled trial of the effects of rofecoxib, a selective cyclooxygenase-2 inhibitor, on rectal polyps in familial adenomatous polyposis patients. *Clin Cancer Res, 9*(13), 4756-4760.

Hoesel, B., & Schmid, J. A. (2013). The complexity of NF-kappaB signaling in inflammation and cancer. *Mol Cancer, 12*, 86.

Hollingsworth, M. A., & Swanson, B. J. (2004). Mucins in cancer: protection and control of the cell surface. *Nat Rev Cancer, 4*(1), 45-60.

Hooper, L. V., & Macpherson, A. J. (2010). Immune adaptations that maintain homeostasis with the intestinal microbiota. *Nat Rev Immunol, 10*(3), 159-169.

Hu, Y., McIntosh, G. H., Le Leu, R. K., Nyskohus, L. S., Woodman, R. J., & Young, G. P. (2013). Combination of selenium and green tea improves the efficacy of chemoprevention in a rat colorectal cancer model by modulating genetic and epigenetic biomarkers. [Research Support, Non-U.S. Gov't]. *PLoS One, 8*(5), e64362.

Hu, Y., McIntosh, G. H., Le Leu, R. K., & Young, G. P. (2010). Selenium-enriched milk proteins and selenium yeast affect selenoprotein activity and expression differently in mouse colon. [Research Support, Non-U.S. Gov't]. *Br J Nutr, 104*(1), 17-23.

Huang, E. H., Park, J. C., Appelman, H., Weinberg, A. D., Banerjee, M., Logsdon, C. D., et al. (2006). Induction of inflammatory bowel disease accelerates adenoma formation in Min +/- mice. *Surgery, 139*(6), 782-788.

Huang, X., Wullschleger, S., Shpiro, N., McGuire, V. A., Sakamoto, K., Woods, Y. L., et al. (2008). Important role of the LKB1-AMPK pathway in suppressing tumorigenesis in PTEN-deficient mice. *Biochem J, 412*(2), 211-221.

Huerta, S., Goulet, E. J., Huerta-Yepez, S., & Livingston, E. H. (2007). Screening and detection of apoptosis. *J Surg Res, 139*(1), 143-156.

Hughes, D. J., Fedirko, V., Jenab, M., Schomburg, L., Meplan, C., Freisling, H., et al. (2014). Selenium status is associated with colorectal cancer risk in the European prospective investigation of cancer and nutrition cohort. *Int J Cancer*.

Hull, M., & Lagergren, J. (2014). Obesity and colorectal cancer. [Comment

Letter]. *Gut, 63*(1), 205.

Hurst, R., Hooper, L., Norat, T., Lau, R., Aune, D., Greenwood, D. C., et al. (2012). Selenium and prostate cancer: systematic review and meta-analysis. [Meta-Analysis

Research Support, Non-U.S. Gov't

Review]. *Am J Clin Nutr, 96*(1), 111-122.

Hwang, J. T., Ha, J., & Park, O. J. (2005). Combination of 5-fluorouracil and genistein induces apoptosis synergistically in chemo-resistant cancer cells through the modulation of AMPK and COX-2 signaling pathways. *Biochem Biophys Res Commun, 332*(2), 433-440.

Ishikawa, M., Kitayama, J., Kazama, S., Hiramatsu, T., Hatano, K., & Nagawa, H. (2005). Plasma adiponectin and gastric cancer. *Clin Cancer Res, 11*(2 Pt 1), 466-472.

Itzkowitz, S. H., & Yio, X. (2004). Inflammation and cancer IV. Colorectal cancer in inflammatory bowel disease: the role of inflammation. *Am J Physiol Gastrointest Liver Physiol, 287*(1), G7-17.

Jemal, A., Bray, F., Center, M. M., Ferlay, J., Ward, E., & Forman, D. (2011). Global cancer statistics. *CA Cancer J Clin, 61*(2), 69-90.

Jensen, J., Pedersen, E. E., Galante, P., Hald, J., Heller, R. S., Ishibashi, M., et al. (2000). Control of endodermal endocrine development by Hes-1. *Nat Genet, 24*(1), 36-44.

Jiang, C., Ganther, H., & Lu, J. (2000). Monomethyl selenium--specific inhibition of MMP-2 and VEGF expression: implications for angiogenic switch regulation. [Research Support, Non-U.S. Gov't

Research Support, U.S. Gov't, Non-P.H.S.
Research Support, U.S. Gov't, P.H.S.]. *Mol Carcinog, 29*(4), 236-250.
Johansson, M. E., Gustafsson, J. K., Holmen-Larsson, J., Jabbar, K. S., Xia, L., Xu, H., et al. (2014). Bacteria penetrate the normally impenetrable inner colon mucus layer in both murine colitis models and patients with ulcerative colitis. *Gut, 63*(2), 281-291.
Johansson, M. E., Gustafsson, J. K., Sjoberg, K. E., Petersson, J., Holm, L., Sjovall, H., et al. (2010). Bacteria penetrate the inner mucus layer before inflammation in the dextran sulfate colitis model. *PLoS One, 5*(8), e12238.
Johansson, M. E., & Hansson, G. C. (2013). Mucus and the goblet cell. *Dig Dis, 31*(3-4), 305-309.
Johansson, M. E., Phillipson, M., Petersson, J., Velcich, A., Holm, L., & Hansson, G. C. (2008). The inner of the two Muc2 mucin-dependent mucus layers in colon is devoid of bacteria. *Proc Natl Acad Sci U S A, 105*(39), 15064-15069.
Kadowaki, T., & Yamauchi, T. (2005). Adiponectin and adiponectin receptors. *Endocr Rev, 26*(3), 439-451.
Kapas, L., Hong, L., Cady, A. B., Opp, M. R., Postlethwaite, A. E., Seyer, J. M., et al. (1992). Somnogenic, pyrogenic, and anorectic activities of tumor necrosis factor-alpha and TNF-alpha fragments. *Am J Physiol, 263*(3 Pt 2), R708-715.
Karmiris, K., Koutroubakis, I. E., Xidakis, C., Polychronaki, M., Voudouri, T., & Kouroumalis, E. A. (2006). Circulating levels of leptin, adiponectin, resistin, and ghrelin in inflammatory bowel disease. *Inflamm Bowel Dis, 12*(2), 100-105.
Kaser, A., Zeissig, S., & Blumberg, R. S. (2010a). Genes and environment: how will our concepts on the pathophysiology of IBD develop in the future? *Dig Dis, 28*(3), 395-405.
Kaser, A., Zeissig, S., & Blumberg, R. S. (2010b). Inflammatory bowel disease. *Annu Rev Immunol, 28*, 573-621.
Kato, M., Watabe, K., Tsujii, M., Funahashi, T., Shimomura, I., & Takehara, T. (2014). Adiponectin inhibits murine pancreatic cancer growth. *Dig Dis Sci, 59*(6), 1192-1196.
Katoh, M. (2007). Notch signaling in gastrointestinal tract (review). *Int J Oncol, 30*(1), 247-251.
Kidane, D., Chae, W. J., Czochor, J., Eckert, K. A., Glazer, P. M., Bothwell, A. L., et al. (2014). Interplay between DNA repair and inflammation, and the link to cancer. *Crit Rev Biochem Mol Biol, 49*(2), 116-139.
Kim, A. Y., Lee, Y. S., Kim, K. H., Lee, J. H., Lee, H. K., Jang, S. H., et al. (2010). Adiponectin represses colon cancer cell proliferation via AdipoR1- and -R2-mediated AMPK activation. *Mol Endocrinol, 24*(7), 1441-1452.
Kim, J. H., Hue, J. J., Kang, B. S., Park, H., Nam, S. Y., Yun, Y. W., et al. (2011). Effects of selenium on colon carcinogenesis induced by azoxymethane and dextran sodium sulfate in mouse model with high-iron diet. *Lab Anim Res, 27*(1), 9-18.
Kim, J. Y., & Scherer, P. E. (2004). Adiponectin, an adipocyte-derived hepatic insulin sensitizer regulation during development. *Pediatr Endocrinol Rev, 1 Suppl 3*, 428-431.
Kishida, K., Funahashi, T., & Shimomura, I. (2014). Adiponectin as a routine clinical biomarker. *Best Pract Res Clin Endocrinol Metab, 28*(1), 119-130.

Korinek, V., Barker, N., Morin, P. J., van Wichen, D., de Weger, R., Kinzler, K. W., et al. (1997). Constitutive transcriptional activation by a beta-catenin-Tcf complex in APC-/- colon carcinoma. *Science, 275*(5307), 1784-1787.

Korsgaard, M., Pedersen, L., Sorensen, H. T., & Laurberg, S. (2006). Reported symptoms, diagnostic delay and stage of colorectal cancer: a population-based study in Denmark. [Comparative Study

Research Support, Non-U.S. Gov't]. *Colorectal Dis, 8*(8), 688-695.

Kosaric, J. V., Cvetkovic, D. M., Zivanovic, M. N., Curcic, M. G., Seklic, D. S., Bugarcic, Z. M., et al. (2014). Antioxidative and antiproliferative evaluation of 2-(phenylselenomethyl)tetrahydrofuran and 2-(phenylselenomethyl)tetrahydropyran. [Research Support, Non-U.S. Gov't]. *J BUON, 19*(1), 283-290.

Krehl, S., Loewinger, M., Florian, S., Kipp, A. P., Banning, A., Wessjohann, L. A., et al. (2012). Glutathione peroxidase-2 and selenium decreased inflammation and tumors in a mouse model of inflammation-associated carcinogenesis whereas sulforaphane effects differed with selenium supply. [Research Support, N.I.H., Extramural

Research Support, Non-U.S. Gov't]. *Carcinogenesis, 33*(3), 620-628.

Kryczyk, J., & Zagrodzki, P. (2013). [Selenium in Graves' disease]. *Postepy Hig Med Dosw (Online), 67*, 491-498.

L'Abbe, M. R., Fischer, P. W., Campbell, J. S., & Chavez, E. R. (1989). Effects of dietary selenium on DMBA-induced carcinogenesis in rats fed a diet high in mixed fats. *J Nutr, 119*(5), 757-765.

Labunskyy, V. M., Hatfield, D. L., & Gladyshev, V. N. (2014). Selenoproteins: molecular pathways and physiological roles. [Research Support, N.I.H., Extramural

Review]. *Physiol Rev, 94*(3), 739-777.

Lampropoulos, P., Zizi-Sermpetzoglou, A., Rizos, S., Kostakis, A., Nikiteas, N., & Papavassiliou, A. G. (2012). TGF-beta signalling in colon carcinogenesis. *Cancer Lett, 314*(1), 1-7.

Lang, T., Hansson, G. C., & Samuelsson, T. (2007). Gel-forming mucins appeared early in metazoan evolution. *Proc Natl Acad Sci U S A, 104*(41), 16209-16214.

Larsson, S. C., & Wolk, A. (2007). Obesity and colon and rectal cancer risk: a meta-analysis of prospective studies. *Am J Clin Nutr, 86*(3), 556-565.

Law, L., Rogers, J., & Eng, C. (2014). Delayed Presentation of DPD Deficiency in Colorectal Cancer. *J Adv Pract Oncol, 5*(3), 205-210.

Le Marchand, L., Wilkens, L. R., Kolonel, L. N., Hankin, J. H., & Lyu, L. C. (1997). Associations of sedentary lifestyle, obesity, smoking, alcohol use, and diabetes with the risk of colorectal cancer. *Cancer Res, 57*(21), 4787-4794.

Leblond, C. P., & Stevens, C. E. (1948). The constant renewal of the intestinal epithelium in the albino rat. *Anat Rec, 100*(3), 357-377.

Lee, D. H., Esworthy, R. S., Chu, C., Pfeifer, G. P., & Chu, F. F. (2006). Mutation accumulation in the intestine and colon of mice deficient in two intracellular glutathione peroxidases. [Research Support, N.I.H., Extramural

Research Support, Non-U.S. Gov't]. *Cancer Res, 66*(20), 9845-9851.

Lee, K. H., & Jeong, D. (2012). Bimodal actions of selenium essential for antioxidant and toxic pro-oxidant activities: the selenium paradox (Review). [Research Support, Non-U.S. Gov't

Review]. *Mol Med Rep, 5*(2), 299-304.

Lee, W. L., Huang, J. Y., & Shyur, L. F. (2013). Phytoagents for cancer management: regulation of nucleic acid oxidation, ROS, and related mechanisms. [Review]. *Oxid Med Cell Longev, 2013*, 925804.

Leow, C. C., Polakis, P., & Gao, W. Q. (2005). A role for Hath1, a bHLH transcription factor, in colon adenocarcinoma. *Ann N Y Acad Sci, 1059*, 174-183.

Li, Y., de Haar, C., Chen, M., Deuring, J., Gerrits, M. M., Smits, R., et al. (2010). Disease-related expression of the IL6/STAT3/SOCS3 signalling pathway in ulcerative colitis and ulcerative colitis-related carcinogenesis. *Gut, 59*(2), 227-235.

Li, Z., Carrier, L., & Rowan, B. G. (2008). Methylseleninic acid synergizes with tamoxifen to induce caspase-mediated apoptosis in breast cancer cells. *Mol Cancer Ther, 7*(9), 3056-3063.

Li, Z., Meng, J., Xu, T. J., Qin, X. Y., & Zhou, X. D. (2013). Sodium selenite induces apoptosis in colon cancer cells via Bax-dependent mitochondrial pathway. *Eur Rev Med Pharmacol Sci, 17*(16), 2166-2171.

Lizcano, J. M., Goransson, O., Toth, R., Deak, M., Morrice, N. A., Boudeau, J., et al. (2004). LKB1 is a master kinase that activates 13 kinases of the AMPK subfamily, including MARK/PAR-1. *EMBO J, 23*(4), 833-843.

Logan, C. Y., & Nusse, R. (2004). The Wnt signaling pathway in development and disease. *Annu Rev Cell Dev Biol, 20*, 781-810.

Luo, H., Yang, Y., Duan, J., Wu, P., Jiang, Q., & Xu, C. (2013). PTEN-regulated AKT/FoxO3a/Bim signaling contributes to reactive oxygen species-mediated apoptosis in selenite-treated colorectal cancer cells. [Research Support, Non-U.S. Gov't]. *Cell Death Dis, 4*, e481.

Makki, K., Froguel, P., & Wolowczuk, I. (2013). Adipose Tissue in Obesity-Related Inflammation and Insulin Resistance: Cells, Cytokines, and Chemokines. [Review]. *ISRN Inflamm, 2013*, 139239.

Maloy, K. J., & Powrie, F. (2011). Intestinal homeostasis and its breakdown in inflammatory bowel disease. *Nature, 474*(7351), 298-306.

Mao, J., & Teng, W. (2013). The relationship between selenoprotein P and glucose metabolism in experimental studies. [Research Support, Non-U.S. Gov't

Review]. *Nutrients, 5*(6), 1937-1948.

Marnett, L. J. (2002). Oxy radicals, lipid peroxidation and DNA damage. *Toxicology, 181-182*, 219-222.

Martinez, F. O., & Gordon, S. (2014). The M1 and M2 paradigm of macrophage activation: time for reassessment. *F1000Prime Rep, 6*, 13.

Maseko, T., Howell, K., Dunshea, F. R., & Ng, K. (2014). Selenium-enriched Agaricus bisporus increases expression and activity of glutathione peroxidase-1 and expression of glutathione peroxidase-2 in rat colon. *Food Chem, 146*, 327-333.

Masferrer, J. L., Leahy, K. M., Koki, A. T., Zweifel, B. S., Settle, S. L., Woerner, B. M., et al. (2000). Antiangiogenic and antitumor activities of cyclooxygenase-2 inhibitors. *Cancer Res, 60*(5), 1306-1311.

Meilleur, K. G., Doumatey, A., Huang, H., Charles, B., Chen, G., Zhou, J., et al. (2010). Circulating adiponectin is associated with obesity and serum lipids in West Africans. *J Clin Endocrinol Metab, 95*(7), 3517-3521.

Metanis, N., & Hilvert, D. (2014). Natural and synthetic selenoproteins. *Curr Opin Chem Biol, 22*, 27-34.

Meyer, F., Galan, P., Douville, P., Bairati, I., Kegle, P., Bertrais, S., et al. (2005). Antioxidant vitamin and mineral supplementation and prostate cancer prevention in the SU.VI.MAX trial. *Int J Cancer, 116*(2), 182-186.

Mikkelsen, H. B., Rumessen, J. J., & Qvortrup, K. (1991). Prostaglandin H synthase immunoreactivity in human gut. An immunohistochemical study. *Histochemistry, 96*(4), 295-299.

Miladi-Abdennadher, I., Abdelmaksoud-Dammak, R., Ayed-Guerfali, D. B., Ayadi, L., Khabir, A., Amouri, A., et al. (2012). Expression of COX-2 and E-cadherin in Tunisian patients with colorectal adenocarcinoma. *Acta Histochem, 114*(6), 577-581.

Mistry, T., Digby, J. E., Desai, K. M., & Randeva, H. S. (2008). Leptin and adiponectin interact in the regulation of prostate cancer cell growth via modulation of p53 and bcl-2 expression. *BJU Int, 101*(10), 1317-1322.

Miyazaki, T., Bub, J. D., Uzuki, M., & Iwamoto, Y. (2005). Adiponectin activates c-Jun NH2-terminal kinase and inhibits signal transducer and activator of transcription 3. *Biochem Biophys Res Commun, 333*(1), 79-87.

Moon, H. S., Liu, X., Nagel, J. M., Chamberland, J. P., Diakopoulos, K. N., Brinkoetter, M. T., et al. (2013). Salutary effects of adiponectin on colon cancer: in vivo and in vitro studies in mice. [In Vitro

Research Support, N.I.H., Extramural

Research Support, Non-U.S. Gov't

Research Support, U.S. Gov't, Non-P.H.S.]. *Gut, 62*(4), 561-570.

Moon, H. S., & Mantzoros, C. S. (2013). Adiponectin and metformin additively attenuate IL1beta-induced malignant potential of colon cancer. [Research Support, N.I.H., Extramural

Research Support, U.S. Gov't, Non-P.H.S.]. *Endocr Relat Cancer, 20*(6), 849-859.

Moser, A. R., Pitot, H. C., & Dove, W. F. (1990). A dominant mutation that predisposes to multiple intestinal neoplasia in the mouse. *Science, 247*(4940), 322-324.

Munkholm, P. (2003). Review article: the incidence and prevalence of colorectal cancer in inflammatory bowel disease. *Aliment Pharmacol Ther, 18 Suppl 2*, 1-5.

Murawaki, Y., Tsuchiya, H., Kanbe, T., Harada, K., Yashima, K., Nozaka, K., et al. (2008). Aberrant expression of selenoproteins in the progression of colorectal cancer. *Cancer Lett, 259*(2), 218-230.

Mutoh, M., Teraoka, N., Takasu, S., Takahashi, M., Onuma, K., Yamamoto, M., et al. (2011). Loss of adiponectin promotes intestinal carcinogenesis in Min and wild-type mice. *Gastroenterology, 140*(7), 2000-2008, 2008 e2001-2002.

Nagaraju, G. P., Aliya, S., & Alese, O. B. (2014). Role of adiponectin in obesity related gastrointestinal carcinogenesis. *Cytokine Growth Factor Rev*.

Nagy, D. T., Fulesdi, B., & Hallay, J. (2013). [The relationship between selenium and gastrointestinal inflammatory diseases]. *Orv Hetil, 154*(41), 1636-1640.

Nigro, E., Scudiero, O., Monaco, M. L., Palmieri, A., Mazzarella, G., Costagliola, C., et al. (2014). New insight into adiponectin role in obesity and obesity-related diseases. *Biomed Res Int, 2014*, 658913.

Nishihara, T., Baba, M., Matsuda, M., Inoue, M., Nishizawa, Y., Fukuhara, A., et al. (2008). Adiponectin deficiency enhances colorectal carcinogenesis and liver tumor

formation induced by azoxymethane in mice. *World J Gastroenterol, 14*(42), 6473-6480.

Nishihara, T., Matsuda, M., Araki, H., Oshima, K., Kihara, S., Funahashi, T., et al. (2006). Effect of adiponectin on murine colitis induced by dextran sulfate sodium. *Gastroenterology, 131*(3), 853-861.

Niv, Y., Byrd, J. C., Ho, S. B., Dahiya, R., & Kim, Y. S. (1992). Mucin synthesis and secretion in relation to spontaneous differentiation of colon cancer cells in vitro. *Int J Cancer, 50*(1), 147-152.

Nolfo, F., Rametta, S., Marventano, S., Grosso, G., Mistretta, A., Drago, F., et al. (2013). Pharmacological and dietary prevention for colorectal cancer. [Research Support, Non-U.S. Gov't]. *BMC Surg, 13 Suppl 2*, S16.

Obeid, S., & Hebbard, L. (2012). Role of adiponectin and its receptors in cancer. *Cancer Biol Med, 9*(4), 213-220.

Okayasu, I., Hatakeyama, S., Yamada, M., Ohkusa, T., Inagaki, Y., & Nakaya, R. (1990). A novel method in the induction of reliable experimental acute and chronic ulcerative colitis in mice. *Gastroenterology, 98*(3), 694-702.

Okuno, T., Honda, E., Arakawa, T., Ogino, H., & Ueno, H. (2014a). Glutathione-dependent cell cycle G1 arrest and apoptosis induction in human lung cancer A549 cells caused by methylseleninic acid: comparison with sodium selenite. *Biol Pharm Bull, 37*(11), 1831-1837.

Okuno, T., Honda, E., Arakawa, T., Ogino, H., & Ueno, H. (2014b). Glutathione-dependent cell cycle G arrest and apoptosis induction in human lung cancer A549 cells caused by methylseleninic acid: comparison with sodium selenite. *Biol Pharm Bull*.

Otake, S., Takeda, H., Suzuki, Y., Fukui, T., Watanabe, S., Ishihama, K., et al. (2005). Association of visceral fat accumulation and plasma adiponectin with colorectal adenoma: evidence for participation of insulin resistance. *Clin Cancer Res, 11*(10), 3642-3646.

Otani, K., Kitayama, J., Yasuda, K., Nio, Y., Iwabu, M., Okudaira, S., et al. (2010). Adiponectin suppresses tumorigenesis in Apc(Min)(/+) mice. *Cancer Lett, 288*(2), 177-182.

Ouchi, N., Kobayashi, H., Kihara, S., Kumada, M., Sato, K., Inoue, T., et al. (2004). Adiponectin stimulates angiogenesis by promoting cross-talk between AMP-activated protein kinase and Akt signaling in endothelial cells. *J Biol Chem, 279*(2), 1304-1309.

Pandurangan, A. K., & Esa, N. M. (2014). Signal transducer and activator of transcription 3 - a promising target in colitis-associated cancer. *Asian Pac J Cancer Prev, 15*(2), 551-560.

Park, S. Y., Kim, J. S., Seo, Y. R., & Sung, M. K. (2012). Effects of diet-induced obesity on colitis-associated colon tumor formation in A/J mice. *Int J Obes (Lond), 36*(2), 273-280.

Paz-Filho, G., Lim, E. L., Wong, M. L., & Licinio, J. (2011). Associations between adipokines and obesity-related cancer. *Front Biosci, 16*, 1634-1650.

Pelissier, M. A., Muller, C., Hill, M., & Morfin, R. (2006). Protection against dextran sodium sulfate-induced colitis by dehydroepiandrosterone and 7alpha-hydroxy-dehydroepiandrosterone in the rat. *Steroids, 71*(3), 240-248.

Perse, M. (2013). Oxidative stress in the pathogenesis of colorectal cancer: cause or consequence? *Biomed Res Int, 2013*, 725710.

Petersen, S., Haroske, G., Hellmich, G., Ludwig, K., Petersen, C., & Eicheler, W. (2002). COX-2 expression in rectal carcinoma: immunohistochemical pattern and clinical outcome. *Anticancer Res, 22*(2B), 1225-1230.

Petersson, J., Schreiber, O., Hansson, G. C., Gendler, S. J., Velcich, A., Lundberg, J. O., et al. (2011). Importance and regulation of the colonic mucus barrier in a mouse model of colitis. *Am J Physiol Gastrointest Liver Physiol, 300*(2), G327-333.

Pillai, S. S., Sugathan, J. K., & Indira, M. (2012). Selenium downregulates RAGE and NFkappaB expression in diabetic rats. *Biol Trace Elem Res, 149*(1), 71-77.

Pretlow, T. P., Edelmann, W., Kucherlapati, R., Pretlow, T. G., & Augenlicht, L. H. (2003). Spontaneous aberrant crypt foci in Apc1638N mice with a mutant Apc allele. *Am J Pathol, 163*(5), 1757-1763.

Qiao, L., & Wong, B. C. (2009). Role of Notch signaling in colorectal cancer. *Carcinogenesis, 30*(12), 1979-1986.

Rayman, M. P. (2012). Selenium and human health. *Lancet, 379*(9822), 1256-1268.

Reid, M. E., Duffield-Lillico, A. J., Slate, E., Natarajan, N., Turnbull, B., Jacobs, E., et al. (2008). The nutritional prevention of cancer: 400 mcg per day selenium treatment. [Randomized Controlled Trial

Research Support, N.I.H., Extramural]. *Nutr Cancer, 60*(2), 155-163.

Renehan, A. G., Tyson, M., Egger, M., Heller, R. F., & Zwahlen, M. (2008). Body-mass index and incidence of cancer: a systematic review and meta-analysis of prospective observational studies. *Lancet, 371*(9612), 569-578.

Roy, S., Dontamalla, S. K., Mondru, A. K., Sannigrahi, S., & Veerareddy, P. R. (2011). Downregulation of apoptosis and modulation of TGF-beta1 by sodium selenate prevents streptozotocin-induced diabetic rat renal impairment. *Biol Trace Elem Res, 139*(1), 55-71.

Rubin, D. C., Shaker, A., & Levin, M. S. (2012). Chronic intestinal inflammation: inflammatory bowel disease and colitis-associated colon cancer. *Front Immunol, 3*, 107.

Saeki, N., Saito, A., Choi, I. J., Matsuo, K., Ohnami, S., Totsuka, H., et al. (2011). A functional single nucleotide polymorphism in mucin 1, at chromosome 1q22, determines susceptibility to diffuse-type gastric cancer. *Gastroenterology, 140*(3), 892-902.

Sag, D., Carling, D., Stout, R. D., & Suttles, J. (2008). Adenosine 5'-monophosphate-activated protein kinase promotes macrophage polarization to an anti-inflammatory functional phenotype. *J Immunol, 181*(12), 8633-8641.

Sakurai, T., Ogasawara, J., Kizaki, T., Sato, S., Ishibashi, Y., Takahashi, M., et al. (2013). The Effects of Exercise Training on Obesity-Induced Dysregulated Expression of Adipokines in White Adipose Tissue. [Review]. *Int J Endocrinol, 2013*, 801743.

Sano, H., Kawahito, Y., Wilder, R. L., Hashiramoto, A., Mukai, S., Asai, K., et al. (1995). Expression of cyclooxygenase-1 and -2 in human colorectal cancer. *Cancer Res, 55*(17), 3785-3789.

Sarkanen, J. R., Kaila, V., Mannerstrom, B., Raty, S., Kuokkanen, H., Miettinen, S., et al. (2012). Human adipose tissue extract induces angiogenesis and adipogenesis in vitro. *Tissue Eng Part A, 18*(1-2), 17-25.

Sasai, H., Masaki, M., & Wakitani, K. (2000). Suppression of polypogenesis in a new mouse strain with a truncated Apc(Delta474) by a novel COX-2 inhibitor, JTE-522. *Carcinogenesis, 21*(5), 953-958.

Saxena, A., Baliga, M. S., Ponemone, V., Kaur, K., Larsen, B., Fletcher, E., et al. (2013). Mucus and adiponectin deficiency: role in chronic inflammation-induced colon cancer. [Research Support, N.I.H., Extramural]. *Int J Colorectal Dis, 28*(9), 1267-1279.

Saxena, A., Chumanevich, A., Fletcher, E., Larsen, B., Lattwein, K., Kaur, K., et al. (2012). Adiponectin deficiency: role in chronic inflammation induced colon cancer. [Research Support, N.I.H., Extramural]. *Biochim Biophys Acta, 1822*(4), 527-536.

Schonhoff, S. E., Giel-Moloney, M., & Leiter, A. B. (2004). Minireview: Development and differentiation of gut endocrine cells. *Endocrinology, 145*(6), 2639-2644.

Sebio, A., Kahn, M., & Lenz, H. J. (2014). The potential of targeting Wnt/beta-catenin in colon cancer. *Expert Opin Ther Targets, 18*(6), 611-615.

Seril, D. N., Liao, J., Yang, G. Y., & Yang, C. S. (2003). Oxidative stress and ulcerative colitis-associated carcinogenesis: studies in humans and animal models. *Carcinogenesis, 24*(3), 353-362.

Shackelford, D. B., & Shaw, R. J. (2009). The LKB1-AMPK pathway: metabolism and growth control in tumour suppression. *Nat Rev Cancer, 9*(8), 563-575.

Shan, Y. S., Hsu, H. P., Lai, M. D., Yen, M. C., Fang, J. H., Weng, T. Y., et al. (2014). Suppression of mucin 2 promotes interleukin-6 secretion and tumor growth in an orthotopic immune-competent colon cancer animal model. *Oncol Rep, 32*(6), 2335-2342.

Shaw, R. J., Kosmatka, M., Bardeesy, N., Hurley, R. L., Witters, L. A., DePinho, R. A., et al. (2004). The tumor suppressor LKB1 kinase directly activates AMP-activated kinase and regulates apoptosis in response to energy stress. *Proc Natl Acad Sci U S A, 101*(10), 3329-3335.

Sheng, X. Z., Xu, G. J., Tang, X. Q., & Zhan, W. B. (2012). Monoclonal antibodies recognizing mucus immunoglobulin and surface immunoglobulin-positive cells of flounder (Paralichthys olivaceus). *Vet Immunol Immunopathol, 145*(1-2), 143-150.

Shibata, R., Sato, K., Pimentel, D. R., Takemura, Y., Kihara, S., Ohashi, K., et al. (2005). Adiponectin protects against myocardial ischemia-reperfusion injury through AMPK- and COX-2-dependent mechanisms. *Nat Med, 11*(10), 1096-1103.

Shroyer, N. F., Helmrath, M. A., Wang, V. Y., Antalffy, B., Henning, S. J., & Zoghbi, H. Y. (2007). Intestine-specific ablation of mouse atonal homolog 1 (Math1) reveals a role in cellular homeostasis. *Gastroenterology, 132*(7), 2478-2488.

Shroyer, N. F., Wallis, D., Venken, K. J., Bellen, H. J., & Zoghbi, H. Y. (2005). Gfi1 functions downstream of Math1 to control intestinal secretory cell subtype allocation and differentiation. *Genes Dev, 19*(20), 2412-2417.

Shu, R. Z., Zhang, F., Wang, F., Feng, D. C., Li, X. H., Ren, W. H., et al. (2009). Adiponectin deficiency impairs liver regeneration through attenuating STAT3 phosphorylation in mice. *Lab Invest, 89*(9), 1043-1052.

Shukla, S., Meeran, S. M., & Katiyar, S. K. (2014). Epigenetic regulation by selected dietary phytochemicals in cancer chemoprevention. *Cancer Lett, 355*(1), 9-17.

Siegel, R., Ma, J., Zou, Z., & Jemal, A. (2014). Cancer statistics, 2014. *CA Cancer J Clin, 64*(1), 9-29.

Siegel, R., Naishadham, D., & Jemal, A. (2013). Cancer statistics, 2013. *CA Cancer J Clin, 63*(1), 11-30.
Siegel, R. L., Miller, K. D., & Jemal, A. (2015). Cancer statistics, 2015. *CA Cancer J Clin, 65*(1), 5-29.
Specian, R. D., & Oliver, M. G. (1991). Functional biology of intestinal goblet cells. *Am J Physiol, 260*(2 Pt 1), C183-193.
Stanger, B. Z., Datar, R., Murtaugh, L. C., & Melton, D. A. (2005). Direct regulation of intestinal fate by Notch. *Proc Natl Acad Sci U S A, 102*(35), 12443-12448.
Tae, C. H., Kim, S. E., Jung, S. A., Joo, Y. H., Shim, K. N., Jung, H. K., et al. (2014a). Involvement of adiponectin in early stage of colorectal carcinogenesis. *BMC Cancer, 14*(1), 811.
Tae, C. H., Kim, S. E., Jung, S. A., Joo, Y. H., Shim, K. N., Jung, H. K., et al. (2014b). Involvement of adiponectin in early stage of colorectal carcinogenesis. *BMC Cancer, 14*, 811.
Tai, E. K., Wong, H. P., Lam, E. K., Wu, W. K., Yu, L., Koo, M. W., et al. (2008). Cathelicidin stimulates colonic mucus synthesis by up-regulating MUC1 and MUC2 expression through a mitogen-activated protein kinase pathway. *J Cell Biochem, 104*(1), 251-258.
Tian, X., Liu, Z., Niu, B., Zhang, J., Tan, T. K., Lee, S. R., et al. (2011). E-cadherin/beta-catenin complex and the epithelial barrier. *J Biomed Biotechnol, 2011*, 567305.
Tong, Y., Yang, W., & Koeffler, H. P. (2011). Mouse models of colorectal cancer. [Research Support, N.I.H., Extramural
Research Support, Non-U.S. Gov't
Review]. *Chin J Cancer, 30*(7), 450-462.
Trayhurn, P., & Wood, I. S. (2004). Adipokines: inflammation and the pleiotropic role of white adipose tissue. *Br J Nutr, 92*(3), 347-355.
Tsai, C. F., Ou, B. R., Liang, Y. C., & Yeh, J. Y. (2013). Growth inhibition and antioxidative status induced by selenium-enriched broccoli extract and selenocompounds in DNA mismatch repair-deficient human colon cancer cells. [Research Support, Non-U.S. Gov't]. *Food Chem, 139*(1-4), 267-273.
Tsai, J. S., Chuang, L. M., Chen, C. S., Liang, C. J., Chen, Y. L., & Chen, C. Y. (2014). Troglitazone and Delta2Troglitazone enhance adiponectin expression in monocytes/macrophages through the AMP-activated protein kinase pathway. *Mediators Inflamm, 2014*, 726068.
Turanov, A. A., Shchedrina, V. A., Everley, R. A., Lobanov, A. V., Yim, S. H., Marino, S. M., et al. (2014). Selenoprotein S is involved in maintenance and transport of multiprotein complexes. *Biochem J, 462*(3), 555-565.
Tytgat, K. M., Buller, H. A., Opdam, F. J., Kim, Y. S., Einerhand, A. W., & Dekker, J. (1994). Biosynthesis of human colonic mucin: Muc2 is the prominent secretory mucin. *Gastroenterology, 107*(5), 1352-1363.
Van der Sluis, M., De Koning, B. A., De Bruijn, A. C., Velcich, A., Meijerink, J. P., Van Goudoever, J. B., et al. (2006). Muc2-deficient mice spontaneously develop colitis, indicating that MUC2 is critical for colonic protection. *Gastroenterology, 131*(1), 117-129.

van Es, J. H., de Geest, N., van de Born, M., Clevers, H., & Hassan, B. A. (2010). Intestinal stem cells lacking the Math1 tumour suppressor are refractory to Notch inhibitors. *Nat Commun, 1*, 18.

van Horssen, R., Ten Hagen, T. L., & Eggermont, A. M. (2006). TNF-alpha in cancer treatment: molecular insights, antitumor effects, and clinical utility. *Oncologist, 11*(4), 397-408.

Van Klinken, B. J., Dekker, J., Buller, H. A., de Bolos, C., & Einerhand, A. W. (1997). Biosynthesis of mucins (MUC2-6) along the longitudinal axis of the human gastrointestinal tract. *Am J Physiol, 273*(2 Pt 1), G296-302.

van Kruijsdijk, R. C., van der Wall, E., & Visseren, F. L. (2009). Obesity and cancer: the role of dysfunctional adipose tissue. *Cancer Epidemiol Biomarkers Prev, 18*(10), 2569-2578.

Vander Heiden, M. G., Cantley, L. C., & Thompson, C. B. (2009). Understanding the Warburg effect: the metabolic requirements of cell proliferation. *Science, 324*(5930), 1029-1033.

Velcich, A., Yang, W., Heyer, J., Fragale, A., Nicholas, C., Viani, S., et al. (2002). Colorectal cancer in mice genetically deficient in the mucin Muc2. *Science, 295*(5560), 1726-1729.

Vetvik, K. K., Sonerud, T., Lindeberg, M., Luders, T., Storkson, R. H., Jonsdottir, K., et al. (2014). Globular adiponectin and its downstream target genes are up-regulated locally in human colorectal tumors: ex vivo and in vitro studies. [Research Support, Non-U.S. Gov't]. *Metabolism, 63*(5), 672-681.

Virchow, R. (1989). Cellular pathology. As based upon physiological and pathological histology. Lecture XVI--Atheromatous affection of arteries. 1858. *Nutr Rev, 47*(1), 23-25.

Waki, H., Yamauchi, T., Kamon, J., Ito, Y., Uchida, S., Kita, S., et al. (2003). Impaired multimerization of human adiponectin mutants associated with diabetes. Molecular structure and multimer formation of adiponectin. *J Biol Chem, 278*(41), 40352-40363.

Wang, Y., Chen, J., Zhang, D., Zhang, Y., Wen, Y., Li, L., et al. (2013). Tumoricidal effects of a selenium (Se)-polysaccharide from Ziyang green tea on human osteosarcoma U-2 OS cells. [Research Support, Non-U.S. Gov't]. *Carbohydr Polym, 98*(1), 1186-1190.

Wang, Y., Lam, K. S., Xu, J. Y., Lu, G., Xu, L. Y., Cooper, G. J., et al. (2005). Adiponectin inhibits cell proliferation by interacting with several growth factors in an oligomerization-dependent manner. *J Biol Chem, 280*(18), 18341-18347.

Wei, E. K., Giovannucci, E., Fuchs, C. S., Willett, W. C., & Mantzoros, C. S. (2005). Low plasma adiponectin levels and risk of colorectal cancer in men: a prospective study. *J Natl Cancer Inst, 97*(22), 1688-1694.

Weiss, R., Dufour, S., Groszmann, A., Petersen, K., Dziura, J., Taksali, S. E., et al. (2003). Low adiponectin levels in adolescent obesity: a marker of increased intramyocellular lipid accumulation. *J Clin Endocrinol Metab, 88*(5), 2014-2018.

Westerink, J., & Visseren, F. L. (2011). Pharmacological and non-pharmacological interventions to influence adipose tissue function. *Cardiovasc Diabetol, 10*, 13.

Whanger, P. D. (2004). Selenium and its relationship to cancer: an update. *Br J Nutr, 91*(1), 11-28.

Whelan, G. (1991). Ulcerative colitis--what is the risk of developing colorectal cancer? *Aust N Z J Med, 21*(1), 71-77.

Williams, C. J., Mitsiades, N., Sozopoulos, E., Hsi, A., Wolk, A., Nifli, A. P., et al. (2008). Adiponectin receptor expression is elevated in colorectal carcinomas but not in gastrointestinal stromal tumors. *Endocr Relat Cancer, 15*(1), 289-299.

Wimmer, I., Hartmann, T., Brustbauer, R., Minear, G., & Dam, K. (2014). Selenium levels in patients with autoimmune thyroiditis and controls in lower Austria. *Horm Metab Res, 46*(10), 707-709.

Wong, M. H. (2004). Regulation of intestinal stem cells. *J Investig Dermatol Symp Proc, 9*(3), 224-228.

Wright, D. H., Ford-Hutchinson, A. W., Chadee, K., & Metters, K. M. (2000). The human prostanoid DP receptor stimulates mucin secretion in LS174T cells. *Br J Pharmacol, 131*(8), 1537-1545.

Xing, S. Q., Zhang, C. G., Yuan, J. F., Yang, H. M., Zhao, S. D., & Zhang, H. (2015). Adiponectin induces apoptosis in hepatocellular carcinoma through differential modulation of thioredoxin proteins. *Biochem Pharmacol, 93*(2), 221-231.

Yamauchi, T., Kamon, J., Ito, Y., Tsuchida, A., Yokomizo, T., Kita, S., et al. (2003). Cloning of adiponectin receptors that mediate antidiabetic metabolic effects. *Nature, 423*(6941), 762-769.

Yamauchi, T., Kamon, J., Minokoshi, Y., Ito, Y., Waki, H., Uchida, S., et al. (2002). Adiponectin stimulates glucose utilization and fatty-acid oxidation by activating AMP-activated protein kinase. *Nat Med, 8*(11), 1288-1295.

Yamauchi, T., Nio, Y., Maki, T., Kobayashi, M., Takazawa, T., Iwabu, M., et al. (2007). Targeted disruption of AdipoR1 and AdipoR2 causes abrogation of adiponectin binding and metabolic actions. *Nat Med, 13*(3), 332-339.

Yan, L., & DeMars, L. C. (2012). Dietary supplementation with methylseleninic acid, but not selenomethionine, reduces spontaneous metastasis of Lewis lung carcinoma in mice. [Research Support, U.S. Gov't, Non-P.H.S.]. *Int J Cancer, 131*(6), 1260-1266.

Yan, L., Yee, J. A., Li, D., McGuire, M. H., & Graef, G. L. (1999). Dietary supplementation of selenomethionine reduces metastasis of melanoma cells in mice. [Research Support, Non-U.S. Gov't]. *Anticancer Res, 19*(2A), 1337-1342.

Yang, Q., Bermingham, N. A., Finegold, M. J., & Zoghbi, H. Y. (2001). Requirement of Math1 for secretory cell lineage commitment in the mouse intestine. *Science, 294*(5549), 2155-2158.

Yang, Y., Huang, F., Ren, Y., Xing, L., Wu, Y., Li, Z., et al. (2009). The anticancer effects of sodium selenite and selenomethionine on human colorectal carcinoma cell lines in nude mice. *Oncol Res, 18*(1), 1-8.

Yoon, S. O., Kim, M. M., & Chung, A. S. (2001). Inhibitory effect of selenite on invasion of HT1080 tumor cells. *J Biol Chem, 276*(23), 20085-20092.

Yu, J., Yao, H., Gao, X., Zhang, Z., Wang, J. F., & Xu, S. W. (2014). The Role of Nitric Oxide and Oxidative Stress in Intestinal Damage Induced by Selenium Deficiency in Chickens. *Biol Trace Elem Res*.

Zeng, H., & Wu, M. (2015). The Inhibitory Efficacy of Methylseleninic Acid Against Colon Cancer Xenografts in C57BL/6 Mice. *Nutr Cancer*, 1-8.

Zheng, X., Tsuchiya, K., Okamoto, R., Iwasaki, M., Kano, Y., Sakamoto, N., et al. (2011). Suppression of hath1 gene expression directly regulated by hes1 via notch signaling is associated with goblet cell depletion in ulcerative colitis. *Inflamm Bowel Dis, 17*(11), 2251-2260.

Zhuo, H., Smith, A. H., & Steinmaus, C. (2004). Selenium and lung cancer: a quantitative analysis of heterogeneity in the current epidemiological literature. [Comparative Study
Meta-Analysis
Research Support, Non-U.S. Gov't
Research Support, U.S. Gov't, P.H.S.
Review]. *Cancer Epidemiol Biomarkers Prev, 13*(5), 771-778.

APPENDIX A

DETAILED PROTOCOL

DAKO/ProHisto IHC Protocol

1. Put slides in a glass slide holder and place in the following solutions serially (rocking at room temperature):
    a. xylene: 5 min., swishing every 2 min. (UNDER THE HOOD)
    b. xylene: 5min., swishing every 2 min. (UNDER THE HOOD)
    c. 100% EtOH: 2 min., swishing every 30 sec.
    d. 95% EtOH: 2 min.,rocking.
    e. 80% EtOH: 2 min., rocking.
    f. f.70% EtOH: 2min., rocking.
    g. 50% EtOH: 2 min., rocking.
    h. dd H_2O: 2x3min., rocking.
    i.
2. Put slides with fixed cells in a glass slide holder and place in the following solutions serially (rocking at room temperature):
    - 1xTBST (pH 7.6) 5 min
    - 2x3min. in 1xTBST
3. Transfer slide holder into plastic container and put in 1xCitrate Antigen Retrieval Buffer (stored at 4°C). To prepare 1xCAR Buffer: add 30ml of 10xCAR Buffer (ProHisto) to 270ml of dH_2O.

Take off metal handle.

4. Autoclave for min 20 min (max 30 min). In 5th floor small autoclave, choose "liquid-slow exhaust" and set time for 25 min. Sign name in log book. Sample done in 1 hour total. If using ProHisto box, add 15 ml Antigen Retrieval Buffer per well. Autoclave 8 min on slow exhaust. Done in 25 - 30 min.

5. Retrieve sample from autoclave using gloves and tray. Let sit 20 min at RT in Citrate Buffer.

6. Wash in 1xTBST for 5 min.

7. Wipe off back and sides of slide with Kimwipe tissues; lay flat on benchtop and cover tissue with 1-3 drops of Peroxidase Block (DAKO), stored at 4°C in the fridge. Incubate 30 min at RT, checking every 5-10 min. to make sure samples don't dry out. Add more Peroxidase Block if slides starting to dry.

8. Put slides back into slide carrier and wash 3x3min in 1xTBST.

9. Dilute primary antibody in ProHisto Antibody Dilution Buffer, stored at 4°C in the fridge. Minimum of 3 ml needed per slide for ProHisto box.

10. Incubate 12 to 72h, rocking at 4° C.

11. Put slides back into glass slide carrier and wash 2x10 min. in 1xTBST.

12. Wipe off back and sides of slides with a Kimwipe, place flat on benchtop, and add 1-3 drops of Labeled Polymer Yellow (DAKO) straight from the bottle, just enough to cover tissue. Make sure to use proper DAKO kit, e.g. DAKO #K400611 for monoclonal primary antibodies (host species is mouse), or DAKO # K400911 for polyclonal primary antibodies (host species is rabbit). Incubate 30 min at RT, adding more polymer if slides start to dry out.

13. As soon as slides are incubating, mix up a DAB solution. The ratio of the solution is 1ml solution 3a (Buffered Substrate): 1 drop 3b (liquid DAB and chromagen). Mix well. Make enough so there is 200 ul per slide. Let the mixed solution sit RT 30-60 min. before using.

14. Put slides in glass slide carrier and wash 2X 5 min. in 1X TBST.

15. Wash slides in dH2O 1X 3 min.

16. Wipe slides with Kimwipe, keeping tissue moist, and add DAB solution. Check the staining of one slide first by testing a positive: Incubate with 100-200 ul of DAB solution, starting at 30 seconds. Check using the microscope at 40X. Keep note of DAB times. Wash slides as soon as staining is optimal with dH2O.

17. Wash slides in dH2O 1 X 3 min.

18. Counterstain using 0.5% Methyl Green. Add 200 ml of methyl green onto tissue and incubate at RT for 2 min. Rinse in containers of dd H2O until slides are clean and let dry, with slides standing vertically on their ends.

19. Add one drop of permount, put on coverslip, and smooth out bubbles using big end of pipettor tip. Label slides with: date, antibody, dilution, and timing. After 4-5 hours, clean off extra permount with xylene. (xylene is optional-only if covering tissue).

ImmunoHistoChemistry Protocol

(for paraffin-embedded tissues)

1. Set the water bath at 95-100^{o}C.

2. **For formalin-fixed, paraffin-embedded tissues, deparaffinize** sections by 3x5 min xylene washes.

3. Prepare 90 ml of 1X solution of the **Epitope Unmasking Solution** from its 10X stock [ProHisto]. This is also called the Citrate Antigen Retrieval Buffer or just Citrate Buffer. It is stored at 4^{o}C. Pour the solution in a **heat-resistant** coplin jar, and put the jar into the water bath. Put a thermometer into the coplin jar and wait for the temperature to rise to 95-100^{o}C.

4. Wash 2x5 min in 100% ETOH.

5. Wash 1x3 min in 95% ETOH and 1x3 min in 70% ETOH.

6. Wash 2x3 min in dH_2O.

7. Wash 1x5 min (1X) Amplifying IHC wash buffer [ProHisto] – kept at R.T., (1X TBST or 1X PBST can also be used). Wash again 2x3 min with the wash buffer.
8. Once the temperature of the epitope unmasking solution/citrate buffer reaches ~95^{o}C, place the slides into it. Place the lid onto the coplin jar loosely. Incubate the slides in the citrate buffer for 30 minutes.

9. Turn off the water bath and remove the coplin jar from it and close it tightly. Keep the jar containing the slides at R.T. for 20-30 minutes, allowing the temperature to slowly come down to R.T.

10. Wash 1x5 min with 1X wash buffer.

11. Wipe off extra liquid from the slides and cover the tissue with **Peroxidase Block** (Dako) – kept at 4^{o}C, and incubate the slides for 30 minutes at R.T., checking every 5-10 minutes so that the slides don't dry out. Add more peroxidase block if slides start to dry out.

12. Wash 3x3 min with 1X wash buffer.

13. Dilute the **primary antibody** in (ProHisto) Amplifying Antibody Dilution Buffer stored at 4^{o}C. [3.5 ml solution is enough to cover a single slide kept in a slide compartment box.

14. Incubate for 12-72 hours at 4^{o}C, rocking.

15. Wash 2x10 min in 1X wash buffer.

16. Wipe off excess liquid from the slides and cover the tissues with Labelled Polymer-HRP-anti-Rabbit (Dako), kept at 4^{o}C, and incubate the slides for 30 min at R.T., adding more polymer if slides start to dry out – [**secondary antibody**]. As soon as the slide incubation starts prepare DAB solution = 1 ml DAB+ Substrate Buffer (Dako) + 1 drop of DAB chromogen (BrdU In-situ Staining Kit), and leave it at R.T. till the slide incubation gets over.

17. Wash 2x5 min with wash buffer.

18. Wash 1x3 min in dH_2O.

19. Wipe off the excess liquid from the slides keeping the tissue moist. Cover the tissues with the prepared **DAB** solution, and incubate 30 sec to a maximum of 8 minutes (till the desired colour intensity is developed), checking it under the microscope.

20. Wash 1x3 min in dH_2O.

21. **Counterstain** with 0.5% Methyl Green, for 30 seconds.

22. Follow the following steps OR keep the counterstained slides, and then rinse thoroughly in water until the stain no longer fades. Keep the slides for drying O/N, OR follow the following steps for **dehydration** :-
23. Wash 1x2 min with 95% EtOH.
    Wash 2x3 min with 100% EtOH.
    Wash 2x5 min with xylene.
    20-30 minutes air dry.

24. Mount the slides with permount, and view under the microscope.

RIPA Homogenization Buffer
(for homogenization of colon samples for Western Blot)

To RIPA buffer (commercially available from SIGMA: R0278-50ML; 091M6007), **add the following:**

Sodium pyrophosphate – 2.5 mM; [Stock prepared – 100mM]

Sodium Flouride – 5 mM; [Stock – 500 mM]

β-glycerophosphate – 1 mM; [Stock – 100 mM]

Sodium orthovandate – 1mM; [Stock – 1M]

Protease inhibitor – 1:100

Use 200 µl of the above **freshly prepared** buffer for homogenization of the tissue (colon) samples weighed beforehand (usually 20-30 mg sample is used).

Once the tissue is homogenized completely, add 200 µl more of the buffer (total 400 µl) to the homogenized tissue sample.

Centrifuge the above contents at 12000 rpm at $4^{O}C$ for 15 minutes.

Perform Bradford protein estimation assay on the samples using 10X dilution.

Protein estimation Protocol

1). **Label eppendorfs** A through J and keep them on ice. Keep the protein samples also on ice.

2). Label the wells of the **template** to be used in the microplate reader.

3). Prepare **BSA standard** concentrations as follows:-

Eppendorf	Protein amount (µg)
A	0
B	1
C	2
D	3
E	4
F	5
G	6
H	7

4). **Loading of samples**: add 10 µl of each protein sample (as per duplicates or triplicates) and the standards (should be loaded after the test samples) to each of the wells.

5). Prepare the **Bradford dye solution** by adding 4 ml of dye (Biorad) to 16 ml of ddH_2O. Add 200 µl of the prepared dye to each of the wells.

6). Incubate in dark at R.T. for 12 minutes, and read the plate using the plate reader:-

* new experiment – template – file – instrument set up – read mode "endpoint" – read speed "step" – measurement filter "595 nm" – mix time "3 sec" – mix speed "low" – instrument control "close door" – read.

7). Collect data and standard curve for **analysis**.

ApopTag™ TUNEL Assay (Kit)

[DO NOT touch dry tissue with film]

1. Purchase Apop-Tag kit from Millipore (Product #S7100).

2. **For formalin-fixed, paraffin-embedded tissues, deparaffinize** sections by 3x5 min xylene washes.
3. Wash 2x5 min in 100% ETOH.
4. Wash 1x3 min in 95% ETOH and 1x3 min in 70% ETOH.
5. Wash 1x5 min in PBS.
6. Dilute **proteinase K** (Millipore product # 21627 **Stock = 200µg/ mL**) to 20 ug/ml in PBS, 40 µl is enough to cover a medium-sized tissue. Incubate with slides for 15 min at RT **(cover the tissue only)**
7. Wash slides 2x2 min in dH2O.
8. **Peroxidase quench / blocking** in 3% H2O2 in PBS for 5 min at RT **(cover the tissue only).**
9. Rinse slides 2x5 min in PBS or dH_2O.
10. Blot off extra liquid.
11. Add equilibration buffer for at least 10 seconds at RT **(cover the tissue only)**
12. Blot off extra liquid.
13. Add TdT enzyme as a working solution: 77uL of reaction buffer + 33uL of TdT enzyme - are sufficient for 2 sections), **(use ~15 µl for each tissue).**
14. Incubate at 37^{o}C for 1 hour in a humidified chamber **(2 to 2.5 hrs).**
15. Add working strength stop solution (1mL stop solution and 34 ml dH_2O). Agitate for 15 sec and incubate for 10 min at RT.
16. Remove an aliquot of anti-digoxigenin conjugate. Warm to RT.
17. Wash slides 3x1 min in PBS.
18. Blot off excess liquid.
19. Add anti-digoxigenin conjugate to each slide.
20. Incubate in humidified chamber for 30 min at RT.
21. Wash slides 4x2 min in PBS.
22. Prepare working strength DAB peroxidase substrate: 1ml DAB buffer + 1-2 drops of DAB chromogen.
23. Incubate slides with DAB for 3-6 min **(8 min)** – keep viewing under the microscope until the desired colour intensity is development.
24. Wash the slides 3x1 min in dH_2O.
25. Wash slides for 1x5 min in dH_2O.
26. Counterstain with hematoxylin **(filter before with whatman filter paper)** – 1-2 min.
27. Counterstain with methyl green (if not using hematoxylin) – 30 sec.
28. Wash the slides with dH_2O until the counterstain no longer fades.
29. **Dehydrate** with 1 x 2 min wash with 95% EtOH.
30. 100% EtOH 2 x 3 min.
31. Xylene 2 x 5 min

32. Air-dry for ~30 minutes (if xylene was used, or O/N if dehydration steps were avoided).
33. Mount with xylene based permount solution.
34. Air-dry for 20 minutes, and view under the microscope.

Western Blot protocol

1. **Protein homogenization:** Ref. RIPA buffer protocol.

2. **Protein normalization:** calculated as the amount of protein that will be loaded on the gel (prepare a proper loading pattern for the gel that is needed to be run); ref. any normalization file on computer.

3. **Gel preparation:**

Resolving gel – 10% polyacrylamide

	for 2 gels	for 1 gel
dH_2O –	4.9 ml	2.45 ml
gel buffer –	2.5 ml	1.25 ml
40% acrylamide –	2.475 ml	1.238 ml
10% SDS –	200 µl	100 µl
10% APS –	50 µl as 10% soln or a pinch in powder form	50 µl as 10% soln
TEMED -	5 µl	4 µl

Stacking gel – 5% polyacrylamide

	for 2 gels
dH_2O –	3.062 ml
gel buffer –	1.25 ml
40% acrylamide –	0.638 ml
10% SDS –	50 µl
10% APS –	25 µl as 10% soln or a pinch in powder form
TEMED -	5 µl

4. Load the Resolving gel on the gel preparation apparatus and add 70% ethanol on top of it immediately using a syringe. Let the gel solidify for 30 minutes.

5. After removing the 70% ethanol from the apparatus (by inverting the apparatus), blot the inside of the gel using a tissue paper.
   Now load the stacking gel on top and put on the gel comb. Let the gel fluid leak out during the comb insertion and do not try to wipe it out immediately. Let the gel solidify for another 30 minutes.
   Prepare the running buffer during this time.

6. Prepare **1X running buffer:**

   Tris – 3 g
   Glycine – 14.4 g
   SDS – 1 g
   in **dH_2O**, and make up the volume to 1 liter

7. Pour running buffer into the gel running tub and place the gel cassette with the gel held into it, inside the tub (use a dummy plate for the gel cassette in case only 1 gel is to be run). Remove the gel comb once the gel is completely submerged in the gel running buffer.

8. Prepare **Laemmli/loading buffer:**

   To make 20 ml of 4X stock:
   0.5 M Tris-HCl (pH 6.8) – 8 ml
   SDS – 1.6 g
   100% glycerol – 8 ml
   14.7 M β-mercaptoethanol – 8 ml
   0.5 M EDTA – 2 ml
   Bromophenol Blue – 16 mg
   dH_2O – 1.2 ml

9. **Denaturation of protein samples and loading:** Add the normalized volumes of the protein samples to 4X Laemmli buffer in the ratio 2:1::protein:buffer and vortex. Keep the eppendorfs in water bath/heating block for **boiling** for 12 minutes. During this time prerun the gel at 100 V for 10 – 15 minutes.
   Spin the eppendorfs for 2-3 seconds, vortex the contents and again give them a short spin.

10. Load the samples on the gel using the prepared loading pattern, and run the gel at 80 V for first 10 minutes and then at 110 – 120 V for the rest of the time.
    *Prepare transfer buffer at this time.
    Stop the gel immediately once the dye starts coming out of the gel in case the protein is low molecular weight and let it run more for around 5 minutes after the dye comes out in case the protein of interest is of a high molecular weight.

11. * **Preparation of 1X transfer buffer:**

    Tris – 3 g
    Glycine – 14.4 g
    Methanol – 200 ml
    in **dH_2O**, and make up the volume to 1 liter

    - Prepare 1.5 liters of transfer buffer for the transfer step.

12. **Tranfer:** Pour the transfer buffer in a glass tray and soak the fiber, filter paper and the nitrocellulose membrane that will be used in the process [use forceps to handle the nitrocellulose membrane].
    Remove the gel from gel plate by hydrating them enough by pouring transfer buffer towards the side of the gel containing wells. Gently remove one of the plates and cut out parts of the gel containing stacking gel and the bottom end that usually contains ripples which may interfere with the transfer process.

13. **Arrange** the contents as below:
    Black side of transfer cassette
    Fiber
    Filter paper
    Gel
    Nitrocellulose membrane
    Filter paper
    Fiber
    Transparent side of transfer cassette

    Close the cassette and put it into the transfer apparatus (black side of transfer cassette facing black side of apparatus).

14. Fill the whole of the transfer apparatus tub with transfer buffer and put at 4^oC, 220 mA for 3 hours, on a stirrer plate. Put a magnetic stirrer inside the transfer apparatus tub and set rotation to 200 rpm.

15. Discard transfer buffer, gel and filter paper; and wash the nitrocellulose membrane with 1X PBS for 10 minutes.

16. Cut out extra membrane based on the size of the protein.

17. **Block** the membrane using 1X PBS with 0.1% tween 20 and 5% milk for 1 hour.

18. Add **primary antibody** to the membrane prepared in a suitable ratio in 1X PBS with 0.1% tween 20 and 5% milk, and incubate for the desired time (16 hours/overnight/24 hours/48 hours/72 hours) at 4^{o}C, shaking.

19. **Wash** membrane 5x10 minutes with 1X PBS containing 0.1% tween 20.

20. Add **secondary antibody** to the membrane prepared at a ratio of 1:2000 – 1:3000 in 1X PBS containing 0.1% tween 20 and 5% milk and incubate for 1 hour at R.T.

21. Repeat the wash as in step 19, using 6 washes. At the start of 4th wash, switch on the chemiluminescent film developer machine. At the start of 5th wash, put the ECL bottles at R.T. from 4^{o}C.

22. Add equal quantities of both the solutions – Detection Reagent 1 (Peroxide solution) and Detection Reagent 2 (Luminol Enhancer solution) from either the ThermoECL or AdvanstaECL kit – to the membrane [1 ml of both solutions (total 2ml) is needed for a single membrane]. Incubate in dark for 10 minutes. Meanwhile, prepare the cellotape, cling wrap and gel developer cassette for developing the membrane.

23. Remove the nitrocellulose membrane from the ECL solution and wrap safely using a transparent wrapping film. Fix the film in the cassette using tape and immediately close the cassette.

24. Switch off all lights in the dark room keeping only the red light. Cut the chemiluminescence film into half or use it full size according to the number of membranes being exposed, and keep it on top of the membrane to be developed. Close the cassette and keep in a dark place (closed drawer) for an appropriate time of exposure; you can switch on the lights at this time.
    Note: some proteins need less time while others may need more time to be obtained on the chemiluminesence film, based on their levels of expression in any sample.

25. Switch off the lights and remove the exposed film from the membrane in the cassette and put it in the developer machine. DO NOT turn on the lights again until a "ready" light appears on the machine and it beeps. Obtain the developed film from the developer machine and analyse.
    Keep another film for exposure on to the gel-blotted membrane for lesser or more time than the previous attempt to get the right amount of exposure level on it; ie, repeat steps 24 and 25 if and when necessary.

Alcian Blue Staining Protocol

Solutions and Reagents:

3% Acetic Acid Solution:
Glacial acetic acid ---------- 3 ml
Distilled water ---------- 97 ml

Alcian Blue Solution (pH 2.5):
Alcian blue, 8GX ---------- 1 g
Acetic acid, 3% solution ---------- 100 ml
Mix well and adjust pH to 2.5 using acetic acid.

0.1% Nuclear Fast Red Solution:
Nuclear fast red ---------- 0.1 g
Aluminum sulfate---------- 5 g
Distilled water ----------100 ml
Dissolve aluminum sulfate in water. Add nuclear fast red and slowly heat to boil and cool. Filter and add a grain of thymol as a preservative.

Procedure:

1. Deparaffinize slides and hydrate to distilled water.
2. Stain in alcian blue solution for 30 minutes.
3. Wash in running tap water for 2 minutes.
4. Rinse in distilled water.
5. Counterstain in nuclear fast red solution for 5 minutes.
6. Wash in running tap water for 1 minute.
7. Dehydrate and through 95% alcohol, 2 changes of absolute alcohol, 3 minutes each.
8. Clear in xylene or xylene substitute.
9. Mount with resinous mounting medium.

Hematoxylin and Eosin Staining Protocol

1. Deparaffinize in Xylene I and II and III (3 minutes)
2. Rehydrate
    a. EtOH 100% (3 minutes)
    b. EtOH 100% (3 minutes)
    c. EtOH 95% (3 minutes)
    d. EtOH 95% (3 minutes)
    e. EtOH 70% (3 minutes)
3. Rinse in distilled water (5 minutes)
4. Stain in hematoxylin (6 minutes) ***Filter before each use to remove oxidized particles***
5. Rinse in running tap water (15 minutes)
6. Decolorize in acid alcohol (1 second)
7. Rinse well in tap water (5 minutes)
8. Immerse in ammonia water (3 Seconds)
9. Rinse in tap water (5 minutes)
10. Counterstain in Eosin (15 seconds)
11. Dehydrate
    a. EtOH 95 % (3 minutes) ***Discard after each use***
    b. EtOH 95% (3 minutes)
    c. EtOH 100 % (3 minutes)
    d. EtOH 100 % (3 minutes)
12. Clear in Xylene I and II (5 minutes)
13. Mount with Cytoseal in fume hood.

Adiponectin ELISA protocol

1. Prepare reagents, standard dilutions, control, and samples as directed in the kit. Make 1:200 dilution of the serum samples.

2. Remove excess microplate strips from the plate frame, return them to the foil pouch containing the desiccant pack, and reseal.

3. Add 50 µL of Assay Diluent RD1W to each well.

4. Add 50 µL of Standard, control, or sample* per well. Tap plate gently for one minute. Cover with the adhesive strip provided. Incubate for 3 hours at room temperature.

5. Aspirate each well and wash, repeating the process four times for a total of five washes. Wash by filling each well with Wash Buffer (400 µL) using a squirt bottle, manifold dispenser, or autowasher. Complete removal of liquid at each step is essential to good performance. After the last wash, remove any remaining Wash Buffer by aspirating or decanting. Invert the plate and blot it against clean paper towels.

6. Add 100 µL of Mouse Adiponectin Conjugate to each well. Cover with a new adhesive strip. Incubate for 1 hour at room temperature.

7. Repeat the aspiration/wash as in step 5. 8. Add 100 µL of Substrate Solution to each well. Incubate for 30 minutes at room temperature. Protect from light. 9. Add 100 µL of Stop Solution to each well. Gently tap the plate to ensure thorough mixing. 10. Determine the optical density of each well within 30 minutes, using a microplate reader set to 450 nm. If wavelength correction is available, set to 540 nm or 570 nm. If wavelength correction is not available, subtract readings at 540 nm or 570 nm from the readings at 450 nm. This subtraction will correct for optical imperfections in the plate. Readings made directly at 450 nm without correction may be higher and less accurate.

IL-6 ELISA protocol

1. Bring all reagents and samples to room temperature (18 - 25°C) prior to use. It is recommended that all standards and samples be run in duplicate. A standard curve is required in each assay run.

2. Remove required quantity of test strips/wells, place in well holder. Note: Wells are provided in breakable 8-well strips. Strips may be "broken" into individual wells, replaced in well holder, and assayed. Return any unused wells to sealed pouch for 2 - 8°C storage.

3. Pipette 50 µL of ELISA Diluent into each well.

4. Pipette 50 µL of each standard (see Reagent Preparation, step 2) and sample into appropriate wells. Gently shake/tap the plate for 5 seconds to mix. Cover wells with Plate Sealer and incubate for 2 hours at room temperature.

5. Prepare Working Detector. Within 15 minutes prior to use, pipette required volume of Detection Antibody into a clean tube or flask. Add in required quantity of Enzyme Concentrate (250×), vortex or mix well. For a full 96-well plate, add 48 µL of Enzyme Concentrate into 12 mL of Detection Antibody.

6. Decant or aspirate contents of wells. Wash wells by filling with at least 300 µL/well prepared Wash Buffer (see Reagent Preparation, step 4), followed by decanting/aspirating. Repeat wash 4 times for a total of 5 washes. After the last wash, blot plate on absorbent paper to remove any residual buffer. Complete removal of liquid is required for proper performance.

7. Add 100 µL of prepared Working Detector (see step 5 above) to each well. Cover wells with Plate Sealer and incubate for 1 hour at room temperature.

8. Wash wells as in Step 6, but a total of 7 times. Note: In this final wash step, soak wells in wash buffer for 30 seconds to 1 minute for each wash. Thorough washing at this step is very important.

9. Add 100 µL of TMB One-Step Substrate Reagent to each well. Incubate plate (without Plate Sealer) for 30 minutes at room temperature in the dark.

10. Add 50 µL of Stop Solution to each well. 11. Read absorbance at 450 nm within 30 minutes of stopping reaction. If wavelength correction is available, subtract the optical density readings at 570 nm from readings at 450 nm.

IL-10 ELISA protocol

1. Coat microwells with 100 µL per well of Capture Antibody diluted in Coating Buffer (1;250 dilution) . Seal plate and incubate overnight at 4° C.

2. Aspirate wells and wash 3 times with ≥ 300 µL/well Wash Buffer. After last wash, invert plate and blot on absorbent paper to remove any residual buffer.

3. Block plates with ≥ 200 µL/well Assay Diluent. Incubate at RT for 1 hour.

4. Aspirate/wash as in step 2.

5. Prepare standard and sample dilutions in Assay Diluent. Standard: 2000 pg/mL will be the highest standard and prepare other standard by serial dilution.

6. Pipette 100 µL of each standard, sample, and control into appropriate wells. Seal plate and incubate for 2 hours at RT.

7. Aspirate/ wash as in step 2, but with 5 total washes.

8. Add 100 µL of Working Detector (Detection Antibody + SAv-HRP reagent 1:250 dilution for detection and HRP dilution is on the bottle) to each well. Seal plate and incubate for 1 hour at RT.

9. Aspirate/ wash as in step 2, but with 7 total washes.

10. Add 100 µL of Substrate Solution to each well. Incubate plate (without plate sealer) for 30 minutes at room temperature in the dark.

11. Add 50 µL of Stop Solution or 1N HCL to each well.

12. Read absorbance at 450 nm within 30 minutes of stopping reaction. If wavelength correction is available, subtract absorbance at 570 nm from absorbance 450 nm.

IL-1β ELISA protocol

1. Coat microwells with 100 µL per well of Capture Antibody diluted in Coating Buffer (1;250 dilution). Seal plate and incubate overnight at 4° C.

2. Aspirate wells and wash 3 times with ≥ 300 µL/well Wash Buffer. After last wash, invert plate and blot on absorbent paper to remove any residual buffer.

3. Block plates with ≥ 200 µL/well Assay Diluent. Incubate at RT for 1 hour.

4. Aspirate/wash as in step 2.

5. Prepare standard and sample dilutions in Assay Diluent. Standard: 1000 pg/mL will be the highest standard and prepare other standard by serial dilution.

6. Pipette 100 µL of each standard, sample, and control into appropriate wells. Seal plate and incubate for 2 hours at RT.

7. Aspirate/ wash as in step 2, but with 5 total washes.

8. Add 100 µL of Detection Antibody diluted in Assay Diluent to each well. Dilution 1:250. Seal plate and incubate for 1 hour at RT.

9. Aspirate/ wash as in step 2, but with 5 total washes.

10. Add 100 µL of Enzyme Reagent diluted in Assay Diluent (dilution on the bottle) to each well. Seal plate and incubate for 30 min at RT.

11. Aspirate/ wash as in step 2, but with 7 total washes.

12. Add 100 µL of Substrate Solution to each well. Incubate plate (without plate sealer) for 30 minutes at room temperature in the dark.

13. Add 50 µL of Stop Solution to each well.

14. Read absorbance at 450 nm within 30 minutes of stopping reaction. If wavelength correction is available, subtract absorbance at 570 nm from absorbance 450 nm.

TNF-α ELISA protocol

1. Bring all reagents and samples to room temperature (18 - 25°C) prior to use. It is recommended that all standards and samples be run in duplicate.

2. Remove the required quantity of test strips/wells and place in well holder.

Note: Wells are provided in breakable 8-well strips. Strips may be “broken” into individual wells, replaced in a well holder, and assayed. Return any unused wells to sealed pouch for 2 - 8°C storage.

3. Pipette 50 µL of ELISA Diluent into each well.

4. Pipette 50 µL of each standard (see Reagent Preparation, step 2) and sample into appropriate wells. Cover wells with Plate Sealer and incubate for 2 hours at room temperature.

5. Decant or aspirate contents of wells. Wash wells by filling with at least300 µL/well prepared Wash Buffer (see Reagent Preparation, step 3)followed by decanting/aspirating. Repeat the wash 4 times for a totalof 5 washes. After the last wash, blot the plate on absorbent paper toremove any residual buffer. Complete removal of liquid is required forproper performance.

6. Add 100 µL of Detection Antibody to each well. Cover wells with Plate Sealer and incubate for 1 hour at room temperature.

7. a. Prepare Enzyme Working Reagent.
b. Pipette the required volume of Enzyme Diluent into a clean tube or flask. Add in the required quantity of Enzyme Concentrate (250×) and vortex or mix well. For a full 96-well plate, add 48 µL of Enzyme Concentrate into 12 mL of Enzyme Diluent.

8. Wash wells as in Step 5.

9. Add 100 µL of Enzyme Working Reagent (see step 7 above) to each well. Cover wells with Plate Sealer and incubate for 30 minutes at room temperature.

10. Wash wells as in Step 5, but a total of 7 times.
Note: In this final wash step, soak wells in wash buffer for 30 seconds to 1 minute for each wash. Thorough washing at this step is very important.

11. Add 100 µL of TMB One-Step Substrate Reagent to each well. Incubate plate (without Plate Sealer) for 30 minutes at room temperature in the dark.

12. Add 50 µL of Stop Solution to each well.

13. Read absorbance at 450 nm within 30 minutes of stopping the reaction. If wavelength correction is available, subtract the optical density readings at 570 nm from readings at 450 nm. A standard curve is required in each assay run.

APPENDIX B

DOCTORAL DISSERTATION PROTOCOL

Adiponectin and Selenium rich diet can act as a complimentary medicine in the treatment of intestinal and chronic inflammation induced colon cancer.

By

Arpit Saxena

March 20, 2015

Summary

Background and Significance: Colon cancer is the second largest cause of cancer death in United States. Chronic inflammation and obesity predispose patients to colon cancer. Adipose tissue is a source of bioactive substances called adipokines. Adiponectin (APN), an adipokine has anti-inflammatory property and found at lower levels in obese patients. Our preliminary data has shown that APN knockout (KO) mice had severe clinical manifestation associated with chemically induced colon cancer. Selenium (Se), a trace mineral and a dietary supplement, is inversely associated with cancer risk and possess anti-inflammatory and anti-carcinogenic properties. Furthermore, Se deficiency is associated with immune dysfunction, impaired resistance to microbial and viral infections, inadequate phagocytosis and antibody production. Colon insults by toxins and gut permeability also induce chronic inflammation caused by gut flora that activates the body's immune system, leading to the vicious cycle of chronic inflammation, which culminates into colorectal cancer. The ***overall purpose*** of this dissertation is to determine if chronic inflammation leading to colon and intestinal cancer are regulated by APN or Se rich diet or both. The ***working hypothesis*** is that APN deficiency will decrease goblet cell mucous production in colon leading to greater chronic inflammation and exacerbate the clinical symptoms and tumor load related to colon cancer. Se rich diet alone or in combination with APN administration will increase goblet cell production and apoptosis of cancer cells leading to reduced clinical symptoms, tumor load and inflammation. To test this hypothesis following specific aims will be used:

Specific Aim 1: **To determine if chronic inflammation induced colon cancer (CICC) is regulated by APN.**

Specific Aim 2: **To determine if Se rich diet can interact with APN to regulate CICC.**

Specific Aim 3: **To determine if APN administration and Se rich diet can act in conjugation to regulate intestinal inflammation and cancer in $APC^{Min/+}$ mice model.**

The ***primary objectives*** of this study are to: 1) determine whether CICC is effected by APN deficiency and to identify its effect on clinical manifestation, tumor load and inflammation, 2) elucidate how APN deficiency have an effect on goblet cell production and hence mucus secretion, 3) determine how Se rich diet could interact with APN to modulate clinical score, tumor load, inflammation and selenoproteins expression, 4) study how Se rich diet and APN deficiency could have an effect on cancer cell apoptosis and goblet cell production, 5) determine how APN administration and Se rich diet could have an effect on intestinal cancer modulating clinical score, tumor load, goblet cell production and cancer cell apoptosis and 6) study how APN and Se rich diet could impact oxidative stress and inflammation. The ***rationale*** for this proposal comes from several published manuscripts and our preliminary data. Our preliminary data indicated that the APNKO mice administered dimethylhydrazine (DMH) to induce colon cancer showed significantly higher clinical score and tumor number when compared to wild type (WT) mice given the same treatment. Se rich diet (0.75 ppm) was found to be effective in reducing clinical score and tumor number in both WT and APNKO mice administered DMH with a greater significance in APNKO mice. Our preliminary results are also supported by the published data of Mutoh et al., 2011 who had shown that $APN^{-/-}$ in $APC^{Min/+}$ mice increased the tumor load by 3.2-fold, by the age of 9 weeks and 3.4-fold by the age of 12 weeks when compared with $APN^{+/+}$ $APC^{Min/+}$ mice. AOM induced colon tumor formation was found to be significantly higher in $APN^{-/-}$ when compared to the $APN^{+/+}$ mice. The ***novelty*** of this

dissertation lies in studying the effect and the different mechanism of action of APN and Se rich diet on chronic inflammation induced by dextran sodium sulfate (DSS), colon cancer (by DMH) and CICC by DSS and DMH. In addition, we will also be studying the role of APN administration either alone or in conjugation with Se rich diet on $APC^{Min/+}$ mice model of intestinal cancer.

Limitations and Pitfalls

1. DSS induced colitis and DSS+DMH induced CICC are 2 different models and vary from DMH induced cancer (preliminary data), in pathology and the stage of cancer. In these new model it is possible that the APNKO and WT mice show similar pathology, clinical score and tumor load.
2. Loss of adiponectin may not have an effect on goblet cell production and hence mucus secretion.
3. APN administration on the goblet cell lines may cause greater apoptosis of the goblet cells rather than being anti-apoptotic and hence leading to lower mucin production.
4. Se administration as shown by previous publications might cause colon tumor cell apoptosis, but may not be effective in epithelial cell recovery or proliferation of epithelial cell to recover from colon insult.
5. There is no published data indicating the role of Se in goblet cell production therefore it might be possible that Se might not increase goblet cell production and hence no increased mucus secretion.

6. Se rich diet might not be effective in reducing the severity of intestinal cancer in the $APC^{Min/+}$ mouse model of intestinal cancer, as it is a completely different model system from the DMH model of colon cancer
7. APN administration might not be effective in reducing the severity of intestinal cancer in the $APC^{Min/+}$ mouse model of intestinal cancer.
8. Combination of Se and APN might not produce additive effects and might not be effective in significantly reducing the pathology, clinical score and tumor number when compared with individual treatments.
9. APN dosage may not be effective in reducing the severity of intestinal cancer.

Working Model

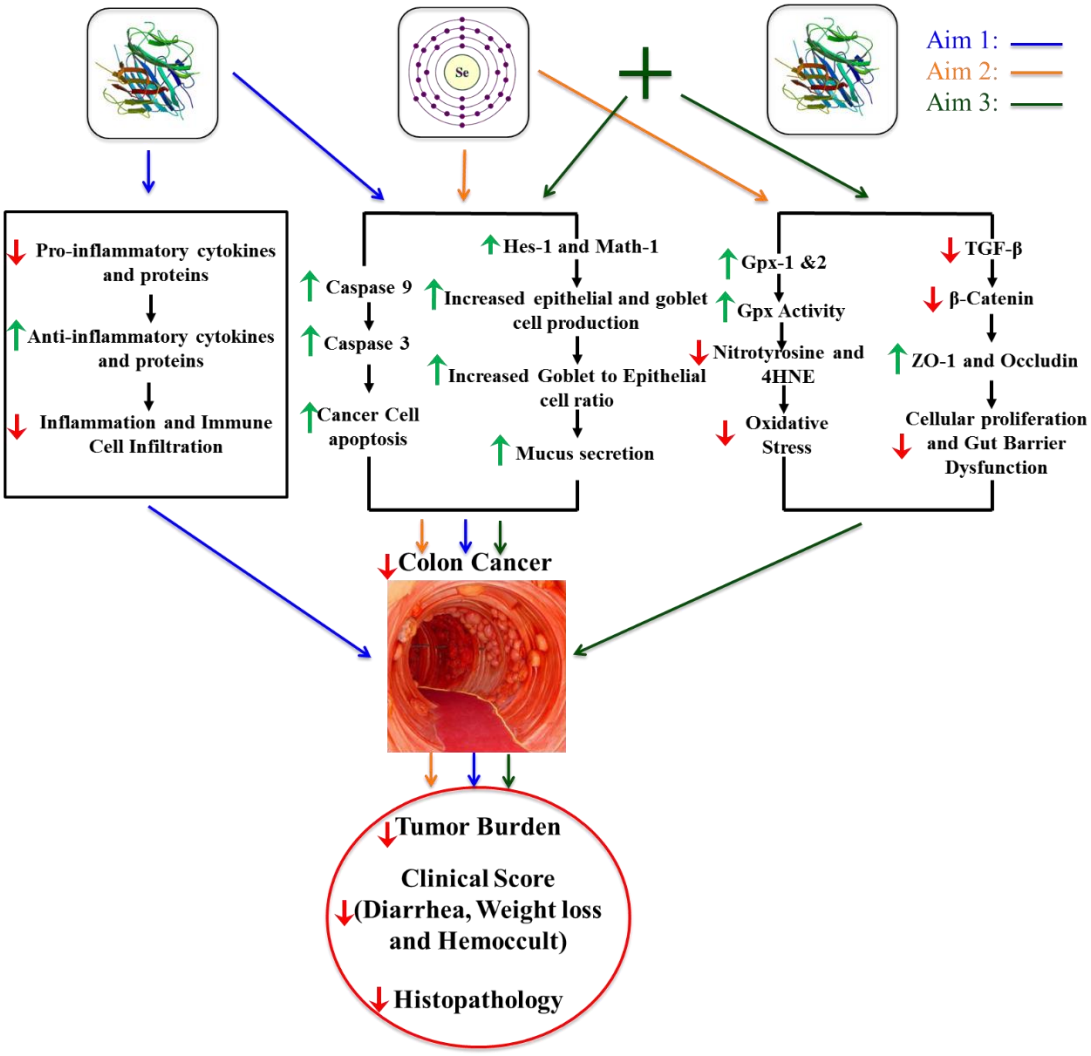

<u>Central idea</u> of this dissertation is to study the protective effect of APN and Se rich diet on intestinal cancer and CICC and delineate the mechanism for this protection. To achieve this, we will be using the inducible (DSS+DMH) model for studying CICC and $APC^{Min/+}$ mice model for studying intestinal cancer. DMH+DMH and $APC^{Min/+}$ mice models are very widely used model for studying colon and intestinal cancer respectively

(Tong, et al., 2011). Colon cancer in most of the cases is preceded by cycles of chronic inflammation and exposure to carcinogen sparking the formation of colon polyp. Colon and intestinal cancer at the clinical level is marked by blood in stools, diarrhea, weight loss, nausea, vomiting, constipation and constant fatigue. At the molecular level, colon and intestinal cancer is marked by increase in pro-inflammatory marker and proteins and suppression of anti-inflammatory response. Earlier stage pathology of the colon and intestine indicates pre-cancerous lesion and inflammation, which later on develops into colon tumors of varying size and shape. Our model of CICC is very near to mimic human stage II and III of colon cancer progression. Additionally, $APC^{Min/+}$ mutation accounts for majority of the intestinal and colon cancer cases along with a large similarity in the symptoms with human condition. There have been published study indicating the role of Se rich diet and APN administration in colorectal or intestinal cancer but these studies are limited in explaining the mechanism of action and most of the studies are *in vitro*. Also the combination of the above intervention has never been used in colon or intestinal cancer related studies.

This thesis is divided in to 3 different aims, where the 1^{st} aim is based on our preliminary experiment, which indicate that APNKO mice showed a significantly higher clinical score when compared to WT mice treated with DMH to induce colon cancer. We also found a significant increase in the tumor number in APNKO mice when compared to WT mice given DMH to induce colon cancer. On the basis of our preliminary data, we are trying to study whether CICC is regulated by APN deficiency. APN has been considered as an anti-inflammatory, antidiabetic and anti-cancer molecule secreted by the adipose

tissue. However, in obese individuals, a reduction in serum APN has been reported (Nigro, et al., 2014). APN has been shown to decrease inflammation by the activation of AMPK (A. Y. Kim, et al., 2010). Our first aim will study the effect of APN deficiency on chronic inflammation induced colon cancer. In this aim, we will determine the effect of APN on clinical score, tumor load and inflammatory markers associated with chronic inflammation and CICC. Aim 1.2 will study the effect of APN through AMPK and STAT3 activation and Cyclooxygenase (Cox) -2 mediated chronic inflammation and cancer. In addition to this we will study the effect of APN on hairy and enhancer of split (Hes)-1 and mouse atonal homolog (Math)-1 mediated goblet cell production and mucus secretion. The last part of this aim will study the how APN administration on goblet cell lines could affect goblet cell production and mucin secretion.

Our second aim is also based on our preliminary data where we found that Se rich diet (0.75ppm) was effective in reducing the clinical score and tumor number of mice with colon cancer. Se has been widely studied for it benefits in reducing inflammation, oxidative stress and to some extent leads to the reduction in cancer pathology. Se has been found to cause apoptosis of the colon cancer cells *in vitro* (Luo, et al., 2013). In this aim, we will study the role of Se and APN in reducing the severity of chronic inflammation and colon cancer by administering Se rich diet to APNKO and WT mice model with chronic inflammation, colon cancer and CICC. Aim 2.1 will study the reduction in tumor and clinical score through the mechanism leading to colon cancer cell apoptosis in the response to Se rich diet and serum APN. Since Se is a well-known antioxidant and anti-inflammatory non-metal, it could be easily derived that Se rich diet might be increasing the production

of antioxidant selenoproteins like Glutathione peroxidase (Gpx) I and II which could reduce overall oxidative stress in the state of CICC and hence reducing inflammation leading to reduce pathology of CICC (Aim 2.2). It could be possible that Se might play an important role in increasing the goblet cell production and the secretion of mucus from goblet cells providing protection form the DSS and DMH induced colon insult, which will be studied under aim 1.3.

There have been very limited studies indicating the protective role of APN administration on colon or intestinal cancer (Luo, et al., 2013). In aim 3 of this proposal will study the protective effect of both APN administration and Se rich diet on intestinal cancer. This will provide a reinforcement of our previous aims by studying a genetic model of intestinal and colon cancer ($APC^{Min/+}$) along-with exploring the effect of APN administration alone and in conjugation with Se rich diet on colon cancer. Aim 3.1 will study the clinical score, colon and intestinal tumor number and area, histopathology and inflammation and infiltration of immune cells; mainly concerning the physical attributes of intestinal and colon cancer in both colon and iliac part of small intestine. Sodium selenite has been shown to cause apoptosis of colon cancer cell *in vitro* by the activation of Bax dependent mitochondrial pathway (Z. Li, et al., 2013). APN treatment has also been shown to increase the apoptosis of the implanted colon cancer cells (Moon, et al., 2013). Aim 3.2 will determine the effect of both co-administration and individual effect of Se rich diet and APN administration on caspase 9 and 3 mediated apoptosis of the cancer cells in addition to goblet cell production. This aim will also study the pathways leading to the change in the phenotype from epithelial to goblet cells (Hes1 and MATH1 expression) and mucin

production (Muc2 and Muc4). Aim 3.3 will further study the in-depth mechanism providing an explanation for the protective effect of the Se rich diet and APN on reducing oxidative stress (Nitrosylation and Lipid Peroxidation) by increasing Gpx1 and Gpx2 expression. This aim will further focus on the downregulation of TGF-β and β – Catenin leading to increase expression of gut barrier proteins and reducing cellular proliferation and gut barrier dysfunction. By the means of this proposal will test the role Se rich diet and APN in murine model of intestinal and colon cancer.

PRELIMINARY DATA

Preliminary data for Experiment 1:

Clinical Score:

Colon cancer was induced in DMH treatment group in both the APNKO (n=5) and WT (n=5) mice by administrating DMH intraperitoneally once a week for 12 weeks at a concentration of 20mg/kg body weight of mice. Clinical score which is a summation of weight loss, diarrhea and fecal hemoccult was determined during the length of the study thrice a week till the date of sacrifice (day 194). We found a significant increase in the clinical score of the APNKO mice on day 76, 105 and 128 as compared to WT mice given the same treatment (figure1). Clinical score of the APNKO mice remain significantly higher than the WT mice from day 128 till day 153 (day of sacrifice).

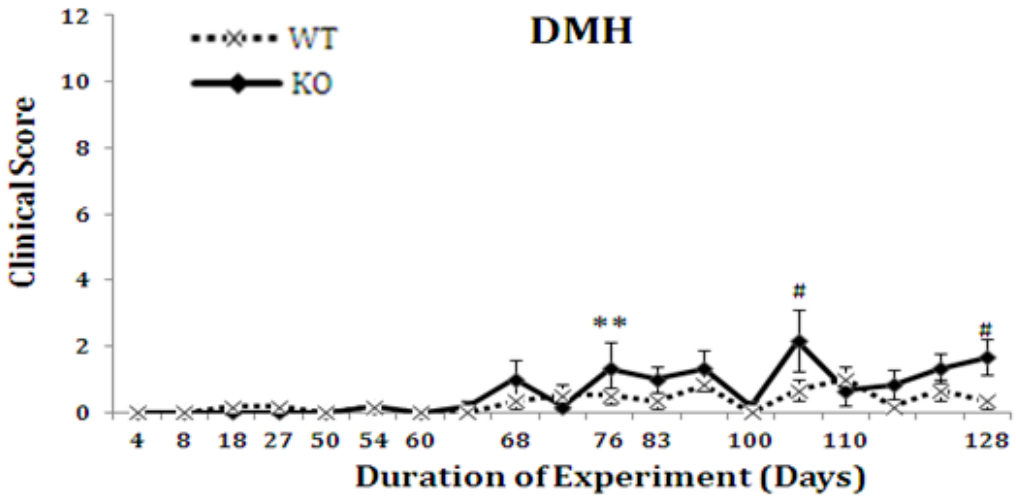

Figure 1: Clinical Score- DMH treatment: The graph compares the clinical score of the APNKO and WT mice given the same DMH treatment starting from day 4 till day 128. Significant difference was determined using TTEST. **p<0.05, #p<0.01.

Mice were sacrificed on day 153 and the colon was excised and flushed with PBS. Colon was cut open longitudinally and stained with 2% methylene blue to count the tumor number and tumor area. Significant increase in the tumor number and area was found in the APNKO mice as compared to the WT mice given the same treatment (figure 2).

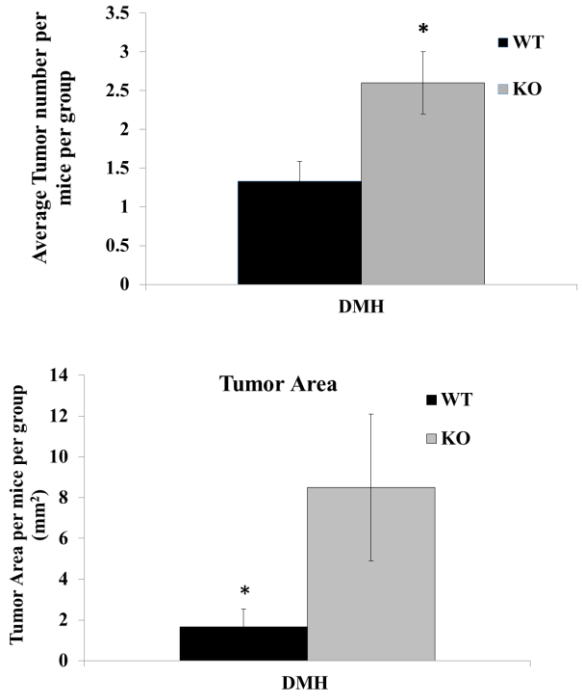

Figure 2: Tumor number and area- DMH treatment: The graph compares the tumor number and area of the APNKO and WT mice given the same DMH treatment. Significant difference was determined using TTEST. *p<0.03.

Preliminary data for Experiment 2:

Clinical Score:

Colon cancer was induced in DMH treatment group in both the APNKO (n=5) and WT (n=5) mice given either control (0.02 ppm Se) or Se rich diet (0.75 ppm Se) by administrating DMH intraperitoneally once a week for 12 weeks at a concentration of 20mg/kg body weight of mice. Clinical score which is a summation of weight loss, diarrhea and fecal hemoccult was determined during the length of the study thrice a week till the date of sacrifice (day 194). We found a significant decrease in the clinical score of both the APNKO and WT mice given Se rich diet as compared to APNKO and WT mice respectively given the control diet (figure 3).

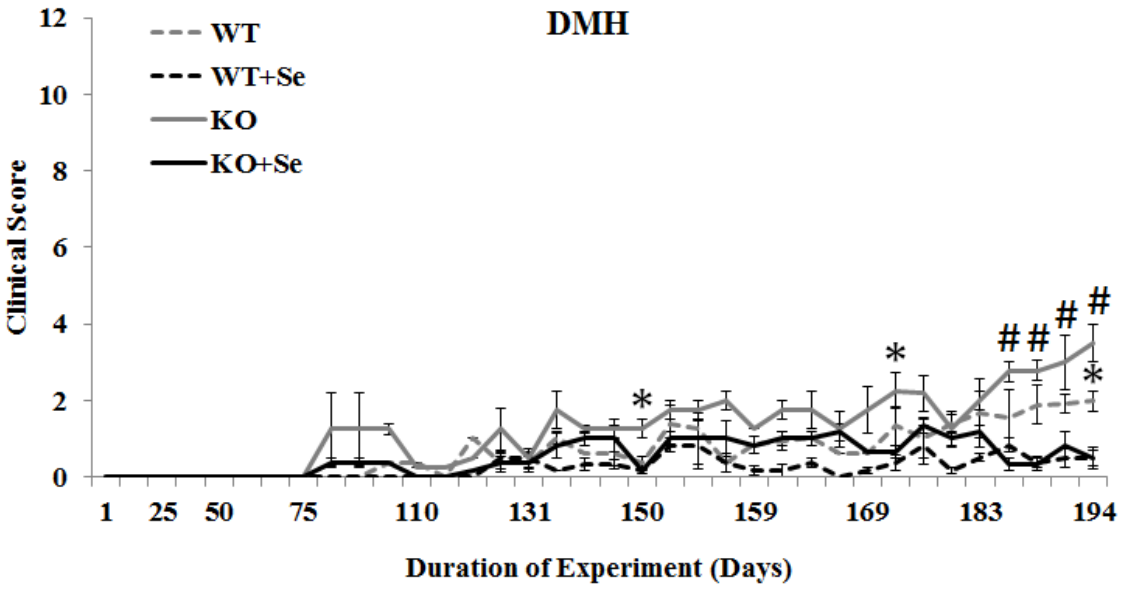

Figure 3: Clinical Score- DMH treatment: The graph compares the clinical score of the APNKO and WT mice given Se rich diet with the same genotype given control diet from day 25 till day 194. Significant difference was determined using TTEST. *p<0.05, #p<0.01.

Mice were sacrificed on day 194 and the colon was excised and flushed with PBS. Colon was cut open longitudinally and stained with 2% methylene blue to count the tumor number and tumor area. Significant decrease in the tumor number was found in both APNKO and WT mice given Se rich diet when compared to the same genotypic mice given control diet (figure 2). However, no significance was found in the tumor area of the APNKO and WT mice given Se rich and control diet. APNKO mice showed a higher tumor area when compared to the WT mice.

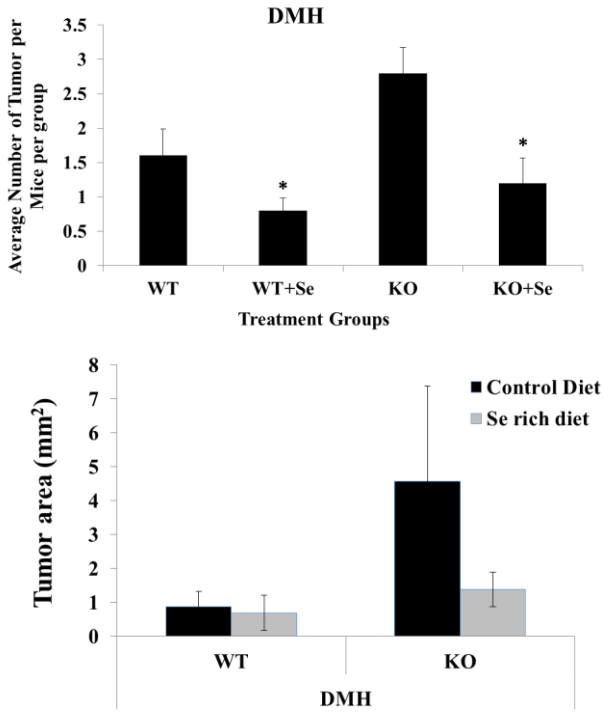

Figure 4: Tumor number and area- DMH treatment: The graph compares the tumor number and area of the APNKO and WT mice given Se rich diet the same genotypic mice given control diet. Significant difference was determined using TTEST. *p<0.05.

RESEARCH DESIGN AND METHODS

Overall research Design: The overall purpose of this study is to determine the effect of Se rich diet, and APN on colon and intestinal cancer. There have been few studies indicating the role of Se rich diet and APN on colon cancer but most of these study lack the mechanism of action of these interventions and there is no study which indicate the combination of these intervention. Since colon cancer is a complex set of condition originating from chronic inflammation, obesity and toxic exposure so it is necessary to use a combination of these intervention to alleviate the symptoms associated with chronic inflammation and colon cancer.

This research proposal has been divided into 3 different aims, where our 1st aim deals with studying effect of APN deficiency on DSS+DMH model of CICC. This aim is based on our preliminary data where we found a significant increase in clinical score and tumor number in APNKO mice when compared to WT mice with DMH induced colon cancer. In the first aim we will study the mechanism of action of APN in reducing the severity of chronic inflammation and CICC. The preliminary data for the 2nd aim indicate that Se rich diet (0.75 ppm) reduces the clinical score and tumor load of both APNKO and WT mice given Se rich diet when compared to the control diet (0.02 ppm). This aim will study the effect of Se rich diet and APN deficiency on chronic inflammation and CICC. Mechanism dealing with the protective effect of Se and APN in reducing the severity of colon cancer will be studied under this aim including colon cancer cell apoptosis, goblet cell production and oxidative stress. In the last aim we will try to replicate the use of Se rich diet in $APC^{Min/+}$ mouse model of intestinal cancer; providing another proof for the use

of Se rich diet in colon and intestinal cancer. Along with this intervention, this aim will also delineate the role of APN administration and the combination of Se rich diet and APN administration on $APC^{Min/+}$ model of intestinal cancer. This aim will provide the first proof of use of combinatorial approach for reducing the severity of intestinal cancer and related inflammation. This aim will also study different signaling pathways related to the effect of Se and APN administration in reducing the severity of intestinal cancer.

AIM 1: To determine if CICC is regulated by APN.

Rationale: Our preliminary data indicated that APN deficiency increase the severity of DMH induced colon cancer as indicated by significantly higher clinical score and tumor number in APNKO mice when compared to the WT mice given the same treatment. APN is an adipocytokine secreted by the adipose tissue which has been identified as an anti-inflammatory and anti-cancer molecule (Byeon, et al., 2010). Studies have linked obesity with increased risk of colon cancer (Calle & Kaaks, 2004; Le Marchand, Wilkens, Kolonel, Hankin, & Lyu, 1997). Lower expression of APN has been found in obese patients when compared to non-obese individuals (Barresi, Tuccari, & Barresi, 2009; Meilleur et al., 2010) reflecting that lower serum of APN is linked with increased risk of human colorectal cancer (Wei, et al., 2005). APN has been shown to stimulate AMPK phosphorylation and mediate its anti-inflammatory and anti-cancer function through the activation of AdipoR1 and AdipoR2 receptors in HT29 and LoVo colon cancer cell lines (A. Y. Kim, et al., 2010). APN has been shown to alleviate stromal cell Cox-2 expression (Awazawa et al., 2011).

Adipocytokines including APN has an effect on carcinogenesis with a little information about its role in chronic inflammation and progression and development of colon cancer. There are several evidences available indicating the protective role of APN in inflammation and cancer but there are very few studies published in colon cancer. Most of the studies conducted in the field are *in vitro* and lacks the mechanistic explanation for APN medicated protection. Very few to none of the studies have identified the role of APN on goblet cell production and mucus secretion which is one of the major pathway leading to colon protection against toxin and gut bacterial invasion. In order to answer the above questions, this aim has been designed to study the effect of APN deficiency on clinical score, tumor load and inflammation in chronic inflammation, colon cancer and CICC. The effect of APN on goblet cell production and mucus secretion along with the effect of APN administration on goblet cell line leading to goblet cell production will be studied in this aim.

AIM 1.1 To study the effect of APN deficiency on clinical score, tumor load and inflammation in CICC.

AIM 1.2 To determine the effect of APN deficiency on AMPK mediated inflammation and mucus secretion.

AIM 1.3 To study how APN administration could affect goblet cell production and epithelial to goblet cell transition with mucin production in goblet cell lines.

Experimental Design Specific AIM 1: Aim 1 will study the effect of APN deficiency on chronic inflammation, colon cancer and CICC. In this aim, 6-8 weeks old, male and female APNKO and C57BL/6 mice will be randomly divided into 4 different treatment groups including control, DSS alone, DMH alone and DSS+DMH. DSS alone group will receive 3 cycle of 2% DSS in the drinking water. DMH alone group will receive intraperitoneally injections of 20mg/kg of DMH, once a week for 12 weeks to induce colon cancer and DSS+DMH groups will receive one intraperitoneal injection of DMH (20mg/kg) on day 4 and 3 cycles of DSS to induce CICC. Mice will be monitored for the clinical score throughout the length of the study and will be sacrificed on day 153. Mice colon will be collected for protein expression studies, secreted cytokines and histochemical analysis. Remaining part of the colon will be stained with 2% methylene blue for counting the tumor number and tumor area. HT29-Cl.16E and Ls174T goblet cell lines cells will be seeded and cultured in the Dulbecco's modified Eagle's medium (DMEM). These cells will be incubated with the different dosages of APN to determine its effect of mucin secretion and goblet cell apoptosis. Aim 1 is subdivided in to 3 different sub-aims exploring the

mechanism of action of APN in reducing the severity of chronic inflammation, colon cancer and CICC. Aim 1.1 will study the effect of APN deficiency clinical score, tumor load and inflammation. Aim 1.2 will study the effect of APN deficiency on AMPK mediated STAT3 phosphorylation, Cox-2 expression and goblet to epithelial cell ratio and mucus secretion. Aim 1.3 will study the effect of differential concentration of APN administration on goblet cell apoptosis and mucin secretion. Unpaired TTEST and One Way ANOVA will be used for statistical analysis with a $p \leq 0.05$ as significant.

Experiment 1: This experiment will identify whether APN play a role in modulating the severity of chronic inflammation, colon cancer and CICC through goblet cell production and mucus secretion.

Animal Model and Handling: Six to eight week old male APNKO and C57BL/6 (WT) were obtained from Jackson Laboratories and bred in the animal facility at the University of South Carolina. They will be housed in conventional animal room and treated in the animal facility at the University of South Carolina. All APNKO mice were homozygous for APN deficiency $^{(-/-)}$. The mice were on a 12:12 h light–dark cycle in a low stress environment (22 °C, 50% humidity and low noise) and had access to food (Purina Chow) and water *ad libitum*. All animal care followed institutional guidelines under a protocol approved by the Institutional Animal Care and Use Committee at the University of South Carolina. APNKO and WT mice were randomly assigned to 8 different treatment groups (n=10 mice per group): 1) APNKO+DMH+DSS; 2) WT+DMH+DSS; 3) APNKO+DMH;

4) WT+DMH; 5) APNKO+DSS; 6) WT+ DSS 7) APNKO+Control 8) WT+ Control. The body weight of both APNKO and WT mice showed no significant difference at the beginning of the study. Mice will be monitored throughout the length of the study for clinical score including weight loss, diarrhea and fecal hemmoccult. Mice will be sacrificed by cervical dislocation on day 153. Blood will be collected before sacrifice through retro-orbital puncture, spin down at 10,000 rpm for 18 minutes and serum will be isolated and stored at -20°C for measuring serum APN. Mice colon will be excised and flushed clean with PBS. 2 mm^2 colon tissue section with tumor and non-tumor area will be fixed in 10% formalin and after 24 hours will be replaced with 70% ethanol followed by paraffin embedding and sectioning to obtain 5-6 mm thin section on glass slide. 2 mm^2 colon tissue section with tumor and non-tumor area will be snap frozen on dry ice and stored at -80°C for protein expression studies and another 2 mm^2 colon tissue section will be incubated in RPMI medium at 37°C for 24 hours followed by centrifugation at 2500 rpm for 15 minutes. Supernatant will be obtained and stored at -20°C for secreted cytokine expression.

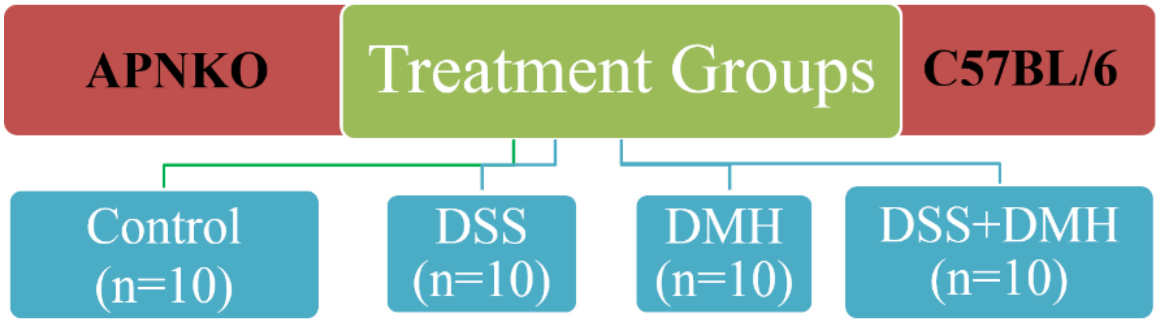

Figure 1: It shows different treatment groups with the number of mice used in each group (n=10) for Aim 1

Material and Methods

Chronic Inflammation and Colon Cancer

Depending on the treatment group, mice will be either administered DSS or DMH or both. DSS will be administered alone to induce chronic inflammation. DMH will be injected to induce cancer while the combination of both will be given to induce CICC. DSS will be administered in 3 cycles where one cycle constitutes 2% DSS (MP Biochemicals, MW: 36,000-50,000) in drinking water for 5 days followed by 5 days of normal drinking water. DSS will be administered on day 4, 27 and 50 to induce chronic inflammation. DMH (Sigma Aldrich) will be injected intraperitoneally at a concentration of 20mg/kg either once for DSS+DMH treatment group on day 4 or once a week for 12 weeks for DMH alone group. These concentration and model have been well established to study chronic inflammation and colon cancer.

Clinical Score

Clinical score will be measured for each mouse in each group from day 25 to day 194. Mice will be sacrificed after the last clinical score measurement. Score for the weight loss is based on the following published scale where 0 = 0–5% weight loss; 1 = 6–10% weight loss; 2 = 11–15% weight loss; 3 = 16–20% weight loss; and 4 = >20% weight loss. Scoring

of diarrhea is as follows: 0 = well-formed pellets, 2 = pasty and semi-formed stools that do not adhere to the anus, 4 = liquid stools that adhere to the anus. Detection of blood in the stools will be determined using hemoccult kit (BECKMAN COULTER). The higher intensity of blue color indicates greater bleeding. The followings are the score rates for the fecal hemoccult: 0 = no blood, 2 = positive hemoccult, 4 = gross bleeding. The total clinical score will be the summation of the individual score of weight loss, diarrhea and fecal hemoccult. The maximum score a mouse could get is 12. The clinical score will be calculated and plotted against days of DSS administration or duration of the experiment. Higher clinical score indicates more severity of colon cancer development in animals.

Colon Tissue and Serum Collection:

Blood will be collected before sacrifice through retro-orbital puncture and spun down at 10,000 rpm for 18 minutes and serum will be obtained and stored at -20°C to measure APN. Mice colon will be excised and flushed clean with PBS. $2mm^2$ colon tissue section with tumor and non-tumor area will be fixed in 10% formalin. 24 hours later, tissues will be submerged in 70% ethanol followed by paraffin embedding and sectioning to obtain 5 µm thin section on glass slide. Sections with tumor and non-tumor areas will then be snap frozen on dry ice and stored at -80°C for protein analysis. Another $2mm^2$ colon tissue section will be incubated in RPMI medium containing 5000 IU/mL and 5000 IU/mL penicillin and streptomycin (CELLGRO) respectively at 37°C and 5% CO_2 for 24 hours. This will be followed by centrifugation at 2500 rpm for 15 minutes. Supernatant will be obtained and stored at -20°C to measure secreted cytokine levels.

Tumor Number and Tumor Area and Histopathology:

Mice colon will be excised and flushed with PBS. Tumor number and area will be counted under the microscope for all mice of different groups and significant difference will be calculated between different groups given different treatment and genotype.

Hematoxylin and Eosin staining will be used to determine the morphology of mice colon. Histopathology will be quantified based on the scoring system indicating the severity of disease and constituting inflammation and immune cell infiltration. Quantification of severity of disease including inflammation and immune cell infiltration was done on the scale of 4 for both the parameters, where 0 = no infiltration or no inflammation; 2 = moderate infiltration or inflammation; and 4 = severe inflammation with distorted crypts or infiltration and formation of lymphatic follicles. All the images were taken in 20× magnification with Nikon e600 microscope. The scale bar represents 120 µm. The score will be measured by two investigators in blinded fashion.

Cell culture

HT29-Cl.16E and Ls174T cells (ATCC) will be seeded on porous nitrocellulose filters (MILLIPORE filters HAHY, porosity 0.45 µm; 2×10^6 cells per filter) to provide improved access to basolateral membrane of cells. The cells will be cultured in Dulbecco's modified Eagle's medium (DMEM) (GIBCO) supplemented with 10 % (*v*/*v*) heat-inactivated fetal

calf serum (FCS) (GIBCO). HT29-Cl.16E and Ls174T cells form at confluence homogeneous monolayer of differentiated goblet cells, secreting a mucus gel in the culture medium. HT29-Cl.16E and Ls174T cells (10^6/well) will be incubated at 37 °C and 5 % CO_2 in the presence of different dosages of recombinant APN (0, 0.25, 0.5, 1.0, 1.5, 2.0 µg/mL) in one experiment and with APN (2 µg/mL), TNF-α (10 ng/mL), and APN+TNF-α (PROSPEC) for 24 h in other experiment.

Protein determination using Western Blot:

Colon tissue frozen at -80°C will be homogenized in RIPA buffer added to protease and phosphatase inhibitors (SIGMA). It will be then centrifuged at 10,000 rpm for 15 minutes and supernatant will be collected for protein analysis. Protein concentration in the supernatant will be determined by using Bradford protein assay. This will be followed by loading equal amounts of protein (50 µg) in each well for a 10% Sodium Dodecyl Sulphate (SDS) gel electrophoresis. The protein from the gel will then be transferred to a nitrocellulose membrane (Pall Scientific) and blocked with 5% non-fat dry milk (Biorad) in phosphate buffer saline (PBS) (cellgro) with 0.1% Tween 20. The membrane will be incubated overnight with the primary antibody. The primary antibodies include AMPK, pAMPK, Cox-2, STAT-3 and pSTAT3 obtained from Cell Signaling Technology. Membrane will be washed by PBS containing 0.1% Tween 20 (Biorad). The membrane will then be incubated with secondary antibody (Santa Cruz) followed by another washing step. The last step includes incubating the membrane in ECL substrate (Western Bright, Advansta). The film will be then developed by using a developer (SRX-101A, Konica

Minolta Medical & Graphic, INC.) in the dark room. Finally the film will be scanned and the density of the protein bands obtained will be analyzed using Image J software.

Mucus Thickness

Mucus thickness will be measured with micropipettes connected to a micromanipulator (LEITZ) with a digimatic indicator (IDC SERIES 543, Mitutoyo). The degraded luminal mucus layer was removed. Glass tubing (borosilicate tubing with 1.2 mm OD and 0.6 mm ID; Frederick Haer) will be pulled with a pipette puller (pp-83; NARISHIGE SCIENTIFIC) to a tip diameter of 1–3 µm and to prevent mucus adhering to glass, the pipettes were siliconized by dipping the tip of the micropipette into a silicone solution followed by drying at 100 °C for 30 min. The luminal surface of the mucus gel will be visualized by placing graphite particles (activated charcoal, extra pure, Merck) on the gel, and the colonic epithelial cell surface was visible through the microscope. The micropipette will be inserted into the mucus gel at an angle of ~30° (θ) to the surface. The distances traveled by the micropipette from the luminal surface of the mucus gel to the epithelial cell surface will be measured with a digimatic indicator connected to the micromanipulator, and a mean value (A) was calculated. The mucus thickness (T) will be calculated using the formula $T=A$ (sin θ). Mean of four to five different measurements will be taken as one thickness value.

Alcian Blue Staining

Standard deparaffinization procedure will be followed using xylene and gradation of ethanol. Alcian blue solution (1 %) of pH 2.5 in 3 % acetic acid and nuclear fast red in aluminum sulfate will be prepared. Tissues will be stained with Alcian blue and counterstained with nuclear fast red solution. Goblet to epithelial cell ratio will be counted per crypt with ten crypts per section and five sections per group.

Enzyme Linked Immunosorbent Assay (ELISA):

Spontaneous secreted cytokines will be measured from the tissue incubated in the RPMI medium for 24 hours at 37°C. The media will be collected and centrifuged at 2500 rpm for 16 minutes. Pellet will be discarded and the supernatant is isolated. Cytokines IL-6, TNF-α, IL-1β and IL-10 levels will be measured by using BD OptEIA ELISA kit obtained from BD biosciences and normalized by total protein content estimated by using standard Bradford assay procedure. Muc1 and Muc2 production was measured both in colonic epithelial cells and in HT29-Cl.16E and Ls174T cell supernatant by ELISA (USCN LIFE SCIENCE) using standard protocol.

Genes knockdown using siRNA

Small interfering RNA (siRNA) (40 nM) targeting MUC2, Bax, APN R1 and R2 (QIAGEN), and Math-1 was transfected in HT29-Cl.16E and Ls174T cells (10^6) using lipofectamine 2000 reagent (Invitrogen) according to the manufacturer's instructions.

Controls were transfected with unrelated siRNA (CsiRNA) (SANTA CRUZ, QIAGEN, and INVITROGEN). Reductions of cell-surface proteins were analyzed with flow cytometry. The efficacy of knockdowns was assessed by conventional semi-quantitative RT-PCR. Assays were performed 2 days after transfection.

TUNEL Assay

Terminal deoxynucleotidyl transferase (TdT)-mediated dUTP-biotin nick-end labeling (TUNEL) technique was used as per manufacturer instructions (R&D systems) to detect DNA strand breaks in situ. After treating cells with APN (2 μg/mL), TNF-α (10 ng/mL), and APN+TNF-α pelleted cells were rinsed with PBS and TUNEL staining procedure was performed. Cells were then counterstained with methyl green. Negative controls were performed by substituting PBS for TdT enzyme, which exhibited no immunostaining. Enumeration of apoptotic nuclei was made on ten slides per treatment, using a Zeiss light microscope with a 40× objective and a 10× eyepiece. All nuclei counted showing a brown labeling. The incidence of apoptotic nuclei was given as the percentage relative to total nuclei (apoptotic ratio). The data are representative of three repeated experiments, all displaying similar results.

Reverse transcription-polymerase chain reaction

Semi-quantitative reverse transcription-polymerase chain reaction (RT-PCR) was used to determine the efficacy of siRNA transfection and relative gene expression in HT29-Cl.16E

and Ls174T cells and colonic epithelial cells. Total cellular RNA was isolated using TRIzol reagent (Invitrogen) according to the manufacturer's instructions. A total of 2.5 mg extracted RNA was used as the template for complementary DNA (cDNA) synthesis using the Thermoscript reverse transcription-polymerase chain reaction system (Invitrogen). Semi-quantitative PCR was performed for Muc2, Bax, APN R1 and R2, Hes-1, and Math-1 using the following primer pairs: MUC2 forward primer (FP) (5-GACATTTGTCAT GTACTCGGC-3) and reverse primer (RP) (5-GCAAGGACTGAACAA AGACTC-3), Bcl-2 (FP-59-GACTTCGCCGAGATGTCCAG-39 and RP-5-TCACTTG TGGCT CAGATAGG-3), Bax (FP-59-GGTTTCATCCAGGATCGAGACGG-3 and RP-5-ACAAAGATG GTCACGGTCTGCC-3), GAPDH (HT29-Cl.16E cells) (FP-5-GCAGGGGGGAGCCAAAAGGG-3 and RP- 5-TGCCAGCCCCAGCGTCAAAG-3), Hes1 (FP-CAGCCAGTGTCAACACG ACAC and RPTCGTTCATGCACTCGCTGAG), Math1 (FP-AGTGACGGAGAGTTTTCCCC and RP-CTGCAGCCGTCCGAAGTCAA), and GAPDH (colonic epithelial cells) (FP- GTCATCA TCTCCGCCCCTTCTGC and RP-GATGCCTGCTTCACCACC TTCTTG). The synthesized cDNA was amplified by RT-PCR assay; the PCR cycle consisted of 94 °C for 1 min, 56 °C for 2 min, and 72 °C for 1 min, with final extension at 72 °C for 10 min. Relative mRNA abundance of Math-1, hes-1, and ratio of Bax/Bcl-2 was calculated using semi-quantitative RT-PCR and Image J software (NCBI) for densitometry. GAPDH was used as a loading control and the gels were run thrice using different samples from the same group to calculate significant difference.

Statistical analysis

Two-way analysis of variance (ANOVA), Two-way repeated measure ANOVA and One-way ANOVA will be used to analyze the data with Tukey post hoc-analyses. A $p<0.05$ will be considered statistically significant. All the statistical analyses will be done using SigmaStat 3.5 (SPSS, Chicago, IL).

Primary Outcomes:

Clinical Score: Clinical score was measured for each mouse in each group from day 4 to day 153. Mice were sacrificed after the last clinical score measurement. Clinical score is a summation of 3 different score including weight loss, diarrhea and fecal hemoccult. The scoring system is as follows:

Weight loss -	**0 = 0-5% weight loss; 1 = 6-10% weight loss; 2 = 11-15% weight loss; 3 = 16-20% weight loss; 4 = >20% weight loss.**
Diarrhea -	**0 = well-formed pellets, 2 = pasty and semi-formed stools that do not adhere to anus 4 = liquid stools that adhere to the anus**
Fecal Hemoccult-	**0 = no blood, 2 = positive hemoccult, 4 = gross bleeding**

Table 1: It shows clinical score measurement criteria.

The maximum score a mouse could get is 12. Fecal hemoccult scoring was obtained using a kit from Beckman Coulter, which turns the fecal blood into blue color. The higher

intensity of blue color indicates greater bleeding. The clinical score was calculated and plotted against days of DSS administration. Higher clinical score indicated more severity of colon cancer.

Tumor Number and Tumor Area: Mice colon was excised and flushed with PBS. At this point the tumor number and area were counted for that part of the colon, which was excised for paraffin embedding, freezing and RPMI medium. The rest of the colon was fixed in 10% formalin for 24 hours and then stored in 70% ethanol. The colon was stained with 2% methylene blue. Tumor number and area was counted under the microscope for all the mice in different groups and significant different was calculated between different groups and a graph was plotted.

Chronic Inflammation: Chronic inflammation will be measured in the colon of all the mice in different group by measuring secreted cytokines. Secreted cytokines will be measured from the tissue incubated in the RPMI medium for 24 hours at 37°C. Cytokines like IL-6, TNF-α, IL-1β and IL-10 will be measured. This will be followed by Hematoxylin and Eosin staining of the colon tissue section fixed in formalin and embedded in paraffin wax to study chronic inflammation and immune cell infiltration. STAT3 is an indicator of inflammation and has been shown to overexpress in many cancers. Phosphorylation of STAT3 will indicate the degree of inflammation and its protein expression will be measured using western blot. Increased expression of pro-inflammatory cytokines and proteins and decrease production of anti-inflammatory cytokines indicates greater

inflammation. Greater degree of inflammation indicated by abnormal crypts and infiltration of the immune cells indicates higher severity of colon cancer.

Goblet Cell Production, Mucus Secretion and Apoptosis: Increase in the goblet cells and hence increase mucus production is one of the protective mechanisms that could play an essential role in the colon cancer prevention. Alcian blue staining will be used to determine the ratio of goblet to epithelial cells in the colon tissue section for all the treatment groups. Higher ratio will be an indication of increase number of goblet cell and hence increase mucus secretion. Hes-1 and Math-1 gene expression will be determined in the colon tissue of the APNKO and WT mice belonging to all treatment groups as they will provide indirect measure for epithelial to goblet transition and goblet cell production. Mucus thickness will also be determined to get a direct measure of mucus secretion and hence mucus mediated protection in the control, DSS, DMH and DSS+DMH treatment groups. Whether mucin secretion is APN dependent will be studied by giving different concentration of APN to the HT29-CI.16E cells and measuring the secretion of Muc1 and Muc2 in the culture media by ELISA. Goblet cell apoptosis will measured under different treatment conditions including APN administration (2 μg/mL), TNF-α mediated apoptosis (10 ng/mL) and co-administration of TNF-α and APN to determine if APN is directly involved in the apoptosis of the goblet cells. Mechanism of goblet cell apoptosis will be further investigated by studying the gene expression of Bax and Bcl_2 in goblet cell under different treatment conditions.

APMK and Cox-2 Expression: AMPK has been known for its ant-inflammatory and anti-cancer properties and is activated during cellular stress. APN increase the rate of phosphorylation of AMPK and has been known to suppress cell growth by downregulating mTOR (Ouchi, et al., 2004). AMPK has been known to inhibit the activity of Cox-2; an enzyme that is overexpressed during inflammation and cancer. This aim will study the protein expression of phospho-AMPK and AMPK by western blot and localization expression of Cox-2 in the colon tissue section by immunohistochemistry.

Serum Adiponectin: Higher levels of serum APN has been reported in trained individuals. Obesity and cancer is linked with lower APN levels making it a prospective candidate in the treatment for colon cancer. Serum APN will be determined in the WT mice in all the treatment groups using ELISA.

AIM 2: To determine if Se rich diet can interact with APN to alleviate CICC.

Rationale: Our preliminary data indicate that Se rich diet (0.75 ppm) was effective in reducing clinical score and tumor number DMH induced colon cancer. APNKO showed greater clinical score and tumor load when compared to WT mice. A recent study by Li et al., 2013 have shown that Se induces G1/M cell cycle arrest and apoptosis of the HCT116 and SW620 colorectal cancer cells (Z. Li, et al., 2013). They also found that Se treatment leads to the upregulation and translocation of Bax from cytosol to mitochondria, increased

expression of caspase 3 and downregulation of Bcl-2 and increased loss of MMP in a dose dependent manner in HCT116 and SW620 colorectal cancer cell lines. Another recent study by Maseko et al., 2014 discovered that Se rich Agaricus bisporus supplementation increased Gpx-1 and Gpx-2 expression level in rat colon (Maseko, et al., 2014). Se deficient diet (0.01mg Se as sodium selenite per kg) has been found to exacerbate colonic tissue injury inflicted by DSS treatment and induced oxidative stress as indicated by DNA damage further culminating in increased inflammation and carcinogenesis (Barrett, et al., 2013). Although there have been few publications indicating the protective role of Se in colorectal cancer but they lack the in depth mechanism of action of Se in reducing the severity of colon cancer. Most of the studies are *in-vitro* and hence lack *in-vivo* approach. In addition, there is no published literature indicating an interaction between Se rich diet and APN and their combined effect on inflammation and colorectal cancer. Therefore to provide more mechanistic explanation and to study whether Se and APN can act synergistically, aim 2 is designed to define the role of Se rich diet and APN on CICC and study the different possible explanations for their protective role on colorectal cancer. These include determining the role of Se and APN on tumor load and clinical score, changes in the different inflammatory markers, modulation of the anti-oxidant potential of the colon through variation in the expression of selenoproteins like Gpx-1 and Gpx-2. Studying the effect of Se rich diet and APN in increasing cancer cell apoptosis by increased expression of cleaved caspase 9 and lastly by determining their role on goblet cell production.

AIM 2.1 To study the effect of selenium rich diet on clinical score and tumor load in CICC.

AIM 2.2 To study the effect of Se rich diet on pro-inflammatory and anti-inflammatory cytokines production and selenoproteins expression.

AIM 2.3 To study the effect of Se rich diet on colon cancer cell apoptosis and goblet cell production.

Experimental Design Specific AIM 2: Aim 2 will study the effect of Se rich diet (0.75) on DSS induced chronic inflammation, DMH mediated colon cancer and CICC. In addition to this we will study the mechanism of action of Se in reducing the severity of colon cancer. Four weeks old male and female C57BL/6 mice (WT) and APNKO mice with C57BL/6 background will be randomized in to 4 different treatment groups including Control, DSS, DMH and DSS+DMH and each group will be fed 2 different types of diet including Se rich (0.75 ppm) and Se deficient (0.02 ppm) diets. This will result in total 16 groups (n=9). Based on the respective group, mice will be administered 2% DSS in the drinking water for 3 different cycles either alone or with a single injection of DMH (20mg/kg mouse weight). In DMH alone group mice will be administered DMH injection intraperitoneally (20mg/kg mouse weight) once a week for 12 weeks. This will result in the formation 3 different treatment groups translating into DSS indicating chronic colitis, DMH indicating mild colon cancer and DSS+DMH reflecting CICC and a control group. Mice will be monitored for clinical score, 3 times a week and will be sacrificed on day 194. Mice colon will be collected for protein expression studies, histochemical analysis, fluorescent staining

and mass spectrometry. Remaining part of the colon will be stained with 2% methylene blue for counting the number of tumors and tumor area. Aim 2 is subdivided in to 3 different sub-aims studying the effect of Se rich diet on chronic inflammation and colon cancer in addition to its mechanism of action in both WT and APNKO mice. Aim 1.1 will study the effect of Se rich diet on chronic inflammation, colon cancer and CICC in WT and APNKO mice. Aim 1.2 will study the effect of Se rich diet on the oxidative potential of the colon and its consecutive effect on oxidative stress and inflammation. Aim 1.3 will study the effect of Se rich diet on colon cancer cell apoptosis with respect to caspase expression and increasing goblet cell production and hence providing protection form the colorectal cancer by increase mucus secretion. Unpaired TTEST and One Way ANOVA will be used for statistical analysis with a $p \leq 0.05$ as significant.

Experiment 2: This experiment will identify the effect of Se rich diet and APN on increasing anti-oxidant potential, apoptosis of cancer cells, goblet cell production and decreasing inflammation and pathology of chronic inflammation and colon cancer.

Animal Model and Handling: Four weeks old C57BL/6 (WT) mice will be obtained from Jackson Laboratories and will be bred in the animal facility at the University of South Carolina under the IACUC guidelines. The mice will be fed regular chow and *ad libitum*. Four weeks old mice will be then randomized in to 16 different treatment groups

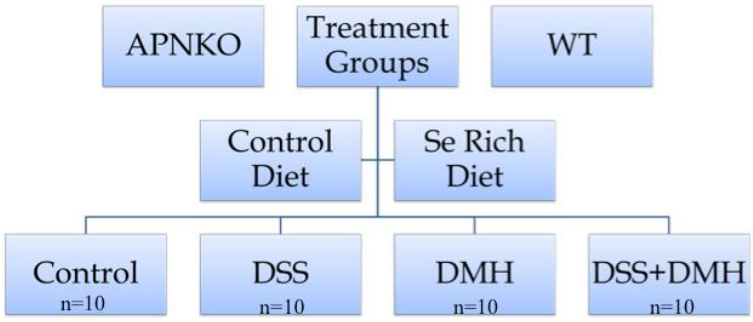

with n=10. The mice will then be acclimatized to the animal facility for 24 days in a low stress environment (22°C, 50% humidity and low noise) with 12:12 hours of light-dark cycle and the first DSS or DMH administration will be done on day 25. The groups include: WT+Normal Diet, WT+Se Diet, APNKO+Normal Diet, APNKO+Se Diet, WT+DSS+Normal Diet, WT+DSS+Se Diet, APNKO+DSS+Normal Diet, APNKO+DSS+Se Diet, WT+DMH+Normal Diet, WT+DMH+Se Diet, APNKO+DMH+Normal Diet, APNKO+DMH+Se Diet, WT+DSS+DMH+Normal Diet, WT+DSS+DMH+Se Diet, APNKO+DSS+DMH+Normal Diet and APNKO+DSS+DMH+Se Diet. Mice will be fed Se rich diet and control diet on day 25. They will be monitored throughout the length of the study for clinical score including weight loss, diarrhea and fecal hemmoccult. Mice will be sacrificed by cervical dislocation on day 194. Blood will be collected before sacrifice through retro-orbital puncture, spin down at 10,000 rpm for 18 minutes and serum was isolated and stored at -20°C for measuring serum APN. Mice colon will be excised and flushed clean with PBS. 2 mm^2 colon tissue section with tumor and non-tumor area will be fixed in 10% formalin and after 24 hours will be replaced with 70% ethanol followed by paraffin embedding and sectioning to obtain 5-6 mm thin section on glass slide. 2 mm^2 colon tissue section with tumor and non-tumor area will be snap frozen on dry ice and stored at -80°C for protein expression studies and another 2 mm^2 colon tissue section will be incubated in RPMI medium at 37°C for 24 hours followed by centrifugation at 2500 rpm for 15 minutes. Supernatant will be obtained and stored at -20°C for secreted cytokine expression studies.

Figure 2: It shows different treatment groups with the number of mice used in each group (n=10) for Aim 2.

Material and Methods

Chronic Inflammation and Colon Cancer

Depending on the treatment group, mice will be either administered DSS or DMH or both. DSS will be administered alone to induce chronic inflammation. DMH will be injected to induce cancer while the combination of both will be given to induce CICC. DSS will be administered in 3 cycles where one cycle constitutes 2% DSS (MP Biochemicals, MW: 36,000-50,000) in drinking water for 5 days followed by 5 days of normal drinking water. DSS will be administered on day 25, 50 and 75 to induce chronic inflammation. DMH (Sigma Aldrich) will be injected intraperitoneally at a concentration of 20mg/kg either once for DSS+DMH treatment group on day 25 or once a week for 12 weeks for DMH alone group. These concentration and model have been well established to study chronic inflammation and colon cancer.

Selenium Diet Administration

Selenium rich diet containing 0.75 ppm of Se per kg will be administered to 8 groups on day 25 simultaneously with the administration of DSS, DMH, or both or to the Control group. The diet will be administered till the day of sacrifice that is day 194. Control diet

contains all the components of the Se rich diet except that the Se content is 0.02 ppm per kg of diet.

Clinical Score

Clinical score will be measured for each mouse in each group from day 25 to day 194. Mice will be sacrificed after the last clinical score measurement that is on day 194. Score for the weight loss is based on the following published scale where 0 = 0–5% weight loss; 1 = 6–10% weight loss; 2 = 11–15% weight loss; 3 = 16–20% weight loss; and 4 = >20% weight loss. Scoring of diarrhea is as follows: 0 = well-formed pellets, 2 = pasty and semi-formed stools that do not adhere to the anus, 4 = liquid stools that adhere to the anus. Detection of blood in the stools will be determined using hemoccult kit (BECKMAN COULTER). The higher intensity of blue color indicates greater bleeding. The followings are the score rates for the fecal hemoccult: 0 = no blood, 2 = positive hemoccult, 4 = gross bleeding. The total clinical score will be the summation of the individual score of weight loss, diarrhea and fecal hemoccult. The maximum score a mouse could get is 12. The clinical score will be calculated and plotted against days of DSS administration. Higher clinical score indicates more severity of colon cancer development in animals.

Colon Tissue and Serum Collection:

Blood will be collected before sacrifice through retro-orbital puncture and spun down at 10,000 rpm for 18 minutes and serum will be obtained and stored at -20°C to

measure APN. Mice colon will be excised and flushed clean with PBS. $2mm^2$ colon tissue section with tumor and non-tumor area will be fixed in 10% formalin. 24 hours later, tissues will be submerged in 70% ethanol followed by paraffin embedding and sectioning to obtain 5 µm thin section on glass slide. Sections with tumor and non-tumor areas will then be snap frozen on dry ice and stored at -80°C for protein analysis. Another $2mm^2$ colon tissue section will be incubated in RPMI medium containing 5000 IU/mL and 5000 IU/mL penicillin and streptomycin (CELLGRO) respectively at 37°C and 5% CO_2 for 24 hours. This will be followed by centrifugation at 2500 rpm for 15 minutes. Supernatant will be obtained and stored at -20°C to measure secreted cytokine levels.

Tumor Number and Tumor Area and Histopathology:

Mice colon will be excised and flushed with PBS. Tumor number and area will be counted under the microscope in all mice of different groups and significant different will be calculated between different groups.

Hematoxylin and Eosin staining will be used to determine the morphology of mice colon. Histopathology will be quantified based on the scoring system indicating the severity of disease and constituting inflammation, immune cell infiltration and degree of tumor. This will be calculated on the scale of 12 where highest score of 4 was given for each parameter, where 0 = no infiltration or no inflammation or no cancer; 2 = moderate infiltration or inflammation or pre-cancerous lesions; and 4 = severe inflammation with distorted crypts or infiltration and formation of lymphatic follicles or visible tumors. All the images will be taken in 20X magnification with Nikon e600 microscope. The score will be measured by two investigators in blinded fashion.

TUNEL Assay*:*

Degree of apoptosis will be measured in the tumor and non-tumor tissue sections of the colon by TUNEL assay. TUNEL assay (EMD Millipore) will be used to determine the number of TUNEL positive cells and total number of epithelial cells of the colon in $2mm^2$ tissue cross-sectional tissue area. 5 sections will then be randomly selected from each tissue section and 10 tissue sections will be randomly selected from each group. The ratio of TUNEL positive cell to total epithelial cell will be used to determine the ratio of apoptosis and plotted as a graph for different treatment groups. All the images will be taken in 20X magnification with Nikon e600 microscope.

Protein determination using Western Blot:

Colon tissue frozen at -80°C will be homogenized in RIPA buffer added to protease and phosphatase inhibitors (SIGMA). It will be then centrifuged at 10,000 rpm for 15 minutes and supernatant will be collected for protein analysis. Protein concentration in the supernatant will be determined by using Bradford protein assay. This will be followed by loading equal amounts of protein (50 µg) in each well for a 10% Sodium Dodecyl Sulphate (SDS) gel electrophoresis. The protein from the gel will then be transferred to a nitrocellulose membrane (Pall Scientific) and blocked with 5% non-fat dry milk (Biorad) in phosphate buffer saline (PBS) (cellgro) with 0.1% Tween 20. The membrane will be incubated overnight with the primary antibody. The primary antibodies include Gpx-1, Gpx-2 and GAPDH obtained from Genetex. phospho-NFκB p65, NFκB p65, phospho-p65, cleaved caspase 9, MDA, 4HNE and Nitrotyrosine will be obtained from cell signaling technology. Membrane will be washed by PBS containing 0.1% Tween 20 (Biorad). The

membrane will then be incubated with secondary antibody (Santa Cruz) followed by another washing step. The last step includes incubating the membrane in ECL substrate (Western Bright, Advansta). The film will be then developed by using a developer (SRX-101A, Konica Minolta Medical & Graphic, INC.) in the dark room. Finally the film will be scanned and the density of the protein bands obtained will be analyzed using Image J software.

Enzyme Linked Immunosorbent Assay (ELISA):

Spontaneous secreted cytokines will be measured from the tissue incubated in the RPMI medium for 24 hours at 37°C. The media will be collected and centrifuged at 2500 rpm for 16 minutes. Pellet will be discarded and the supernatant is isolated. Cytokines IL-6, TNF-α, IL-1β and IL-10 levels will be measured by using BD OptEIA ELISA kit obtained from BD biosciences and normalized by total protein content estimated by using standard Bradford assay procedure.

Immunofluorescence:

Colon tumor tissue sections will be deparaffinzed by xylene and dehydrated by different concentrations of ethanol. The sections will then undergo heat mediated antigen retrieval step with 10nM citrate buffer (Prohisto), 0.05% Tween 20, pH 6.0 in an autoclave at 121°C, 15 psi for 20 minutes. The tissues will be then blocked with 10% goat anti-rabbit serum with PBS. Tissues will be incubated in a primary antibody that is cleaved caspase 9 (Cell Signaling Technology) for overnight incubation. This will be followed by 5 washing steps and 2 hour- incubation with anti-rabbit secondary antibody (Aexa Flour 488) (Cell Signaling Technology). Finally the tissue section will be mounted with a DAPI based

mounting media (Genetex) and covered with a coverslip. 10 random 20X magnification, 2x2 images of the 8 slides per group belonging to different mice will be taken and quantified by using Image J software.

Mass Spectrometry:

Colon tissues will be freeze-dried using lyophilizer and weight prior to be used for mass spectrometry. The tissue will then be digested using aqua regia (1 mL of optima grade nitric acid plus 3 mL of optima grade hydrochloric acid) at 140°C and the final volume will then be brought to 10 ml. The samples will be analyzed for Selenium using the Finnigan ELEMENT2 double focusing magnetic sector field inductively coupled plasma-mass spectrometer (ICP-MS). Iridium will be used as the internal standard. The instrument will be calibrated for element ^{82}Se. The samples will be analyzed immediately after the initial calibration. The samples will then be diluted (5X) and the instrument blank will be set at 0.31 ppb of Se.

Statistical analysis

Two-way analysis of variance (ANOVA), Two-way repeated measure ANOVA and One-way ANOVA will be used to analyze the data with Tukey post hoc-analyses. A p value<0.05 will be considered statistically significant. All the statistical analyses will be done using SigmaStat 3.5 (SPSS, Chicago, IL).

Primary Outcomes:

Clinical Score: Clinical score will be measured for each mouse in each group from day 25 to day 194. Mice were sacrificed after the last clinical score measurement. Clinical score is a summation of 3 different score including weight loss, diarrhea and fecal hemoccult. The scoring system is as follows:

Weight loss -	**0 = 0-5% weight loss; 1 = 6-10% weight loss; 2 = 11-15% weight loss; 3 = 16-20% weight loss; 4 = >20% weight loss.**
Diarrhea -	**0 = well-formed pellets, 2 = pasty and semi-formed stools that do not adhere to anus 4 = liquid stools that adhere to the anus**
Fecal Hemoccult-	**0 = no blood, 2 = positive hemoccult, 4 = gross bleeding**

Table 1: It shows clinical score measurement criteria.

The maximum score a mouse could get is 12. Fecal hemoccult scoring was obtained using a kit from Beckman Coulter, which turns the fecal blood into blue color. The higher intensity of blue color indicates greater bleeding. The clinical score was calculated and plotted against days of DSS administration. Higher clinical score indicated more severity of colon cancer.

Tumor Number and Tumor Area: Mice colon will be excised and flushed with PBS. At this point the tumor number and area will be counted for that part of the colon, which was excised for paraffin embedding, freezing and RPMI medium. The rest of the colon was fixed in 10% formalin for 24 hours and then stored in 70% ethanol. The colon will then be stained with 2% methylene blue. Tumor number and area will be counted under the microscope for all the mice in different groups and significant difference will be calculated between different groups and a graph was plotted.

Selenium Content: Se content in the colon of each mice belonging to different groups will be measured by mass spectrometry which would provide a direct measure of colon Se content. Se content will measured as nmol/gm of the colon tissue and significant difference between different groups will be calculated and represented on a graph.

Chronic Inflammation: Chronic inflammation will be measured in the colon of all the mice in different group by measuring secreted cytokines. Secreted cytokines will be measured from the tissue incubated in the RPMI medium for 24 hours at 37°C. Cytokines like IL-6, TNF-α, IL-1β and IL-10 will be measured followed by pNFκB protein expression. This will be followed by Hematoxylin and Eosin staining of the colon tissue section fixed in formalin and embedded in paraffin wax to study chronic inflammation and immune cell infiltration. Increased expression of pro-inflammatory cytokines and proteins and decrease production of anti-inflammatory cytokines indicates greater inflammation.

Greater degree of inflammation indicated by abnormal crypts and infiltration of the immune cells indicates higher severity of colon cancer.

Oxidative Stress: Oxidative stress will be measured in the colon tissue sample which were snap frozen at -80°C by performing western blot for 4HNE, a marker for lipid peroxidation, nitrotyrosine, a marker of nitrosylation and iNOS (inducible nitric oxide synthase) a well-known marker for increased oxidative stress. Higher oxidative stress measured by increased nitrosylation, lipid peroxidation and NO production is indicative of greater severity of chronic inflammation and colon cancer.

Apoptosis: Apoptosis will be measured in the tumor tissue and the normal tissue section of the colon by TUNEL assay. TUNEL positive cells and total number of epithelial cells will be counted and the ratio of TUNEL positive cell to total epithelial cell will determine the degree of apoptosis. Degree of apoptosis will also be measured by determining the protein expression for caspase 9 and caspase 3 in both tumor and non-tumor colon tissue section of all the treatment groups. Greater degree of epithelial cell apoptosis in the non-tumor area of the colon tissue section is indicative of increase pathology and severity of colon cancer. However, increased colon cancer cell apoptosis is indicative of an effective treatment and better prognosis.

Goblet Cell: Increase in the goblet cells and hence increase mucus production is one of the protective mechanisms that could play an essential role in the colon cancer prevention. Alcian blue staining will be used to determine the ratio of goblet to epithelial cells in both the tumor and non-tumor colon tissue section for all the treatment groups. Higher ratio will be an indication of increase number of goblet cell and hence increase mucus secretion. This will be further confirmed by studying the expression of Hes-1 and Math-1, which are involved in the differentiation of epithelial cell to goblet cells. Along with this protein expression study for mucins, indicator of mucus production including Muc 1 and Muc 2 will be studied. Higher number of goblet cells, mucin production and increased expression of Math-1 is indicative of reduced severity and pathology of chronic inflammation and colon cancer.

AIM 3: To study the effect of Adiponectin and Selenium administration on intestinal cancer.

Rationale: Aim 3 will study the role and the mechanism of action of both Se and APN administration on intestinal cancer. Our preliminary data indicated that APN deficiency leads to greater severity of CICC with greater tumor number and area. Higher pathology scoring was observed with APN deficiency with CICC when compared to WT mice. APNKO mice showed greater incidence of aberrant crypts as compared to WT mice. This data was further supported by increase pro-inflammatory cytokine and protein production in APNKO mice when compared to WT mice. Recent study by Tae et al., 2014 has shown

that the patients with advanced adenoma and colorectal cancer (CRC) has lower serum APN concentration when compared to the control group (Tae et al., 2014a). APN Receptor showed higher expression in normal epithelium when compared to epithelium tissue of CRC patients (Tae, et al., 2014a). APN has always been considered to have dual opposite functions with globular variant of APN as a pro-inflammatory marker and full-length protein to be anti-inflammatory. Globular APN mRNA showed increased expression in the colorectal tumors as compared to the adjacent mucosa indicating a pro-inflammatory and pro-cancerous role of globular APN in CRC carcinogenesis (Vetvik et al., 2014). Intraperitoneal administration of full length APN (1.5 mg/kg/week) has been shown to significantly reduced polyps, especially polyps larger than 2mm diameter in small intestine in $APC^{Min/+}$ mice model of intestinal cancer (Otani, et al., 2010). Another recent study has shown that administration of APN alone or in combination with an anti-diabetic drug metformin reduces the IL-1β regulated malignancy in human (LoVo) and mouse (MCA38) cell lines in a STAT3 and AMPK/LKB1 dependent manner (Moon & Mantzoros, 2013). One the basis of the published literature, our preliminary data of AIM 1 and our published manuscript, we hypothesize that the administration of full length APN alone and/or in addition to Se rich diet will reduce the severity of intestinal inflammation and cancer in the $APC^{Min/+}$ mouse model of intestinal cancer.

AIM 3.1 To study the effect of APN administration and Se rich diet on clinical score and tumor load in $APC^{Min/+}$ mice model of intestinal cancer.

AIM 3.2 To study the effect of APN administration and Se rich diet on goblet cell production and cancer cell apoptosis.

AIM 3.3 To determine the effect of APN administration and Se rich diet on oxidative stress, TGF- β, β catenin and ZO-1 mediated gut barrier alterations cellular proliferation and tumor invasion.

Experimental Design Specific AIM 3: Aim 3 will study the study the effect of Se rich diet (0.75 ppm) and APN administration (1.5mg/kg/week) on the $APC^{Min/+}$ mouse model of intestinal cancer. This aim is further divided in to three separate aims where the first aim deals with the role of APN administration and Se rich diet either in combination or alone on clinical score which includes diarrhea, fecal hemoccult and weight loss and intestinal tumor number and area. Four weeks old male and female $APC^{Min/+}$ mice with C57BL/6 background will been randomized in to 3 different treatment groups including $APC^{Min/+}$ mice with control diet (Se = 0.02 ppm) and APN administration, $APC^{Min/+}$ mice with Se rich diet (Se=0.75ppm) and $APC^{Min/+}$ mice with Se rich diet and APN administration. C57BL/6 will be used as a control group. 4 weeks old $APC^{Min/+}$ mice will be administered APN (1.5mg/kg/week) for 20 weeks. Depending on the group, the mice population will either be administered Se rich diet or control diet at 4 weeks of age till 20 weeks of age. $APC^{Min/+}$ mice have been known to develop larger polyps at 16 weeks of age with a peek at 19-20 weeks. Mice will be sacrificed at the end of the study at day 140 and serum, small intestine, colon and spleen will be collected for further proteomic and genomic studies. Aim 3.2 will study the mechanism of action of APN and Se rich diet on reducing the severity of intestinal cancer. This aim will study the how APN and Se rich diet could play a role in prevention of intestinal cancer by increasing mucus production through increase differentiation of epithelial cells to goblet cells. Another mechanism that will be studied

includes studying their role in the cancer cell apoptosis through the activation of caspases. The third sub aim (3.3) will further study the role of both APN and Se rich diet on oxidative stress which has been considered as one of the major mechanism leading to chronic inflammation and hence intestinal cancer. It will also study their effect on β- catenin, TGF-β and junctional proteins like ZO1 and occludin which are responsible for severe inflammation, cellular proliferation and EMT. Unpaired TTEST and One Way ANOVA will be used for statistical analysis with a $p \leq 0.05$ as significant.

Experiment 3: This experiment will study the effect of Se rich diet and APN administration on increasing anti-oxidant potential, apoptosis of cancer cells, goblet cell production and decreasing inflammation and pathology of intestinal cancer.

Animal Model and Handling: Six to Eight weeks old $APC^{Min/+}$ mice were obtained from Jackson Laboratories and bred in the animal facility at the University of South Carolina under the IACUC guidelines. The mice were fed regular chow and *ad libitum*. Four weeks old $APC^{Min/+}$ mice were then randomized in to 6 different treatment. Se rich diet and control diet will be administered to mice on day 28. The groups include: $APC^{Min/+}$+Control Diet (n=10), $APC^{Min/+}$+Se Diet (n=10), $APC^{Min/+}$+APN (n=6), $APC^{Min/+}$+Se+APN (n=6) and Control group (C57BL/6, n=10). Mice were monitored throughout the length of the study for clinical score including weight loss, diarrhea and fecal hemmoccult. Food and water consumption of the mice will be monitored. Mice will be sacrificed by cervical dislocation on day 113. Blood will be collected before sacrifice through retro-orbital puncture, spin

down at 10,000 rpm for 18 minutes and serum will be isolated and stored at -20°C for measuring serum APN. Mice colon will be excised and flushed clean with PBS. 2 mm^2 colon tissue section with tumor and non-tumor area will be fixed in 10% formalin and after 24 hours will be replaced with 70% ethanol followed by paraffin embedding and sectioning to obtain 5-6 mm thin section on glass slide. 2 mm^2 colon tissue section with tumor and non-tumor area will be snap frozen on dry ice and stored at -80°C for protein expression studies and another 2 mm^2 colon tissue section will be incubated in RPMI medium at 37°C for 24 hours followed by centrifugation at 2500 rpm for 15 minutes. Supernatant w obtained and stored at -20°C for secreted cytokine expression.

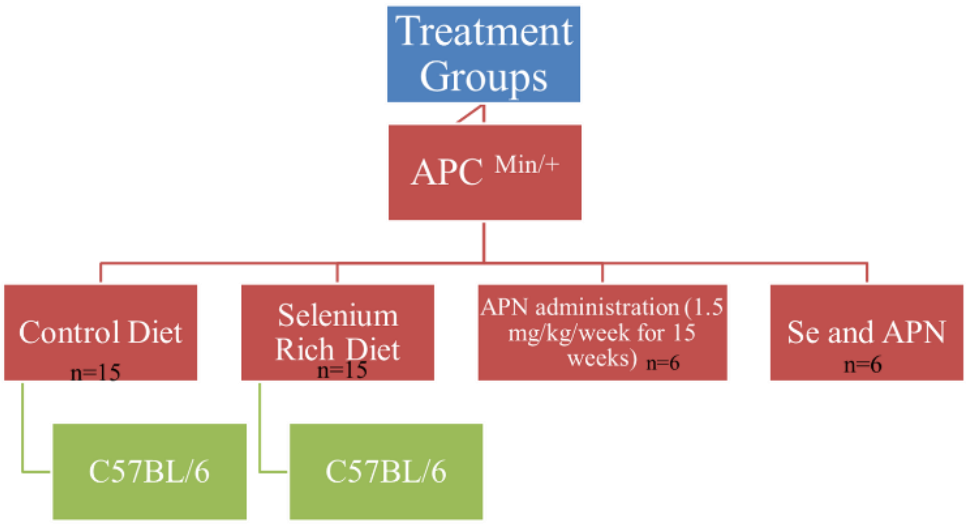

Figure 3: It shows different treatment groups with the number of mice used in each group (n=10) for Aim 2.

Material and Methods

Selenium Diet Administration

Selenium rich diet containing 0.75 ppm of Se per kg will be administered to 2 groups on day 1 of the study. The diet will be administered till the day of sacrifice that is day 114. Control diet contains all the components of the Se rich diet except that the Se content is 0.02 ppm per kg of diet.

Adiponectin Administration

APN (Creative Biochemicals, NY) will be administered intraperitoneally (1.5mg/kg/mouse) once a week for 16 weeks starting day 1 in four weeks old $APC^{Min/+}$ mice belonging to group $APC^{Min/+}$ mice+APN and $APC^{Min/+}$ mice+Se+APN.

Clinical Score

Clinical score will be measured for each mouse in each group from day 1 to day 113. Mice will be sacrificed after the last clinical score measurement. Score for the weight loss is based on the following published scale where 0 = 0–5% weight loss; 1 = 6–10% weight loss; 2 = 11–15% weight loss; 3 = 16–20% weight loss; and 4 = >20% weight loss. Scoring of diarrhea is as follows: 0 = well-formed pellets, 2 = pasty and semi-formed stools that do not adhere to the anus, 4 = liquid stools that adhere to the anus. Detection of blood in the stools will be determined using hemoccult kit (BECKMAN COULTER). The higher intensity of blue color indicates greater bleeding. The followings are the score rates for the fecal hemoccult: 0 = no blood, 2 = positive hemoccult, 4 = gross bleeding. The total clinical

score will be the summation of the individual score of weight loss, diarrhea and fecal hemoccult. The maximum score a mouse could get is 12. The clinical score will be calculated and plotted against length of the study. Higher clinical score indicates more severity of colon cancer development in animals.

Colon Tissue and Serum Collection:

Blood will be collected before sacrifice through retro-orbital puncture and spun down at 10,000 rpm for 18 minutes and serum will be obtained and stored at -20°C to measure APN. Mice colon and SI will be excised and flushed clean with PBS. $2mm^2$ SI and colon tissue section with tumor and non-tumor area will be fixed in 10% formalin. 24 hours later, these tissues will be submerged in 70% ethanol followed by paraffin embedding and sectioning to obtain 5 µm thin section on glass slide. Sections with tumor and non-tumor areas will then be snap frozen on dry ice and stored at -80°C for protein analysis. Another $2mm^2$ colon tissue section will be incubated in RPMI medium containing 5000 IU/mL and 5000 IU/mL penicillin and streptomycin (CELLGRO) respectively at 37°C and 5% CO_2 for 24 hours. This will be followed by centrifugation at 2500 rpm for 15 minutes. Supernatant will be obtained and stored at -20°C to measure secreted cytokine levels.

Tumor Number and Tumor Area and Histopathology:

Mice colon and SI will be excised and flushed with PBS. This will be followed by fixing the tissue in 10% formalin followed by 70% ethanol. Colon and SI will be stained with 2% methylene blue. Tumor number and area will be counted under the microscope in all mice belonging to different treatment groups and significant difference will be calculated.

Hematoxylin and Eosin staining will be used to determine the morphology of mice colon. Histopathology will be quantified based on the scoring system indicating the severity of disease and constituting inflammation, immune cell infiltration and degree of tumor. This will be calculated on the scale of 12 where highest score of 4 was given for each parameter, where 0 = no infiltration or no inflammation or no cancer; 2 = moderate infiltration or inflammation or pre-cancerous lesions; and 4 = severe inflammation with distorted crypts or infiltration and formation of lymphatic follicles or visible tumors. All the images will be taken in 20X magnification with Nikon e600 microscope. The score will be measured by two investigators in blinded fashion.

TUNEL Assay*:*

Degree of apoptosis will be measured in the tumor and non-tumor tissue sections of the SI and colon by TUNEL assay. TUNEL assay (EMD Millipore) will be used to determine the number of TUNEL positive cells and total number of epithelial cells of the colon in $2mm^2$ tissue cross-sectional tissue area. 5 sections will then be randomly selected from each tissue section and 10 tissue sections will be randomly selected from each group. The ratio of TUNEL positive cell to total epithelial cell will be used to determine the ratio of apoptosis and plotted as a graph for different treatment groups. All the images will be taken in 20X magnification with Nikon e600 microscope.

Protein determination using Western Blot:

Colon tissue frozen at -80°C will be homogenized in RIPA buffer added to protease and phosphatase inhibitors (SIGMA). It will be then centrifuged at 10,000 rpm for 15 minutes and supernatant will be collected for protein analysis. Protein concentration in the

supernatant will be determined by using Bradford protein assay. This will be followed by loading equal amounts of protein (50 µg) in each well for a 10% Sodium Dodecyl Sulphate (SDS) gel electrophoresis. The protein from the gel will then be transferred to a nitrocellulose membrane (Pall Scientific) and blocked with 5% non-fat dry milk (Biorad) in phosphate buffer saline (PBS) (cellgro) with 0.1% Tween 20. The membrane will be incubated overnight with the primary antibody. The primary antibodies include Gpx-1, Gpx-2 and GAPDH obtained from Genetex. phospho-NFκB p65, NFκB p65, phospho-p65, cleaved caspase 9, MDA, 4HNE and Nitrotyrosine will be obtained from cell signaling technology. Membrane will be washed by PBS containing 0.1% Tween 20 (Biorad). The membrane will then be incubated with secondary antibody (Santa Cruz) followed by another washing step. The last step includes incubating the membrane in ECL substrate (Western Bright, Advansta). The film will be then developed by using a developer (SRX-101A, Konica Minolta Medical & Graphic, INC.) in the dark room. Finally the film will be scanned and the density of the protein bands obtained will be analyzed using Image J software.

Enzyme Linked Immunosorbent Assay (ELISA):

Spontaneous secreted cytokines will be measured from the tissue incubated in the RPMI medium for 24 hours at 37°C. The media will be collected and centrifuged at 2500 rpm for 16 minutes. Pellet will be discarded and the supernatant is isolated. Cytokines IL-6, TNF-α, IL-1β and IL-10 levels will be measured by using BD OptEIA ELISA kit obtained from BD biosciences and normalized by total protein content estimated by using standard Bradford assay procedure.

Immunofluorescence:

Colon tumor tissue sections will be deparaffinzed by xylene and dehydrated by different concentrations of ethanol. The sections will then undergo heat mediated antigen retrieval step with 10nM citrate buffer (Prohisto), 0.05% Tween 20, pH 6.0 in an autoclave at 121°C, 15 psi for 20 minutes. The tissues will be then blocked with 10% goat anti-rabbit serum with PBS. Tissues will be incubated in a primary antibody that is ZO-1 () for overnight incubation. This will be followed by 5 washing steps and 2 hour- incubation with anti-rabbit secondary antibody (Aexa Flour 488) (Cell Signaling Technology). Finally the tissue section will be mounted with a DAPI based mounting media (Genetex) and covered with a coverslip. 10 random 20X magnification, 2x2 images of the 8 slides per group belonging to different mice will be taken and quantified by using Image J software.

Statistical analysis

Two-way analysis of variance (ANOVA), Two-way repeated measure ANOVA and One-way ANOVA will be used to analyze the data with Tukey post hoc-analyses. A p value<0.05 will be considered statistically significant. All the statistical analyses will be done using SigmaStat 3.5 (SPSS, Chicago, IL).

Primary Outcomes:

Clinical Score: Clinical score will be measured for each mouse in each group from day 1 to day 112. Mice will be sacrificed after the last clinical score measurement. Clinical score is a summation of 3 different score including weight loss, diarrhea and fecal hemoccult. The scoring system is as follows:

Weight loss -	**0 = 0-5% weight loss; 1 = 6-10% weight loss; 2 = 11-15% weight loss; 3 = 16-20% weight loss; 4 = >20% weight loss.**
Diarrhea -	**0 = well-formed pellets, 2 = pasty and semi-formed stools that do not adhere to anus 4 = liquid stools that adhere to the anus**
Fecal Hemoccult-	**0 = no blood, 2 = positive hemoccult, 4 = gross bleeding**

Table 1: It shows clinical score measurement criteria.

The maximum score a mouse could get is 12. Fecal hemoccult scoring will be obtained using a kit from Beckman Coulter, which turns the fecal blood into blue color. The higher intensity of blue color indicates greater bleeding. The clinical score will be calculated and plotted against duration of study. Higher clinical score indicated more severity of colon cancer.

Tumor Number and Tumor Area: Mice colon and small intestine (SI) will be excised and flushed with PBS. At this point the tumor number and area will be counted for that part of the colon and SI, which was excised for paraffin embedding, freezing and RPMI medium. The rest of the colon and SI will be fixed in 10% formalin for 24 hours and then stored in 70% ethanol. The fixed SI and colon will be stained with 2% methylene blue. Tumor number and area will be counted under the microscope for all the mice in different groups and significant difference will be calculated between different groups and a graph will be plotted.

Chronic Inflammation: Chronic inflammation will be measured in the colon and SI of all the mice in different group by measuring secreted cytokines. Secreted cytokines will be measured from the tissue incubated in the RPMI medium for 24 hours at 37°C. Cytokines like IL-6, TNF-α, IL-1β and IL-10 will be measured followed by pNFκB protein

expression. This will be followed by Hematoxylin and Eosin staining of the colon tissue section fixed in formalin and embedded in paraffin wax to study chronic inflammation and immune cell infiltration. Increased expression of pro-inflammatory cytokines and proteins and decrease production of anti-inflammatory cytokines indicates greater inflammation. Greater degree of inflammation indicated by abnormal crypts and infiltration of the immune cells indicates higher severity of intestinal cancer.

Oxidative Stress: Oxidative stress will be measured in the SI and the colon tissue sample which were snap frozen at -80°C by performing western blot for 4HNE, a marker for lipid peroxidation, nitrotyrosine, a marker of nitrosylation and iNOS (inducible nitric oxide) a well-known marker for increased oxidative stress. Higher oxidative stress measured by increased nitrosylation, lipid peroxidation and NO production is indicative of chronic inflammation and intestinal cancer.

Apoptosis: Apoptosis will be measured in the tumor tissue and the normal tissue section of the colon and SI by TUNEL assay. TUNEL positive cells and total number of epithelial cells will be counted and the ratio of TUNEL positive cell to total epithelial cell will determine the degree of apoptosis. Degree of apoptosis will also be measured by determining the protein expression for caspase 9 and caspase 3 in both tumor and non-tumor colon and SI tissue section of all the treatment groups. Greater degree of epithelial cell apoptosis in the non-tumor area of the colon and the SI tissue section is indicative of increase pathology and severity of colon cancer. However, increased cancer cell apoptosis is indicative of an effective treatment and better prognosis.

Goblet Cell: Increase in the goblet cells and hence increase mucus production is one of the protective mechanisms that could play an essential role in the colon cancer prevention. Alcian blue staining will be used to determine the ratio of goblet to epithelial cells in both the tumor and non-tumor intestine tissue section for all the treatment groups. Higher ratio will be an indication of increase number of goblet cell and hence increase mucus secretion. This will be further confirmed by studying the expression of Hes-1 and Math-1, which are involved in the differentiation of epithelial cell to goblet cells. Along with this protein expression study for mucins, indicator of mucus production including Muc 1 and Muc 2 will be studied. Higher number of goblet cells, mucin production and increased expression of Math-1 is indicative of reduced severity and pathology of colon cancer.

TGF-β and Cellular Proliferation: TGF-β is a 25 kDa cytokines that plays a critical role in carcinogenesis, homeostasis, cell proliferation, migration, apoptosis, fibrosis, differentiation of cell and wound healing. TGF-β signaling pathway is one of the most common altered signaling. It can play a dual role as a tumor suppressor and as a cancer promotor. Higher TGF-β protein levels is associated with an increased incidence of tumor reoccurrence (Friedman, et al., 1995). TGF-β alongwith β catenin has been shown to enhance EMT and angiogenesis leading to greater severity of colon cancer (Lampropoulos, et al., 2012). We will study the protein expression of TGF-β through western blot. Lower TGF-β expression will provide an indication of reduced severity of colon cancer.

Canonical Wnt Pathway and β Catenin: Wnt pathway is well known pathway leading to cellular proliferation. In $APC^{Min/+}$ mice model of intestinal cancer there is mutation of APC gene leading to intestinal cancer. APC protein is a negative regulator of β catenin and prevents cellular proliferation and epithelial to mesenchymal transition (EMT). β catenin

and junctional protein expression of ZO-1 and occludin by Western blot will be studied to show the effect of APN or Se or both on cellular proliferation and EMT. β catenin alongwith TGF- β has been shown to induce morphogenetic changes in epithelial cells leading to greater proliferation, inflammation and intestinal cancer.

APPENDIX C

PERMISSION TO REPRINT

ELSEVIER LICENSE
TERMS AND CONDITIONS

Jun 20, 2015

This is a License Agreement between ARPIT SAXENA ("You") and Elsevier ("Elsevier") provided by Copyright Clearance Center ("CCC"). The license consists of your order details, the terms and conditions provided by Elsevier, and the payment terms and conditions.

All payments must be made in full to CCC. For payment instructions, please see information listed at the bottom of this form.

Supplier	Elsevier Limited The Boulevard,Langford Lane Kidlington,Oxford,OX5 1GB,UK
Registered Company Number	1982084
Customer name	ARPIT SAXENA
Customer address	100 RIVERBEND DR. APT A44 WEST COLUMBIA, SC 29169
License number	3652860798674
License date	Jun 20, 2015
Licensed content publisher	Elsevier
Licensed content publication	Biochimica et Biophysica Acta (BBA) - Molecular Basis of Disease
Licensed content title	Adiponectin deficiency: Role in chronic inflammation induced colon cancer
Licensed content author	Arpit Saxena,Alexander Chumanevich,Emma Fletcher,Bianca Larsen,Kirby Lattwein,Kamaljeet Kaur,Raja Fayad
Licensed content date	April 2012
Licensed content volume number	1822
Licensed content issue number	4
Number of pages	10
Start Page	527
End Page	536
Type of Use	reuse in a thesis/dissertation
Portion	full article
Format	both print and electronic
Are you the author of this Elsevier article?	Yes
Will you be translating?	No
Title of your thesis/dissertation	ADIPONECTIN AND SELENIUM RICH DIET CAN ACT AS A COMPLIMENTARY MEDICINE IN THE TREATMENT OF INTESTINAL

AND CHRONIC INFLAMMATION INDUCED COLON CANCER.

Expected completion date	Jul 2015
Estimated size (number of pages)	300
Elsevier VAT number	GB 494 6272 12
Permissions price	0.00 USD
VAT/Local Sales Tax	0.00 USD / 0.00 GBP
Total	0.00 USD

Terms and Conditions

INTRODUCTION

1. The publisher for this copyrighted material is Elsevier. By clicking "accept" in connection with completing this licensing transaction, you agree that the following terms and conditions apply to this transaction (along with the Billing and Payment terms and conditions established by Copyright Clearance Center, Inc. ("CCC"), at the time that you opened your Rightslink account and that are available at any time at http://myaccount.copyright.com).

GENERAL TERMS

2. Elsevier hereby grants you permission to reproduce the aforementioned material subject to the terms and conditions indicated.

3. Acknowledgement: If any part of the material to be used (for example, figures) has appeared in our publication with credit or acknowledgement to another source, permission must also be sought from that source. If such permission is not obtained then that material may not be included in your publication/copies. Suitable acknowledgement to the source must be made, either as a footnote or in a reference list at the end of your publication, as follows:

"Reprinted from Publication title, Vol /edition number, Author(s), Title of article / title of chapter, Pages No., Copyright (Year), with permission from Elsevier [OR APPLICABLE SOCIETY COPYRIGHT OWNER]." Also Lancet special credit - "Reprinted from The Lancet, Vol. number, Author(s), Title of article, Pages No., Copyright (Year), with permission from Elsevier."

4. Reproduction of this material is confined to the purpose and/or media for which permission is hereby given.

5. Altering/Modifying Material: Not Permitted. However figures and illustrations may be altered/adapted minimally to serve your work. Any other abbreviations, additions, deletions and/or any other alterations shall be made only with prior written authorization of Elsevier Ltd. (Please contact Elsevier at permissions@elsevier.com)

6. If the permission fee for the requested use of our material is waived in this instance, please be advised that your future requests for Elsevier materials may attract a fee.

7. Reservation of Rights: Publisher reserves all rights not specifically granted in the combination of (i) the license details provided by you and accepted in the course of this

SPRINGER LICENSE
TERMS AND CONDITIONS

Jun 20, 2015

This is a License Agreement between ARPIT SAXENA ("You") and Springer ("Springer") provided by Copyright Clearance Center ("CCC"). The license consists of your order details, the terms and conditions provided by Springer, and the payment terms and conditions.

All payments must be made in full to CCC. For payment instructions, please see information listed at the bottom of this form.

License Number	3652861011147
License date	Jun 20, 2015
Licensed content publisher	Springer
Licensed content publication	International Journal of Colorectal Disease
Licensed content title	Mucus and adiponectin deficiency: role in chronic inflammation-induced colon cancer
Licensed content author	Arpit Saxena
Licensed content date	Jan 1, 2013
Volume number	28
Issue number	9
Type of Use	Thesis/Dissertation
Portion	Full text
Number of copies	1
Author of this Springer article	Yes and you are a contributor of the new work
Order reference number	None
Title of your thesis / dissertation	ADIPONECTIN AND SELENIUM RICH DIET CAN ACT AS A COMPLIMENTARY MEDICINE IN THE TREATMENT OF INTESTINAL AND CHRONIC INFLAMMATION INDUCED COLON CANCER.
Expected completion date	Jul 2015
Estimated size(pages)	300
Total	0.00 USD
Terms and Conditions	

Introduction
The publisher for this copyrighted material is Springer Science + Business Media. By clicking "accept" in connection with completing this licensing transaction, you agree that the following terms and conditions apply to this transaction (along with the Billing and Payment terms and conditions established by Copyright Clearance Center, Inc. ("CCC"), at the time that you opened your Rightslink account and that are available at any time at http://myaccount.copyright.com).

Limited License

With reference to your request to reprint in your thesis material on which Springer Science and Business Media control the copyright, permission is granted, free of charge, for the use indicated in your enquiry.

Licenses are for one-time use only with a maximum distribution equal to the number that you identified in the licensing process.

This License includes use in an electronic form, provided its password protected or on the university's intranet or repository, including UMI (according to the definition at the Sherpa website: http://www.sherpa.ac.uk/romeo/). For any other electronic use, please contact Springer at (permissions.dordrecht@springer.com or permissions.heidelberg@springer.com).

The material can only be used for the purpose of defending your thesis limited to university-use only. If the thesis is going to be published, permission needs to be re-obtained (selecting "book/textbook" as the type of use).

Although Springer holds copyright to the material and is entitled to negotiate on rights, this license is only valid, subject to a courtesy information to the author (address is given with the article/chapter) and provided it concerns original material which does not carry references to other sources (if material in question appears with credit to another source, authorization from that source is required as well).

Permission free of charge on this occasion does not prejudice any rights we might have to charge for reproduction of our copyrighted material in the future.

Altering/Modifying Material: Not Permitted
You may not alter or modify the material in any manner. Abbreviations, additions, deletions and/or any other alterations shall be made only with prior written authorization of the author(s) and/or Springer Science + Business Media. (Please contact Springer at (permissions.dordrecht@springer.com or permissions.heidelberg@springer.com)

Reservation of Rights
Springer Science + Business Media reserves all rights not specifically granted in the combination of (i) the license details provided by you and accepted in the course of this licensing transaction, (ii) these terms and conditions and (iii) CCC's Billing and Payment terms and conditions.

Copyright Notice:Disclaimer
You must include the following copyright and permission notice in connection with any reproduction of the licensed material: "Springer and the original publisher /journal title, volume, year of publication, page, chapter/article title, name(s) of author(s), figure number(s), original copyright notice) is given to the publication in which the material was originally published, by adding; with kind permission from Springer Science and Business Media"

Warranties: None

Example 1: Springer Science + Business Media makes no representations or warranties with respect to the licensed material.

Example 2: Springer Science + Business Media makes no representations or warranties with

respect to the licensed material and adopts on its own behalf the limitations and disclaimers established by CCC on its behalf in its Billing and Payment terms and conditions for this licensing transaction.

Indemnity
You hereby indemnify and agree to hold harmless Springer Science + Business Media and CCC, and their respective officers, directors, employees and agents, from and against any and all claims arising out of your use of the licensed material other than as specifically authorized pursuant to this license.

No Transfer of License
This license is personal to you and may not be sublicensed, assigned, or transferred by you to any other person without Springer Science + Business Media's written permission.

No Amendment Except in Writing
This license may not be amended except in a writing signed by both parties (or, in the case of Springer Science + Business Media, by CCC on Springer Science + Business Media's behalf).

Objection to Contrary Terms
Springer Science + Business Media hereby objects to any terms contained in any purchase order, acknowledgment, check endorsement or other writing prepared by you, which terms are inconsistent with these terms and conditions or CCC's Billing and Payment terms and conditions. These terms and conditions, together with CCC's Billing and Payment terms and conditions (which are incorporated herein), comprise the entire agreement between you and Springer Science + Business Media (and CCC) concerning this licensing transaction. In the event of any conflict between your obligations established by these terms and conditions and those established by CCC's Billing and Payment terms and conditions, these terms and conditions shall control.

Jurisdiction
All disputes that may arise in connection with this present License, or the breach thereof, shall be settled exclusively by arbitration, to be held in The Netherlands, in accordance with Dutch law, and to be conducted under the Rules of the 'Netherlands Arbitrage Instituut' (Netherlands Institute of Arbitration).***OR:***

All disputes that may arise in connection with this present License, or the breach thereof, shall be settled exclusively by arbitration, to be held in the Federal Republic of Germany, in accordance with German law.

Other terms and conditions:

v1.3

Questions? customercare@copyright.com or +1-855-239-3415 (toll free in the US) or +1-978-646-2777.